Imperial College of Science and Technology

(University of London)

A FINITE ELEMENT ANALYSIS OF CRACK PROPACATION PROBLEMS WITH APPLICATIONS TO SEISMOLOGY

by

Hossein Javaherian

Thesis submitted for the Degree of Doctor of Philosophy

January 1978

To my parents and teachers

ABSTRACT

Plate tectonic forces are known to give rise to strain accumulation in the crust of the earth. The stress field can be released by the extension of the existing fault-planes. The process of stress accumulation and its subsequent release are studied from a fracture view point.

A systematic simulation of the process is carried out in three phases. In phase I, the process of gradual stress build-up in a static field containing a crack is considered. Phase II concerns wave propagation in a cracked structure and possible mechanisms for fracture initiation. Phase III concerns the transient field generated by a crack extending in a medium. In each case simple models are chosen to represent the process.

These models are formulated in their equivalent weak variational form. Proofs of existence and uniqueness of solutions to stationary crack problems are given. For the running crack problem a new variational form taking into account the energy dissipation at the crack tip is presented.

Regularity of the solutions to stationary problems, for angular domains, is studied. The problem is then numerically approximated by the finite element method. It is demonstrated that due to the presence of sharp re-entrant corners, convergence of the standard method of finite elements fails for these problems. This is remedied by the inclusion of proper singular basis functions in the approximating spaces. Using singular basis functions optimum rates of convergence in different norms are established.

Using embedded singularity elements, computational results for the stationary crack problem giving dynamic stress intensity factors, crack-opening displacements and transient response at an arbitrary point in the

medium are presented. A numerical procedure for computer implementation of the moving crack problem is suggested and the elastic field in the limiting case of a crack propagating at the Rayleigh velocity is numerically evaluated. The suitability and power of the method in the analysis of fracture problems are emphasized.

ACKNOWLEDGEMENTS

The research reported in the thesis was carried out at the Department of Computing and Control, Imperial College, under the supervision of Dr. Richard B. Vinter. I would like to sincerely thank him for his encouragement and much technical advice throughout the period of this research.

I would also like to express my gratitude to the following:

To Professor N. Ambrayses from the Seismology Section who encouraged me to take up research in the field and discussed the scope of the problems involved, particularly, in the initial stages of the work.

To Dr. C. Atkinson from the Mathematics Department with whom I had many valuable discussions during this period.

To Dr. L.P.R. Lyons from the Civil Engineering Department who generously made his frontal solution processor available for further extension to my problems and also for his expert programming advice during the computing stage of the project.

To my past and present fellow students, in particular to Miss. F. Javadi with whom I discussed the work.

Last, but not least, to Linden for her excellent typing of the thesis.

This research was supported by the Technical Cooperation Training Department of the British Council while the author was on leave from Arya-Mehr University, Tehran, Iran.

LIST OF CONTENTS

OUTLINE OF THE THESIS AND CONTRIBUTION

The physical problem considered in the thesis, together with the objectives to be achieved and the approach adopted here are explained in Chapter I where simple models of the problem are introduced and then some of the well-established tools, in particular the finite element method, for their analysis are reviewed.

Chapter II is devoted to the analysis of static crack problems. The problem is first written in a weak variational form as the basis for any finite element analysis. Using symmetry, single mode crack problems are reduced to boundary value problems for which existence of a unique solution is already provided. As an alternative approach for the general mixed-mode crack problems, the definition of Sobolev spaces is extended to slit domains and it is then proved that the bilinear form in the problem is V-elliptic from which existence and uniqueness of solutions follows. Study of regularity of solutions is regarded as an important step in obtaining approximate solutions. The solution is expanded as the sum of singular and smooth functions on slit domains and these expansions are then employed in the approximations to show that by inclusion of these singular functions the optimum rate of convergence can be recovered. Estimates, in terms of data, for the approximation errors in displacements and stresses are also derived. Results concerning domains with cracks are treated as special cases.

In Chapter III the equations of dynamic elasticity on slit domains are studied. For a finite element analysis of the system, the problem is written in its equivalent variational form. With the V-ellipticity of the bilinear form established in Chapter II, the existence and uniqueness of a solution to the system of equations is

straightforward. Then, using singular functions, an approximate solution to the problem is sought. Using finite elements on spatial variables in conjunction with singular functions, the approximate problem is reduced to the solution of a system of ordinary differential equations with time as the variable. The problem is further approximated by a full discretization in both time and space. In each case, rates of convergence for the solution are established.

The problem of moving cracks is dealt with in Chapter IV. In order to apply finite element method a new variational form for the problem is proposed which is closely related to the rate of energy balance equation. This form takes into account the energy dissipation from the tip of the crack. In a manner consistent with the analysis of Chapter II, the asymptotic near field is re-derived. Using finite elements in both time and space a numerical scheme for approximation of the variational form is suggested. Due to the complexity of the problem only the special case of a crack running at the Rayleigh velocity is computationally implemented. The relevance of this velocity as an acceptable velocity is discussed.

In Chapter V after a brief introduction to conformity and patch test different methods of inclusion of singular functions in the approximating spaces are discussed. It turns out that distorted isoparametric elements yield highly accurate results with a relatively coarse mesh, if the solution is interpreted correctly. A numerical procedure for consistent extraction of stress intensity factors for the general mixed-mode crack problems using 6-node quarter-point elements is suggested. The resulting set of simultaneous equations is solved by a direct method and the general organisation of the program is explained.

Chapter V concludes by presentation of results for a number of stationary and non-stationary crack problems.

Chapter I

PROBLEM AND BACKGROUND

I.1 PROBLEM STATEMENT

I.1.1 Description of the Physical Problem

A large class of earthquakes, classified as shallow-focus type, occur by fracture of the earth's crust. It is generally hypothesized that plate-tectonic forces give rise to a gradual stress build-up in the crust. The strain energy accumulated in this way is then rapidly released by the fracture of the crust. The process of fracture is normally initiated by extension of the existing fault planes. This sets off waves of high intensity into the medium. The resulting motion is then recorded at different seismological stations around the globe.

The ground shaking is dominated by the way in which the fracture proceeds in the medium. From a physical view point this process, in turn, must depend on the structural and geometrical properties of the crust and the initial strain in it. However, the complete physical knowledge regarding the fracture phenomenon is lacking.

This motivates one to develop a theoretical model of the process for a systematic approach to study the fracture phenomenon.

I.1.2 Objectives

In this work we are interested in obtaining the complete near and far field solutions for plane crack problems.

I.1.3 Approach

In strong-motion seismology the main interest is in a complete

knowledge of the field. While analytical methods have provided a partial solution to the problem, the complete solution can only be given by a reliable numerical technique.

The numerical approximation method adopted here is that of the finite elements. This method has been very successful in solving many partial differential equations of mathematical physics.

For elliptic equations the method is standard for smooth domain and data. However, for hyperbolic systems of equations defined over domains with non-smooth boundaries, the method should further be developed. This step is regarded as essential in the study since important aspects of the problem are both the sharp reentrant corner present and its dynamic feature.

Some theoretical aspects of the problem such as the question of existence and uniqueness of solutions to different crack problems are dealt with. The modified approximation procedure is discussed and shown to converge. Also the theoretical rates of convergence of the approximations are given.

Finally, a computer implementation of the scheme is undertaken and numerical results reported. The power and value of the method is evident in its application to a wide range of problems.

I.1.4 Simple Models of the Problem

In this work we will confine ourselves to linear elasticity and ignore any thermal effect. The assumption of linearity in fracture might seem to be restrictive and in certain cases give rise to physically unacceptable results. However, a linear analysis provides some insight into the complicated process. Also, regarding fracture in seismology, the

thermal effects are usually secondary and have little significance.

Within the linear theory of elasticity the material can be regarded as inhomogeneous and anisotropic. For ease of presentation, in some parts of the theory we will concentrate on homogeneous isotropic material, nevertheless this should not be regarded as any restriction. The material is assumed to satisfy the minimum requirement of having positive-semi-definite strain energy density. Throughout, the body is assumed to be brittle.

We will also be dealing with plane problems only, as the case of anti-plane crack problems have been well treated in the literature.

We consider three different problems:

I.1.4.1 Stationary crack in a static field

The body and boundary forces are gradually applied to the medium so that we essentially have a static problem Fig. (1). The governing equations constitute an elliptic system with respect to the variables of interest (i.e. displacements u_i, $i = 1, 2$)

$$Au_i = f_i \text{ on } \Omega \tag{1}$$

where A is an elliptic matrix of differential operators given by

$$(Au)_i = -\frac{\partial}{\partial x_j}(\sigma_{ij}(u)) \tag{2}$$

where

$u = (u_1, u_2)$ = displacement vector

$\sigma_{ij}(u) = a_{ijkh}\varepsilon_{kh}(u)$ = stress tensor component

$\varepsilon_{ij}(u) = \frac{1}{2}\left(\frac{\partial u_i}{\partial x_j} + \frac{\partial u_j}{\partial x_i}\right)$ = linearized strain tensor component

Solution of this problem, apart from its individual character, would simulate the initial strain required for the next phase of dynamic analysis.

I.1.4.2 Stationary crack in a dynamic field

In this case we study the transient response of the field due to dynamic forces acting in the medium while the crack tip remains stationary. The governing equations of motion constitute a conservative system of hyperbolic equations. Taking $u(t)$ = a function $x \to u(x,t)$ and $u'(t) = \partial u/\partial t$ we have

$$u''(t) + Au(t) = f(t) \quad \text{in} \quad Q = \Omega \times I; \quad I =]0,T[\qquad (3)$$

where A was defined earlier.

This system of equations together with the specified body and boundary forces as well as initial conditions obtained from the static analysis ($u(0) = u_0$, $u'(0) = 0$) define a well-posed problem for analysis.

I.1.4.3 Moving crack problem

Throughout our analysis we will consider the material to be ideal brittle so that no plastic zone is formed ahead of the crack tip and the assumption of linear elasticity is valid.

It is assumed that, under the influence of applied forces, when a certain critical condition is reached the crack tip starts to move. The direction of crack extension and position of the crack tip is not, a priori, known and needs to be determined. Evidently from physical considerations the crack tip position in time influences the complete elastic field and therefore knowledge of one should, in principle, be equivalent to the knowledge of both (see Fig. 2).

The governing equations of motion constitute a locally-dissipative

system of hyperbolic equations. Part of the dissipative energy is spent on formation of new surfaces in the material by extension of the crack faces. Here again we have the same equations as in (3) with the additional condition that *the position* a(t) *of the crack tip* (p) *is time-dependent*. Later it will be shown how to incorporate this statement into our formulation.

I.2 SOLUTION TECHNIQUES

A large number of techniques have been applied to crack problems. While most of these techniques are related and hence cannot be regarded as distinct from each other we attempt to, very briefly, classify some of the more important of these analytical and numerical methods.

I.2.1 Analytical Methods

I.2.1.1 Complex variable theory and conformal mapping

This method has been intensively applied to two-dimensional problems of elasticity. The method essentially consists of introducing the Airy Stress function $\chi(x,y)$. Then the equations of motion reduce to a biharmonic equation

$$\nabla^4 \chi(x,y) = 0$$

The solution can then be written (Muskhelishvili [1]) in terms of the complex variable $z = x + iy$ and two analytic functions $\phi(z)$ and $\psi(z)$ as

$$\chi(x,y) = \text{Re}\,[\bar{z}\phi(z) + \int \psi(z)\,dz]$$

Then the stresses are:

$$\sigma_x + \sigma_y = 4\,\mathrm{Re}\,[\phi'(z)]$$

$$\sigma_y - \sigma_x + 2i\tau_{xy} = 2[\bar{z}\phi''(z)+\phi'(z)]$$

where

$$\phi' = \frac{d\phi}{dz} \text{ etc.}$$

Introducing a complex stress-intensity factor $k = k_1 - ik_2$, Sih [2] expressed the first stress invariant of the near tip solution as

$$\sigma_x + \sigma_y = \mathrm{Re}\left[\frac{2\sqrt{k}}{\sqrt{z-z^*}}\right]$$

where z^* expresses the location of the crack tip on the positive side of the x-axis, i.e.

$$k = 2\sqrt{2} \lim_{z\to z^*} \sqrt{z-z^*}\ \phi'(z)$$

This relation indicates that a local near tip knowledge of $\phi(z)$ would be sufficient for the determination of the complex stress intensity factor k.

With the aid of a conformal transformation $z = \omega(s)$ we can map suitably regular domains into a unit circle or a half plane. The equations of motion would then be transformed to

$$\sigma_x + \sigma_y = 4\ \mathrm{Re}\left[\frac{\phi'(\xi)}{\omega'(\xi)}\right]$$

$$\sigma_y - \sigma_x + 2i\tau_{xy} = 2\left\{\frac{\bar{\omega}(\bar{\xi})}{[\omega'(\xi)]^3}\left(\omega'(\xi)\phi''(\xi)-\phi'(\xi)\omega''(\xi) + \frac{\psi'(\xi)}{\omega'(\xi)}\right)\right\}$$

and k is expressed as

$$k = 2\sqrt{2} \lim_{\xi \to \xi^*} \sqrt{\omega(\xi) - \omega(\xi^*)} \; \frac{\phi'(\xi)}{\omega'(\xi)}$$

with $\lim_{\xi \to \xi^*} \omega'(\xi) \to 0$ where z^* is mapped into ξ^* in ξ-plane. It has further been shown that

$$k = 2 \frac{\phi'(\xi^*)}{\sqrt{\omega''(\xi^*)}}$$

This form has been used in solving Laplace equations in conjunction with Schwartz-Christoffel transformation to yield closed form solutions. See Sih [3], Bowie [4], [5] and Neal [6].

I.2.1.2 Eigenfunction expansion

For a wedge-shaped domain of a homogeneous linear isotropic material Williams [7], [8] has obtained the form of singularities at the corners. We make the polar coordinate transformation

$$x_1 = r \cos \theta$$

$$x_2 = r \sin \theta$$

and introduce $R = \{(r,\theta) \mid 0<r<\infty, -\pi \leq \theta \leq \pi\}$ with R^0 as the interior of R. Now take u_i and σ_{ij} as the components of displacement and stress field, respectively. The equilibrium and compatability conditions would then reduce to

$$\begin{cases} \nabla^4 \chi = 0 \\ \qquad\qquad \text{on } R^0 \\ \sigma_{ij} = \varepsilon_{ki} \varepsilon_{\ell j} \chi_{,k\ell} \end{cases}$$

where χ is the Airy Stress function, $\chi_{,k\ell} = \frac{\partial^2 \chi}{\partial x_k x_\ell}$ and ε_{ij} are the components of the 2-D alternator. For plane strain

$$\sigma_{ij} = 2\mu \{\frac{\nu}{1-2\nu} \delta_{ij} u_{k,k} + u_{(i,j)}\} \text{ on } R^0$$

where

$$u_{(i,j)} = \tfrac{1}{2}(u_{i,j} + u_{j,i})$$

and δ_{ij} is the Kronecker delta, μ and ν are the shear modulus and poisson ratio. The boundary conditions take the form

$$\sigma_{i2}(r_1 \pm \pi) = 0 \qquad 0 < r < \infty$$

Now choosing

$$\chi(r,\theta) = r^{m+1} F(\theta)$$

for m a constant and F an unknown function of θ, he finds that the solution χ is a combination of the following biharmonic functions

$$r^{m+1} \cos (m \pm 1)\theta, \; r^{m+1} \sin (m \pm 1)\theta$$

The function χ satisfying the specified boundary conditions leads to

$$\sin 2m\pi = 0$$

$$F(\theta) = c_1[\sin(m-1)\theta - \frac{m-1}{m+1} \sin (m+1)\theta] + c_2[\cos(m-1)\theta - \cos (m+1)\theta]$$

The roots of these equations are

$$2m\pi = k\pi \qquad \text{or} \qquad m = \frac{k}{2}\,; \quad k \text{ is a positive integer}$$

Williams has also given the eigenequations corresponding to different boundary conditions on angular corners.

I.2.1.3 Green's function approach

If the fundamental solution to concentrated forces are known then we can always find the solution to an arbitrary loading by employing the Green function. In particular, if the stress intensity factors (Fig. (3)) due to normal and longitudinal point forces H and V at x = b is known (See the end of the chapter)

$$k = k_1 - ik_2 = \frac{H+iV}{2\pi\sqrt{a}}\left\{\frac{\kappa-1}{\kappa+1} + \sqrt{\frac{b+a}{b-a}}\right\};\ b < a,\ \kappa = 3-4\nu \text{ for plane strain}$$

Then the solution to arbitrary σ_y^0 and τ_{xy}^0 are obtained from

$$k_1 = \frac{1}{2\pi\sqrt{a}}\int_{-a}^{a} \sigma_y^0 \sqrt{\frac{a+x}{a-x}}\,dx + \frac{1}{2\pi\sqrt{a}}\left(\frac{\kappa-1}{\kappa+1}\right)\int_{-a}^{a} \tau_{xy}^0\,dx$$

$$k_2 = -\frac{1}{2\pi\sqrt{a}}\left(\frac{\kappa-1}{\kappa+1}\right)\int_{-a}^{a} \sigma_y^0\,dx + \frac{1}{2\pi\sqrt{a}}\int_{-a}^{a} \tau_{xy}^0 \sqrt{\frac{a+x}{a-x}}\,dx$$

I.2.1.4 Riemann-Hilbert problem

This method is particularly convenient for a system of cracks along a line or perimeter of a circle. Representing by σ_y^+ and τ_{xy}^+, the stresses on the upper crack face and σ_y^- and τ_{xy}^- on the lower one, the boundary value problem is reduced to the following form

$$F^+(x) - \alpha F^-(x) = p(x) \text{ on } L \quad \text{(the crack line)}$$

α and $p(x)$ are known functions.

Now we have to find an analytic function $F(z)$ which assumes the values $F^+(x)$ and $F^-(x)$ on the upper and lower crack line, resepctively, except at the crack tips. When the cracks are represented by branched cuts whose ends are a_i and b_i $(i = 1, \ldots, n)$ then the appropriate function for describing these cuts is

$$Q(z) = \prod_{i=1}^{n} (z-a_i)^{-\frac{1}{2}} (z-b_i)^{-\frac{1}{2}}$$

and the solution $F(z)$ is given by:

$$F(z) = \frac{Q(z)}{2\pi j} \int_L \frac{p(x)}{Q^+(x)\,(x-z)}\, dx + Q(z) P_n(z)$$

where P_n is a polynomial of degree n whose coefficients are determined from conditions on displacements and stresses, see [9] and [10]. (This is also a standard method in seismology and dislocations theory.)

I.2.1.5 Wiener-Hopf technique

This is one of the most celebrated techniques in analysis of crack problems. Its power lies in its potential to deal with mixed boundary conditions.

Using integral transforms one can reduce a crack problem to an equation of the following form (Noble 1958) [11]: (Fig. 4))

$$A(s)H_+(S) + B(s)K_-(s) + C(s) = 0; \quad s = \alpha + i\omega \qquad (1)$$

and

$$-\infty < \alpha < +\infty$$

$$\omega_- < \omega < \omega_+$$

the unknown function $H_+(s)$ is regular in the half plane $\omega > \omega_-$ and $K_-(s)$ is regular in the $\omega < \omega_+$ plane. A(s), B(s) and c(s) are known functions in the strip.

Basically we have to find

$$M_+(s) \text{ in } \omega > \omega_-$$

$$M_-(s) \text{ in } \omega < \omega_+$$

such that

$$\frac{M_+(s)}{M_-(s)} = \frac{A(s)}{B(s)} \tag{2}$$

Then the equation (1) can be rearranged as

$$M_+(s)H_+(s) + M_-(s)K_-(s) = -M_-(s)\frac{c(s)}{B(s)} \tag{3}$$

The r.h.s. in (3) can be decomposed as

$$M_-(s)\frac{c(s)}{B(s)} = C_+(s) + C_-(s) \tag{4}$$

where $C_+(s)$ is regular in $\omega > \omega_-$

and

$C_-(s)$ is regular in $\omega < \omega_+$

using (4) in (3) we have

$$M_+(s)H_+(s) + C_+(s) = -[M_-(s)K_-(s)+c_-(s)] = J(s) \tag{5}$$

Since

$$M_+(s)H_+(s) + c_+(s) \text{ is regular in } \omega > \omega_-$$

and

$$M_-(s)K_-(s) + c_-(s) \text{ is regular in } \omega < \omega_+$$

then J(s) can analytically be continued over the whole s-plane.

Assuming that

$$|M_+(s)H_+(s)+C_+(s)| < |s|^m \quad \text{as} \quad s \to \infty; \quad \omega > \omega_-$$

and (6)

$$|M_-(s)K_-(s) + C_-(s)| < |s|^n \quad \text{as} \quad s \to \infty; \quad \omega < \omega_+$$

then using the extended form of Liouville's theorem, we can represent J(s) as a polynomial P(s) with deg {P(s)} = min (m,n) and hence

$$M_+(s)H_+(s) + C_+(s) = P(s)$$

(7)

$$M_-(s)K_-(s) + C_-(s) = -P(s)$$

These equations determine $H_+(s)$ and $K_-(s)$ to within polynomials P(s) whose coefficients may be found from other conditions. It can be observed that this technique is identical to the Riemann-Hilbert representation of a semi-infinite crack parallel to the x-axis.

This technique has been employed by Koiter [12], Knauss [13] and Westman [14]. Baker [15] has solved the problem of a uniformly moving crack in plane using the Wiener-Hopf technique.

I.2.1.6 Singular-integral equations

A large number of crack and contact problems can be formulated as singular-integral equations on the boundary of a half-plane. For a crack problem we usually get a couple of dual integral equations corresponding to the boundary conditions on the crack line. The singular equation has a kernel of Cauchy-type singularity

$$\alpha\phi(x) + \frac{\beta}{\pi j}\int_L \frac{\phi(t)}{t-x}\,dt = P(x) \qquad (1)$$

α and β are constants s.t. $\alpha^2-\beta^2 \neq 0$ and L represents the crack arc. For more general forms of the equations refer to [16]. Muskhelishvili [1] has given the solution $\phi(x)$ to (1) as

$$\phi(x) = \frac{\alpha}{\alpha^2-\beta^2}P(x) - \frac{\beta}{(\alpha^2-\beta^2)\pi j\sqrt{(x-a)\,x-b)}}\int_L \frac{\sqrt{(t-a)\,(t-b)}}{t-x}\,P(t)\,dt + \frac{c}{\sqrt{(x-a)\,(x-b)}} \qquad (2)$$

a and b are the end points of L and c is a constant

The stress intensity factors are obtained by, say, displacements ahead of the crack. ($\phi(x)$ could represent displacements.)

Representation of cracks by a continuous distribution of dislocation singularities also results in singular integral equations. The Burger's vector b_i in terms of the distribution $D_i(t)$ is

$$b_i = \int_c D_i(t)\,dt \qquad (3)$$

where c is a path around the dislocation distribution and the net Burger's vector around a crack is zero, i.e.

$$\int_L D_i(t)\,dt = 0 \tag{4}$$

Consider a central crack of length 2a in Mode I with traction $\sigma_y(x,0) = -P(x)$ on the crack faces $-a \leq x \leq a$. This crack can be modelled as a continuous array of dislocations of density D_y. The stress on the crack line are then

$$\sigma_x = -\frac{2\mu}{\pi(\kappa+1)} \int_L \frac{D_y(t)}{x-t}\,dt$$

$$\sigma_y = \frac{2\mu}{\pi(\kappa+1)} \int_L \frac{D_y(t)}{x-t}\,dt \tag{5}$$

$$\tau_{xy} = 0$$

Hence we have

$$\frac{2\mu}{\pi(\kappa+1)} \int_L \frac{D_y(t)}{t-x}\,dt = P(x) \tag{6}$$

also the displacement is singled-valued if

$$\int_L D_y(t)\,dt = 0 \tag{7}$$

In a continuous dislocation model the stress-intensity factor k_1 can be expressed in terms of the density distributions D_y as

$$D_y(t) = \frac{(\kappa+1)}{2\sqrt{2}\mu} \frac{k_1}{\sqrt{a-x}} \qquad \text{(see [17])}$$

The equations (6) and (7) represent a special case for the general singular integral equations.

I.2.1.7 Boundary collocation method

This method is applicable to internal cracks in homogeneous isotropic materials. The method uses the Laurent series expansion of the relevant complex potentials which satisfy the boundary conditions. The unknown coefficients in the expansion are then written in terms of a parameter λ which represents the non-dimensional crack length. Finally a set of linear system of equations are constructed from segment s_i, $i = 1, \ldots, n$, of the boundary, Isida [18]. This method is shown to give results with an accuracy as high as 0.1%.

I.2.2 Numerical Methods

In this category fall the method of finite differences and finite elements. We briefly review these techniques as applied to crack problems.

I.2.2.1 Method of finite differences

This method is based on a direct approximation of differential equations. In this method one discretizes a differential operator at any point in terms of neighbouring unknown values. With regard to stationary crack problems Chen [19], among others, has used a Lagrangian code, initially developed for problems in gas dynamics; etc., to determine stress intensity factors. As he recognises, no finite-difference technique can deal with unbounded strains in the vicinity of the crack tips and hence a local refinement of meshes seems to be necessary in order to get reliable results. While the mesh refinement idea for finite difference methods as applied to crack problems is a natural one, it is not clear how one would go about establishing improved rates of convergence, and this has not been attempted.

As a consequence of the required mesh refinement a much larger system of equations must be solved. This would impose difficulties on computer storage and processing time of problems. Still even with the extreme near tip mesh refinement reported there, results obtained in the vicinity of the crack tip are not reliable and one has to revert to extrapolation techniques beyond this zone.

Two main drawbacks of any finite-difference scheme are the difficulties in dealing with general mixed boundary conditions and domains of arbitrary shape. However, its formulation and computer implementation is straightforward and does not require a great deal of experience. We will return to these points, in a more specific manner, in the course of presentation of numerical results.

I.2.2.2 The finite element method

This is an elegant mathematical tool in solving systems of partial differential equations. It is perhaps the most versatile numerical technique available for this purpose that can deal with general mixed boundary conditions over domains of arbitrary shape.

In this method we start by writing the variational form corresponding to the classical partial differential equations. The domain is divided into a finite number of elements with piecewise polynomials describing the variables of interest over each element. We then try approximately to satisfy the variational form.

For static problems, the technique is essentially an optimization problem and the exact solution corresponds to the minimum of the cost function involved. For problems in linear elasticity the cost function corresponds to the potential strain energy, i.e. the exact solution is the solution that minimizes the potential strain energy.

However, there are two basic inherent difficulties involved. The first is the variational formulations of a given dynamic problem and the second is computer implementation of any finite element method requires a good deal of experience and computer system engineering.

Once a problem is formulated in finite elements one can analyse the problem for the errors involved with relative ease before trying to implement it. And when the problem is implemented and tested the same routine would be sufficient for a wide variety of problems in that category.

One of the most beautiful aspects of finite elements is the fact that basis functions are specified over each *element* as piecewise polynomials with their support extended over few elements. This would give a unique opportunity to include any desired behaviour of the solution in the scheme. In particular, for the crack problems it is possible to incorporate the proper singular forms obtained from an asymptotic near tip analysis of the problem.

Many authors have studied the finite element approximation of stationary crack problems, see [20], [21] and [22].

Tong and Pian [23] show that for problems with singularities the rate of convergence depends on the nature of the singularities. In particular for plane problems of elasticity with a sharp crack the displacement rate of convergence, in energy norm, is of the order ½. In other words using any finite element with polynomial basis functions of any order this rate cannot be improved. Chan et al [24] have used conventional finite element routines and mesh refinement around the crack tip. Their numerical results indicate the need for a very large system of equations to be solved and also the very poor convergence of the solution in the zone surrounding the

tip. In fact, solutions away from the tip are more reliable. According to Nitsche [25] this is to be expected as the one-half order of convergence is true only on the neighbourhood of the tip and away from this area it is better (order one).

Babuska [26] has theoretically supported the idea of mesh refinement and for domains with corners proves that by a 'proper' refinement it is possible to get the same order of convergence, in energy norm, as for smooth domains. No numerical results to show how to approximate his model-problem are presented. However it would not be surprising if the same difficulties and inherent shortcomings as in [24] were to arise in the implementation of this scheme.

Hilton and Sih [21] divide the plane into two regions: on the core region surrounding the tip singularity-imbedded elements are used and over the rest of the plane the usual constant strain elements are defined. With this arrangement the potential energy is written as the sum of energies from these regions. The potential energy of the static problem is then minimized with respect to the unknown displacements at nodes and the unknown stress intensity factor. The resulting system of equations would determine both the displacement field and the stress intensity factor. For the results reported, using this method reasonable accuracies are obtained while the computational time is unreasonably large for typical problems.

Wilson [22] has surrounded the crack tip with elements over which different singular functions are defined to represent the proper asymptotic forms associated with the problem. He has analytically worked out the stiffness matrices of these special elements. For the case using singular strain triangulars at the tip in conjunction with constant strain triangles

the accuracy of the results is improved by increasing the number of special elements at the tip. The difficulty in the convergence of the scheme arises from the fact that these special elements are not in equilibrium and do not possess compatibility conditions required to match the neighbouring elements in the circumferential direction, i.e. the convergence of the method is questionable. Indeed, while the vertex angle of the elements is reduced to zero to improve the accuracy we are violating the basic requirement for the convergence of the finite element method, i.e. there should be a lower bound on this angle for any element. It is, heuristically, accepted that incompatible elements give convergent results if they pass the patch test. We have implemented Wilson's SST elements and observed that it does not pass the patch test.

Another couple of special elements have been suggested by Aberson et al [20]. They employ two special symmetric and asymmetric elements which contain high order asymptotic behaviour of the solution near the tip. The corresponding stiffness and mass matrices are then calculated analytically and stored, once and for all. They apply these elements for the stationary dynamic problems. No results for the simple static problems are presented to check the errros involved in the method, but good accuracy is expected.

I.2.3 Standard Methods for Simulation of Source Mechanism in Seismology

Due to the complexity of possible source mechanisms of earthquakes, different theories have been put forward to, at least partially, explain some of the observed phenomena in each event. In the 'force system' theory [27] a prescribed pattern of single/double forces and/or couples cause fracture within an elastic medium. Here, the process of extension of actual rupture is simulated by the propagation of applied forces along the fault planes.

Basic tools such as Fourier transformation are normally employed. However, due to a large arbitrariness in adopting any pattern of forces/couples these results are almost inconclusive, Fig. 5.

Haskell [28] applied dynamic dislocation theory, which was developed in [29], for specific dislocation functions in an unbounded medium. Ida [30] and Ida and Aki [31] obtained analytical results for propagating faults of known displacement discontinuities in the simple model of longitudinal shear (Mode III). The main difficulty in applying this theory is the lack of a priori knowledge about dislocation functions, Fig. 6.

A third theory which is speculated to be mainly associated with deep-focus earthquakes is known as the 'relaxation theory' [32]. This theory assumes a fundamental structural change in the properties of the material (such as fluidization) as the cause of earthquakes. Since we are not concerned with this type of earthquake we will not elaborate more on it.

I.3 PATH-INDEPENDENT INTEGRALS FOR STATIONARY PROBLEMS

I.3.1 Static Problems

For an elastic body containing a crack Eshelby [33] and Rice [34] have shown that the following integral

$$J = \oint_c (w dx_2 - T_i u_{i,1} d\ell)$$

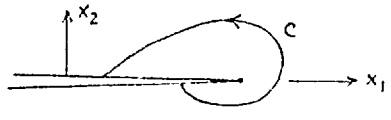

taken around any closed curve surrounding the tip in x_1-x_2 plane has a constant value. In this expression w is the strain energy density, $w = \int_0^{\varepsilon} \sigma_{ij} d\varepsilon_{ij}$, $\varepsilon = [\varepsilon_{ij}]$ is the infinitesimal strain tensor, $T_i = \sigma_{ij} n_j$ is the stress component on c and u_i is the displacement component.

Knowles and Sternberg [35] in introducing new conservative laws point out that J integral is actually the first component of the vector

$$J_k = \oint_c (wn_k - T_i u_{i,k})\, d\ell$$

where n is the unit outward normal to c. J_1 and J_2 vanish over all closed curves in a region in which w depends only on the strain $\varepsilon_{ij} = \frac{1}{2}(u_{i,j}+u_{j,i})$ and in which the stresses σ_{ij} satisfy

$$\sigma_{ij} = \frac{1}{2}\left(\frac{\partial}{\partial \varepsilon_{ij}} + \frac{\partial}{\partial \varepsilon_{ji}}\right) w$$

and

$$\sigma_{ij,i} = 0$$

This would mean that the values of J_1 and J_2 are constant over any path enclosing the crack.

For isotropic plane elasticity Budiansky and Rice [36] have represented these integrals in complex variables using the complex potential functions $\phi(z)$ and $\psi(z)$ (defined earlier):

$$J_1 + iJ_2 = -\frac{2i}{E}\left[\oint_c (\phi'^2)\, dz - 2\overline{\oint_c \phi'\psi'\, dz}\right]$$

Hellen and Blackburn [37] have derived J_k in terms of stress intensity factors as

$$J_1 + iJ_2 = \frac{(1+\nu)(1+\kappa)}{4E}\left[(K_I^2 + K_{II}^2) - 2iK_I K_{II}\right]$$

where K_I, K_{II} are mode I, mode II stress intensity factors, respectively, and

$\kappa = 3-4\nu$ for plane strain.

The great attraction of J_k for crack problems is its path-independency. On the other hand, any approximation of crack problems introduce errors which pollute the whole region but the error is greater in a zone closer to the tip.

So by choosing contours of integration c away from the tip we expect to get better results for J_k values. Consequently the representation of J_k in terms of K_I and K_{II} would immediately enable one to extract K_I and K_{II}.

Obviously J_k can also be interpreted as the energy release rate for virtual crack extensions. We note that the maximum energy release rate is for a crack extending at an angle $\Theta = \tan^{-1}(\frac{2K_I K_{II}}{K_I^2+K_{II}^2})$.

I.3.2 Dynamic Problems

In parallel to the J-integral for the static problem, Nilsson [38] suggests a path independent integral for dynamic problems. In a linear isotropic visco-elastic material he Laplace transforms the dynamic equations of elasticity. The transformed equations then constitute an elliptic system of equations. Then with an argument almost similar to the static case it can be shown that the following integral, in the frequency domain, is path independent

$$\bar{I} = \int_c \{(\bar{w}+\tfrac{1}{2}\rho p^2 \bar{u}_i^2)\, dx_2 - \bar{T}_i \bar{u}_{i,1}\, d\ell\}$$

where a bar denotes Laplace transformations with the parameter p. In this expression $\bar{W} = \tfrac{1}{2}\bar{\sigma}_{ij}\bar{\varepsilon}_{ij}$ and $\bar{T}_i = \bar{\sigma}_{ij} n_j$ represents the transformed traction on the closed curve c. He shows that the value of $\bar{I}$ is independent of the choice of c.

The $\bar{I}$-integral can be written in terms of the stress intensity factors. For mode I crack the relation between $\bar{I}$ and $\bar{K}_I$ is shown to be essentially the same as in the static case, i.e.

$$\bar{I}(p) = \frac{(1+\nu)(1+\kappa)}{4E} \bar{K}_I^{-2}(p)$$

However the interpretation of I in terms of the energy release rate, as in the static case, is no longer valid.

Nilsson applies $\bar{I}$-integral to an infinite strip problem with a semi-infinite crack and by calculating the $\bar{I}$-integral obtains the dynamic stress intensity factor K_I.

While this representation of stress intensity factors in terms of $\bar{I}$-integral is interesting, the evaluation of $\bar{I}$-integral for typical problems is extremely difficult, if not impossible. Hence this formulation for obtaining stress intensity factors could be regarded as a conceptual one.

Recently Gurtin [39] has given a time-domain representation of the $\bar{I}$-integral in the form

$$I = \tfrac{1}{2}\int_c [\sigma_{jk} * u_{j,k} + \rho u_j * u''_j] dx_2 - \int_c \sigma_{jk} n_k * u_{j,1} ds$$

where * denotes convolution.

I.4 MATHEMATICAL BACKGROUND TO THE FINITE ELEMENT METHOD

In this section we will briefly review some standard results on the application of the finite element method to a model problem. The aim is to clarify the necessary steps in any variational treatment of elliptic boundary

problems. This section is based on Raviart's lecture notes [40]. For an engineering approach to the finite elements one can consult [41] while essential mathematical foundations of the method are presented in [42]-[44] as well as the research papers [45]-[50].

I.4.1 Notation and Preliminary Definitions

Let $\Omega \subset R^n$ be an open set with boundary $\Gamma = \partial\Omega$. We define the following spaces:

(1) $L_p(\Omega)$: space of measurable functions f such that for $1 \leq p \leq \infty$

$$||f||_{L_p(\Omega)} = \left(\int_\Omega |f(x)|^p dx\right)^{1/p} < \infty \qquad (p \neq \infty)$$

$$||f||_{L_\infty(\Omega)} = \operatorname{ess\,sup}_{x\in\Omega} |f(x)| < \infty$$

$L_p(\Omega)$ with the norms is a Banach space. For $p = 2$, $L_2(\Omega)$ is a Hilbert space where the scalar product corresponding to the norm is given by

$$(f,g) = \int_\Omega f(x)g(x)dx$$

$c^\infty(R^n)$ denotes the space of infinitely differentiable functions in R^n and $c^\infty(\Omega)$ comprises elements which are restrictions of elements in $c^\infty(R^n)$ to Ω.

(2) $D(\Omega)$: space of c^∞ functions with compact support in Ω; for a given sequence $\phi_j \in D(\Omega)$ we will say that $\phi_j \to 0$ in $D(\Omega)$ if

(i) The ϕ_j have their support in a fixed compact subset E of Ω;

(ii) We have $D^\alpha\phi_j \to 0$ uniformly on Ω, for all α where

$$\alpha = (\alpha_1,\ldots,\alpha_N), \quad \alpha_i \geq 0 \text{ integers}$$

$$|\alpha| = \sum_{i=1}^{N} \alpha_i$$

$$D^{\alpha}\phi = \prod_{i=1}^{N} \left(\frac{\partial}{\partial x_i}\right)^{\alpha_i}\phi$$

(3) $D'(\Omega)$: space of distributions over Ω i.e. spaces of forms $\phi \to (f,\phi)$, which are linear and continuous on $D(\Omega)$ (i.e. $(f,\phi_i) \to 0$ when $\phi_i \to 0$ in $D(\Omega)$). We will say that $f_j \to f$ in $D'(\Omega)$ if $(f_j,\phi) \to (f,\phi)$, for all $\phi \in D(\Omega)$. Now suppose Ω is a Lipschitz domain, defined as follows:

Definition 1

A region $\Omega \in E_N$ (N-dimensional Euclidean space) is called Lipschitz if it is bounded and its boundary Γ has the following properties:

(i) To each point $x \in \Gamma$ an open hypersphere s_x about x exists, such that the intersection $s_x \cap \Gamma$ may be described by means of a Lipschitz function and,

(ii) $s_x \cap \Gamma$ divides s_x into exterior and interior parts w.r.t. Ω.

We may now introduce the Sobolev space $W^{m,p}(\Omega)$ of order m on $L_p(\Omega)$.

Definition 2

For any integer $m \geq 1$, any $1 \leq p \leq \infty$.

$$W^{m,p}(\Omega) = \{v \,|\, v \in L_p(\Omega),\ D^{\alpha}v \in L_p(\Omega),\ |\alpha| \leq m\}$$

with the norm

$$||v||_{m,p,\Omega} = \left(\sum_{|\alpha|\leq m} ||D^{\alpha}v||_{p,\Omega}^{p}\right)^{1/p}, \quad 1 \leq p < \infty$$

where

$$||\cdot||_{p,\Omega} = \left(\int_{\Omega} ||\cdot||^{p} dx\right)^{1/p}$$ It is a Banach space.

Notation

$$|v|_{m,p,\Omega} = \Big(\sum_{|\alpha|=m} ||D^{\alpha} v||^{p}_{p,\Omega} \Big)^{1/p}$$ denotes semi-norm, $1 \leq p < \infty$.

For $p = \infty$

$$||v||_{m,\infty,\Omega} = \max \{ ||D^{\alpha} v||_{\infty,\Omega};\ 0 \leq |\alpha| \leq m \}$$

and

$$|v|_{m,\infty,\Omega} = \max \{ ||D^{\alpha} v||_{\infty,\Omega},\ |\alpha| = m \}$$

As a special case for $p = 2$ we have the Sobolev space, $H^{m}(\Omega) = W^{m,2}(\Omega)$. It is a Hilbert space.

We have

$$D(\Omega) \subset H^{m}(\Omega)$$

So we may define $H_0^m(\Omega)$ as the closure of $D(\Omega)$ in $H^{m}(\Omega)$.

I.4.2 Abstract Variational Problems

We are given:

(i) V (real) Hilbert space with norm $||\cdot||$

(ii) A bilinear form $u, v \to a(u,v)$ continuous on V

There exists M such that $|a(u,v)| \leq M||u|| \cdot ||v||$

(iii) A linear continuous functional f defined on V

Let us denote by V^* the dual of V i.e. the space of linear continuous functions

Given $f \in V^*$, (f,v) value of f on V

$$||f||^* = \sup_{v \in V} \frac{|(f,v)|}{||v||}$$

The *problem* (P) is as follows:

$$(P)\begin{cases} \text{Find } u \in V \text{ such that} \\ a(u,v) = (f,v), \text{ for all } v \in V \end{cases}$$

Fix u and consider $v \to a(u,v) : V \to R$ then there exists $Au \in V^*$ such that

$$a(u,v) = (Au,v), \quad \text{for all } v \in V$$

Claim

$$A \in L(V,V^*)$$

in fact

$$||Au||^* = \sup_{v \in V} \frac{|(Au,v)|}{||v||} = \sup_{v \in V} \frac{|a(u,v)|}{||v||} \leq M||u||$$

or

$$||A|| \leq M$$

The problem (P) then can, equivalently, be written as

$$(P)\begin{cases} \text{Find } u \in V \text{ such that} \\ Au = f \end{cases}$$

Definition 3

The bilinear form a(u,v) is called V-elliptic if there exists a constant $\alpha > 0$ such that

$$a(v,v) \geq \alpha||v||^2, \quad \text{for all } v \in V$$

Theorem 1 (Lax-Milgram)

Assume that the bilinear form $a(u,v)$ is V-elliptic, then the problem (P) has a unique solution. This result is proved by simple application of the Browder Fixed Point Theorem [51].

Adjoint Problem

We introduce the adjoint bilinear form

$$a^*(u,v) = a(v,u)$$

$$a(u,v) \to A$$

Similarly $a^*(u,v) \to A^*$ = adjoint of A. The bilinear form $a(u,v)$ is symmetric if and only if

$$a(u,v) = a^*(u,v)$$

Introduce $J(v) = \frac{1}{2}a(v,v) - (f,v)$ and find $u \in V$ such that

$$J(u) = \underset{v \in V}{\text{Min}}\, J(v)$$

Theorem 2

Assume that $a(u,v)$ is symmetric and V-elliptic, then there exists a unique $u \in V$ such that

$$J(u) = \underset{v \in V}{\text{Min}}\, J(v)$$

Moreover, u is the solution of the problem (P).

Theorem 3 (Poincaré-Friedrichs)

Assume that Ω is a bounded open set in R^n, then there exists a constant $c = c(\Omega)$ such that

$$||v||_{0,\Omega} \leq c|v|_{1,\Omega} \quad \text{, for all } v \in H_0^1(\Omega)$$

where

$$H_0^1(\Omega) = \{v \in H^1(\Omega), v|_\Gamma = 0\}$$

Theorem 4

Assume Ω is bounded. Then the semi-norm $|\cdot|_{m,\Omega}$ is a norm over the space $H_0^m(\Omega)$ which is equivalent to the norm $||\cdot||_{m,\Omega}$

Theorem 5

Assume that Ω is Lipschitz. There exists a constant $c = c(\Omega)$ such that

$$||v||_{L_2(\Gamma)} \leq c||v||_{1,\Omega} \quad \text{, for all } v \in c^\infty(\bar{\Omega})$$

Theorem 6

Assume Ω is Lipschitz. The space $c^\infty(\bar{\Omega})$ is dense in $H^1(\Omega)$.

Now define $\gamma_0 : v \to v|_\Gamma : c^\infty(\bar{\Omega}) \to L_2(\Gamma)$.

Trace Theorem

There exists a constant c such that

$$||v|_\Gamma||_{L_2(\Gamma)} \leq c||v||_{1,\Omega} \quad \text{, for all } v \in H^1(\Omega)$$

Green's Formula

Suppose u and v are smooth. Then

$$\int_\Omega \frac{\partial u}{\partial x_i} v dx = -\int_\Omega u \frac{\partial v}{\partial x_i} dx + \int_\Gamma uv\nu_i d\gamma, \quad \text{for all } v \in C^1(\Omega)$$

where $\nu = \{\nu_1, \ldots, \nu_N\}$ is the outward normal to the boundary Γ.

Example 1 Dirichlet Problem (bounded Ω)

$V = H_0^1(\Omega)$. Given $c \in L_\infty(\Omega)$, $c \geq 0$ almost everywhere in Ω. Define

$$a(u,v) = \int_\Omega \{ \sum_{i=1}^N \frac{\partial u}{\partial x_i} \frac{\partial v}{\partial x_i} + cuv \} dx$$

$$(f,v) = \int_\Omega fv dx; \quad f \in L_2(\Omega)$$

By the Cauchy-Schwarz inequality $a(u,v)$ and (f,v) are continuous. Also we have

$$a(v,v) = \int_\Omega \{ \sum_{i=1}^N |\frac{\partial v}{\partial x_i}|^2 + c|v|^2 \} dx \geq \sum_{i=1}^N \int_\Omega |\frac{\partial v}{\partial x_i}|^2 dx$$

or

$$a(v,v) \geq |v|^2_{1,\Omega} \quad \text{(semi-norm)}$$

Since $|v|_{1,\Omega}$ is a norm equivalent to $||v||_{1,\Omega}$ we have

$$a(v,v) \geq c||v||^2_{1,\Omega}$$

i.e. $a(u,v)$ is V-elliptic.

Applying abstract results we conclude that there exists $u \in H_0^1(\Omega)$ such that

$$a(u,v) = (f,v), \quad \text{for all } v \in H_0^1(\Omega)$$

Interpretation of the Problem

We know that $D(\Omega) \subset H_0^1(\Omega)$, therefore

$$\int_\Omega \{ \sum_{i=1}^N \frac{\partial u}{\partial x_i} \frac{\partial \phi}{\partial x_i} + cu\phi \} dx = \int_\Omega f\phi dx, \quad \text{for all } \phi \in D(\Omega)$$

Also by definition of distributional derivatives

$$\langle \frac{\partial u}{\partial x_i}, \phi \rangle = -\langle u, \frac{\partial \phi}{\partial x_i} \rangle$$

Hence

$$\langle -\Delta u + cu, \phi \rangle = \langle f, \phi \rangle; \quad \text{for all } \phi \in D(\Omega)$$

So (Δ is the Laplace operator)

$$-\Delta u + cu = f \text{ in } \Omega \quad \text{(in distribution sense)}$$

$$u \in H_0^1(\Omega)$$

i.e. homogeneous Dirichlet problem for the operator $(-\Delta+c)$. Note that u minimizes $J(v) = \frac{1}{2}a(v,v) - (f,v)$ over $H_0^1(\Omega)$.

Essential and Natural Boundary Conditions

Given the following elliptic boundary problem

$$\begin{cases} Lu = f \text{ in } \Omega \\ B_j u = g_j \text{ on } \Gamma; \quad j = 1, \ldots, \ell \end{cases}$$

where L and B_j are differential operators of order 2ℓ and m_j, respectively. The boundary condition $B_j u = g_j$ will be called *essential* if $m_j < \ell$. Otherwise for $m_j \geq \ell$ the boundary conditions are *natural*. Natural boundary conditions are not imposed on u in the variational problem as they are

automatically satisfied by the minimizing u. However, the admissible solution u must, necessarily, satisfy the essential boundary conditions. This is illustrated by the following example.

Example 2

$$\begin{cases} -\Delta u + cu = f \text{ in } \Omega \\ u = 0 \text{ on } \Gamma_0 \qquad \text{(essential boundary condition)} \\ \dfrac{\partial u}{\partial \nu} = 0 \text{ on } \Gamma_1 \qquad \text{(natural boundary condition)} \end{cases}$$

Take

$$V = \{v \in H^1(\Omega) \,|\, v|_{\Gamma_0} = 0\}$$

We show that V is a closed subspace of $H^1(\Omega)$. By trace theorem the mapping $v \to v|_\Gamma \to v|_{\Gamma_0}$ is continuous. So if $v_i \to v_0$ in $H^1(\Omega)$ and $v_i|_{\Gamma_0} = 0$ then by continuity of the above mapping $v_0|_{\Gamma_0} \to 0$ and therefore V is a closed subspace of $H^1(\Omega)$. The problem can, equivalently, be written as

$$\begin{cases} \text{Find } u \in v \text{ such that} \\ a(u,v) = (f,v), \quad \text{for all } v \in V \end{cases}$$

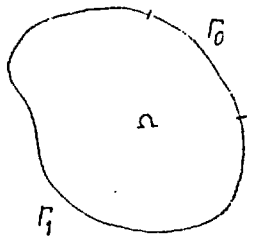

where

$$a(u,v) = \int_\Omega \{\sum_i \frac{\partial u}{\partial x_i} \frac{\partial v}{\partial x_i} + cuv\} dx$$

and

$$(f,v) = \int_\Omega fv dx$$

By the general theory, a unique solution $u \in H^1(\Omega)$ exists. To interpret u, suppose $u \in H^2(\Omega)$, then in particular

$$a(u,\phi) = (f,\phi), \quad \text{for all } \phi \in D(\Omega)$$

implying

$$(-\Delta u+cu,\phi) = (f,\phi), \quad \text{for all } \phi \in V$$

But by Green's formula, for any $\phi \in V$

$$(-\Delta u+cu,\phi) = (f,\phi) - \int_{\Gamma_1} \frac{\partial u}{\partial \nu} \phi d\gamma, \quad \text{for all } \phi \in V$$

giving

$$\int_{\Gamma_1} \frac{\partial u}{\partial \nu} \phi d\gamma = 0, \quad \text{for all } \phi \in V$$

or

$$\frac{\partial u}{\partial \nu} = 0 \text{ on } \Gamma_1$$

i.e. the natural boundary condition is satisfied.

I.4.3 The Approximating Problem

In the approximation of the problem (P) basically we replace V by a finite-dimensional subspace $V_h \subset V$. So the approximating problem (P_h) can be expressed as

$$(P_h) \begin{cases} \text{Find } u_h \in V_h \text{ such that} \\ a(u_h,v_h) = (f,v_h), \quad \text{for all } u_h \in V_h \end{cases}$$

Then from Lax-Milgram theorem we know that there exists a unique solution $u_h \in V_h$ of (P_h). The approximation error is given by the following:

Theorem 7

For the problem (P_h) there exists a constant c independent of v_h such that

$$||u-u_h|| \leq c \inf_{v_h \in V_h} ||u-v_h||$$

Graphically:

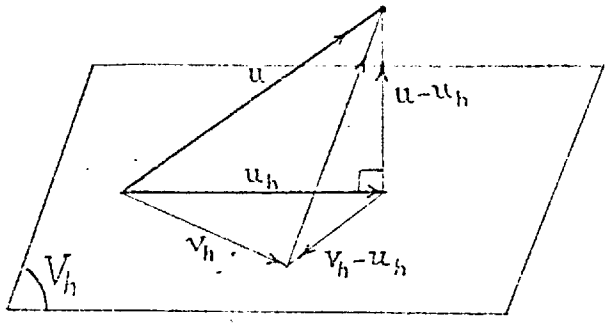

Proof

We have

$$a(u-u_h,\omega_h) = (f,\omega_h) - (f,\omega_h) = 0, \quad \text{for all } \omega_h \in V_h$$

Also

$$a(u-u_h,u-u_h) = a(u-u_h,u-v_h) + a(u-u_h,\overset{0}{v_h-u_h}), \quad \text{for all } v_h \in V_h$$

Since

$$a(u-u_h,u-u_h) \geq \alpha||u-u_h||^2 \quad \text{(i.e. } a(u,v) \text{ is V-elliptic)}$$

and

$$a(u-u_h,u-v_h) \leq M||u-u_h||.||u-v_h|| \quad \text{(i.e. } a(u.v) \text{ is continuous)}$$

We conclude

$$\alpha||u-u_h||^2 \leq M||u-u_h||.||u-v_h||$$

or

$$||u-u_h|| \leq \frac{M}{\alpha}||u-v_h|| \leq \inf_{v_h \in V_h} \frac{M}{\alpha}||u-v_h|| \qquad \#$$

Remark 1

Suppose $a(u,v)$ is symmetric. Then $J(u) = \min_{v\in V} J(v)$ and $J(u_h) = \min_{v_h \in V_h} J(v_h)$

Given that V_h is spanned by basis functions $\{\omega_j \mid j=1,\ldots,M\}$ i.e.

$u_h = \sum_{j=1}^{M} a_j\omega_j; \quad a_j \in R.$

The problem (P_h) is written as

$$a(u_h,\omega_i) = (f,\omega_i), \qquad 1 \leq i \leq M$$

or

$$\sum_{j=1}^{M} a(\omega_j,\omega_i)a_j = (f,\omega_i), \qquad 1 \leq i \leq M$$

where $a(\omega_j,\omega_i)$ represents the (j,i) element of the *stiffness matrix.*

Remark 2

a(u,v) symmetric implies symmetric stiffness matrix and V-ellipticity implies positive-definiteness of stiffness matrix.

I.4.4 Interpolation Results

In the finite element method a knowledge of the errors involved in interpolating a function is of fundamental importance. [52] unifies previous results in this respect and develops new results. We review some of these results that we need later on.

I.4.4.1 Lagrange interpolation

Given an integer $m \geq 1$, let P_k denote the space of polynomials of degree $\leq m$ defined over R^n and we let

$$N = N(m) = \dim P_m$$

We shall say that N distinct points a_i of R^n form an m-*unisolvent set* provided that given any real numbers α_i, $1 \leq i \leq N$, there exists one and only one polynomial $p \in P_m$ such that

$$p(a_i) = \alpha_i, \qquad 1 \leq i \leq N$$

Given a function u defined on an m-unisolvent set Σ, we say that $\tilde{u}$ is its *interpolating polynomial* if it is the unique polynomial of degree $\leq m$ with the property that

$$\tilde{u}(a_i) = u(a_i), \quad 1 \leq i \leq N$$

Let $\Sigma = \{a_i\}_{i=1}^N$ and $\hat{\Sigma} = \{\hat{a}_i\}_{i=1}^N$ be two sets of N points of R^n. Then we say that the two sets are *equivalent* if and only if there exists an invertible element $B \in L(R^n)$ and a vector $b \in R^n$ such that

$$a_i = B\hat{a}_i + b, \quad 1 \leq i \leq N$$

We say that a subset $K \subset R^n$ is a Σ-*admissible* if and only if whenever it contains a point x, it also contains the closed-segments joining the points x and a_i, for all $1 \leq i \leq N$ (i.e. K is a star-shaped with reference to any point of Σ).

Given a function $u : K \to R$, we say that u *belongs to the class* $\tau^{k+1}(K)$ if and only if the Taylor formula

$$u(a_i) = u(x) + Du(x)(a_i-x) + \ldots + \frac{1}{k!} D^k u(x) \cdot (a_i-x)^k + \frac{1}{(k+1)!} D^{k+1} u(\eta_i(x))(a_i-x)^{k+1}$$

holds for all points $x \in K$ and all $1 \leq i \leq N$, where $\eta_i(x) = \theta_i x + (1-\theta_i)a_i$ for some $0 < \theta_i < 1$. In particular, this will be the case if K is the closed convex hull of Σ, $u \in C^k(K)$ and $D^{k+1}u(x)$ exists for all points x in K.

Given a set $\Sigma = \{a_i\}_{i=1}^N$ we denote by $K = K(\Sigma)$ the closed convex hull of Σ, and we associate with K, the two following geometrical parameters:

$$\begin{cases} h = h(\Sigma) = \text{diameter of } K \\ \rho = \rho(\Sigma) = \sup \{\text{diameter of the spheres contained in } K\} \end{cases}$$

(in many applications, K is an n-simplex, so that ρ is the diameter of the inscribed sphere). Likewise we define $\hat{\rho}$, $\hat{h}$ for $\hat{K}$ and $\hat{\Sigma}$. If Σ is any k-unisolvent set ($k \geq 1$), the interior $\overset{\circ}{K}$ of K is non-empty, so that $\rho > 0$.

Theorem 8

Let $\Sigma = \{a_i\}_{i=1}^{N}$ be a k-unisolvent set of points of R^n, with h and ρ defined as before. Let $u \in \tau^{k+1}(K)$ be given with

$$M_{k+1} = \sup \{||D^{k+1}u(x)||;\ x \in K\} < +\infty$$

If $\tilde{u}$ is the unique interpolating polynomial of degree $\leq k$ of u we have for any integer m with $0 \leq m \leq k$,

$$(1) \qquad \sup \{||D^m u(x) - D^m \tilde{u}(x)||;\ x \in K\} \leq c M_{k+1} \frac{h^{k+1}}{\rho^m}$$

for some constant

$$c = c(n,k,m,\hat{\Sigma})$$

which are the same for all equivalent k-unisolvent sets and which can be computed once and for all in a k-unisolvent set $\hat{\Sigma}$ equivalent to Σ. #

Remark 3

It is clear that the estimates of (1) for $m \geq 1$ are better when

the ratio h/ρ is small. The intuitive significance of this is that one should not consider k-unisolvent sets Σ whose closed convex hull is "too flat", i.e. which is "almost" contained in an (n-1)-dimensional manifold of R^n. For example, if K is a 2-simplex (i.e. a triangle) in R^2, one has the estimate

$$\frac{1}{2 \tan \frac{\theta}{2}} \leq \frac{h}{\rho} \leq \frac{2}{\sin \theta}$$

where θ is the smallest angle of K. This shows the smaller θ is the poorer the estimate.

I.4.4.2 Interpolation in Sobolev spaces

We denote by $(W^{m,p}(\Omega))'$ the strong dual space of $W^{m,p}(\Omega)$, by (f,u) the pairing between an element of $f \in (W^{m,p}(\Omega))'$ and an element $u \in W^{m,p}(\Omega)$, and by

$$||f||^*_{m,p,\Omega} = \sup \frac{|(f,v)|}{||v||_{m,p,\Omega}} ; \quad v \in W^{m,p}(\Omega), v/0\}$$

the dual norm. We have the following lemma.

Lemma 1

Let Ω be a bounded open subset of R^n with a continuous boundary (in the sense of Nečas), let p be given with $1 \leq p \leq \infty$, let $k \geq 0$ be a fixed integer and $f \in (W^{k+1,p}(\Omega))'$ be such that

$$(f,u) = 0, \quad \text{for all } u \in P_k$$

Then there exists a constant

$$c = c(n,k,P,\Omega)$$

such that

$$|(f,u)| \leq c||f||^{*}_{k+1,p,\Omega} \, |u|_{k+1,p,\Omega} \quad \text{, for all } u \in W^{k+1,p}(\Omega)$$

#

Lemma 2

Let Ω be a bounded open subset of R^n with a continuous boundary, let p be given with $1 \leq p \leq \infty$, let $k \geq 0$ be a fixed integer and let m be an integer with $0 \leq m \leq k+1$. Let $\pi \in L(W^{k+1,p}(\Omega); W^{m,p}(\Omega))$ be such that

$$\pi u = u, \quad \text{for all } u \in P_k$$

Then there exists a constant

$$c = c(n,k,p,\Omega)$$

(the same as in Lemma 1) such that

$$||u-\pi u||_{m,p,\Omega} \leq c||I-\pi||_{L(W^{k+1,p}(\Omega);W^{m,p}(\Omega))} |u|_{k+1,p,\Omega}$$

$$\text{for all } u \in W^{k+1,p}(\Omega) \quad \#$$

We need to define the notion of equivalent domains. Let Ω (resp. $\hat{\Omega}$) be a bounded open subset of R^n. Then we say that Ω and $\hat{\Omega}$ are *equivalent* if and only if there exists an invertible element $B \in L(R^n)$ and a vector $b \in R^n$ such that

$$\Omega = \{x \in R^n;\ x=B\hat{x}+b \text{ for each } \hat{x} \in \hat{\Omega}\}$$

With each function u defined over Ω, we associate a function $\hat{u}$ defined over $\hat{\Omega}$ by letting

$$\hat{u}(\hat{x}) = u(B\hat{x}+b) \qquad \text{for each } \hat{x} \in \hat{\Omega}$$

It can be shown that the correspondence $u \to \hat{u}$ is an isomorphism between $W^{m,p}(\Omega)$ and $W^{m,p}(\hat{\Omega})$ for each m and p.

Likewise, if π is an element of $L(W^{k+1,p}(\Omega); W^{m,p}(\Omega))$, we associate with π an element $\hat{\pi} \in L(W^{k+1,p}(\hat{\Omega}); W^{m,p}(\Omega))$ by letting

$$\hat{\pi}\hat{u} = \widehat{\pi u} \qquad \text{for each } u \in W^{k+1,p}(\Omega)$$

It can easily be seen that P_k is left invariant by π if and only if it is left invariant by $\hat{\pi}$.

Theorem 9

Let Ω be a bounded open subset of R^n with a Lipschitz continuous boundary, let p be given with $1 \leq p \leq \infty$, let $k \geq 0$ be a fixed integer, and let m be an integer with $0 \leq m \leq k+1$. Let $\pi \in L(W^{k+i,p}(\Omega); W^{m,p}(\Omega))$ be such that

$$\pi u = u, \quad \text{for all } u \in P_k$$

Then for any $u \in W^{k+1,p}(\Omega)$ (and for h small enough if $p < \infty$, i.e. $h \leq \rho$),

$$||u-\pi u||_{m,p,\Omega} \leq C|u|_{k+1,p,\Omega} \frac{h^{k+1}}{\rho^m}$$

for some constant

$$C = C(n,k,p,\hat{\Omega},\hat{\pi})$$

which are the same for all equivalent domains Ω and which can be computed once and for all in a domain $\hat{\Omega}$ equivalent to Ω. #

Now we shall apply this theorem to finite elements of Lagrange type.

Remark 4 (Sobolev embedding theorem)

Let Ω be a bounded open subset of R^n with Lipschitz continuous boundary. Then

$$W^{q,p}(\Omega) \subset \begin{cases} L^q(\Omega) & \text{if } \frac{1}{q} = \frac{1}{p} - \frac{1}{n} > 0 \\ L^q(\Omega) & \text{for all } q, \ \frac{1}{p} - \frac{1}{n} = 0 \\ C^0(\bar{\Omega}) & \frac{1}{p} - \frac{1}{n} < 0 \end{cases}$$

Then one can conclude

$$W^{k+1,p}(\Omega) \subset \begin{cases} W^{m,q}(\Omega) & \text{if } \frac{1}{q} = \frac{1}{p} - \frac{k+1-m}{n} > 0 \\ W^{m,q}(\Omega) & \text{for all } q, \ \frac{1}{p} - \frac{k+1-m}{n} = 0 \\ C^m(\bar{\Omega}) & \frac{1}{p} - \frac{(k+1-m)}{n} < 0 \end{cases}$$ #

Theorem 10

Let the triple $(\hat{K},\hat{\Sigma},\hat{P})$ be a finite element of Lagrange type. Assume that

$$W^{k+1,p}(\hat{K}) \subset C^0(\hat{K})$$

$$W^{k+1,p}(\hat{K}) \subset W^{m,q}(\hat{K}) \qquad \text{(continuous injection)}$$

and

$$P_k \subset \hat{P} \subset W^{m,q}(\hat{K})$$

Then for any $u \in W^{k+1,p}(K)$

$$||u-\pi u||_{m,q,K} \leq \hat{c}\ \text{meas}\ (K)^{\frac{1}{q}-\frac{1}{p}}\ |u|_{k+1,p,K}\ \frac{h_k^{k+1}}{\rho_k^m}$$

for some constants

$$\hat{c} = \hat{c}\ (\hat{K},\hat{\Sigma},\hat{P})$$

which are the same for all affine equivalent finite elements (K,Σ, P) and which can be computed once and for all in domain $\hat{K}$ equivalent to K.

I.4.5 Error Estimates in the Finite Element Method

Recall the problem (P)

$$(P) \qquad \begin{cases} \text{find } u \in V \text{ such that} \\ a(u,v) = (f,v), \quad \text{for all } u \in V \end{cases}$$

and the approximating problem (P_h)

$$(P_h) \qquad \begin{cases} \text{find } u_h \in V_h \text{ such that} \\ a(u_h,v_h) = (f,v_h), \quad \text{for all } u_h \in V_h \end{cases}$$

where V_h is a finite-dimensional subspace $V_h \subset V$.

Assume Ω is a polyhedral domain in R^n, τ_h a collection of subsets K. Assume:

(i) $\bar{\Omega} = \bigcup_{K\in\tau_h} K$

(ii) K is a closed polyhedron whose diameter $\leq h$

(iii) any (n-1)-dim face of K is either a portion of the boundary Γ or an (n-1)-dim face of an adjacent element.

Associate $K \rightarrow (K,\Sigma_K,P_K)$

$$P_K \subset C^0(K) \cap H^1(K)$$

We have the following:

Theorem 11

Given

$$V_h \subset C^0(\Omega)$$

$$P_k \subset H^1(K), \quad \text{for all } K \subset \tau_h$$

then

$$V_h \subset H^1(\Omega). \qquad \#$$

Definition 4

A finite element (K,Σ,P) is a C^0-*element* if the following property holds:

For any (n-1)-dim face K' of K, the set $\Sigma|_{K'} = \Sigma \cap K$ is $P|_{K'}$-unisolvent where

$$P|_{K'} = \{p|_{K'},\ p \in P\} \qquad \#$$

Definition 5

The triangulation $\{(K,\Sigma_K,P_K) \mid K \in \tau_h\}$ is a C^0-*triangulation* if the following conditions hold:

(i) each element (K,Σ_K,P_K) is a C^0-element

(ii) for any pair of adjacent elements K_1, $K_2 \in \tau_h$ we have

$$\Sigma_{K_1} \cap K_2 = \Sigma_{K_2} \cap K_1$$

$$P|_{K_1}|_{K'} = P|_{K_2}|_{K'} \quad \text{where} \quad K' = K_1 \cap K_2 \qquad \#$$

Define $X_h = \{v \in C^0(\bar{\Omega})$; for all $K \in \tau_h$, $v|_K \subset P_k\}$ it follows that $X_h \subset H^1(\Omega)$.

Take

$$\Sigma_h = \bigcup_{K \in \tau_h} \Sigma_K = \{\text{d.o.f. of function } v \in X_h\}$$

$$\pi_h v = X_h \text{ interpolate of } v \text{ on } \Sigma_h$$

By definition $\pi_h v \in X_h$. For $v \in C^0(\Omega)$: $\pi_h v(a) = v(a)$, for all $a \in \Sigma_h$. Also we have the obvious result: $\pi_h v|_K = \pi_K v$.

Definition 6

Let τ_h be a family of triangulations of Ω. We shall say that τ_h is an affine *regular family* of triangulations if:

(i) all (K, Σ_K, P_K) are affine equivalent to a reference finite element $(\hat{K}, \hat{\Sigma}, \hat{P})$,

(ii) there exists a constant $\sigma > 0$ independent of h such that $h_K \leq \sigma \rho_K$, for all $K \in \tau_h$.

Theorem 12

Let τ_h be an affine regular family of C^0-triangulations of $\bar{\Omega}$ associated with the reference finite element $(\hat{K}, \hat{\Sigma}, \hat{P})$ which satisfies:

$$P_k \subset \hat{P} \subset C^0(\hat{K}) \cap H^1(\hat{K})$$

for some integer $k \geq 1$ with $k+1 - \frac{n}{2} > 0$. Then if $u \in H^{k+1}(\Omega)$, there

exists a constant c > 0 independent of h and u such that:

$$||u-u_h||_{1,\Omega} \leq ch^k|u|_{k+1,\Omega} \qquad \#$$

Corollary 1

From Theorems (3) and (12) we conclude:

$$||u-u_h||_{0,\Omega} \leq ch^k|u|_{k+1,\Omega} \qquad \#$$

However using the duality argument of Nitsche we can get better estimates i.e. $0(h^{k+1})$. To do so we introduce the following:

Take V and H two Hilbert spaces with inner product and norms as:

$$H \longleftrightarrow (\cdot,\cdot),\ |\cdot|$$

$$V \longleftrightarrow ||\ \ ||$$

$A \in L(V,V')$ such that $a(u,v) = (Au,v)$ and A^{-1} exists also the adjoint bilinear form $a^*(u,v) = a(v,u) = (A^*u,v)$ and $(A^*)^{-1}$ exists.

Theorem 13

Let the spaces V and H satisfy the above properties. Then

$$|u-u_h| \leq M||u-u_h|| \sup_{g\in H} \{\frac{1}{|g|} \inf_{\phi_h \in V_h} ||(A^*)^{-1}g-\phi_h||\} \qquad \#$$

Definition 7

The adjoint problem is *regular* if A^* is an isomorphism $A^* : H^2(\Omega) \cap V \to L^2(\Omega)$.

If $f \in L_2(\Omega)$ then one can show that for sufficiently smooth boundary Γ, the solution to the adjoint problem $\phi = (A^*)^{-1} g \in H^2(\Omega)$. In fact using Kontradev's results (to be explained in the next chapter) one can conclude that for polyhedral *convex* domains $||\phi||_{2,\Omega} \leq c||f||_{0,\Omega}$.

Using Theorem 13 we have:

Theorem 14

Assume $n \leq 3$. Let $\{\tau_h\}$ be an affine regular family of C^0—triangulations of $\bar{\Omega}$ associated with a reference finite element $(\hat{K}, \hat{\Sigma}, \hat{p})$ such that

$$P_k \subset \hat{p} \subset C^0(\hat{K}) \cap H^1(\hat{K}) \quad \text{for some integer } k \geq 1$$

Assume that the adjoint problem is regular and that $u \in H^{k+1}(\Omega)$. Then there exists a constant $c > 0$ independent of h and u such that:

$$||u-u_h||_{0,\Omega} \leq ch^{k+1}|u|_{k+1,\Omega} \qquad \#$$

Remark 5

Nitsche also gives the following estimates ($p = \infty$):

$$||u-u_h||_{W^{1,\infty}(\Omega)} \leq ch^k||u||_{W^{k+1,\infty}(\Omega)}$$

$$||u-u_h||_{L^\infty(\Omega)} \leq ch^{k+1}||u||_{W^{k+1,\infty}(\Omega)} \qquad \#$$

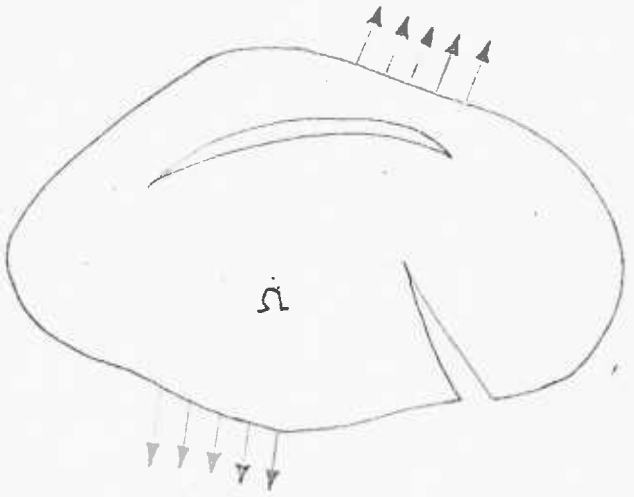

Fig (1)

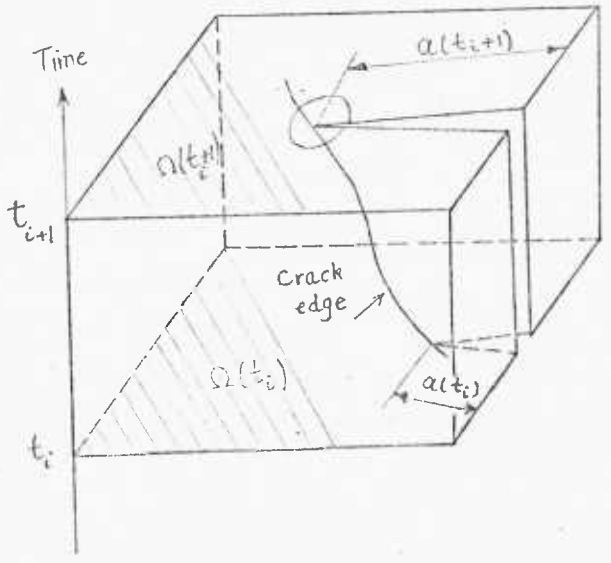

Fig (2)

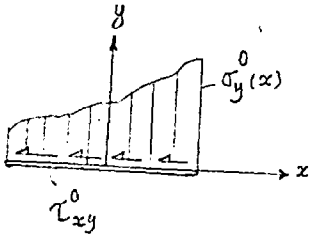

Fig 3 (a)

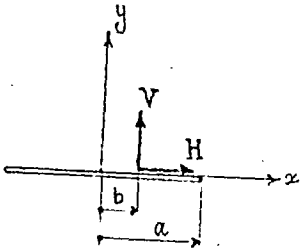

Fig 3 (b)

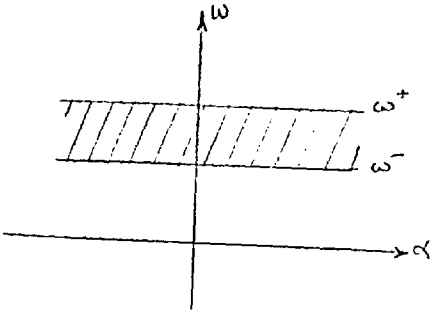

Fig (4)

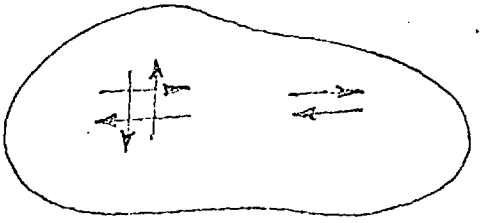

Elements of 'force-system' theory

Fig (5)

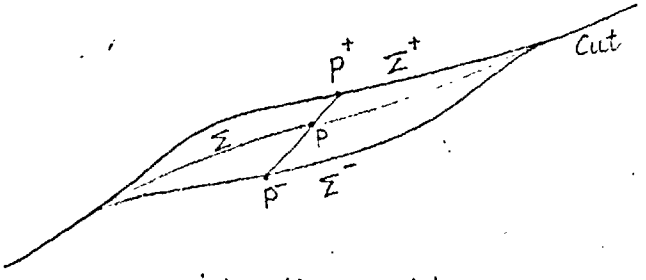

Dislocation Model

Fig (6)

Chapter II

ANALYSIS OF THE STATIC CRACK PROBLEM

In this chapter we are concerned with the questions of existence and uniqueness of solutions to crack problems. We also study the regularity of solutions to the problem and obtain estimates for the errors involved in our approximating scheme.

With an extension of the definition of Sobolev spaces, it is shown that the bilinear form in the problem is elliptic on slit domains. With this property, one then uses the usual arguments to establish the existence and uniqueness of solutions.

Some general regularity results for solutions to equations of elasticity are obtained. Results concerning smoothness of solutions on convex domains and domains containing cracks are treated as special cases. In particular, it is shown that the solution near a vertex of the domain can asymptotically be expanded into 'smooth' and 'singular' parts. Estimates, in terms of data, for the "smooth" part are also derived.

Furthermore, by using the 'singular' functions in our approximating subspaces we obtain estimates for the rate of convergence of the solution which are known to be the best in both L_2 and H^1 norms.

I.1 VARIATIONAL FORMULATION OF ELASTIC BOUNDARY VALUE PROBLEMS

Consider the equations of elasticity in a Lipschitz domain Ω with boundary Γ.

$$\sigma_{ik,k}(u) + K_i = 0 \quad \text{in } \Omega \tag{1}$$

where the generalized Hooke's law

$$\sigma_{ik}(u) = C_{ik\ell m}\varepsilon_{\ell m}(u) \tag{2}$$

and the strain-displacement relations

$$\varepsilon_{ik}(u) = \tfrac{1}{2}(u_{i,k}+u_{k,i}) \tag{3}$$

hold. Here u_i, ε_{ik} and σ_{ik} denote the components of the displacement vector u, the strain tensor ε and the stress tensor σ, respectively. We use the usual summation convention and write $u_{i,k} = \dfrac{\partial u_i}{\partial x_k}$. The elastic coefficients $C_{ik\ell m}$ are assumed to be measurable and bounded on Ω and satisfy the *symmetry relations:*

$$C_{ik\ell m} = C_{ki\ell m} = C_{\ell mik} \tag{4}$$

We also assume the *ellipticity property*:

$$C_{ik\ell m}(x)\varepsilon_{ik}\varepsilon_{\ell m} \geq \mu_0 \sum_{i,k=1}^{3} \varepsilon_{ik}^2 , \quad \text{for some } \mu_0 > 0 \tag{5}$$

Consider initially the boundary conditions:

$$u_i\big|_{\Gamma_U} = 0 \tag{6}$$

and

$$\sigma_{ik}\, n_k\big|_{\Gamma_F} = f_i \tag{7}$$

(n_k is the component of the unit outward normal n to Γ) where Γ_U is an open subset of Γ, and Γ_F is its complement. Let the body forces $K_i \in L_2(\Omega)$ and surface tractions $f_i \in L_2(\Gamma)$ be prescribed. We comment on more complicated boundary conditions below.

To adapt this problem to the general abstract framework of Chapter I, introduce

$$V = (H^1(\Omega))^3 \tag{8}$$

and

$$V_0 = \{v \,|\, v \in V,\ v_i\big|_{\Gamma_U} = 0\} \tag{9}$$

In view of the trace theorem, V_0 is a closed space.

The bilinear form is taken as:

$$a(u,v) = \int_\Omega \sum_{i,j=1}^{3} \sigma_{ij}(u)\,\epsilon_{ij}(v)\,dx \tag{10}$$

and the linear functional $g \in V_0$ is defined by:

$$g(v) = \int_\Omega K_i v_i\,dx + \int_{\Gamma_F} f_i v_i\,d\gamma \tag{11}$$

We address the abstract problem:

$$\begin{cases} \text{find } u \in V_0 \text{ such that} \\ a(u,v) = g(v), \text{ for all } v \in V_0 \end{cases} \tag{12}$$

A solution to the abstract problem may be interpreted as a solution to our problem; indeed taking $v \in (\mathcal{D}(\Omega))^3$ we see a solution u to the abstract problem satisfies:

$$\sigma_{ik,k}(u) + K_i = 0 \qquad (13)$$

(in a distribution sense), and (assuming that $u \in (H^2(\Omega))^3$ which it is probably not) an application of Green's theorem shows:

$$\sigma_{ik} n_k = f_i \quad \text{on} \quad \Gamma_F \qquad (14)$$

of course u satisfies the remaining boundary condition by definition of V_0.

II.2 EXISTENCE AND UNIQUENESS RESULTS

Existence and uniqueness of solutions will follow from the previous chapter, if we can establish V-ellipticity of the bilinear form $a(\cdot,\cdot)$.

Definition 1

The system of operators $\varepsilon_{ij}(v)$ is called V-*coercive* if there exists a constant $C > 0$ such that:

$$\int_\Omega \varepsilon_{ij}(v)\varepsilon_{ij}(v)dx + \int_\Omega v_i v_i dx \geq C||v||_V^2, \quad \text{for all } v \in V \qquad (15) \ \#$$

The following result is proved in [53]. For more smooth domains see [60].

Theorem 1

For Ω a Lipschitz domain, $\varepsilon_{ij}(v)$ is V-coercive. #

This theorem asserts, loosely speaking, that the norm on the linear combinations of derivatives implicit in ε_{ij} is equivalent to the norm on the derivatives themselves.

Remark

For a more general domain having the cone property, Gobert [54] using the theory of singular integrals has proved that $\varepsilon_{ij}(v)$ is again V-coercive.

Now, using the property that the boundary condition $u_i\big|_{\Gamma_U} = 0$ excludes rigid-body motion, we may deduce the following:

Theorem 2

For V defined as above, $a(\cdot,\cdot)$ is V-elliptic. #

Whence the problem has a unique solution.

Proof of this result [53] uses the compactness of the injection $V \to (L_2(\Omega))^3$ to get the *Korn's inequality*:

$$\int_\Omega \varepsilon_{ik}(v)\,\varepsilon_{ik}(v)\,dx \geq c_0 ||v||_V^2, \text{ all } v \in V, \text{ for some } c_0 > 0 \quad (16)$$

Korn's inequality together with the ellipticity property gives the desired result.

II.3 MORE GENERAL BOUNDARY CONDITIONS

The existence and uniqueness results of the last section also apply under more general conditions along the boundary.

Let us assume the following decomposition of the boundary Γ:

$$\Gamma = \Gamma_U \cup \Gamma_F \cup \Gamma_K \cup \Gamma_V \cup N \tag{17}$$

meas $N = \emptyset$ (N = a set of surface measure zero)

where Γ_U, Γ_F, Γ_K and Γ_V are mutually disjoint sets, which are either empty or open in Γ. These sets are defined for:

$$u\big|_{\Gamma_U} = u_0 \tag{18}$$

$$\sigma_{ik} n_k \big|_{\Gamma_F} = f_i \tag{19}$$

$$u_n\big|_{\Gamma_K} = 0, \quad T_t\big|_{\Gamma_K} = 0 \tag{20}$$

$$u_t\big|_{\Gamma_V} = u_{0t}, \quad T_n\big|_{\Gamma_V} = 0 \tag{21}$$

where u_n and $u_t = \{u_{tj}\}$ are normal and tangential components of displacement, respectively.

$$u_n = u_k n_k, \quad u_{tj} = u_j - u_i n_i n_j, \quad i, j, k = 1, 2, 3 \tag{22}$$

and

$$T_n = \sigma_{ik} n_i n_k, \quad T_{tj} = \sigma_{jk} n_k - \sigma_{ik} n_i n_k n_j, \quad i, j, k = 1, 2, 3 \tag{23}$$

T_n and $T_t = \{T_{tj}\}$ denote normal and tangential stresses, respectively.

Now we introduce:

$$W = \{v \in V \;\big|\; u_n\big|_{A_n} = 0 \text{ and } u_t\big|_{A_t} = 0\} \tag{24}$$

where

$$A_n = \{x \in \Gamma, \; u_n = u_{on}\}$$

and

$$A_t = \{x \in \Gamma, \; u_t = u_{0t}\}$$

Also define

$$\mathcal{B}_n = \{x \in \Gamma,\ T_n = f_n\} \tag{25}$$

$$\mathcal{B}_t = \{x \in \Gamma,\ T_t = f_t\} \tag{26}$$

We consider the problem (1)-(5) with the more general boundary conditions (17)-(21). By a *weak solution* we mean a function $u \in W$ such that:

$$a(u,v) = b(v), \quad \text{all } v \in W \tag{27}$$

where

$$b(v) = \int_\Omega K_i v_i \, dx + \int_{\mathcal{B}_n} f_n v_n \, ds + \int_{\mathcal{B}_t} f_t v_t \, ds$$

and

$$K_i \in L_2(\Omega),\ f_n n_s,\ f_{tj},\ f_{tj} n_s n_i \in L_2(\Gamma);\quad i, j, s = 1, 2, 3$$

If the boundary conditions exclude rigid body motion, it may be shown that $a(\cdot,\cdot)$ is again V-elliptic.

If rigid body motion is possible, we may still demonstrate existence and uniqueness of solutions in the class of functions, modulo rigid body motions, provided the body forces are invariant under rigid motions.

These results are summarized in the following theorem [53]:

Theorem 3

Let any of the following conditions be satisfied:

(i) $$\Gamma_U \neq \emptyset \tag{28}$$

(ii) $$v = \alpha + \beta \times r \text{ implies } v = \underline{0}, \text{ all } v \in W \tag{29}$$

(iii) $\quad (v = \alpha + \beta \times r,\ v_n|_{A_n} = 0)$ implies $v = \underline{0}$ (30)

(α, β are constant vectors and r denotes radius vector).

Then the Korn's inequality

$$\int_\Omega \varepsilon_{ik}^2(v)\,dx \geq c||v||_V^2, \text{ all } v \in W, \text{ for some } c > 0 \qquad (31)$$

holds, one and only one solution $u \in W$ to the mixed boundary value problem exists, and the inequality

$$||u||_W \leq c(||K||_{(L_2(\Omega))^3} + ||f_n||_{L_2(B_n)} + ||f_t||_{(L_2(B_t))^3}) \qquad (32)$$

holds for the solution. #

II.4 APPLICATION TO SINGLE-MODE CRACK PROBLEMS

Due to non-standard nature of boundary value problems on non-smooth domains (including domains with cracks), existence of a unique solution to these problems does not follow from well-known theories on elliptic boundary value problems.

However, the results of the previous section for Lipschitz domains can be adopted for symmetric crack problems. Since in II.3 we dealt with a rather general decomposition of the boundary we show that single-mode crack problems (i.e. the three basic modes of fracture) can be considered as mixed boundary value problems on Lipschitz domains but with more complicated boundary conditions. The problem of mixed-mode cracks will be analysed in Section II.5.

A. Crack in Pure Tension (Mode I)

An example for this problem is given in figure (1)[1]. (See end of this chapter) Using conditions of symmetry this problem can be reduced to that of figure (2) with the indicated homogeneous boundary conditions on the crack line. Obviously Γ_U is empty in this case. However, from other boundary conditions it can be verified that the condition (29) holds. For this problem

$$\Gamma_V = \phi, \ \Gamma_k = \bigcup_{i=1}^{2} \Gamma_{k_i} \text{ and } \Gamma_F = \bigcup_{i=1}^{3} \Gamma_{F_i} \quad \text{(nonhomogeneous conditions only on } \Gamma_{F_3}\text{)}$$

and therefore

$$\Gamma = \Gamma_K \cup \Gamma_F$$

With the condition (29) satisfied, the existence of a unique solution to this problem and its continuous dependence on the data follows from Theorem 3.

B. Crack in Pure Shear (Mode II)

We consider the problem of figure (3) and reduce it to figure (4). Here $\Gamma_U = \emptyset$ and we have the following decomposition of the boundary Γ

$$\Gamma_k = \emptyset, \ \Gamma_F = \bigcup_{i=1}^{3} \Gamma_{F_i}, \ \Gamma_V = \bigcup_{i=1}^{2} \Gamma_{V_i} \quad \text{(nonhomogeneous conditions only on } \Gamma_{F_3}\text{)}$$

i.e.

$$\Gamma = \Gamma_V \cup \Gamma_F$$

Again it can be seen that the condition (29) is satisfied whence by Theorem 3 a weak solution exists and is unique.

C. Crack Under Anti-plane Loading

This simple problem is shown in figure (5). As the symmetry of the problem with reference to the crack line indicates there is no rigid body motion and $\Gamma_U = \emptyset$. With the condition (28) satisfied, Theorem 3 gives the desired results.

So the question of existence and uniqueness of solutions to the single-mode crack problems was resolved in this section.

II.5 MIXED-MODE CRACK PROBLEMS

To establish existence and uniqueness of solutions, under conditions of combined loading on domains with cracks we need to introduce Sobolev spaces on *slit domains*.

The difficulty in defining such spaces arises from the fact that we must permit elements in the space to take different values on either side of the crack line. Consequently we cannot define them as restrictions of functions defined on the whole plane. The required modifications were suggested by Vinter.

II.5.1 Sobolev Spaces on Slit Domains

Take Ω, an open, connected subset of R^n.

Definition 2

Ω is a *regular slit domain* in case there exists a family $\{\Omega_i\}_{i=1}^{K}$ of subsets such that

$$\Omega = \bigcup_i \Omega_i$$

and

(i) for each i, Ω_i has non-empty interior, is bounded, connected with

Lipschitz boundary $\partial\Omega_i = \bar{\Omega}_i \setminus \mathring{\Omega}_i$ ($\bar{\Omega}$ denotes closure, $\mathring{\Omega}$ denotes interior).

(ii) $\mathring{\Omega}_i \cap \mathring{\Omega}_j = \emptyset$, $i \neq j$.

(iii) (boundary measure) $|\Omega_i \cap \Omega_{i+1}| > 0$, $i = 1, \ldots, K-1$.

The Ω_i's are not assumed open or closed.

Example

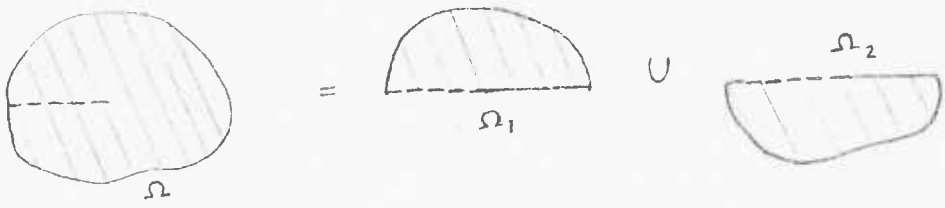

Assumption (iii) excludes such domains as

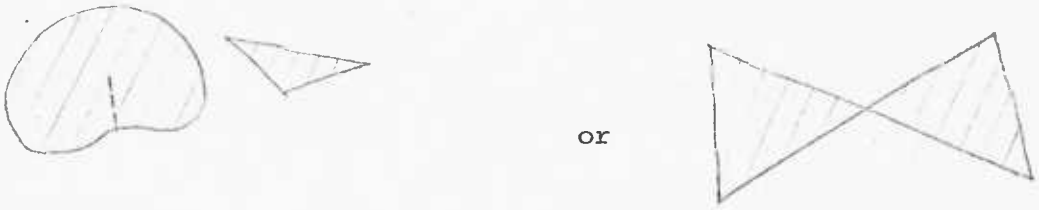

Definition 3

We say $\phi \in C^\infty(\Omega)$ in case ϕ is infinitely differentiable for all $x \in \Omega$ and there exists a collection $\{\phi_i\}_{i=1}^K$ of $C^\infty(R^n)$ elements such that

$$\phi\big|_{\Omega_i} = \phi_i\big|_{\Omega_i}, \quad i = 1, 2, \ldots, K$$

(Ω_i's as above).

Definition 4

$H^k(\Omega)$, $k \geq 1$ integer, is the completion of $C^\infty(\Omega)$ with respect to the inner product

$$(u,v) \to \sum_{|\alpha| \leq k} \int_\Omega D^\alpha u D^\alpha v dx$$

$H_0^k(\Omega)$ is the completion of $\{\phi \in C^\infty(R^n) \,|\, \text{supp}\,\{\phi\} \subset \Omega\}$ with respect to inner product $(u,v) \to \sum_{|\alpha| \leq k} \int_\Omega D^\alpha u D^\alpha v dx$

Proposition 1

The mapping

$$u \to u|_{\Omega_i} : H^k(\Omega) \to H^k(\mathring{\Omega}_i)$$

is continuous and onto (for each i). #

Proof

(i) Since

$$|u|_{H^k(\Omega_i)} \leq |u|_{H^k(\Omega)}$$

the mapping is continuous.

(ii) Choose $\psi \in H^k(\mathring{\Omega}_i)$. By definition of $H^k(\mathring{\Omega}_i)$, ψ is the restriction of some $\tilde{\psi} \in H^k(R^n)$. We may choose a sequence $\{\psi_j\}$ in $C^\infty(R^n)$ such that

$$\psi_j \to \tilde{\psi} \text{ in } H^k(R^n)$$

Select

$$\phi_{ij} = \psi_j|_{\Omega_i}, \quad i = 1, \ldots, K, \quad j = 1, 2, \ldots$$

Then, for each j, $\{\phi_{ij}\}_{i=1}^K$ defines an element $\psi_j \in C^\infty(R^n)$. Further,

$$\psi_j \to \tilde{\psi}|_\Omega \text{ in } H^k(\Omega)$$

and

$$\psi_j|_{\mathring{\Omega}_i} \to \tilde{\psi}|_{\mathring{\Omega}_i} = \psi \text{ in } H^k(\mathring{\Omega}_i)$$

Thus $\tilde{\psi}|_{\Omega} \in H^k(\Omega)$ has restriction ψ. Recalling that ψ was arbitrary, the mapping is onto. #

Write

$$\Sigma_i = \bar{\Omega}_i \cap \partial\Omega$$

Definition 5

Given $\phi \in C^\infty(\Omega)$, the *trace of* ϕ, written $\phi|_{\partial\Omega}$, is the collection of functions

$$\phi_1|_{\Sigma_1}, \ldots, \phi_K|_{\Sigma_K}$$

(the ϕ_i's as above). Example:

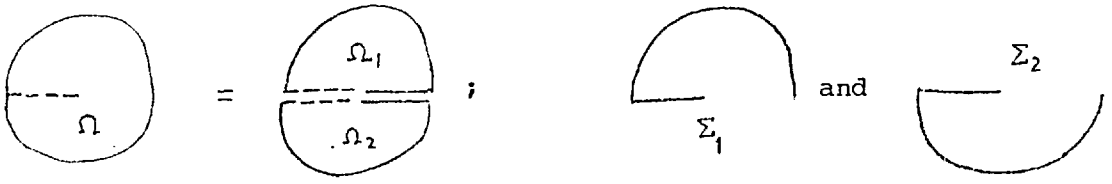

Proposition 2 (A trace theorem.)

The map

$$\phi \to \phi|_{\partial\Omega} : H^1(\Omega) \to L^2(\Sigma_1) \times \ldots \times L^2(\Sigma_K)$$

on $\phi \in C^\infty(\Omega)$ is continuous, and may therefore be extended to all of $H^1(\Omega)$, so defining "trace" as a $L^2(\bar{\Omega}_1 \cap \partial\Omega) \times \ldots \times L^2(\bar{\Omega}_K \cap \partial\Omega)$ valued function on $H^1(\Omega)$.

Proof

Take $\phi \in C^\infty(\Omega)$, and let $\{\phi_i\}_{i=1}^K$ define ϕ (as above). Then [55, p. 15], there exists a constant c, independent of ϕ, such that

$$\left|\phi_i\right|_{\partial\Omega_i}\Big|^2_{L^2(\Sigma_i)} \leq c^2\left|\phi^i\right|^2_{H^1(\Omega_i)}$$

Similarly over i,

$$\left|\phi\right|_{\partial\Omega}\Big|_{L^2(\Sigma_1)x\ldots xL^2(\Sigma_k)} \leq c\left|\phi\right|_{H^1(\Omega)}$$

which establishes continuity. #

Proposition 3

The mapping

$$u \to d/dx : H^1(\Omega) \to L^2(\Omega)$$

on $C^\infty(\Omega)$ is continuous, whence $d/dx(\cdot)$ may be defined on $H^1(\Omega)$ and is a continuous mapping into $L^2(\Omega)$.

Proof

Given $\phi \in C^\infty(\Omega)$, let $\{\phi^i\}$ be as above. Then by standard results, there exists c (independent of ϕ) such that

$$\left|\frac{d}{dx}\ \phi\right|^2_{H^1(\Omega_i)} \leq c^2\left|\phi\right|^2_{L^2(\Omega)}$$

Summing over i gives continuity. #

Proposition 4

(Compactness of the injection $H^1(\Omega) \to L^2(\Omega)$.)

$u_i \to \bar{u}$, weakly in $H^1(\Omega)$ implies $u_i \to \bar{u}$, strongly in $L^2(\Omega)$.

Proof

Suppose $u_i \to \bar{u}$ (weakly in $H^1(\Omega)$).

Since the mapping

$$u \to u\big|_{\Omega_i} : H^1(\Omega) \to H^1(\Omega_i)$$

is onto,

$$u_i\big|_{\Omega_j} \to \bar{u}\big|_{\Omega_j} \quad \text{(weakly in } H^1(\mathring{\Omega}_j)) \quad j = 1, 2, \ldots, K$$

(Ω_j's as above). But, by [55, p. 17] then,

$$u_i\big|_{\Omega_j} \to \bar{u}\big|_{\Omega_j} \quad \text{(strongly in } L^2(\Omega_j))$$

i.e.

$$\int_{\Omega_1 \cup \ldots \cup \Omega_k} |u_i - \bar{u}|^2 dx = \int_{\Omega} |u_i - \bar{u}|^2 dx \to 0, \quad i \to \infty$$

Thus

$$u_i \to \bar{u} \quad \text{(strongly in } L^2(\Omega))$$

II.5.2 V-ellipticity on Slit Domains

Let Ω be a regular slit domain. $\Gamma_F(\Gamma_U)$ is a collection $\{\Gamma_F^i\}_{i=1}^K$ ($\{\Gamma_U^i\}_{i=1}^K$) of measurable subsets of $\{\partial\Omega_i\}_{i=1}^K$.

We consider

$$\begin{cases} \sigma_{ij,j} + f_i = 0 \text{ in } \Omega \\ \sigma_{ij} n_j = F_i \text{ "on } \Gamma_F\text{"} \\ u_i\big|_{\partial\Omega} = U_i \text{ "on } \Gamma_U\text{"} \end{cases} \tag{33}$$

Assume:

(i) $F_i \in \prod_i L^2(\Sigma_i \cap \Gamma_F^i)$

(ii) U_i lies in the range of the canonical injection

$$\phi \to \{\phi\big|_{\partial\Omega_i \cap \Gamma_U^i}\}_{i=1} : H^1(\Omega) \to \prod_k L^2(\partial\Omega_k \cap \Gamma_U^k)\}$$

(iii) (boundary measure) $|\partial\Omega_k \cap \Gamma_U^k| > 0$ (for some k).

Define

$$\bar{V} = \{\phi \in (H^1(\Omega))^3 \,|\, \phi\big|_{\partial\Omega} = u_i \text{ on } \Gamma_U^i\}$$

We have shown that the canonical injection $\phi \to \phi\big|_{\partial\Omega} : H^1 \to L^2$ is continuous, whence $\bar{V}$ is a closed, affine subspace.

Define

$$a(u,v) = \int_\Omega \sigma_{ij}(u)\varepsilon_{ij}(v)dx, \quad (u,v) \in (H^1(\Omega))^3$$

where

$$\varepsilon_{ij}(u) = \tfrac{1}{2}(\partial u_i/\partial x_j + \partial u_j/\partial x_i); \quad \sigma_{ij} = c_{ijk\ell}\varepsilon_{k\ell}$$

We interpret weak solutions of (33) as $u \in \bar{V}$ such that

$$a(u,v-u) = \sum_k \int_{\partial\Omega_k \cap \Gamma_F^k} F(v-u)ds + \int_\Omega f(v-u)dx$$

all $v \in \bar{V}$.

With this definition, $a(\cdot,\cdot)$ is a continuous bilinear form on $\bar{V}$ (continuous since, as shown above $\phi \to d/dx\ \phi : H^1 \to L^2$ is continuous).

To establish existence and uniqueness then, we need only show

ellipticity of $a(\cdot,\cdot)$ on $V_0 = \{v \in V \mid v|_{\partial\Omega}=0\}$.†

Proposition 6 (V-coercivity)

There exists a constant $c > 0$ such that

$$\int_\Omega \varepsilon_{ij}\varepsilon_{ij}dx + \int_\Omega v_i v_i dx \geq c||v||_V^2 \text{ , all } v \in V \tag{34}$$

Proof

Since $\phi \to d/dx\ \phi : H^1 \to L^2$ is continuous, we need only establish the result for $v \in (C^\infty(\Omega))^3$. Let v^k be the $C^\infty(\bar{\Omega}_k)$ elements associated with v. By [55],

$$\int_{\Omega_k} \varepsilon_{ij}(v)\varepsilon_{ij}(v)dx + \int_{\Omega_k} v_i v_i dx \geq c||v||^2_{H^1(\Omega_k)}$$

and summing over k gives the result.

Theorem 4 (ellipticity of $a(\cdot,\cdot)$ on V_0)

There exists a constant c such that

$$a(u,u) = \int_\Omega \sigma_{ij}(u)\varepsilon_{ij}(u)dx \geq c||u||_V^2 \tag{35}$$

all $u \in V_0$,

$$V_0 = \{u \in V | u=0 \text{ on } \Gamma_U\}$$

---

† Take u_0 such that $u_0|_{\partial\Omega} = \underline{U}$. Then ellipticity on V_0 suffices since u is a weak solution of the above problem iff $\tilde{u} = (u-u_0)$ is a weak solution of

$$a(\tilde{u},\tilde{v}) = \sum_k \int_{\Omega_k \cap \Gamma_F^k} F\tilde{v}ds + \int_\Omega f\tilde{v}dx$$

all $\tilde{v} \in V_0$, $\tilde{u} \in V_0$

and ellipticity on V_0 suffices for existence of a weak solution to this problem.

Proof

First note that

$$\left.\begin{array}{l} a(u,u) = 0 \\ \\ u \in V_0 \end{array}\right\} \Longleftrightarrow u = 0$$

($\Longleftarrow$) is obvious. In the forward direction, assume $u \in V_0$, $a(u,u) = 0$. Suppose (without loss of generality) $|\partial\Omega_1 \cap \Gamma_U^1| > 0$. Then by a standard result,

$$u|_{\Omega_1} = 0$$

But by assumption (iii) (Definition 2)

$$|\Omega_1 \cap \Omega_2| > 0$$

whence (by the same standard result)

$$u|_{\Omega_2} = 0$$

Likewise we show that $u|_{\Omega_2}, \ldots, u|_{\Omega_K} = 0$, whence $u|_{\Omega} = 0$.

It is now easy to deduce that $a(\cdot,\cdot)$ defines an inner product on V_0. Write the resulting inner product space as V.

Now suppose the theorem is false. Then there exists a sequence $\{u_i\}$ in V_0 such that

$$|u_i|_{L^2} = 1, \quad a(u_i,u_i) \to 0, \quad i \to \infty$$

In view of Proposition 6, $\{u_i\}$ is a bounded sequence in $(H^1(\Omega))^3$. $\{u_i\}$ is obviously also bounded as a sequence in V. We may therefore extract a subsequence (also written $\{u_i\}$) such that

$$\begin{aligned} &u_i \to \bar{u} \text{ in } (H^1(\Omega))^3 \quad \text{(weakly)} \\ &u_i \to \bar{u} \text{ in } V \quad \text{(weakly)} \end{aligned} \tag{36}$$

But by a standard result, the norm $a(u,u)$ (on V) is weakly lower semi-continuous. It follows that

$$0 = \lim_i a(u_i,u_i) \geq a(\bar{u},\bar{u}) \geq 0$$

so that $\bar{u} = 0$.

On the other hand (36) implies

$$u_i \to \bar{u} \quad \text{strongly in } L^2(\Omega)$$

It follows,

$$1 = \lim_i |u_i|_{L_2} = |\bar{u}|_{L_2}$$

whence $\bar{u} \neq 0$.

The theorem statement follows from this contradiction. #

Theorem 4 gives existence and uniqueness of solution by the general results of Section 4.2 (Chapter I).

II.6 REGULARITY RESULTS

In error analysis of partial differential equations usually some degree of smoothness for solutions is assumed. From approximation theory we can get estimates for the error involved in the form, (see Chapter I, Theorem 14):

$$\|u-u_h\|_{L_2(\Omega)} \leq Ch^k \|u\|_{H^k(\Omega)} \tag{1}$$

Now if we *assume* that $u \in H^k(\Omega)$ then the right hand side is of finite value and the rate of convergence of solutions is entirely dependent on the order of polynomials used in the approximating subspaces. For smooth data and domain, the solution is smooth and therefore the assumption is valid. However, for certain physical problems this is not the case and hence, irrespective of the degree of interpolating ploynomials used, solutions do not converge. Solutions of the following types of problems are smooth to only a certain degree:

1. Problems with non-smooth data
2. Problems in which the differential operators have non-smooth parameters
3. Problems on domains with interfaces
4. Problems on non-smooth domains

etc.

In fact, it is known that these problems give rise to singularities in the solutions.

We will only be dealing with non-smooth domains in two dimensions where there are a number of corners in the domain and assume data to be as smooth as required. It will be seen that these singularities are

present only over a small region very close to the vertices and vanish outside the areas. However, the local singular behaviour influences the accuracy of the solutions throughout the domain.

The regularity of the solution depends on the angle of the vertices. For example, the Dirichlet problem:

$$\begin{cases} -\Delta u = f \text{ in } \Omega, \ f \in H^m(\Omega) \\ \\ u = 0 \text{ on } \partial\Omega \end{cases} \tag{2}$$

does not have square integrable second derivatives on *non-convex* domains, while for convex domains we have [56]

$$||u||_{m+2} \leq c||f||_m \qquad -3/2 < m \leq 0 \tag{3}$$

Our purpose in this section is to study the smoothness properties of solutions to equations of elasticity on slit domains. It is shown that the solution vector u can be written as the sum of a finite number of 'singular' functions χ_j and a 'smooth' function $\tilde{u}$:

$$u = \tilde{u} + \sum_j \chi_j \tag{4}$$

where $\tilde{u}$ depends on data while χ_j is only dependent on the differential equations and the domain. In particular, estimates for the smooth part $\tilde{u}$ in terms of data are obtained. This expansion is then employed to obtain improved rates of convergence in both L_2 and H^1 norms by including

singular functions in the approximating subspaces. Domains containing cracks and convex domains are treated as special cases.

II.6.1 Regularity of Solutions for Slit Domains

In dealing with the equations of elasticity we need some general results concerning the regularity of solutions to a single differential equation. The available results [59, pp. 287-288] for two-dimensional angular domains are first quoted in their general form and then exploited for the equations of elasticity on slit domains.

II.6.1.1 General theory

Take $\Omega \subset R^2$ an angular sector with vertex at the origin. The vertex angle is ω and the boundary is denoted by Γ.

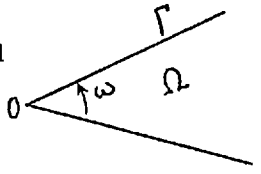

We denote by $H^k(\Omega)$ the usual Sobolev space ($k \geq 0$) and by $H^{k-\frac{1}{2}}(\Gamma)$ the space of functions given on the boundary Γ defined by

$$||\phi||_{H^{k-\frac{1}{2}}(\Gamma)} = \inf_{v|_\Gamma=\phi} ||v||_{H^k(\Omega)}$$

We may also define the space $H^k(\Omega)$ for $k < 0$ as the closure of $C^\infty(\bar{\Omega})$ in the norm $||\cdot||_{H^k(\Omega)}$ where $k < 0$

$$||u||_{H^k(\Omega)} = \sup_{v \in H^{-k}(\Omega)} \frac{\int uv dx}{||v||_{H^k(\Omega)}}$$

Consider now the elliptic boundary problem

$$L(x; \frac{\partial}{\partial x})u = f(x) \text{ in } \Omega$$

$$B_j(x; \frac{\partial}{\partial x})u = \phi_j(x) \text{ on } \Gamma, \; j = 1, \ldots, m \tag{5}$$

where $L(\cdot,\cdot)$ is an elliptic differential operator of order $2m$ and B_j's constitute a normal system of boundary operators of order $m_j \leq 2m-1$

covering $L(\cdot,\cdot)$ (the details of the assumptions are given in [57]. For the sake of brevity we omit them here). $x = (x_1, x_2)$ represents the Cartesian coordinates.

Let $L_0(0,\cdot)$ and $B_j^0(0,\cdot)$ denote the principal part of the operators $L(\cdot,\cdot)$ and $B_j(\cdot,\cdot)$ respectively with coefficients fixed at the origin 0, We consider the following problem:

$$\begin{aligned} &L_0(0; \frac{\partial}{\partial x})u = f(x) \text{ in } \Omega \\ &B_j^0(0; \frac{\partial}{\partial x})u = \phi_j(x) \text{ on } \Gamma,\ j = 1, \ldots, m \end{aligned} \tag{6}$$

where $f \in H^k(\Omega)$ and $\phi_j \in H^{k+2m-m_j-\frac{1}{2}}(\Gamma)$, $j = 1, \ldots, m$. As we shall see, the essential features of the solution to equation (5) will be obtained by studying equation (6).

We transform (6) to polar coordinates (r,θ) and, make the change of variable $r = e^{-\tau}$ so that the domain Ω becomes the strip S,

$S = \{(\tau,\theta),\ 0<\theta<\omega;\ -\infty<\tau<+\infty\}$ with boundary ∂S. System (6) will become

$$\begin{cases} L_1(\tau,\theta;\cdot)u = e^{-2m\tau}f = F \text{ in } S \\ \\ B_j^1(\tau,\theta;\cdot)u = e^{-m_j\tau}\phi_j = \Phi_j,\ (j = 1,\ldots,m) \text{ on } \theta = 0,\ \omega \end{cases} \tag{7}$$

Introducing the Fourier transform $\hat{u}(\xi,\theta)$ by $(Fu)(\xi,\theta) = \hat{u}(\xi,\theta) = \int_{-\infty}^{+\infty} e^{-i\xi\tau}u(\tau,\theta)d\tau$ the system (7) is transformed to

$$\begin{cases} L_1(\cdot;i\xi)\hat{u}(\xi,\theta) = \hat{F}(\xi-2mi,\theta),\ 0 < \theta < \omega \\ \\ B_j^1(\cdot;i\xi)\hat{u}(\xi,\theta) = \hat{\Phi}_j(\xi-m_ji,\theta),\ \theta = 0,\ \omega \end{cases} \tag{8}$$

Then it is known [58] that there exists a meromorphic function $R(\xi)$

$$R(\xi) : H^k(S)\times H^{k+2m-m_j-\frac{1}{2}}(\partial S) \to H^{k+2m}(S)$$

such that

$$\{L_1(\cdot;i\xi),\ B_j^1(\cdot;i\xi)\}R(\xi) = I$$

where the vector operator $\{L_1,\ B_j^1\}$ maps $\hat{u}$ into $\{L_1\hat{u},\ B_j^1\hat{u}\}$.

In fact $R(\xi)$ can be regarded as the solution operator for the given elliptic problem and the behaviour of solutions to system (5) is dominated by the positions of the poles of $R(\xi)$ in the ξ-plane. Kondratev has studied system (5) and gives the following result [59, pp. 287-288]:

Theorem 1:

Let $u \in H^{k+2m}(\Omega)$ be a solution to system (5) and suppose that $f \in H^{k_1}(\Omega)$ and $\phi_j \in H^{k_1+2m-m_j-\frac{1}{2}}(\Gamma)$, $1 \leq j \leq m$, $k_1 > k$. Then provided that f and ϕ_j are 'suitably behaved' at the origin and that k_1 does not take certain pathological values, we have a decomposition of u into regular and singular components w and χ_j's respectively:

$$u = w + \sum_j \alpha_j \chi_j \tag{9}$$

where $w \in H^{k_1+2m}(\Omega)$ and the χ_j's do not depend on the data f and ϕ_j and furthermore we have the bound:

$$\sum_j |\alpha_j| + ||w||_{H^{k_1+2m}(\Omega)} \leq c\{||f||_{H^{k_1}(\Omega)} + \sum_j ||\phi_j||_{H^{k_1+2m-m_j-\frac{1}{2}}(\Gamma)} + ||u||_{H^{k+2m}(\Omega)}\} \tag{10}$$

with $c > 0$ a constant. #

Remark

The singular functions χ_j in (9-a) are given by

$$\chi_j = \sum_{s=0}^{n_j} r^{-i\xi_j}\{(\ell nr)^s P_{jsq}(r\ell n^q r)\} + \sum_{\ell \geq k+2m-1} c_{\ell p} r^{\ell}\{(\ell nr)^p g_{\ell p}(\theta)\}$$

where ξ_j with $k+2m-1 \leq Im\xi_j < h_1 = k_1+2m-1$ are poles of $R(\xi)$ of multiplicity n_j, $c_{\ell p}$ is a constant, P_{jsq} are polynomials of degree $(h_1 - Im\lambda_j)$ with coefficients that are infinitely differentiable functions of θ, p, $q \geq 0$ integers and $g_{\ell p}(\theta)$ is an infinitely differentiable function of θ.

II.6.1.2 Regularity results for slit domains

The above theory has been developed for angular sector domains. We are primarily interested however in slit domains. It is easy to show, using coordinate transformations and partition of unity ideas, that for these more general domains Theorem 1 still applies with the following modification: each corner contributes singular functions with asymptotic properties determined by the corner angle and the analogous bound to inequality (10) applies.

We consider equations of elasticity on a slit domain G and assume the material to be homogeneous and isotropic. The equations of elasticity can be written as:

$$\frac{\partial}{\partial x_j}(\sigma_{ij}(u)) = f_i \text{ in } G \tag{11}$$

$$\sigma_{ij}(u)n_j = g_i \text{ on } \partial G \tag{12}$$

where $u = (u_1, u_2)$ is the displacement vector.

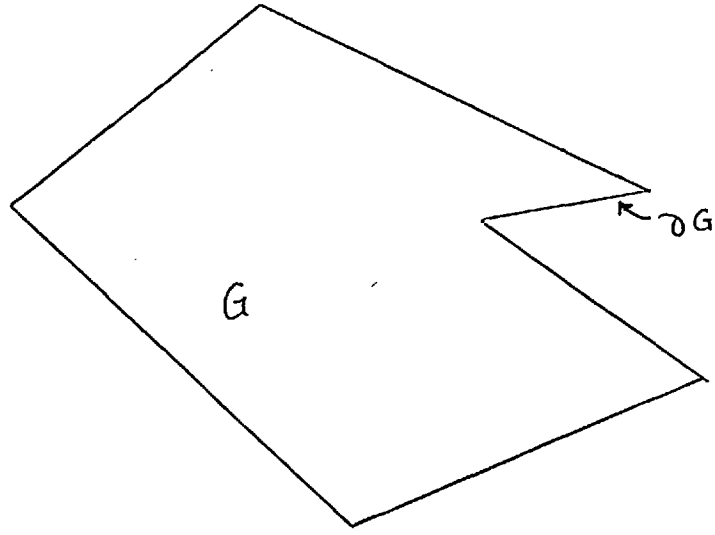

The system of equations (11) together with the given boundary conditions (12) constitute a well-posed elliptic problem (in the sense of Agmon-Douglis-Nirenberg [57]).

II.6.1.2.1 Smoothness and boundedness of Airy's stress function

Let Ω with vertex angle ω be placed at the origin and its two sides lie along $\omega = 0$ and $\theta = \omega$ in the polar coordinates (r,θ). In applying results of Section II.6.1.1 to the equations of elasticity we have to reduce the above system to a single partial differential equation. This is possible by introducing the well-known Airy's stress function.

Suppose that the body forces $f = (f_1, f_2)$ are derived from a potential function $V \in H^1(\Omega)$ such that

$$f_i = \frac{\partial V}{\partial x_i}$$

Then we take

$$\sigma_{ij} = (-\frac{\partial^2}{\partial x_i \partial x_j} + \delta_{ij}\Delta)S + \delta_{ij}V \tag{16}$$

substituting for σ_{ij} from (16) into the system (11) we arrive at the nonhomogeneous biharmonic equation

$$\Delta^2 S = F \quad \text{in } \Omega \tag{17}$$

where

$$F = -2\alpha(\frac{\partial f_i}{\partial x_i}) = -2\alpha\Delta V \tag{18}$$

and

$$\alpha = \frac{\mu}{\lambda+2\mu}$$

With a series of polar coordinate transformations (r,θ), change of variables $r \to e^{-\tau}$ and Fourier transformation with respect to τ (with the transformation variable ξ) we get the following ordinary differential equation in terms of θ:

$$\begin{cases} \hat{S}''''-2(\xi^2-2i\xi-2)\hat{S}'' + \xi^2(\xi^2-4i\xi-4)\hat{S} = \hat{F}(\xi-4i,\theta) & 0 < \theta < \omega \\ i\xi(1+i\xi)\hat{S} = \hat{g}_1(\xi-2i,\theta) & \theta = 0,\ \omega \\ (i\xi+1)\hat{S}' = \hat{g}_2(\xi-2i,\theta) & \theta = 0,\ \omega \end{cases} \tag{19}$$

where

$$\sigma_{\theta\theta} = g_1(r,\theta)$$

and $i = 1, 2$

$$\sigma_{r\theta} = g_2(r,\theta)$$

are given functions along the boundary.

We now aim at finding the poles of the function $R(\xi)$ associated with the problem. For this purpose consider the homogeneous boundary problem in the transformed form. The general solution of the homogeneous problem (19) is given by $(\xi \neq 0,\ i,\ 2i)$

$$\hat{S} = c_1 \cos i\xi\theta + c_2 \sin i\xi\theta + c_3 \sin (i\xi+2)\theta + c_4 \cos (i\xi+2)\theta$$

It is straightforward to see that the solution satisfying the homogeneous boundary conditions is non-trivial provided the determinant of the coefficients c_i, $i = 1, \ldots, 4$ is non-zero. Calculation shows that a unique solution exists if

$$\left(\frac{\sin \omega z}{\omega z}\right)^2 - \left(\frac{\sin \omega}{\omega}\right)^2 \neq 0 \qquad (20)$$

where $z = -(1+i\xi)$. Roots of this transcendental equation then give the poles of $R(\xi)$. For $\xi = i$ we let

$$\hat{S} = c_1 \sin \theta + c_2 \theta \sin \theta + c_3 \cos \theta + c_4 \theta \cos \theta$$

then the determinant in question is

$$\Lambda(i) = \det \begin{bmatrix} 1 & 0 & 0 & 1 \\ \cos \omega & \omega \cos \omega + \sin \omega & -\sin \omega & \cos \omega - \omega \sin \omega \\ 0 & 0 & 1 & 0 \\ \sin \omega & \omega \sin \omega & \cos \omega & \omega \cos \omega \end{bmatrix}$$

$$= \omega^2 - \sin^2 \omega > 0$$

since $\omega > 0$.

For $\xi = 0$ or $\xi = 2i$ we let

$$\hat{S} = c_1 \sin 2\theta + c_2 \cos 2\theta + c_3 \theta + c_4$$

The determinant of the coefficients corresponding to the solution satisfying homogeneous boundary conditions is

$$\Lambda(0) = \det \begin{bmatrix} 2 & 0 & 1 & 0 \\ 2 \cos 2\omega & -2 \sin 2\omega & 1 & 0 \\ 0 & 1 & 0 & 1 \\ \sin 2\omega & \cos 2\omega & \omega & 1 \end{bmatrix}$$

$$= 8 \sin \omega (\omega \cos \omega - \sin \omega)$$

which vanishes when either $\sin\omega = 0$ or $\tan\omega = \omega$.

The equation (20) has a finite number of real roots and an infinite number of complex roots. Real roots, if any, are always smaller than the real part of any complex root of (20), i.e. the dominant pole of $R(\xi)$ is given by the smallest real rool of (20) if such a root exists. Also we have

$$\text{Re } z > c_0$$

where

$$c_0 = \begin{cases} 1/2 & \pi < \omega < 2\pi \\ 1 & 0 < \omega < \pi \end{cases}$$

the following figure (1) shows the real roots of equation (20), i.e.

$$\frac{\sin \omega z}{\omega z} = \pm \frac{\sin \omega}{\omega} \qquad (21)$$

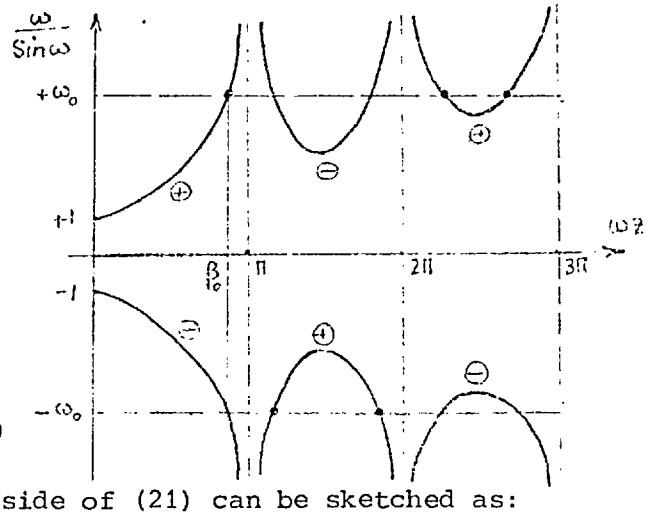

Fig. 1 The Roots of Eq. (21) for real z

The function on the left hand side of (21) can be sketched as:

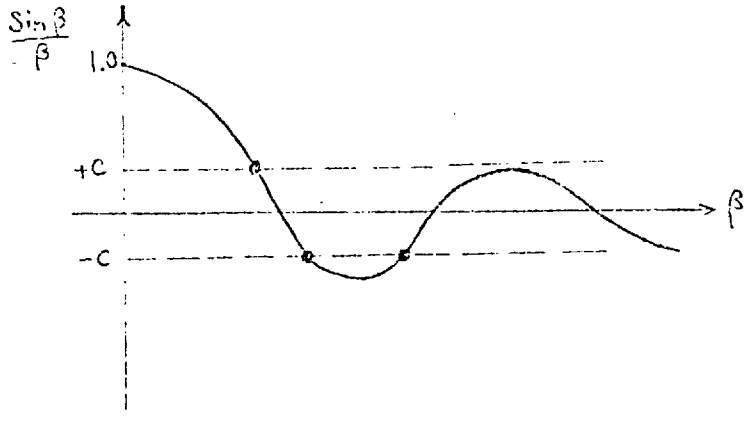

Fig. 2.

We have the following:

Theorem 2

Let $m \geq 0$ be an integer. Assume $f \in (H^m(\Omega))^2$, $g \in (H^{m+\frac{1}{2}})^2$ and conditions of Theorem (1) are satisfied. Then there exists an $\omega_0 > 0$ (dependent on m) such that for all $\omega < \omega_0$.

$$S \in H^{m+3}(\Omega) \tag{22}$$

and

$$||S||_{H^{m+3}(\Omega)} \leq c\{||f||_{(H^m(\Omega))^2} + ||g||_{(H^{m+\frac{1}{2}}(\Gamma))^2} + ||S||_{H^2(\Omega)}\},$$

$m \geq 0$ #

Proof

It is enough to show that the equation (21) has no roots in the strip $0 < \text{Re } z < m+1$ for $\omega < \omega_0$, $m = 0, 1, \ldots$. Fix ω at an arbitrary value $\bar{\omega}_0$ then from Figure (1) it is seen that associated with $\bar{\omega}_0$ is a smallest root β_0 such that there are no roots in the region $0 < \bar{\omega}_0 z < \beta_0$ of equation (21). We choose m such that $\beta_0/\omega_0 = m+1$. This can be done for $0 < \bar{\omega}_0 < \pi$, $\pi < \bar{\omega}_0 < 3\pi/2$ and $3\pi/2 < \bar{\omega}_0 < 2\pi$ with $\beta_0/\omega_0 \geq 1$. As there are no roots of equation (21) in the strip $0 < \text{Re } z < m+1$ from Theorem (1) we see, that there are no terms of the form $e^{-i\xi_j} f_j(\theta)$ in the expansion of S. Indeed, $S \equiv w$ and therefore the assertion follows when we notice that F is a linear functional of f (see equation (18)), i.e.

$$||F||_{H^{m-1}(\Omega)} \leq C||f||_{(H^m(\Omega))^2} \tag{24}$$

The proof is now complete. #

Corollary

For convex domains (i.e. $0 < \omega < \pi$; $\omega_0 = \pi$) and square integrable data, Theorem (2) holds with $m = 0$.

II.6.1.2.2 Regularity properties of displacements

In order to establish bounds on displacements u or 'smooth' part of u we need the following:

Proposition 1

Take Ω a slit domain. Suppose that $u \in (L^2(\Omega))^3$ and $\{\varepsilon_{ij}(u)\} \in (H^k(\Omega))^{3x3}$. Then $u \in (H^{k+1}(\Omega))^3$ and

$$||\varepsilon_{ij}(u)||^2_{H^k(\Omega)} + ||u||^2_{(L_2(\Omega))^3} \geq c||u||^2_{(H^{k+1}(\Omega))^3} \qquad (25)$$

#

Proof

We prove the result for Lipschitz domains. The result follows for regular slit domains by decomposing Ω into Lipschitz components and considering sequences of smooth functions in an obvious way.

We use induction. The assertion is true for $k = 0$ (see Chapter II Proposition 6).

Suppose it is true for all $k \leq \bar{k}-1$. We shall show it is true for $k = \bar{k}$.

Set $E = \{u \in (H^{\bar{k}}(\Omega))^3 | \varepsilon_{ij}(u) \in H^{\bar{k}}\}$

This is a Banach space with norm

$$(||\varepsilon_{ij}(u)||^2_{H^{\bar{k}}} + ||u||^2_{(L_2)^3})^{\frac{1}{2}}$$

Take $u \in E$, arbitrarily. In particular, $\{\varepsilon_{ij}(u)\} \in (H^{\bar{k}-1})^{3x3}$ and by the

induction hypothesis $u \in (H^{\bar{k}}(\Omega))^3$.

Now choose arbitrary α

$$D^{\alpha} = (\frac{\partial}{\partial x_1})^{\alpha_1} \ldots\ldots (\frac{\partial}{\partial x_3})^{\alpha_3}; \quad |\alpha| = \bar{k}$$

we have

$$\frac{\partial}{\partial x_j} (D^{\alpha} u_i) \in H^{-1}(\Omega), \quad \text{for each } i, j$$

(since $u \in (H^{\bar{k}}(\Omega))^3$).

On the other hand

$$\frac{\partial^2}{\partial x_j \partial x_k}(D^{\alpha} u_i) = D^{\alpha} \frac{\partial^2 u_i}{\partial x_j \partial x_k}$$

$$= D^{\alpha}[\frac{\partial}{\partial x_j} \varepsilon_{ik}(u) + \frac{\partial}{\partial x_k} \varepsilon_{ij}(u) - \frac{\partial}{\partial x_i} \varepsilon_{jk}(u)]$$

$$\in H^{-1}(\Omega)$$

(since $\{\varepsilon_{ij}(u)\} \in (H^{\bar{k}}(\Omega))^{3x3}$).

Thus $\frac{\partial}{\partial x_j} (D^{\alpha} u_i)$ and $\frac{\partial}{\partial x_k}[\frac{\partial}{\partial x_j}(D^{\alpha} u_i)]$ lie in $H^{-1}(\Omega)$ and by a property of Sobolev spaces on Lipschitz domains

$$\frac{\partial}{\partial x_j}(D^{\alpha} u_{,i}) \in L_2(\Omega)$$

i.e. $u \in (H^{\bar{k}+1}(\Omega))^3$, and we have shown $E \subset (H^{\bar{k}+1})^3$. The reverse inclusion is obvious and we have the algebraic equality

$$E = (H^{\bar{k}+1}(\Omega))^3$$

By the closed graph theorem, the norms on E and $(H^{\bar{k}+1})^3$ are equivalent

and

$$||\varepsilon_{ij}(u)||^2_{H^{\bar{k}}(\Omega)} + ||u||^2_{(L_2(\Omega))^3} \geq c||u||^2_{(H^{\bar{k}+1}(\Omega))^3} \quad \#$$

Proposition 2

Take Ω a slit domain. Assume that $S \in H^{k+2}(\Omega)$ and $\{\varepsilon_{ij}(u)\} \in (H^k(\Omega))^{3x3}$. Then there exists a constant $c > 0$ such that

$$||\varepsilon_{ij}(u)||_{H^k(\Omega)} \leq c||S||_{H^{k+2}(\Omega)} \qquad (26)$$

##

This follows immediately from the known relation between ε_{ij}, σ_{ij} and S (see equation (16).

Now we can prove the following main result:

Theorem 3

Let $u \in H^1(\Omega)$ be a solution of (11)-(12). Suppose $f \in (H^k(\Omega))^2$ and $g \in (H^{k+\frac{1}{2}}(\Gamma))^2$ ($k \geq 0$ integer). Let f, g and u satisfy the hypothesis of Theorem 1.

Then we may write

$$u = \tilde{u} + \sum_j \chi_j \qquad (27)$$

where $\tilde{u} \in (H^{k+2}(\Omega))^2$. Furthermore, there is a constant $c > 0$ (independent of f, g) such that

$$||\tilde{u}||^2_{(H^{k+2}(\Omega))^2} \leq c\{||f||^2_{(H^k(\Omega))^2} + ||g||^2_{(H^{k+\frac{1}{2}}(\Gamma)^2}\} \qquad (28)$$

The functions χ_j called the 'singular functions' are independent of data but depend on the differential equations and the vertex angle. These functions may be taken to vanish outside a neighbourhood of the

vertices of Ω. #

Proof

With the hypothesis of Theorem (1) satisfied we apply Theorem (1) to the biharmonic equation in terms of Airy's stress function S, (equation (17)).

Then it follows that

$$S = w + \sum_j \Psi_j \tag{29}$$

where Ψ_j are 'singular' functions of the form given there and w is 'smoother' than S. Hence, there is a corresponding expansion for u as

$$u = \tilde{u} + \sum_j \chi_j \tag{30}$$

Similarly $\sigma_{ij}(u)$ can be written as

$$\sigma_{ij} = \tilde{\sigma}_{ij} + \sum_m \Phi_{ijm} \tag{31}$$

The smooth parts of u, σ_{ij} and S can be related according to

$$\tilde{\sigma}_{ij} = \sigma_{ij}(\tilde{u}) = (-\frac{\partial^2}{\partial x_i \partial x_j} + \delta_{ij}\Delta)w + \delta_{ij}V \tag{32}$$

Now combining Propositions (1) and (2) and applying them to the smooth parts of the solutions we get

$$||\tilde{\sigma}_{ij}(u)||_{k+1} \leq c\{||w||_{k+3}\} \tag{33}$$

and

$$||\tilde{u}||_{k+2} \leq c\{||w||_{k+3}+||\tilde{u}||_0\} \tag{34}$$

From Theorem (1) we have

$$||w||_{k+3} \leq c\{||F||_{k-1}+||g||_{k+\frac{1}{2}}+||s||_2\}$$

or as F is a linear functional of f given by (18)

$$||F||_{k-1} \leq c||f||_k$$

we obtain

$$||w||_{H^{k+3}(\Omega)} \leq c\{||f||_{(H^k(\Omega))^2} + ||g||_{(H^{k+\frac{1}{2}}(\Gamma))^2} + ||s||_{H^2(\Omega)}\} \tag{35}$$

substituting (35), into (33)and (34) we have

$$||\tilde{\sigma}_{ij}||_{H^{k+1}(\Omega)} \leq c\{||f||_{(H^k(\Omega))^2} + ||g||_{(H^{k+\frac{1}{2}}(\Gamma))^2} + ||s||_{H^2(\Omega)}\}$$

and (36)

$$||\tilde{u}||_{(H^{k+2}(\Omega))^2} \leq c\{||f||_{(H^k(\Omega))^2} + ||g||_{(H^{k+\frac{1}{2}}(\Gamma))^2} + ||s||_{H^2(\Omega)}$$

$$+ ||\tilde{u}||_{(L_2(\Omega))^2}\}$$

$$\leq c\{||f||_{(H^k(\Omega))^2} + ||g||_{(H^{k+\frac{1}{2}}(\Gamma))^2} + ||s||_{H^2(\Omega)} +$$

$$+ ||\tilde{u}||_{(H^1(\Omega))^2}\} \tag{37}$$

using usual arguments on the uniqueness of solutions $\tilde{u}$ and S

$$||S||^2_{H^2(\Omega)} \leq c\{||f||^2_{(H^k(\Omega))^2} + ||g||^2_{(H^{k+\frac{1}{2}}(\Gamma))^2}\} \tag{38}$$

$$||\tilde{u}||^2_{H^1(\Omega)} \leq c\{||f||^2_{(H^k(\Omega))^2} + ||g||^2_{(H^{k+\frac{1}{2}}(\Gamma))^2}\} \tag{39}$$

The assertion of the theorem follows. #

Also, it can easily be seen from (36) that:

$$||\tilde{\sigma}_{ij}||^2_{H^{k+1}} \leq c\{||f||^2_{(H^k(\Omega))^2} + ||g||^2_{(H^{k+\frac{1}{2}}(\Gamma))^2}\} \tag{40}$$

Corollary

Let Ω be *convex* domain with a finite number of vertices. Let $f \in (L_2(\Omega))^2$ and $g \in (H^{\frac{1}{2}}(\Gamma))^2$ and let u be a solution of (11)-(12). Then

$$u \in (H^2(\Omega))^2 \tag{41}$$

Moreover, there exists a constant $c > 0$ such that

$$||u||^2_{(H^2(\Omega))^2} \leq c\{||f||^2_{(L_2(\Omega))^2} + ||g||^2_{(H^{\frac{1}{2}}(\Gamma))^2}\} \quad \# \tag{42}$$

This follows from the above theorem when we notice that $R(\xi)$ has no poles in the strip $1 \leq \mathrm{Im}\xi < 2$ for convex domains (see Corollary to Theorem 2) and hence $u \equiv \tilde{u}$. #

II.6.1.3 Application to crack problems

The preceeding results are now applied to the crack problem. This corresponds to the special case where $\omega = 2\pi$. The poles of $R(\xi)$ are roots

of the equation

$$\sin 2\pi(1+i\xi) = 0 \tag{43}$$

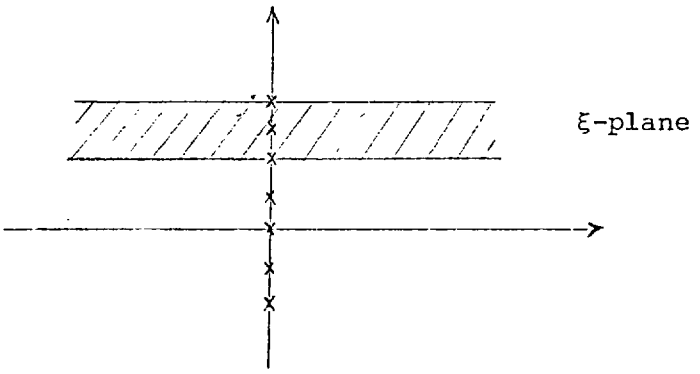

This equation has no repeated pole and therefore according to Theorem (1) the following expansion holds for $S \in H^2(\Omega)$

$$S = \sum_j a_j r^{-i\xi_j} f_{jq}(r\ell n^q r) + \sum_{\ell \geq 1} c_{\ell p} r^{\ell} \ell n^p r\, g_{\ell p}(\theta) + w \tag{44}$$

$$1 \leq \mathrm{Im}\xi_j \leq m+2,\ m \geq 0$$

We have assumed $f \in (H^m(\Omega))^2$, $g \in (H^{m+\frac{1}{2}}(\Gamma))^2$ and hypothesis of Theorem (1) are satisfied.

The behaviour of the solution is seen to be dependent on ξ_j. Suppose $V \in H^1(\Omega)$ so that we have square integrable data. We consider the pole distribution in the strip $1 \leq \mathrm{Im}\xi_j < 2$. In this region there is only one non-integer pole at $\xi = 3/2\, i$. This pole introduces the dominant singular term of the form $r^{3/2}\psi(\theta)$ in the expansion of S. The other poles at $\xi = i,\ 2i$ give rise to polynomials rf_{jq} and $r^2 f_{jq}$. We can also find the function $\psi(\theta)$ at the pole $\xi = 3/2\, i$ from (19), as $\psi(\theta) = c_1 \cos \theta/2 + c_2 \sin \theta/2 + c_2 \sin 3\theta/2 + 3c_1 \cos 3\theta/2$ where c_1 and c_2 can be interpreted in terms of stress intensity factors K_I and K_{II}.

$$\begin{cases} K_I = 3c_1 \\ K_{II} = -c_2 \end{cases}$$

The following expansions are therefore derived for S, σ_{ij} and u. (For a heuristic derivation of the expansion for S we refer to the work of Williams [8].)

$$S = w + \sum_j r^{j+\frac{1}{2}} \psi_j(\theta), \quad w \in H^{j+2}(\Omega) \qquad (j > 0 \text{ integer}) \tag{45}$$

$$\sigma_{ij} = \tilde{\sigma}_{ij} + \sum_\ell r^{\ell-3/2} \rho_{ij\ell}(\theta), \quad \tilde{\sigma}_{ij} \in H^{\ell}(\Omega) \qquad (\ell > 0 \text{ integer}) \tag{46}$$

and

$$u = \tilde{u} + \sum_j r^{j-\frac{1}{2}} \chi_j(\theta), \quad \tilde{u} \in H^{j+1}(\Omega) \qquad (j > 0 \text{ integer}) \tag{47}$$

with the usual bounds on $\tilde{u}$, $\tilde{\sigma}_{ij}$ and w in terms of data.

For example with $f \in (L_2(\Omega))^2$ and $g \in H^{\frac{1}{2}}(\Gamma))^2$ we have

$$||\tilde{u}||_{(H^2(\Omega))^2} \leq c\{||f||_{(L_2(\Omega))^2} + ||g||_{(H^{\frac{1}{2}}(\Gamma))^2}\} \tag{48}$$

$$||\tilde{\sigma}_{ij}||_{,H^1(\Omega)} \leq c\{||f||_{(L_2(\Omega))^2} + ||g||_{(H^{\frac{1}{2}}(\Gamma))^2}\} \tag{49}$$

$$||w||_{H^3(\Omega)} \leq c\{||f||_{(L_2(\Omega))^2} + ||g||_{(H^{\frac{1}{2}}(\Gamma))^2}\} \tag{50}$$

where only one singular term is taken in the expansions.

II.7 ERROR ESTIMATES IN L_2 AND H^1 NORMS

In this section we develop some error estimates for crack problems. We use the previous results on the expansion of displacement for domains

with cracks in the form:

$$u = \sum_j \chi_j + \tilde{u}$$

where χ_i are the singular functions present due to thin cracks.

Notation

We denote by S^k the finite-dimensional space of singular functions $\{\chi_i\}_{i=1}^k$.

$(\tilde{H}^k(\Omega))^3$ means the space $(H^k(\Omega))^3$, $k > 0$, from which has been factored out the singular functions $\chi_i \in (H^k(\Omega))^3$, $i = 1,\ldots,k$.

We also note that $\tilde{H}^1(\Omega) \times S^k$ is isometrically isomorphic to $H^1(\Omega)$ (because $\chi_i \in H^1(\Omega)$, for all i).

Set

$$V^k(\Omega) = (\tilde{H}^k(\Omega))^3 \times S^k \cap B \qquad (51)$$

where

$$B = \{\phi \in (H^1(\Omega))^3 \mid \phi \text{ satisfies 'essential' homogeneous boundary conditions}\}$$

Then $u \in V^r$ and $||u||_{\tilde{(H^r(\Omega))}^3}$ means $||\tilde{u}||_{(H^r(\Omega))^3}$.

Further we assume that

(i) $a(u,v)$ is elliptic on V^1, bounded on $V^1 \times V^1$.

(ii) For all $f \in L_2(\Omega)$

$$a(v,u) = (f,v) \quad \text{for all } v \in V^1$$

has a unique solution $u \in V^2$.

The mapping so defined is written $(A^*)^{-1}$.

Now in the notation of [60] we introduce the family of finite-dimensional subspaces S_h^r of V^1 such that

$$\inf_{\chi \in S_h^r} ||v-\chi||_{(L_2(\Omega))^3} \leq ch^s ||v||_{(\tilde{H}^s(\Omega))^3} \tag{52}$$

$$\inf_{\chi \in S_h^r} ||v-\chi||_{V^1} \leq ch^{s-1} ||v||_{(\tilde{H}^s(\Omega))^3} \tag{53}$$

for all $1 \leq s \leq r$.

These approximating subspaces which include the singular basis functions are assumed to exist.

We have the following estimates in both V^1 and $L_2(\Omega)$:

Theorem 4

Fix r and h. Given $u \in V^1$, there exists a unique $u_h \in S_h^r$ such that

$$a(u_h,v) = a(u,v), \quad \text{for all } v \in S_h^r \tag{54}$$

If further we suppose that

$$u \in V^s, \quad 1 \leq s \leq r$$

then

(a) $$||u-u_h||_{V^1} \leq ch^{s-1} ||u||_{(\tilde{H}^s(\Omega))^3}$$

(b) $$||u-u_h||_{(L_2(\Omega))^3} \leq ch^s ||u||_{(\tilde{H}^s(\Omega))^3}$$

where c is a constant independent of u and h.

Proof

(a) For $w_h \in S_h^r$

$$a(u-u_h, w_h) = 0$$

It follows that for arbitrary $\chi \in S_h^r$

$$a(u-u_h, u-u_h) = a(u-u_h, u-\chi) + a(u-u_h, \overbrace{\chi-u_h}^{\in 0})$$

so

$$\alpha ||u-u_h||^2_{V^1} \leq a(u-u_h, u-u_h) \leq M||u-u_h||_{V^1} . ||u-\chi||_{V^1}$$

whence

$$||u-u_h||_{V^1} \leq \frac{M}{\alpha} \inf_{\chi \in S_h^r} ||u-\chi||_{V^1}$$

(a) follows from (53).

(b) (Nitsche-Aubin duality argument)

Given $g \in L_2$, define $\phi = (A^*)^{-1} g$

then

$$(u-u_h, g)_{L_2} = (u-u_h, A^*\phi) = a(u-u_h, \phi)$$

But

$$a(u-u_h, \chi) = 0, \quad \text{for all } \chi \in S_h^r$$

so

$$(u-u_h, g)_{L_2} = a(u-u_h, \phi-\chi)$$

whence

$$(u-u_h, g)_{L_2} \leq M||u-u_h||_{V^1} \inf_{\chi \in S_h^r} ||\phi-\chi||_{V^1}$$

$$\leq C||u-u_h||_{V^1} . h . ||\phi||_{\underset{H}{\sim}2} \quad \text{(by (53))}$$

but

$$||u-u_h||_{L_2} = \sup_{g\in L_2} \frac{(u-u_h,g)_{L_2}}{||g||_{L_2}}$$

so

$$||u-u_h||_{L_2} \leq (\sup_{g\in L_2} \frac{||\phi||_{\tilde{H}^2}}{||g||_{L_2}}).c.||u-u_h||_{V^1}.h$$

Recalling $\phi = (A^*)^{-1}g$,

$$(\sup_{g\in L_2} \frac{||\phi||_{\tilde{H}^2}}{||g||_{L_2}}) \leq ||A^{*-1}||_{L(L_2,\tilde{H}^2)}$$

and

$$||u-u_h||_{L_2} \leq ch||A^{*-1}||_{L(L_2,\tilde{H}^2)}.||u-u_h||_{V^1}$$

(b) now follows from (53). #

Corollary

When the conditions of Theorem (3) and Theorem (4) are satisfied we further conclude that

$$||u-u_h||^2_{(L_2(\Omega))} \leq ch^{k+2}\{||f||^2_{(H^k(\Omega))} + ||g||^2_{(H^{k+\frac{1}{2}}(\Gamma))}\} \qquad (55)$$

and

$$||u-u_h'||^2_{V^1} \leq ch^{k+1}\{||f||^2_{(H^k(\Omega))} + ||g||^2_{(H^{k+\frac{1}{2}}(\Gamma))}\} \qquad (56)$$

for some integer $k \geq 0$.

In particular, for $k = 0$, i.e. for square integrable data by including only the leading singular term in the subspace S_h^r and using polynomials of degree one as $\hat{p}$ (see Chapter I, Theorem (14)) so that we have the inclusion $p_1 \subset \hat{p}$ then

$$||u-u_h||_{V^1} \leq ch\{||f||_{(L_2(\Omega))^2} + ||g||_{(H^{\frac{1}{2}}(\Gamma))^2}\} \tag{57}$$

$$||u-u_h||_{(L_2(\Omega))^2} \leq ch^2\{||f||_{(L_2(\Omega))^2} + ||g||_{(H^{\frac{1}{2}}(\Gamma))^2}\} \tag{58}$$

which gives the best rates of convergence that can be achieved.

Remark

From the Corollary to Theorem (3) and the singular expansion for u it is clear that for *convex* domains $u \in (H^2(\Omega))^2$ but u does not necessarily belong to $(H^3(\Omega))^2$. This implies that when using interpolating polynomials of degree one over convex domains, inclusion of singularities could be avoided while still having h^2 rate of convergence in L_2 norm. However, *using higher order polynomials on convex domains without including singularities of appropriate form in the approximating subspaces will not give any improvement over linear elements.*

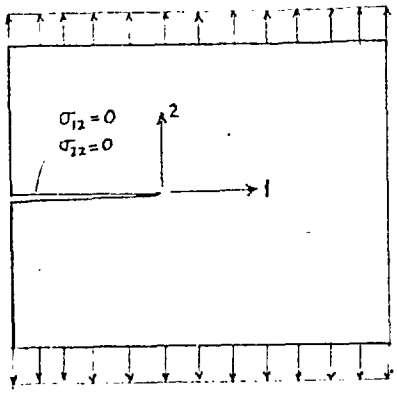

Fig (1)

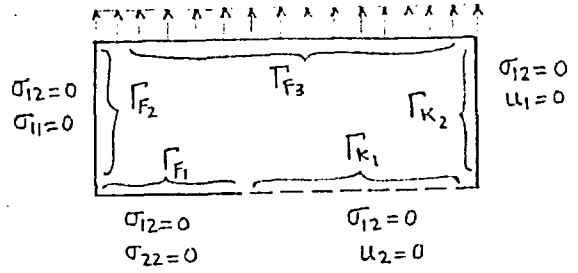

Fig (2)

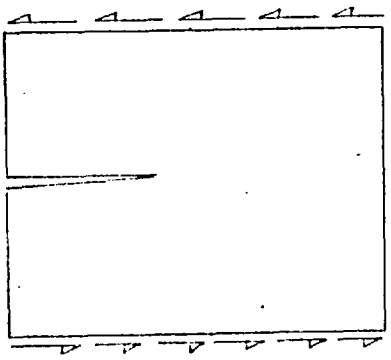

Fig (3)

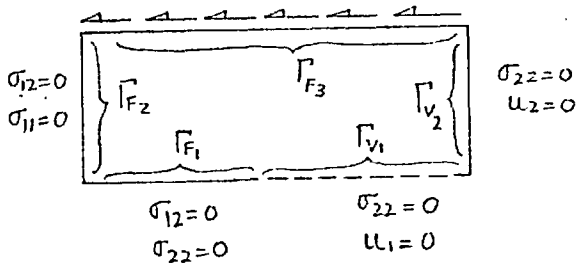

Fig (4)

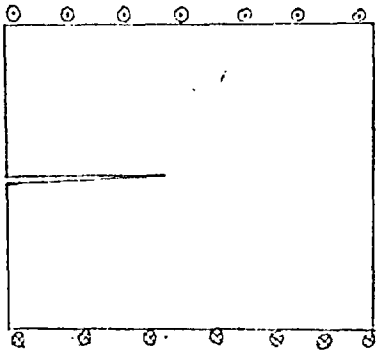

Fig (5)

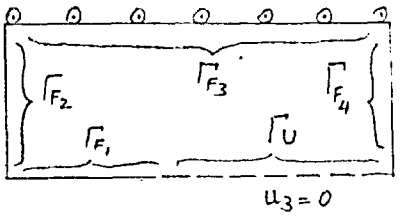

Fig (6)

Chapter III

ANALYSIS OF THE DYNAMIC STATIONARY CRACK PROBLEM

Equations of dynamic elasticity on regular slit domains are studied in this chapter. The problem is first put into a weak form and shown to possess a unique solution. In the existence and uniqueness proofs we heavily rely on our earlier result concerning ellipticity of the bilinear operator $a(\cdot,\cdot)$ on regular slit domains which was established in Chapter II (Section 5). We then proceed to obtain an approximate solution to the problem. It is to be noted that the treatment here is general and can be applied to any domain including convex domains or domains with cracks.

By *spatial* approximation of the weak form we reduce the problem to a system of ordinary differential equations in time. Using the earlier regularity results (see II.6) we obtain estimates for the continuous-time approximation error in terms of the 'smooth' part $\tilde{u}$ of the solution.

Since in any computational algorithm for field calculations we inevitably deal with finite dimensions we require a fully discrete approximation of the weak form in both time and space. In this respect we combine the approximations using finite elements in space and finite differences in time. A variety of difference approximations in time can be employed. We adopt the Newmark's scheme for its known unconditional stability and minimum truncation error. With the time-discretization we carry on to obtain estimates for the combined spatial-termporal approximation. It is formally proved that by inlcusion

of proper singular basis functions we can recover the best rates of convergence in time and space for the slit domains considered here, (e.g. crack problems).

Earlier Dupont [61] and Baker [62] have analysed a *single* hyperbolic equation on domains with *smooth* boundaries (see also [63]). The present work can be regarded as an extension of these results to the *system* of elastodynamic equations on *slit domains*.

III.1 NOTATIONS

Let Ω be a regular slit domain with boundary $\partial\Omega$. On the interval $[0,T] \subset R$ $(T < +\infty)$ and X a Banach space with the norm $||\cdot||_X$ we denote by $L_p([0,T];X)$ the space of functions $t \to f(t)$ measurable on $[0,T] \to X$ (for the measure dt) such that

$$||f||_{L_p([0,T];X)} > \left(\int_0^T ||f(t)||_X^p dt\right)^{1/p} < +\infty \quad (p \neq +\infty)$$

$$||f||_{L_\infty([0,T];X)} = \operatorname{ess\,sup}_{t\in[0,T]} ||f(t)||_X < +\infty$$

when X is a Hilbert space with the inner product $(\cdot,\cdot)_X$, the space $L_2([0,T];X)$ is also Hilbert for the scalar product

$$(f,g)_{L_2([0,T];X)} = \int_0^T (f,g)_X dt$$

We will also make use of the spaces $\tilde{H}^k(\Omega)$, $V^k(\Omega)$ and $S_h^r(\Omega)$ introduced in Chapter II.7

III.2 WEAK FORMULATION OF THE PROBLEM

For u a vector-valued function $u = (u_1, u_2)$ consider the equations of dynamic elasticity:

$$\frac{\partial u^2}{\partial t^2}(x,t) + Au(x,t) = f(x,t), \quad (x,t) \in \Omega \times I; \quad I =]0,T[\tag{1}$$

with the boundary conditions as either

$$u_i(x,t) = \bar{u}_i(x,t), \quad (x,t) \in \partial\Omega \times I \tag{2}$$

or

$$\sigma_{ij}(x,t)n_j = \bar{f}_i(x,t), \quad (x,t) \in \partial\Omega \times I \tag{3}$$

and the initial conditions

$$\begin{aligned} u(x,0) &= u_0(x,0), \quad x \in \Omega \\ \frac{\partial u}{\partial t}(x,0) &= v_0(x,0), \quad x \in \Omega \end{aligned} \tag{4}$$

In (1) A is the operator of elasticity:

$$(Au)_i = -\frac{\partial}{\partial x_j}(\sigma_{ij})$$

The corresponding weak variational problem is to find a solution (see Chapter II.7 for definition of V^1)

$$u \in L_2([0,T];V^1)$$

with $\frac{\partial^2 u}{\partial t^2} \in L_2([0,T];(V^1)')$, (duality with respect to $L^2(\Omega)$) such that

$$(\frac{\partial^2 u}{\partial t^2}(\cdot,t),v) + a(u(\cdot,t),v) = (f(\cdot,t),v), \quad \text{for all } v \in V^1, \ t > 0 \tag{5}$$

and

$$\begin{cases} (u(\cdot,0),v) = (u_0,v), & \text{for all } u_0 \in V^1 \\ (\frac{\partial u}{\partial t}(\cdot,0),v) = (v_0,v), & \text{for all } v_0 \in (L_2(\Omega))^3 \end{cases} \tag{6}$$

where

$$f(\cdot,t) \in L^2([0,T];(V^1)')$$

and

$$a(u,v) = \int_\Omega \sigma_{ij}(u)\varepsilon_{ij}(v)dx$$

is the bilinear form defined earlier (see Chapter II.1).

III.3 EXISTENCE OF A UNIQUE SOLUTION TO THE EQUATIONS OF DYNAMIC ELASTICITY

We introduce $\Phi(t)$ such that

$$\Phi(t) \in (H^1(\Omega))^3 \quad \text{and} \quad \Phi(t) = 0 \text{ on } \Gamma_U \tag{7}$$

(see Chapter II.1 for the meaning of Γ_U) and define

$$V_0 = \{v | v \in (H^1(\Omega))^3, \ v = 0 \text{ on } \Gamma_U\} \tag{8}$$

Then, replacing $u(t)$ by $u(t) - \Phi(t)$, the problem is reduced to finding a function $t \to u(t) : [0,T] \to V_0$ such that

$$(\frac{\partial^2 u}{\partial t^2},v) + a(u,v) = (\Psi(t),v) \quad \text{for all } v \in V_0 \tag{9}$$

where

$$(\Psi(t),v) = (f,v) + (\frac{\partial^2 \Phi}{\partial t^2},v) + a(\Phi(t),v) \tag{10}$$

with the previous initial conditions.

We introduce $H = (L^2(\Omega))^3$ and note that

$$V_0 \subset H, \quad V_0 \text{ is dense in } H \tag{11}$$

We denote the norm in V_0 (resp. H) by $||\cdot||$ (resp. $|\cdot|$) and the scalar product in H by $(\cdot,\cdot)$.

We identify H with its dual, then

$$H \subset V_0' \tag{12}$$

By $||\cdot||_*$ we denote the norm in V_0', dual to $||\cdot||$, then

$$||f||_* = \sup |(f,v)|, \quad v \in V_0, \quad ||v|| \leq 1$$

We have the following: [64, p. 125]:

Theorem 1

We assume that

$$\Psi, \Psi' \in L_2(0,T;(V^1)') \tag{13}$$

$$u_0 \in V^1, \quad v_0 \in H \tag{14}$$

There exists one and only one function u such that

$$u \in L_\infty(0,T;V^1) \tag{15}$$

$$u' \in L_\infty(0,T;H) \tag{16}$$

$$u'' \in L_\infty(0,T;(V^1)') \tag{17}$$

which satisfies (5) and (6).

Proof

With the previous results concerning V-ellipticity of a(u,v) for regular slit domains, the proof goes through in the standard way. We present the proof for the sake of completeness.

Assume that w_i, $i = 1, \ldots, m$ spans V^1 and

$$w_1 = u_0$$

We define u_m, the "approximate solution of order m" by

$$\begin{cases} u_m(t) \in [w_1,\ldots,w_m] \\ (u_m'',v) + a(u_m,v) = (\Psi(t),v), \quad \text{for all } v \in [w_1,\ldots,w_m] \\ u_m(0) = u_o \\ u_m'(0) = v_{0m}, \quad v_{0m} \in [w_1,\ldots,w_m], \quad v_{0m} \to v_0 \text{ in } H \text{ when } m \to \infty \end{cases} \tag{18}$$

(18) defines a system of m linear second order differential equations which is non-singular and therefore u_m is uniquely determined from it.

A Priori Estimates for u_m

If we take $v = u_m'(t)$ in (18) it follows that

$$\tfrac{1}{2}\frac{d}{dt}|u_m'(t)|^2 + \tfrac{1}{2}\frac{d}{dt}a(u_m,u_m) = (\Psi(t),u_m')$$

Integrating both sides,

$$|u_m'|^2 + a(u_m,u_m) = |v_{0m}|^2 + a(u_0,u_0) + 2\int_0^t (\Psi(\sigma),u_m'(\sigma))d\sigma$$

$$= |v_{0m}|^2 + a(u_0,u_0) + 2(\Psi(t),u_m(t)) - 2(\Psi(0),u_0)$$

$$- 2\int_0^t (\Psi'(\sigma),u_m(\sigma))d\sigma \qquad (19)$$

We also have

$$a(v,v) \geq \alpha||v||^2 - c|v|^2$$

$$|v_{0m}| \leq c|v_0|$$

$$2|(\Psi(t),u_m(t))| \leq \tfrac{1}{2}\alpha||u_m(t)||^2 + c||\Psi(t)||_*^2$$

So that (19) is written as

$$|u_m'(t)|^2 + \tfrac{1}{2}\alpha||u_m(t)||^2 \leq c(|v_0|^2 + ||u_0||^2 + ||\Psi(0)||_*^2)$$

$$+ c||\Psi(t)||_*^2 + c|u_m(t)|^2$$

$$+ c\int_0^t ||\Psi'(\sigma)||_* ||u_m(\sigma)||d\sigma \qquad (20)$$

But

$$u_m(t) = u_0 + \int_0^t u_m'(\sigma)\,d\sigma$$

$$|u_m(t)|^2 \leq 2|u_0|^2 + c\int_0^t |u_m'(\sigma)|^2 d\sigma$$

so that (20) becomes

$$|u_m'(t)|^2 + ||u_m(t)||^2 \leq c(|v_0|^2+||u_0||^2+||\Psi(0)||_*^2+||\Psi(t)||_*^2 + \int_0^t ||\Psi'(\sigma)||^2 d\sigma) + c\int_0^t (|u_m'(\sigma)|^2+||u_m(\sigma)||^2)\,d\sigma \quad (21)$$

We set

$$|||\Psi|||^2 = \int_0^t (||\Psi(t)||_*^2 + ||\Psi'(t)||_*^2)\,dt \quad (22)$$

and

$$\phi_m(t) = |u_m'(t)|^2 + ||u_m(t)||^2 \quad (23)$$

Then from (21) we have

$$\phi_m(t) \leq c(|v_0|^2+||u_0||^2+|||\Psi|||^2) + c\int_0^t \phi_m(\sigma)\,d\sigma \quad (24)$$

using Gronwall's inequality we get

$$\phi_m(t) \leq c(|v_0|^2+||u_0||^2+|||\Psi|||^2)\exp(ct) \quad (25)$$

and hence we conclude that

$$\left\| \begin{array}{l} u_m \text{ (resp. } u_m') \text{ remains in a bounded subset of } L_\infty(0,T;V^1) \\ \text{(resp. } L_\infty(0,T;H)) \text{ when } m \to \infty \end{array} \right. \quad (26)$$

This means that we can select a subsequence u_μ from u_m such that

$$\| \quad u_\mu(\text{resp. } u'_\mu) \to u(\text{resp. } u') \text{ weakly star in } L_\infty(0,T;V^1)(\text{resp. } L_\infty(0,T;H \tag{27}$$

Now we have to verify that u is *a solution* to the problem. We introduce the space E of functions ϕ of the form

$$\phi(t) = \sum_{j=1}^{\mu_0} \phi_j(t) w_j, \quad \phi_j \in C^1(0,T), \quad \phi_j(T) = 0 \tag{28}$$

μ_0 is an arbitrary finite integer.

From (18) we conclude for $m = \mu > \mu_0$ that

$$(u''_\mu, \phi) + a(u_\mu, \phi) - (\Psi, \phi) = 0 \text{ for } \phi \text{ given by (28)}$$

or

$$\int_0^T [-(u'_\mu, \phi') + a(u_\mu, \phi) - (\Psi, \phi)]dt = (v_{0\mu}, \phi(0)) \tag{29}$$

passing to the limit with μ in (29)

$$\int_0^T [-(u', \phi') + a(u, \phi) - (\Psi, \phi)]dt = (v_0, \phi(0)), \quad \text{for all } \phi \in E \tag{30}$$

Since the finite linear combination of the w_j are dense in V^1, we obtain (30), for all $\phi \in C^1(0,T;(V^1)')$, $\phi(T) = 0$.

From this we deduce that, in the sense of distributions, on $]0,T[$ with values in V^1

$$u'' + Au = \Psi \tag{31}$$

where $A \in L(V^1;(V^1)')$ is defined by

$$a(u,v) = (Au,v), \quad \text{for all } u, v \in V^1 \tag{32}$$

Therefore $u'' = \Psi - Au \in L_\infty(0,T;(V^1)')$. Taking the scalar product of the two sides of (31) with, say, $\phi \in E$ and comparing with (30) we conclude that

$$(v_0,\phi(0)) = (u'(0),\phi(0)), \quad \text{for all } \phi \in E$$

from which follows that $u'(0) = v_0$. Since (27) implies that $u_\mu(0)=u_0 \to u(0)$ we have $u(0) = u_0$ and u satisfies the conditions of Theorem (1).

We now prove the *uniqueness* of the solution. Let u satisfy (15), (16) and (17) with

$$u'' + Au = 0 \qquad u(0) = 0 \qquad u'(0) = 0 \tag{33}$$

For, say,

$$\phi \in C^1(0,T;(V^1)')$$

according to the first part of the proof, changing t to t-T, there exists a function w such that

$$w \in L_\infty(0,T;V^1), \quad w' \in L_\infty(0,T;H), \quad w'' \in L_\infty(0,T;(V^1)') \tag{34}$$

$$w'' + Aw = \phi \tag{35}$$

$$w(T) = 0, \quad w'(T) = 0 \tag{36}$$

The formula for integration by parts is valid

$$\int_0^T (u'',w)\,dt = \int_0^T (u,w'')\,dt \tag{37}$$

Thus taking the scalar product of the two sides of (33) with $\dot{w}$ and making use of (37) we obtain (using symmetry of $a(u,v)$)

$$\int_0^T (u,w''+Aw)\,dt = 0$$

i.e.

$$\int_0^T (u,\phi)\,dt = 0, \text{ for all } \phi \in C^1(0,T;(V^1)'). \quad \text{Therefore } u \equiv 0$$

The proof is now complete. #

III.4 THE CONTINUOUS-TIME GALERKIN APPROXIMATION

Let h, $0 < h < 1$, be a parameter and $r \geq 2$ be a fixed integer. Now introduce the family of finite-dimensional subspaces $S_h^r(\Omega)$ of $V^1(\Omega)$ (see II.7 for definition of S_h^r). The continuous-time Galerkin approximation to the problem (5)-(6) consists of finding a differentiable function $U_h(\cdot,t) \in S_h^r(\Omega)$ such that

$$\left(\frac{\partial^2 U_h}{\partial t^2}(\cdot,t),v\right) + a(U_h(\cdot,t),v) = (f(\cdot,t),v), \quad \text{for all } v \in S_h^r(\Omega), \quad t > 0 \tag{38}$$

$$(U_h(\cdot,0),v) = (u_0,v), \quad \text{for all } v \in S_h^r(\Omega) \tag{39}$$

$$\left(\frac{\partial U_h}{\partial t}(\cdot,0),v\right) = (v_0,v), \quad \text{for all } v \in S_h^r(\Omega) \tag{40}$$

In the following we investigate the existence of a unique solution U_h to (38)-(40) and give estimates for the approximation error $u - U_h$. We need the following two lemmas:

Lemma 1

Suppose that for some $k \geq 0$

$$\frac{\partial^k u(t)}{\partial t^k} \in L_p(0,T;V)$$

and

$$a(\omega_h(t),v) = a(u(t),v), \text{ for all } v \in S_h^r(\Omega) \text{ (elliptic projection)}$$

Then

$$\frac{\partial^k \omega_h(t)}{\partial t^k} \in L_p(0,T;S_h^r)$$

and

$$a\left(\frac{\partial^k \omega_h(t)}{\partial t^k},v\right) = a\left(\frac{\partial^k u(t)}{\partial t^k},v\right), \quad \text{for all } v \in S_h^r(\Omega)$$

Proof (by induction).

The lemma is obviously true for $k = 0$. Suppose it holds for $k = \bar{k}$ and furthermore

$$\frac{\partial^{\bar{k}+1}}{\partial t^{\bar{k}+1}} u \in L_p(0,T;V) \tag{41}$$

Define $\tilde{\omega}(t) \in S_h^r$ by

$$a(\tilde{\omega}(t),v) = a\left(\frac{\partial^{\bar{k}+1} u}{\partial t^{\bar{k}+1}},v\right), \quad \text{for all } v \in S_h^r(\Omega) \tag{42}$$

Setting $v = \tilde{\omega}(t)$, ellipticity of $a(\cdot,\cdot)$ on V gives

$$|\tilde{\omega}(t)|_V^2 \leq \text{const } \left|\frac{\partial^{\bar{k}+1} u(t)}{\partial t^{\bar{k}+1}}\right|_V \cdot |\tilde{\omega}(t)|_V$$

whence by (41)

$$\tilde{\omega}(t) \in L_p(0,T;S_h^r)$$

integrating both sides of (42)

$$a(\int_0^t \tilde{\omega}(\tau)d\tau, v) = a(\int_0^t \frac{\partial^{\bar{k}+1} u(\tau)}{\partial t^{\bar{k}+1}} d\tau, v)$$

$$= a(\frac{\partial^{\bar{k}} u(t)}{\partial t^{\bar{k}}}, v) - a(\frac{\partial^{\bar{k}} u(0)}{\partial t^{\bar{k}}}, v)$$

Now define $z \in S_h^r$ by

$$a(z,v) = a(\frac{\partial^{\bar{k}} u(0)}{\partial t^{\bar{k}}}, v), \quad \text{for all } v \in S_h^r(\Omega)$$

Then

$$a(z+\int_0^t \tilde{\omega}(\tau)d\tau, v) = a(\frac{\partial^{\bar{k}} u(t)}{\partial t^{\bar{k}}}, v), \quad \text{for all } v \in S_h^r(\Omega)$$

By the induction hypothesis

$$\frac{\partial^{\bar{k}} \omega_h}{\partial t^{\bar{k}}} = z + \int_0^t \tilde{\omega}(\tau)d\tau$$

and since $\tilde{\omega} \in L_p(0,T;S_h^r)$

$$\frac{\partial^{\bar{k}+1}}{\partial t^{\bar{k}+1}} \omega_h = \tilde{\omega} \in L_p(0,T;S_h^r)$$

(42) now gives

$$a(\frac{\partial^{\bar{k}+1}}{\partial t^{\bar{k}+1}} \omega_h(t), v) = a(\frac{\partial^{\bar{k}+1}}{\partial t^{\bar{k}+1}} u(t), v), \quad \text{for all } v \in S_h^r(\Omega)$$

as required. #

Lemma 2

Let $u(t)$ solve the dynamic problem (5)-(6). Then there exists a unique mapping $\omega_h \in L_2(0,T;S_h^r)$ such that

$$a(\omega_h(t),v) = a(u(t),v), \quad \text{for all } v \in S_h^r \tag{43}$$

If, for some $k \geq 0$

$$\frac{\partial^k u}{\partial t^k} \in L_p(0,T;(\tilde{H}^s(\Omega))^2)$$

Then

$$\frac{\partial^k \omega_h}{\partial t^k} \in L_p(0,T;S_h^r)$$

and

$$\left|\left|\left(\frac{\partial}{\partial t}\right)^k [u-\omega_h]\right|\right|_{L_p(0,T;(L_2(\Omega))^2)} \leq ch^s \left|\left|\left(\frac{\partial}{\partial t}\right)^k u\right|\right|_{L_p(0,T;(\tilde{H}^s(\Omega))^2)}$$

for some constant c independent of u and h and $1 \leq s \leq r$.

Proof

The lemma follows immediately from Theorem 4 (Chapter II.7) and Lemma 1. #

Now we can give estimates for the rate of convergence of the semi-discrete approximation error involved in our scheme.

Theorem 2

Let $u(t)$ solve the dynamic problem (5)-(6). For each h there exists a unique mapping $U_h(t) \in L_2(0,T;S_h^r)$ such that (38)-(40) hold. Furthermore if $u(t) \in L_\infty(0,T;V^r(\Omega))$ and $\frac{\partial u(t)}{\partial t} \in L_2(0,T;V^r(\Omega))$ then there exists a constant $c = c(T)$ independent of h and $u(t)$ such that

$$||(u-U_h)(t)||_{L_\infty(0,T;(L_2(\Omega))^2)} \leq ch^r[||u(t)||_{L_\infty(0,T;(\tilde{H}^r(\Omega))^2)}$$

$$+ ||\frac{\partial u}{\partial t}(t)||_{L_2(0,T;(\tilde{H}^r(\Omega))^2)} \quad \#$$

Proof

Except for some changes in the functional spaces and the fact that u is a vector-valued function the arguments of Baker [62] go through exactly in our setting. However, for the sake of completeness we write the proof out here.

The existence of a unique solution $U_h(t) \in S_h^r$ (finite-dimensions) follows from the standard arguments in the theory of ordinary differential equations.

Now let ω_h be defined by (43) and set

$$\eta = u - \omega_h, \quad \psi = U_h - \omega_h \quad \text{and} \quad \ell = u - U_h$$

From (38), (43) and (15)

$$(\frac{\partial^2 \psi}{\partial t^2}(t),v) + a(\psi(t),v) = (f(t),v) - (\frac{\partial^2 \omega_h}{\partial t^2}(t),v) - a(\omega_h(t),v)$$

$$= (f(t),v) - a(u(t),v) - (\frac{\partial^2 \omega_h}{\partial t^2}(t),v)$$

$$= (\frac{\partial^2 \eta}{\partial t^2}(t),v) \quad \text{for all } v \in S_h^r(\Omega),\ t > 0 \tag{44}$$

Now rewriting (44)

$$\frac{d}{dt}(\frac{\partial \psi}{\partial t},v) - (\frac{\partial \psi}{\partial t},\frac{\partial v}{\partial t}) + a(\psi,v) = \frac{d}{dt}(\frac{\partial \eta}{\partial t},v) - (\frac{\partial \eta}{\partial t},\frac{\partial v}{\partial t}) \quad \text{for all } v \in S_h^r(\Omega) \tag{45}$$

Since $\ell = \eta - \psi$, (45) is written as

$$-(\frac{\partial \psi}{\partial t},\frac{\partial v}{\partial t}) + a(\psi,v) = -\frac{d}{dt}(\frac{\partial \ell}{\partial t},v) - (\frac{\partial \eta}{\partial t},\frac{\partial v}{\partial t}), \text{ for all } v \in S_h^r(\Omega),\ t > 0 \tag{46}$$

With the particular choice of

$$\hat{v}(\cdot,\tau) = \int_t^\xi \psi(\cdot,\tau)d\tau, \quad 0 \le t \le T \quad \text{and} \quad 0 < \xi \le T \tag{47}$$

in (46) we have

$$\tfrac{1}{2}\frac{d}{dt}\{||\psi||^2\} - \tfrac{1}{2}\frac{d}{dt}a(\hat{v},\hat{v}) = \frac{d}{dt}(\frac{\partial \ell}{\partial t},\hat{v}) + (\frac{\partial \eta}{\partial t},\psi) \tag{48}$$

(note that from (47) $\frac{\partial \hat{v}}{\partial t}(t) = -\psi(t)$, $0 \le t \le T$ and $\hat{v}(\xi) = 0$). Now integrating (48) from $t = 0$ to $t = \xi$ we have

$$||\psi(\xi)||^2 - ||\psi(0)||^2 + a(\hat{v}(0),\hat{v}(0)) = -2(\frac{\partial \ell}{\partial t}(0),\hat{v}(0)) + 2\int_0^\xi (\frac{\partial \eta}{\partial t}(t),\psi(t))dt \tag{49}$$

Now from (40) it follows that

$$(\frac{\partial \ell}{\partial t}(0),v) = 0, \quad \text{for all } v \in S_h^r(\Omega) \tag{50}$$

Hence using (50) and ellipticity of the bilinear form $a(\cdot,\cdot)$ we reduce (49) to

$$\begin{aligned} ||\psi(\xi)||^2 &\le ||\psi(0)||^2 + 2\int_0^\xi (\frac{\partial \eta}{\partial t}(t),\psi(t))dt \\ &\le ||\psi(0)||^2 + 2\sqrt{T}||\psi||_{L_\infty(0,T;(L^2(\Omega))^2)}||\frac{\partial \eta}{\partial t}||_{L_2(0,T;(L_2(\Omega))^2)} \\ &\le ||\psi(0)||^2 + \tfrac{1}{2}||\psi||^2_{L_\infty(0,T;(L^2(\Omega))^2)} + 2T||\frac{\partial \eta}{\partial t}||^2_{L_2(0,T;(L^2(\Omega))^2)} \end{aligned} \tag{51}$$

Now taking the supremum in (51) over the variable $0 \leq \xi \leq T$, we obtain

$$\tfrac{1}{2}||\psi||^2_{L_\infty(0,T;(L^2(\Omega))^2)} \leq ||\psi(0)||^2 + 2T||\frac{\partial \eta}{\partial t}||^2_{L_2(0,T;(L^2(\Omega))^2)} \tag{52}$$

or

$$||\psi||_{L_\infty(0,T;(L^2(\Omega))^2)} \leq \sqrt{2}||\psi(0)|| + 2\sqrt{T}||\frac{\partial \eta}{\partial t}||_{L_2(0,T;(L^2(\Omega))^2)} \tag{53}$$

From (53),

$$||\ell||_{L_\infty(0,T;(L^2(\Omega))^2)} \leq ||\eta||_{L_\infty(0,T;(L^2(\Omega))^2)} + ||\psi||_{L_\infty(0,T;(L^2(\Omega))^2)}$$

$$\leq ||\eta||_{L_\infty(0,T;(L^2(\Omega))^2)} + 2\sqrt{T}||\frac{\partial \eta}{\partial t}||_{L_2(0,T;(L^2(\Omega))^2)} + \sqrt{2}||\psi(0)||$$

$$\leq ||\eta||_{L_\infty(0,T;(L^2(\Omega))^2)} + 2\sqrt{T}||\frac{\partial \eta}{\partial t}||_{L_2(0,T;(L^2(\Omega))^2)} + \sqrt{2}||\eta(0)|| + \sqrt{2}||\ell(0)|| \tag{54}$$

Now from (39) and equations (52)-(53) (chapter II.7) we have

$$||\ell(0)|| \leq ch^r||u_0||_r \leq ch^r||u(t)||_{L_\infty(0,T;(\tilde{H}^r(\Omega))^2)} \tag{55}$$

Hence using (55) and Lemma 2 in (54) we get

$$||\ell||_{L_\infty(0,T;(L^2(\Omega))^2)} \leq c(T)h^r\{||u||_{L_\infty(0,T;(\tilde{H}^r(\Omega))^2)} + ||\frac{\partial u}{\partial t}||_{L_2(0,T;(\tilde{H}^r(\Omega))^2)}\}$$

The result of Theorem 2 now follows. #

Remark

It is noted that similar results can be obtained in V^1 norm.

III.5 THE DISCRETE-TIME GALERKIN APPROXIMATION

In this section we study the fully-discrete approximation to the equations of dynamic elasticity and derive estimates for the rate of convergence of the solution in $L_2(0,T;L_2)$ norm. Our analysis differs from Baker [62] in that we use a different approximation scheme in time for the *system* of equations on *slit domains*.

Let $T = N\tau$ for some integer $N \geq 1$; for a sequence $\{W^n\}_{n=0}^N \subset (L^2(\Omega))^2$, we define

$$\partial_+ W^n = \frac{W^{n+1}-W^n}{\tau} \tag{56}$$

$$\partial_- W^n = \frac{W^n-W^{n-1}}{\tau} \tag{57}$$

$$W^{n+\frac{1}{2}} = \frac{W^{n+1}+W^n}{2} \tag{58}$$

$$W^{n,\theta} = \theta W^{n+1} + (1-2\theta)W^n + \theta W^{n-1}, \quad \theta \in [0,1] \tag{59}$$

for $n = 1, 2, \ldots, N-1$.

Also for a continuous mapping $W : [0,T] \to (H^1(\Omega))^2$, we define $W^n = W(\cdot,n\tau)$, $1 \leq n \leq N$.

Define the discrete-time Galerkin approximation to be a sequence $\{U_h^n\}_{n=0}^N \subset S_h^r$ such that U_h^n approximates u^n optimally in $(L^2(\Omega))^2$.

The following lemma defines the Galerkin approximation $\{U_h^n\}_{n=0}^N$

in terms of an auxiliary sequence $\{V_h^n\}_{n=1}^N \subset S_h^r(\Omega)$.

Lemma 3

There exists a unique sequence $\{U_h^n\}_{n=0}^N \subset S_h^r$ and a corresponding unique sequence $\{V_h^n\}_{n=1}^N$ which simultaneously satisfy the equations

$$\begin{cases} (U_h^1,\chi) \equiv (u_1,\chi) & \text{for all } \chi \in S_h^r(\Omega) \quad (60) \\ (V_h^1,\chi) \equiv (\left(\frac{\partial u}{\partial t}\right)^1,\chi) & \text{for all } \chi \in S_h^r(\Omega) \quad (61) \end{cases}$$

and

$$\begin{cases} (\partial_+ V_h^n,\chi) + a(U_h^{n,\frac{1}{4}},\chi) = (f^{n,\frac{1}{4}},\chi), & \text{for all } \chi \in S_h^r(\Omega) \quad (62) \\ \partial_- U_h^n = V_h^n, \quad 1 \le n \le N-1 & (63) \end{cases}$$

Proof

It is clear that U_h^1 and V_h^1 exist uniquely. (And hence from (63) so does U_h^0.)

From (56) and (62)-(63) V_h^{n+1} satisfies

$$B_\tau(V_h^{n+1},\chi) = F^n\chi, \quad \text{for all } \chi \in S_h^r, \quad 1 \le n \le N-1$$

where $B_\tau(\cdot,\cdot)$ is the bilinear form given by

$$B_\tau(U,V) = \frac{\tau^2}{4}\, a(U,V) + (U,V)$$

and F^n is the linear functional given by

$$F^n V = \tau[(F^{n,\frac{1}{4}},V) - a(U_h^n,V)] + (V_h^n,V) + \frac{\tau^2}{4}\, a(V_h^n,V)$$

From ellipticity of $a(\cdot,\cdot)$, $B_\tau(\cdot,\cdot)$ is positive definite, so V_h^{n+1} exists uniquely and hence from (63) U_h^{n+1} exists uniquely for $1 \leq n \leq N-1$. #

Note

In the above definition of the discrete-time Galerkin approximation we have chosen $\theta = \frac{1}{4}$. The reason for this choice, rather than Baker's one, is due to the well-known unconditional stability of the scheme for $\theta \geq \frac{1}{4}$. In particular, the resulting spectral radius would remain constant for the choice of $\theta = \frac{1}{4}$ which indicates the minimal truncation error is achieved. This will be explained in more detail in the chapter on computational results. #

Before proceeding to get estimate for the error $||u^n - u_h^n||$ we introduce the following functions

$$\xi^n = U_h^n - \omega_h^n, \qquad 0 \leq n \leq N \tag{64}$$

$$W^n = V_h^n - \left(\frac{\partial \omega_h}{\partial t}\right)^n, \qquad 1 \leq n \leq N \tag{65}$$

$$\eta = u - \omega_h \tag{66}$$

where ω_h is defined by (43). We prove the following lemma.

Lemma 4

Let $u(t)$ be the solution of (5)-(6) and suppose that

$$\frac{\partial u}{\partial t} \in L_2(0,T;V^r(\Omega)) \quad \text{and} \quad \left(\frac{\partial}{\partial t}\right)^k u \in L_2(0,T;(L_2(\Omega))^2)$$

for $k = 3, 4$; then for some constant $c = c(T)$ independent of h and τ,

$$\max_{1\le n\le N} ||\xi^n|| \le \sqrt{2}\,||\xi^1|| + c\{h^r ||\frac{\partial u}{\partial t}||_{L_2(0,T;(\tilde{H}^r(\Omega))^2)} +$$

$$\tau^2[||\frac{\partial^3 u}{\partial t^3}||_{L_2(0,T;(L_2(\Omega))^2)} + ||\frac{\partial^4 u}{\partial t^4}||_{L_2(0,T;(L_2(\Omega))^2)}]\}$$

Proof

With the given time-discretization the proof requires some modifications to Baker's argument. From (5) for $t = n\tau$ we have

$$((\frac{\partial^2 u}{\partial t^2})^{n,\frac{1}{4}},\chi) + a(u^{n,\frac{1}{4}},\chi) = (f^{n,\frac{1}{4}},\chi) \quad \text{for all } \chi \in S_h^r(\Omega),\ t > 0 \tag{67}$$

or

$$(\partial_+(\frac{\partial u}{\partial t})^n,\chi) + a(u^{n,\frac{1}{4}},\chi) = (f^{n,\frac{1}{4}}+\rho^n,\chi)$$

where

$$\rho^n = \partial_+(\frac{\partial u}{\partial t})^n - (\frac{\partial^2 u}{\partial t^2})^{n,\frac{1}{4}} \qquad 1 \le n \le N-1 \tag{68}$$

Now from (62), (64), (65), (43) and (67), for all $\chi \in S_h^r(\Omega)$ we have

$$\begin{aligned}(\partial_+ W^n,\chi) + a(\xi^{n,\frac{1}{4}},\chi) &= (\partial_+ V_h^n,\chi) + a(U_h^{n,\frac{1}{4}},\chi) - (\partial_+(\frac{\partial \omega_h}{\partial t})^n,\chi) \\ &\quad - a(\omega_h^{n,\frac{1}{4}},\chi) \\ &= (f^{n,\frac{1}{4}},\chi) - a(u^{n,\frac{1}{4}},\chi) - (\partial_+(\frac{\partial \omega_h}{\partial t})^n,\chi) \\ &= (\partial_+(\frac{\partial u}{\partial t})^n,\chi) - (\partial_+(\frac{\partial \omega_h}{\partial t})^n,\chi) - (\rho^n,\chi) \\ &= (\partial_+(\frac{\partial \eta}{\partial t})^n - \rho^n,\chi) \qquad 1 \le n \le N-1 \end{aligned} \tag{69}$$

Also from (63) and (65) we obtain

$$\partial_+\xi^n = \partial_+(U_h^n-\omega_h^n) = \partial_- U_h^{n+1} - \partial_+\omega_h^n = V_h^{n+1} - \partial_+\omega_h^n$$

$$= W^{n+1} + (\frac{\partial\omega_h}{\partial t})^{n+1} - \partial_+\omega_h^n$$

$$= W^{n+1} + \partial_+\eta^n - (\frac{\partial\eta}{\partial t})^{n+1} - \sigma^n \qquad (70)$$

where

$$\sigma^n = \partial_+ u^n - (\frac{\partial u}{\partial t})^{n+1} \qquad 1 \le n \le N-1 \qquad (71)$$

From (70)

$$\partial_+\xi^n = W^1 + \tau\sum_{k=1}^{n}\partial_+ W^k + \partial_+\eta^n - (\frac{\partial}{\partial t}\eta)^{n+1} - \sigma^n \qquad (72)$$

Now we define a sequence $\{\mu^m\}_{m=0}^N$ by

$$\begin{cases} \mu^0 = -\tau\xi^1 \\ \\ \mu^n = \tau\sum_{k=1}^{n}\xi^k \qquad 1 \le n \le N \end{cases} \qquad (73)$$

Then

$$\mu^{n,\frac{1}{4}} = \tau\sum_{k=1}^{n}\xi^{k,\frac{1}{4}} + \frac{\tau}{4}(\xi^1-\xi^0) \qquad (74)$$

and

$$\mu^{\frac{1}{2}} = 0 \qquad (75)$$

and hence from (72), (74) and (69), for any $\chi \in S_h^r(\Omega)$ and $1 \le n \le N-1$ we get

$$(\partial_+\xi^n,\chi) + a(\mu^{n,\frac{1}{4}},\chi) = (W^1+\partial_+\eta^n-(\frac{\partial}{\partial t}\eta)^{n+1}-\sigma^n,\chi)$$

$$+ (\tau\sum_{k=1}^{n}\partial_+ W^k,\chi) + a(\tau\sum_{k=1}^{n}\xi^{k,\frac{1}{4}},\chi) + \frac{\tau}{4}a(\xi^1-\xi^0,\chi)$$

$$= (W^1+\partial_+\eta^n-(\frac{\partial\eta}{\partial t})^{n+1}-\sigma^n,\chi) + (\tau[\sum_{k=1}^{n}\partial_+(\frac{\partial\eta}{\partial t})^k-\rho^k],\chi)$$

$$+ \frac{\tau}{4}a\,(U^1-u^1+u^1-\omega_h^1-(U^0-u^0+u^0-\omega_h^0),\chi)$$

using the elliptic projection property

$$= W^1+\partial_+\eta^n-(\frac{\partial\eta}{\partial t})^{n+1}-\sigma^n,\chi) + ((\frac{\partial\eta}{\partial t})^{n+1}-(\frac{\partial\eta}{\partial t})^1-\tau\sum_{k=1}^{n}\rho^k,\chi)$$

$$+ \frac{\tau}{4}a\,(U^1-u^1-(U^0-u^0),\chi) \quad (U^0-u^0 \to 0)$$

$$= (W^1-(\frac{\partial\eta}{\partial t})^1,\chi) + (\partial_+\eta^n-\sigma^n-\tau\sum_{k=1}^{n}\rho^k,\chi)$$

$$= (\partial_+\eta^n-\sigma^n-\tau\sum_{k=1}^{n}\rho^k,\chi) \qquad (76)$$

where in the last step we have used the fact that from (61) and (65)

$$(W^1-(\frac{\partial\eta}{\partial t})^1,\chi) = (V_h^1-(\frac{\partial u}{\partial t})^1,\chi) = 0 \qquad \text{for all } \chi \in S_h^r$$

Now we define

$$\varepsilon^n = \partial_+\eta^n - \sigma^n - \tau\sum_{k=1}^{n}\rho^k \qquad 1 \le n \le N-1 \qquad (77)$$

Then (76) reduces to

$$(\partial_+\xi^n,\chi) + a(\mu^{n,\frac{1}{4}},\chi) = (\varepsilon^n,\chi), \qquad \text{for all } \chi \in S_h^r(\Omega),\ 1 \le n \le N-1 \qquad (78)$$

We may use the particular test function χ defined as

$$\hat{\chi} = \frac{\mu^{n+1} - \mu^{n-1}}{2\tau}$$

Then from (73) we have

$$\hat{\chi} = \frac{\xi^{n+1} + \xi^{n}}{2} = \xi^{n+\frac{1}{2}}$$

Substituting for $\hat{\chi}$ in (78) we get

$$\left(\frac{\xi^{n+1} - \xi^{n}}{\tau}, \frac{\xi^{n+1} + \xi^{n}}{2}\right) + a\left(\frac{(\mu^{n+1} + \mu^{n}) + (\mu^{n} + \mu^{n-1})}{4}, \frac{\mu^{n+1} - \mu^{n-1}}{2\tau}\right) = (\varepsilon^{n}, \xi^{n+\frac{1}{2}})$$

or

$$||\xi^{n+1}||^2 - ||\xi^{n}||^2 + a(\mu^{n+\frac{1}{2}}, \mu^{n+\frac{1}{2}}) - a(\mu^{n-\frac{1}{2}}, \mu^{n-\frac{1}{2}}) = 2\tau(\varepsilon^{n}, \xi^{n+\frac{1}{2}})$$

$$1 \leq n \leq N-1 \qquad (79)$$

Summing in (79) from n = 1 to n = m-1, for any $1 < m \leq N$ and using (75) and V-ellipticity of $a(\cdot,\cdot)$ we obtain

$$||\xi^{m}||^2 \leq ||\xi^{1}||^2 + 2\tau \sum_{n=1}^{m-1} (\varepsilon^{n}, \xi^{n+\frac{1}{2}})$$

$$\leq ||\xi^{1}||^2 + 4T\tau \sum_{n=1}^{m-1} ||\varepsilon^{n}||^2 + \frac{\tau}{4T} \sum_{n=1}^{m-1} ||\xi^{n+\frac{1}{2}}||^2$$

$$\leq ||\xi^{1}||^2 + 4T\tau \sum_{n=1}^{m-1} ||\varepsilon^{n}||^2 + \tfrac{1}{2} \max_{1 \leq n \leq N} ||\xi^{n}||^2 \qquad (80)$$

hence follows

$$\max_{1 < n \leq N} ||\xi^{n}||^2 \leq 2||\xi^{1}||^2 + 8T\tau \sum_{n=1}^{N-1} ||\varepsilon^{n}||^2 \qquad (81)$$

Now from (68) we can obtain

$$\rho^k = \frac{1}{12} \int_{(k-1)\tau}^{k\tau} [(k-1)\tau - s][2(\frac{(k-1)\tau - s}{\tau})^2 - 3] \frac{\partial^4 u}{\partial t^4}(s)ds$$

$$- \frac{1}{12} \int_{k\tau}^{(k+1)\tau} [(k+1)\tau - s][2(\frac{(k+1)\tau - s}{\tau})^2 - 3] \frac{\partial^4 u}{\partial t^4}(s)ds$$

and hence by Schwarz inequality

$$||\rho^k||^2 \leq c\tau^3 \int_{(k-1)\tau}^{(k+1)\tau} ||\frac{\partial^4 u}{\partial t^4}(s)||^2 ds$$

Therefore

$$\tau \sum_{k=1}^{N-1} ||\rho^k||^2 \leq c_1 \tau^4 ||\frac{\partial^4 u}{\partial t^4}||^2_{L^2(0,T;(L^2(\Omega))^2)} \tag{82}$$

In a similar manner from (71) using integration by parts twice we have

$$\sigma^k = \frac{1}{2\tau} \int_{k\tau}^{(k+1)\tau} [(k+1)\tau - s][k\tau - s] \frac{\partial^3 u}{\partial t^3}(s)ds$$

and therefore

$$\tau \sum_{k=1}^{N-1} ||\sigma^k||^2 \leq c_2 \tau^4 ||\frac{\partial^3 u}{\partial t^3}||^2_{L_2(0,T;(L^2(\Omega))^2)} \tag{83}$$

Also from Lemma 2 and the fact that

$$\partial_+ \eta^k = \frac{1}{\tau} \int_{k_\tau}^{(k+1)\tau} \frac{\partial \eta}{\partial t}(s)ds$$

$$||\partial_+ \eta^k||^2 \leq \frac{1}{\tau} \int_{k\tau}^{(k+1)\tau} ||\frac{\partial \eta}{\partial t}(s)||^2 ds$$

we have

$$\tau \sum_{k=1}^{N-1} ||\partial_+ \eta^k||^2 \leq ||\frac{\partial \eta}{\partial t}||^2_{L_2(0,T;(L^2(\Omega))^2)} \leq ch^{2r} ||\frac{\partial u}{\partial t}||^2_{L_2(0,T;(\tilde{H}^r(\Omega))^2)} \tag{84}$$

Now from (77)

$$||\varepsilon^n||^2 \leq c\{||\partial_+ n^n||^2 + ||\sigma^n||^2 + \tau^2||\sum_{k=1}^{n} \rho^k||^2\}$$

$$\leq c\{||\partial_+ n^n||^2 + ||\sigma^n||^2 + \tau^2 N \sum_{k=1}^{N-1} ||\rho^k||^2\}$$

$$\leq c\{||\partial_+ n^n||^2 + ||\sigma^n||^2 + 2T(\tau \sum_{k=1}^{N-1} ||\rho^k||^2)\} \qquad (85)$$

Hence from (82)-(85)

$$\tau \sum_{n=1}^{N-1} ||\varepsilon^n||^2 \leq c_3 h^{2r} ||\frac{\partial u}{\partial t}||^2_{L_2(0,T;(\tilde{H}^r(\Omega))^2)} +$$

$$+ c_4 \tau^4 ||\frac{\partial^4 u}{\partial t^4}||^2_{L_2(0,T;(L_2(\Omega))^2)} + c_5 \tau^4 ||\frac{\partial^3 u}{\partial t^3}||^2_{L_2(0,T;(L_2(\Omega))} \qquad (86)$$

Finally combining (86) and (81) we obtain

$$\max_{i<n\leq N} ||\xi^n|| \leq \sqrt{2}||\xi^1|| + c(T)\{h^r ||\frac{\partial u}{\partial t}||_{L_2(0,T;(\tilde{H}^r(\Omega))^2)}$$

$$+ \tau^2[||\frac{\partial^3 u}{\partial t^3}||_{L_2(0,T;(L_2(\Omega))^2)} +$$

$$+ ||\frac{\partial^4 u}{\partial t^4}||_{L_2(0,T;(L_2(\Omega))^2)}]\}$$

The result of the lemma now follows. #

Now we give our main theorem for the fully-discrete approximation of the equations of dynamic elasticity on slit domains.

Theorem 3

Let u be the solution of (5)-(6) and let $\{U_h^n\}_{n=0}^N \subset S_h^r$ be the sequence defined by (60)-(63). Suppose that $u \in L_\infty(0,T;V^r(\Omega))$, $\frac{\partial u}{\partial t} \in L_2(0,T;V^r(\Omega))$ and $(\frac{\partial}{\partial t})^k u \in L_2(0,T;(L_2(\Omega))^2)$, for k = 3, 4. Then there exists a constant c = c(T) independent of h and τ such that

$$\max_{1<n\leq N} ||u^n - U_h^n|| \leq c\{h^r + \tau^2\}$$

Proof

From (52) (Chapter II.7) and (60)

$$||u(\cdot,\tau) - U_h^1|| \leq ch^r ||u_1||_r \leq ch^r ||u||_{L_\infty(1,T;(\tilde{H}^r(\Omega))^2)}$$

and so from Lemma 2

$$||\xi^1|| \leq ||\eta^1|| + ||u(\cdot,\tau) - U_h^1|| \leq ch^r ||u||_{L_\infty(1,T;(\tilde{H}^r(\Omega))^2)} \tag{87}$$

From Lemma (4)

$$||u(\cdot,n\tau) - U_h^n|| \leq ||\eta^n|| + ||\xi^n||$$

$$\leq ||\eta^n|| + \sqrt{2}||\xi^1|| + c\{h^r ||\frac{\partial u}{\partial t}||_{L_2(0,T;(\tilde{H}^r(\Omega))^2)} +$$

$$+ \tau^2 [||\frac{\partial^3 u}{\partial t^3}||_{L_2(0,T;(L_2(\Omega))^2)} +$$

$$+ ||\frac{\partial^4 u}{\partial t^4}||_{L_2(0,T;(L_2(\Omega))^2)}]\} \tag{88}$$

Using Lemma 2 and (87) in (88) we get

$$||u(\cdot,n\tau)-U_h^n|| \leq c(T)\{h^r[||u||_{L_\infty(1,T;(\tilde{H}^r(\Omega))^2)} +$$

$$+ ||\frac{\partial u}{\partial t}||_{L_2(0,T;(\tilde{H}^r(\Omega))^2)} +$$

$$+ \tau^2[||\frac{\partial^3 u}{\partial t^3}||_{L_2(0,T;(L_2(\Omega))^2)} +$$

$$+ ||\frac{\partial^4 u}{\partial t^4}||_{L_2(0,T;(L_2(\Omega))^2)}]\}$$

The result of the theorem now follows. #

This completes our error analysis for the system of hyperbolic equations of elasticity. Clearly, the above general results can be applied to dynamic *crack* problems at once.

Chapter IV

THE MOVING CRACK PROBLEM

The problem of a moving crack arising from the fracture of solids is dealt with in this chapter. As our approach in solving the problem is that of numerical approximation by the finite element method it is essential to have the basic variational form of the problem which takes into account the flow of energy into the moving crack tip. For this purpose we first investigate the relationship between the already known variational form corresponding to stationary crack problems and rate of energy balance equations of the system. It is demonstrated that for a particular choice of test functions the variational form is an expression of total energy conservation. We will then extend this argument to moving crack problems to derive the required form. In this new variational form an additional term representing the 'fracture power' is incorporated.

IV.1 VARIATIONAL FORMULATION OF MOVING CRACK PROBLEMS

IV.1.1 The Stationary Crack Problem Revisited

Let D be a plane domain whose boundary C consists of the union of a finite number of disjoint, piecewise smooth, simple closed curves, and let L be a straight line segment lying in D. Denote by D_0 the domain consisting of those points in D which are not in L. Choose a Cartesian coordinate system x_1, x_2 so that L consists of the points (x_1, x_2) for which $-a \leq x_1 \leq a$, $x_2 = 0$. Also let L_0 be the interior of L: $L_0 = \{(x_1,x_2) \mid -a < x_1 < a,\ x_2=0\}$.

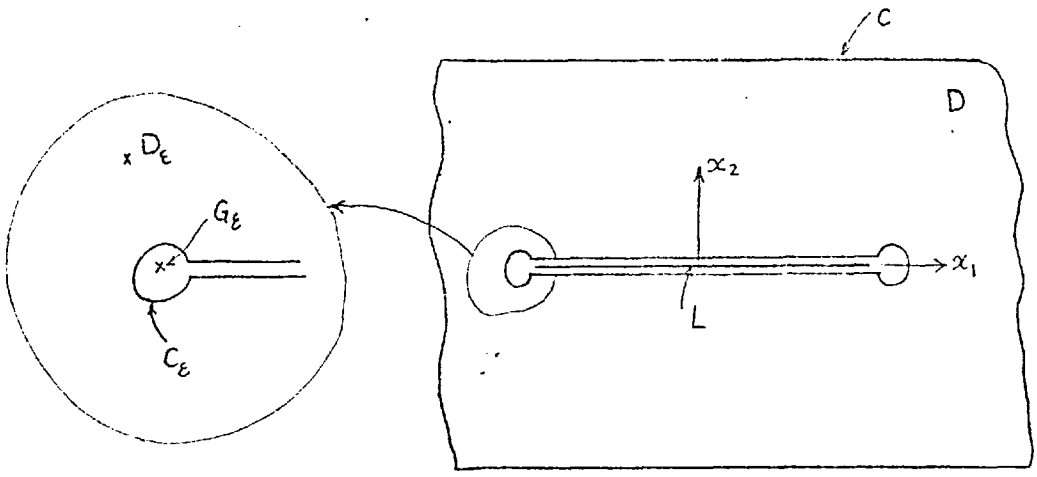

Finally let $C_\varepsilon^{(\alpha)}$, $\alpha = 1, 2$ be circles of radius $\varepsilon > 0$ centered at $(-a,0)$ and $(a,0)$, respectively, and denote by $G_\varepsilon^{(\alpha)}$, $\alpha = 1, 2$, the set of points inside $C_\varepsilon^{(\alpha)}$ which do not lie on the crack L. Let $C_\varepsilon = \underset{\alpha}{\cup} C_\varepsilon^{(\alpha)}$, $\alpha = 1, 2$ $G_\varepsilon = \underset{\alpha}{\cup} G_\varepsilon^{(\alpha)}$, $\alpha = 1, 2$, and let D_ε consist of those points in D_0 which are outside both circles $C_\varepsilon^{(\alpha)}$. (It is assumed that ε is small enough to assure that G_ε is contained in D_0.) In order to state the traction problem for D_0, it is convenient to introduce the following notation. Let D^+ be defined by

$$D^+ = \{(x_1,x_2) \,|\, (x_1,x_2) \in D \cup C,\ x_2 \geq 0,\ (x_1 \pm a)^2 + x_2^2 \neq 0\} \qquad (1)$$

so that D^+ consists of all those points in D U C which lie on or above the x_1-axis except for the crack tips $x_1 = \pm a$, $x_2 = 0$. Similarly let D^- be the set of points in D U C lying on or below the x_1-axis excluding the crack tips. The standard traction problem for D_0 requires the determination of u_i, σ_{ij} with the following properties

$$\text{(I)} \quad \begin{cases} u_i \in C^1(D^+) \cap C^1(D^-) \cap C^2(D_0) \\ \\ \sigma_{ij} \in C(D^+) \cap C(D^-) \cap C^1(D_0) \end{cases} \qquad (2)$$

(II) There exists a constant $M > 0$ such that

$$|u_i| < M \text{ on } D_0 \tag{3}$$

$$(III) \qquad \tfrac{1}{2}(u_{i,j} + u_{j,i}) = a_{ij\alpha\beta}\sigma_{\alpha\beta} \text{ on } D_0 \tag{4}$$

$$(IV) \qquad \sigma_{ij,j} + f_i = \ddot{u}_i, \quad \sigma_{ij} = \sigma_{ji} \text{ on } D_0 \tag{5}$$

$$(V) \qquad \delta_i \equiv \sigma_{ij} n_j = t_i \text{ on } C \tag{6}$$

$$(VI) \qquad \sigma_{21} = \sigma_{22} = 0 \text{ on } L_0 \tag{7}$$

In the stress strain relations (4) $a_{ij\alpha\beta}$ are the components of the given elastic compliance tensor and are assumed to be continuously differentiable functions of position on $D \cup C$ which satisfy

$$a_{ij\alpha\beta} = a_{ji\alpha\beta} = a_{\beta\alpha ij} \text{ on } D \cup C \tag{8}$$

The elastic material under consideration may therefore be nonhomogeneous and anisotropic. Finally it is assumed that the quadratic form

$$W(\xi, x) = \tfrac{1}{2}a_{ij\alpha\beta}(x)\xi_{ij}\xi_{\alpha\beta}, \quad x \in D \cup C \tag{9}$$

is uniformly positive definite in the sense that there exists a positive constant a_0 such that

$$W(\xi, x) \geq a_0^2 \xi_{ij}\xi_{ij}, \quad x \in D \cup C \quad \text{for all } \xi \text{ symmetric} \tag{10}$$

For plane strain of a homogeneous isotropic material with shear modulus μ and Poisson's ratio ν, (10) holds with $a_0^2 = \min(\frac{1}{4}\mu, (1-2\nu)/4\mu)$ provided $\mu > 0$, $(1-2\nu) > 0$.

In the equations of motion (5), f_i are the components of body force per unit volume and assumed to be continuous on $D \cup C$. The components of traction δ_i acting on a curve whose unit normal vector has components n_i are defined in (6), t_i is the prescribed traction on C. In (6) the unit normal vector on C is taken to be outward with respect to D_0.

The boundary conditions (7) express the requirement that the crack be traction free. The generalization to the case in which suitably restricted non-zero tractions are prescribed on the crack offers no difficulty.

The boundedness condition (3) on the displacement is the restriction on the singular behaviour at the crack tips.

IV.1.2 Weak Variational Formulation of the Stationary Crack Problem

Suppose that u_i, σ_{ij} satisfy (2)-(7). An application of the 2-dimensional divergence theorem yields:

$$\int_{D_\varepsilon} \ddot{u}.v\,dA + \int_{D_\varepsilon} \sigma_{ij}(u).\varepsilon_{ij}(v)\,dA = \int_{D_\varepsilon} f.v\,dA + \int_C t.v\,ds + \oint_{C_\varepsilon} \delta.v\,ds \qquad (11)$$

or alternatively

$$(\ddot{u},v)_{D\varepsilon} + a(u,v)_{D\varepsilon} = (f,v)_{D\varepsilon} + (t,v)_C + (\delta,v)_{C\varepsilon} \quad \text{for all } v \in V \qquad (12)$$

where $V = \{v \mid v_i$ satisfying (I), (II), (V), (VI)$\}$

(In the above relation we have used the usual notations.)

When the crack is stationary we have

$$\oint_{C_\varepsilon} \delta \cdot v \, ds \equiv 0, \quad \text{for all } \varepsilon \text{ and } v \in V \tag{13}$$

(This can be demonstrated by writing down the form of singularities at the crack tip and carrying out the integration.) So that the variational form reduces to

$$(\ddot{u},v)_{D\varepsilon} + a(u,v)_{D\varepsilon} = (f,v)_{D\varepsilon} + (t,v)_C \quad \text{for all } v \in V, \text{ when } \varepsilon \to 0 \tag{14}$$

Now it can be observed that, with the particular choice of $v \equiv \dot{u}$, this form expresses the *power balance* in our conservative system, i.e.

$$(\ddot{u},\dot{u})_{D_\varepsilon} + a(u,\dot{u})_{D_\varepsilon} = (f,\dot{u})_{D_\varepsilon} + (t,\dot{u})_C, \quad \text{when } \varepsilon \to 0 \tag{15}$$

The first and second terms in (15) are the time rates of change of kinetic and potential energy, respectively. The terms on the right hand side indicate the power supplied by body and boundary forces. So our weak form can be interpreted as a sound physical law (i.e. first law of thermodynamics) for a special choice of test functions.

Comment

In Chapter III it was shown that a weak solution u to the traction problem (2)-(7) is given by the corresponding weak form (14). We also note that u satisfies equation (15), therefore, one can regard the weak form (14) as a linearised version of the power balance equation (15).

IV.1.3 The Moving-Crack Problem

We replace all the domains in the previous section by their dynamic counterpart e.g. $D \to DXI = \bar{D}$, $I=]0,T[$, $D^+ \to D^+XI = \bar{D}^+$ etc.

We also note that, due to the movement of the tip, some of the domains, such as C_ε, are time dependent. With these modifications the problem could be described by (2)-(7). We have the following weak formulation ($v \to \dot{v}$ without any difficulty)

$$(\ddot{u},\dot{v})_{\bar{D}_\varepsilon(t)} + a(u,\dot{v})_{\bar{D}_\varepsilon(t)} = (f,\dot{v})_{\bar{D}_\varepsilon(t)} + (t,\dot{v})_{\bar{C}} + (\delta,\dot{v})_{\bar{C}_\varepsilon(t)} \tag{16}$$

for all $v \in \bar{V}$, $\varepsilon \to 0$

where

$$\bar{V} = \{v | v_i \text{ satisfying (I), (II), (V), (VI) with } D \to \bar{D} \text{ etc.}\}$$

and

$$(f,g)_{\bar{D}} = \int_0^T (f,g)_D dt, \text{etc.}$$

The important difference between the stationary and moving crack cases arises from the fact that

$$\lim_{\varepsilon \to 0} \oint_{C_\varepsilon(t)} \delta \cdot \dot{v} ds \neq 0, \quad \text{for all } v \in \bar{V} \tag{17}$$

when the tip is running at a speed $V \neq 0$ along x_1-axis. (This can be demonstrated by substituting for the elastic near field into (17) and verifying directly.)

For a special choice of test functions i.e. $v \equiv u$ we get

$$(\ddot{u},\dot{u})_{\bar{D}_\varepsilon(t)} + a(u,\dot{u})_{\bar{D}_\varepsilon(t)} = (f,\dot{u})_{\bar{D}_\varepsilon(t)} + (t,\dot{u})_{\bar{C}} + (\delta,\dot{u})_{\bar{C}_\varepsilon(t)} \qquad \varepsilon \to 0 \qquad (18)$$

Now we try to give a physical interpretation of equation (18) and show that it is the limiting form (i.e. $\varepsilon \to 0$) of the first law of thermodynamics on the physical grounds that fracture process is dissipative in nature. For a general discussion on the energy balance equation we refer to the work of Craggs [65], Atkinson and Eshelby [66], Freund [67], Kostrov [68] and [69, Chapter V].

It was already shown in the stationary crack problem that the principle of conservation of energy could be derived from the weak formulation of the problem by only using differential equations (i.e. principle of conservation of momentum). In other words, in the absence of heat processes, sinks and sources of energy, first law of thermodynamics would not give *additional* information over the principle of conservation of momentum.

However for a moving crack problem and on physical grounds, there is a mechanism of energy dissipation from the tip of the crack. Naturally we must use both the principle of conservation of momentum (i.e. differential equations) and conservation of energy as the differential equations *would not* be sufficient to explain the process.

Define

$$K = \lim_{\varepsilon \to 0} \int_{D_\varepsilon(t)} \tfrac{1}{2}\rho \dot{u} \cdot \dot{u}\, dx, \qquad \text{kinetic energy}$$

$$U = \lim_{\varepsilon \to 0} \int_{D_\varepsilon(t)} \tfrac{1}{2}\sigma_{ij}(u)\varepsilon_{ij}(u)\, dx, \qquad \text{potential energy}$$

$$T = \int_C t \cdot \dot{u}\, ds, \qquad F = (f,\dot{u})_{D_\varepsilon(t)}$$

Then the power balance is written as

$$\frac{d}{dt}(K+U) + E = T + F \tag{19}$$

where E = rate of energy dissipation from the tip.

Due to the time dependence of $D_\varepsilon(t)$ and $C_\varepsilon(t)$ in deriving the time differentials, the amount of energy convection through the boundary $C_\varepsilon(t)$ must also be accounted for i.e.

$$\dot{K} = \lim_{\varepsilon\to 0}\left[\int_{D_\varepsilon(t)} \rho\dot{u}\,\dot{u}\,dx + \int_{C_\varepsilon(t)} [\tfrac{1}{2}\rho\dot{u}\,\dot{u}\,]V_n ds\right] \tag{20}$$

where V_n is the velocity vector of curve $C_\varepsilon(t)$. Also

$$\dot{U} = \lim_{\varepsilon\to 0} \int_{D_\varepsilon(t)} \sigma_{ij}(u).\varepsilon_{ij}(\dot{u})dx + \int_{C_\varepsilon(t)} [\tfrac{1}{2}\sigma_{ij}(u).\varepsilon_{ij}(u)]V_n ds \tag{21}$$

Substituting (20) and (21) into (19) and using the divergence theorem we arrive at

$$E = -\lim_{\varepsilon\to 0}\left[\oint_{C_\varepsilon(t)} \{\delta.\dot{u} + \tfrac{1}{2}[\sigma_{ij}(u)\varepsilon_{ij}(u) + \rho\dot{u}\,\dot{u}\,]V_n\}ds\right] \tag{22}$$

Let us choose $C_\varepsilon(t)$ as the loop in the figure. Now we show that for the particular choice of $C_\varepsilon(t)$ the contributions from the second and third terms in the above integrand vanish as ε_x and $\varepsilon_y \to 0$.

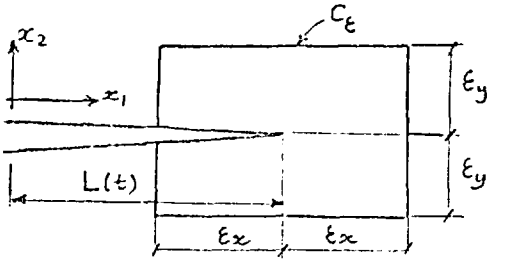

Along the horizontal sides of the rectangle, $V_n = V_i n_i = 0$ and we only have to compute the second and third terms on the vertical sides. Now if we shrink this loop to zero by first letting $\varepsilon_y \to 0$ and then $\varepsilon_x \to 0$ then we can expect that the vertical sides contribute nothing to the integral (in fact by various methods of calculating the rate of energy release it has been demonstrated that this expectation is valid). So we are left with

$$E = - \lim_{\varepsilon_x \to 0} \lim_{\varepsilon_y \to 0} \oint_{C_\varepsilon(t)} \delta . \dot{u} \, ds \tag{23}$$

With this result for the rate of energy release, our rate of energy balance equation would become (from (19)-(23))

$$(\ddot{u} \ , \dot{u} \ )_{D_\varepsilon(t)} + a(u, \dot{u} \ )_{D_\varepsilon(t)} = (f, \dot{u} \ )_{D_\varepsilon(t)} + (t, \dot{u} \ )_{C} + (\delta, \dot{u} \ )_{C_\varepsilon(t)}$$

$$\varepsilon \to 0 \tag{24}$$

Integrating both sides of the equation with respect to time we arrive at the same relation as (18) and hence a physical interpretation of the weak formulation (17) is provided.

Remark 1

We note that our weak formulation will only be valid if $\varepsilon \to 0$ i.e. in any numerical approximation of the problem we expect to get the exact solution for very fine meshes around the tip. In fact as the mesh size $h \to 0$ we expect to get both *convergence* and *convergence to the right values*. However, this dependence on the value ε of the solution has not been studied.

Remark 2

The integration in (23) can only be carried over two horizontal

sides of the rectangle as $\varepsilon_y \to 0$. Then E would correspond to the power required to remove the stresses δ through the velocity $\dot{u}$ to create new surfaces and hence can be termed as the '*fracture power*'.

Summarizing, the solution u to the moving crack problem is given by

$$(\ddot{u}\ ,\dot{v})_{\bar{D}_\varepsilon} + a(u,\dot{v})_{\bar{D}_\varepsilon} + b(u,\dot{v})_{\bar{C}_\varepsilon} = (f,\dot{v})_{\bar{D}_\varepsilon} + (t,\dot{v})_{\bar{C}}$$
$$\text{for all } v \in \bar{V},\ \varepsilon_x \to 0,\ \varepsilon_y \to 0 \qquad (25)$$

where the bilinear form $b(\cdot,\cdot)$ is given by

$$b(u,v)_{\bar{C}} = -\int_0^T \oint_{C_\varepsilon} \sigma_{ij}(u) n_j . v ds dt \begin{cases} > 0 & 0 < V < V_R \\ = 0 & V = 0, \text{ and } V = V_R \end{cases}$$

i.e. fracture power is nonzero for $0 < \dot{V} < V_R$ (for $V > V_R$ the fracture process acts as a source of energy and hence, in the absence of any external source of power applied at the crack tip, this velocity range is excluded).

The proof of the existence of a unique solution u to this problem seems to be a difficult task and is left unresolved. However, we assume that we have a unique solution to this formulation and try to approximate the solution.

IV.2 ASYMPTOTIC SOLUTION AND REGULARITY

The equations of dynamic elasticity in terms of displacements are a set of two coupled equations. The solution to the equations would be easily determined if we could decouple them. This can be done by decomposing the displacement field into irrotational and solenoidal fields, see Sternberg [70].

IV.2.1 Lamé-Clebsch Representation of Equations of Dynamic Elasticity

The equations of elasticity in displacement can be written as

$$\mu \Box_2^2 \vec{u} + (\lambda+\mu) \text{ grad div } \vec{u} + \vec{F} = 0 \tag{1}$$

where μ and λ are Lame's constants, and

$$\Box_n^2 = \nabla^2 - \frac{1}{c_n^2} \frac{\partial^2}{\partial t^2} ; \quad n = 1, 2 \tag{2}$$

$$c_1^2 = \frac{2(1-\nu)}{1-2\nu} c_2^2 \quad \text{and} \quad c_2^2 = \frac{\mu}{\rho}, \quad \rho = \text{mass density}$$

By decomposing the displacement vector into the sum of a gradient and a curl

$$\vec{u} = \nabla\phi + \nabla x \vec{\psi} \qquad \text{(i.e. grad } \phi + \text{curl } \vec{\psi}) \tag{3}$$

we can decouple system (1) into

$$\begin{cases} \Box_1^2 \phi = 0 \\ \\ \Box_2^2 \vec{\psi} = 0 \end{cases} \tag{4}$$

as can be verified directly. However, the *completeness of the representation* (i.e. whether every solution to (1) can also be represented as (3)) remains to be shown. In the following we assume in the region Ω under consideration with boundary Γ the solution $\vec{u}$ together with its time and space derivatives of the first and second order are continuous for $x \in \Omega$, $t_1 < t < t_2$.

Note: Eventhough these assumptions are violated in crack problems we

conjecture that they are not necessary for the following theorem as long as the displacement field satisfies the condition of boundedness of strain energy density.

Clebsch Theorem (due to Duhem)

Let $\vec{u}$ be a particular solution of (1), in the region Ω and for $t_1 < t < t_2$. Then there exists a scalar function $\phi(x,t)$ and a vector function $\vec{\psi}(x,t)$ such that $\vec{u}(x,t)$ is represented by (3) with

$$\nabla.\vec{\psi} = 0 \qquad \text{(i.e. div } \vec{\psi} = 0) \tag{5}$$

and ϕ, $\vec{\psi}$ satisfy (4). #

Remark

The condition (5) which corresponds to a solenoidal field is unnecessary for the Lame equation as long as (4) holds even for a non-solenoidal field $\vec{\psi}$. #

This theorem assures the completeness of the solution.

In the plane strain case

$$u_1 = u(x,y,t), \quad u_2 = v(x,y,t), \quad u_3 = 0 \tag{6}$$

the Lame solution remains complete if the generating potentials are taken in the restricted form

$$\phi = \phi(x,y,t), \quad \psi_3 = \psi(x,y,t), \quad \psi_1 = \psi_2 = 0 \tag{7}$$

Equations (3), (4) and (5) now lead to

$$\begin{cases} u = \dfrac{\partial \phi}{\partial x} + \dfrac{\partial \psi}{\partial y} \\ \\ v = \dfrac{\partial \phi}{\partial y} - \dfrac{\partial \psi}{\partial x} \end{cases} \tag{8}$$

(u and v are components of $\vec{u}$ in x and y directions, respectively)

and

$$\begin{cases} \Box_1^2 \phi = 0 \\ \\ \Box_2^2 \psi = 0 \end{cases} \qquad \text{in } \Omega \times I \tag{9}$$

Then stresses at any point can be written in terms of displacement potentials as

$$\begin{cases} \sigma_x = \lambda \nabla^2 \phi + 2\mu \left(\dfrac{\partial^2 \phi}{\partial x^2} + \dfrac{\partial^2 \psi}{\partial x \partial y} \right) \\ \\ \sigma_y = \lambda \nabla^2 \phi + 2\mu \left(\dfrac{\partial^2 \phi}{\partial y^2} - \dfrac{\partial^2 \psi}{\partial x \partial y} \right) \\ \\ \sigma_{xy} = \mu \left(2 \dfrac{\partial^2 \phi}{\partial x \partial y} - \dfrac{\partial^2 \psi}{\partial x^2} + \dfrac{\partial^2 \psi}{\partial y^2} \right) \end{cases} \tag{10}$$

So equations (9) together with specified values of displacement and/or stresses on the boundary Γ (equations (8) or (10)) and *initial* displacements and/or stresses in the plane would determine a well-posed initial-boundary value problem.

Remark

The previous theorem can be extended to include *volume forces* F represented by

$$\vec{F} = \text{grad } \Phi + \text{curl } \Psi \tag{11}$$

where Φ and Ψ are given and the equations (9) would become

$$\begin{cases} \Box_1^2 \phi + \dfrac{1-2\nu}{1-\nu}\Phi = 0 \\ \Box_2^2 \psi + 2\Psi = 0 \end{cases} \tag{12}$$

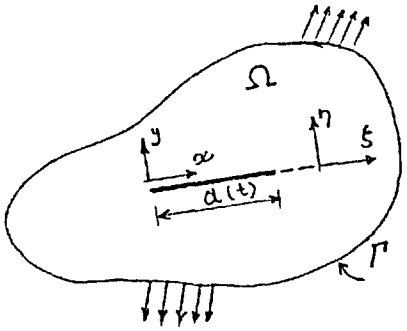

where ν is the poisson ratio.

Remark

The previous results equally apply to some special *viscoelastic materials* where, due to damping, disturbances die out. In this case we substitute the operator

$$(\rho \frac{\partial^2}{\partial t^2} + k \frac{\partial}{\partial t}) \quad \text{for} \quad (\rho \frac{\partial^2}{\partial t^2})$$

so that (2) is replaced by

$$\Box_n^2 = \nabla^2 - \frac{1}{c_n^2}(\frac{\partial^2}{\partial t^2} + \frac{k}{\rho}\frac{\partial}{\partial t}), \quad (n = 1, 2) \tag{13}$$

IV.2.2 Steady Crack Propagation

An isotropic elastic material with a stationary crack of length a is subjected to general plane strain loading. By an increase in the loading along the boundaries, at time t = 0, one end of the crack starts to move. The asymptotic elastic field near the tip of a crack moving with a constant speed V is obtained in the next section. See also Yoffe [71], Craggs [72], Broberg [73] and Baker [15].

IV.2.2.1 Asymptotic solution of the elastic field

Using the previous analysis and decomposing the displacement field into irrotational, Φ, and solenoidal, Ψ, fields we write the equation of motion in the moving coordinate system (ξ,η) with the origin at the tip:

$$\left[1 - \left(\frac{V}{C_1}\right)^2\right] \frac{\partial^2 \Phi}{\partial \xi^2} + \frac{\partial^2 \Phi}{\partial \eta^2} = 0 \qquad (15)$$

$$\left[1 - \left(\frac{V}{C_2}\right)^2\right] \frac{\partial^2 \Psi}{\partial \xi^2} + \frac{\partial^2 \Psi}{\partial \eta^2} = 0 \qquad (16)$$

In this way the system of equations is reduced to two *elliptic* equations for $V < C_2 < C_1$.

Now we can use Kondratev's analysis (see Chapter II) to find the local field near the tip of the crack.

Equations (15)-(16) reduces to:

$$\begin{cases} \dfrac{\partial^2 \Phi}{\partial \xi^2} + \dfrac{\partial^2 \Phi}{\partial \eta_1^2} = 0 \\ \dfrac{\partial^2 \Psi}{\partial \xi^2} + \dfrac{\partial^2 \Psi}{\partial \eta_2^2} = 0 \end{cases} \tag{17}$$

where $\begin{cases} \eta_1 = \alpha_1 \eta \\ \eta_2 = \alpha_2 \eta \end{cases}$ (18)

and $\begin{cases} \alpha_1^2 = 1 - (\dfrac{V}{c_1})^2 \\ \alpha_2^2 = 1 - (\dfrac{V}{c_2})^2 \end{cases}$

Introducing the polar coordinates (r_1,θ_1) and (r_2,θ_2) as

$$\begin{cases} r_1 e^{i\theta_1} = \xi + i\eta_1 \\ r_2 e^{i\theta_2} = \xi + i\eta_2 \end{cases} \tag{19}$$

we have

$$\begin{cases} (\dfrac{\partial^2}{\partial r_1^2} + \dfrac{1}{r_1}\dfrac{\partial}{\partial r_1} + \dfrac{1}{r_1^2}\dfrac{\partial^2}{\partial \theta_1^2})\Phi = 0 \\ (\dfrac{\partial^2}{\partial r_2^2} + \dfrac{1}{r_2}\dfrac{\partial}{\partial r_2} + \dfrac{1}{r_2^2}\dfrac{\partial^2}{\partial \theta_2^2})\Psi = 0 \end{cases} \tag{20}$$

making the change of variables $r_1 = e^{-\tau_1}$ and $r_2 = e^{-\tau_2}$, (20) becomes

$$\begin{cases} (\dfrac{\partial^2}{\partial \tau_1^2} + \dfrac{\partial^2}{\partial \theta_1^2})\Phi = 0 \\ (\dfrac{\partial^2}{\partial \tau_2^2} + \dfrac{\partial^2}{\partial \theta_2^2})\Psi = 0 \end{cases} \tag{21}$$

Fourier transforming Φ with respect to τ_1 and Ψ with respect to τ_2 we get

$$\begin{cases} \dfrac{\partial^2 \tilde{\Phi}}{\partial \theta_1^2} - \lambda_1^2 \tilde{\Phi} = 0 \\ \dfrac{\partial^2 \tilde{\Psi}}{\partial \theta_2^2} - \lambda_2^2 \tilde{\Psi} = 0 \end{cases} \tag{22}$$

which have the general solutions

$$\begin{cases} \tilde{\Phi} = A \sin i\lambda_1\theta_1 + B \cos i\lambda_1\theta_1 \\ \qquad\qquad (i = \sqrt{-1}) \\ \tilde{\Psi} = C \sin i\lambda_2\theta_2 + D \cos i\lambda_2\theta_2 \end{cases} \tag{23}$$

In order to find those $\tilde{\Phi}$ and $\tilde{\Psi}$ which result in stress free crack surfaces

$$\begin{cases} \sigma_{\eta\eta} = 0 \\ \sigma_{\xi\eta} = 0 \end{cases} \tag{24}$$

we calculate $\sigma_{\eta\eta}$ and $\sigma_{\xi\eta}$ from (10). We notice that along the crack faces $\eta = 0$, any point $(r_i = r, \pm\pi)$, $i = 1, 2$ is mapped into $(\lambda_i = \lambda, \pm\pi)$ $i = 1, 2$, in the λ-plane. We substitute into the equations (1) the following identities

$$\begin{cases} \dfrac{\partial \Phi}{\partial y} = \dfrac{\partial \Phi}{\partial \eta_1} \cdot \dfrac{\partial \eta_1}{\partial \eta} = \alpha_1 \dfrac{\partial \Phi}{\partial \eta_1} \\ \dfrac{\partial \Phi}{\partial x} = \dfrac{\partial \Phi}{\partial \xi}, \text{ etc.} \end{cases}$$

and the Cartesian-polar transformation relations:

$$\begin{cases} \dfrac{\partial^2}{\partial\xi^2} = \cos^2\theta\,\dfrac{\partial^2}{\partial r^2} + \dfrac{\sin^2\theta}{r}\dfrac{\partial}{\partial r} - \dfrac{\sin 2\theta}{r}\dfrac{\partial^2}{\partial r\partial\theta} + \dfrac{\sin 2\theta}{r^2}\dfrac{\partial}{\partial\theta} + \dfrac{\sin^2\theta}{r^2}\dfrac{\partial^2}{\partial\theta^2} \\ \dfrac{\partial^2}{\partial\eta^2} = \sin^2\theta\,\dfrac{\partial^2}{\partial r^2} + \dfrac{\cos^2\theta}{r}\dfrac{\partial}{\partial r} + \dfrac{\sin 2\theta}{r}\dfrac{\partial^2}{\partial r\partial\theta} - \dfrac{\sin 2\theta}{r^2}\dfrac{\partial}{\partial\theta} + \dfrac{\cos^2\theta}{r^2}\dfrac{\partial^2}{\partial\theta^2} \\ \dfrac{\partial^2}{\partial\xi\partial\eta} = \sin\theta\cos\theta\dfrac{\partial^2}{\partial r^2} - \dfrac{\sin\theta\cos\theta}{r}\dfrac{\partial}{\partial r} + \dfrac{\cos 2\theta}{r}\dfrac{\partial^2}{\partial r\partial\theta} - \dfrac{\cos 2\theta}{r^2}\dfrac{\partial}{\partial\theta} - \\ \qquad - \dfrac{\sin\theta\cos\theta}{r^2}\dfrac{\partial^2}{\partial\theta^2} \end{cases} \tag{25}$$

which on the crack faces ($\theta = \pm\pi$) reduce to:

$$\begin{cases} \dfrac{\partial^2}{\partial\xi^2} = \dfrac{\partial^2}{\partial r^2} \\ \dfrac{\partial^2}{\partial\eta^2} = \dfrac{1}{r}\dfrac{\partial}{\partial r} + \dfrac{1}{r^2}\dfrac{\partial^2}{\partial\theta^2} \\ \dfrac{\partial^2}{\partial\xi\partial\eta} = \dfrac{1}{r}\dfrac{\partial^2}{\partial r\partial\theta} - \dfrac{1}{r^2}\dfrac{\partial}{\partial\theta} \end{cases} \tag{26}$$

in (26) we have

$$\begin{cases} \dfrac{\partial}{\partial r} = -e^{\tau}\dfrac{\partial}{\partial\tau} \\ \dfrac{\partial^2}{\partial r^2} = e^{2\tau}\left(\dfrac{\partial^2}{\partial\tau^2} + \dfrac{\partial}{\partial\tau}\right) \end{cases} \tag{27}$$

With (26) and (27) used in (24) we arrive at the following boundary conditions

$$\begin{cases} 2\alpha_1\tilde{\Phi}' + \mu(1+\alpha_2^2)\tilde{\Psi} = 0 \\ \qquad\qquad \text{on } \theta_1 = \theta_2 = \pm\pi \\ 2\alpha_2\tilde{\Psi}' - \mu(1+\alpha_2^2)\tilde{\Phi} = 0 \end{cases} \tag{28}$$

where $\mu = i\lambda$ and $\tilde{\Phi}' = \frac{\partial\tilde{\Phi}}{\partial\Theta_1}$, $\tilde{\Psi}' = \frac{\partial\tilde{\Psi}}{\partial\Theta_2}$ etc. Substituting for $\tilde{\Phi}$ and $\tilde{\Psi}$ from (23) into (28) we get

$$\begin{cases} 2\alpha_1(A\cos\mu\pi \mp B\sin\mu\pi) + (1+\alpha_2^2)(\pm C\sin\mu\pi + D\cos\mu\pi) = 0 \\ \\ 2\alpha_2(C\cos\mu\pi \mp D\sin\mu\pi) - (1+\alpha_2^2)(\pm A\sin\mu\pi + B\cos\mu\pi) = 0 \end{cases} \tag{29}$$

which reduces to two independent sets of equations:

$$\begin{cases} 2\alpha_1 A\cos\mu\pi + (1+\alpha_2^2)D\cos\mu\pi = 0 \\ \\ (1+\alpha_2^2)A\sin\mu\pi + 2\alpha_2 D\sin\mu\pi = 0 \end{cases} \tag{30}$$

$$\begin{cases} (1+\alpha_2^2)C\sin\mu\pi - 2\alpha_1 B\sin\mu\pi = 0 \\ \\ 2\alpha_2 C\cos\mu\pi - (1+\alpha_2^2)B\cos\mu\pi = 0 \end{cases} \tag{31}$$

A nontrivial solution is obtained if the determinants Λ_1 and Λ_2 of the system (30) and (31), respectively, vanish, i.e.

$$\Lambda_1 = \Lambda_2 = [(1+\alpha_2^2)^2 - 4\alpha_1\alpha_2]\sin 2\pi\mu = 0 \tag{32}$$

For (32) we can consider two cases

(i) $\sin 2\pi\mu = 0$

(ii) $[(1+\alpha_2^2)^2 - 4\alpha_1\alpha_2] = 0$

and discuss the implications of each case. Case (ii) will be discussed later in IV.4.

(i) $\sin 2\pi\mu = 0$

The roots of the equation are $\mu = \pm j/2$, j integer, where for the physical condition that energy is finite we only accept

$$\mu = -j/2, \quad j > 1 \text{ integer}$$

or

$$-i\lambda_j = j/2, \quad j > 1 \text{ integer} \quad (i = \sqrt{-1})$$

upon substitution for μ into (30) and (31) we have

$$\begin{cases} C = \dfrac{2\alpha_1}{1+\alpha_2^2} B \\ D = -\dfrac{1+\alpha_2^2}{2\alpha_2} A \end{cases} \quad j > 1 \text{ odd integer} \qquad \begin{cases} C = \dfrac{1+\alpha_2^2}{2\alpha_2} B \\ D = -\dfrac{2\alpha_1}{1+\alpha_2^2} A \end{cases} \quad j > 1 \text{ even integer} \qquad (34)$$

So the potentials from (23) are

$$\begin{cases} \tilde{\Phi} = -A \sin \dfrac{j}{2}\theta_1 + B \cos \dfrac{j}{2}\theta_1 & j > 1 \\ \tilde{\Psi} = \dfrac{-2\alpha_1}{1+\alpha_2^2} B \sin \dfrac{j}{2}\theta_2 - \dfrac{1+\alpha_2^2}{2\alpha_2} A \cos \dfrac{j}{2}\theta_2 & j > 1 \text{ odd integer} \\ \tilde{\Psi} = -\dfrac{1+\alpha_2^2}{2\alpha_2} B \sin \dfrac{j\theta_2}{2} - \dfrac{2\alpha_1}{1+\alpha_2^2} A \cos \dfrac{j\theta_2}{2} & j > 1 \text{ even integer} \end{cases} \qquad (35)$$

Therefore, according to Kondratev's analysis (see Chapter II) the following expansions hold

$$\begin{cases} \Phi = \sum_j a_j r_1^{j/2} P_j(r_1 \ell n^q r_1) + W\phi_j \\ \Psi = \sum_j b_j r_2^{j/2} Q_j(r_2 \ell n^q r_2) + W\psi_j \end{cases} \quad j > 1 \text{ integer} \qquad (36)$$

where q is an integer and P_j and Q_j are polynomials with coefficients infinitely smooth functions of θ_1 and θ_2, respectively. (These are given by eigen functions in (35).)

Relations (36) together with (8) and (15) would determine the actual displacement and stress field e.g. when A = 0 *(Mode I)* the dominant singular terms given for j = 3 are:

$$\begin{cases} u = \frac{3}{2} B(t)\{r_1^{\frac{1}{2}} \cos\frac{\theta_1}{2} - \frac{2\alpha_1\alpha_2}{1+\alpha_2^2} r_2^{\frac{1}{2}} \cos\frac{\theta_2}{2}\} + 0(1) \\ v = \frac{3}{2} \alpha_1 B(t)\{\frac{2}{1+\alpha_2^2} r_2^{\frac{1}{2}} \sin\frac{\theta_2}{2} - r_1^{\frac{1}{2}} \sin\frac{\theta_1}{2}\} + 0(1) \end{cases} \tag{37}$$

The corresponding well-known stresses and velocities are then:

$$\begin{cases} \sigma_{11} = \frac{3}{4}\mu B\{(1+2\alpha_1^2-\alpha_2^2) \frac{\cos(\frac{\theta_1}{2})}{r_1^{\frac{1}{2}}} - \frac{4\alpha_1\alpha_2}{(1+\alpha_2^2)} \cdot \frac{\cos(\frac{\theta_2}{2})}{r_2^{\frac{1}{2}}}\} + 0(1) \\ \sigma_{12} = \frac{3}{2}\mu B\ \alpha_1\{\frac{\sin(\frac{\theta_1}{2})}{r_1^{\frac{1}{2}}} - \frac{\sin(\frac{\theta_2}{2})}{r_2^{\frac{1}{2}}}\} + 0(1) \\ \sigma_{22} = \frac{3}{4}\mu B\{-(1+\alpha_2^2) \frac{\cos(\frac{\theta_1}{2})}{r_1^{\frac{1}{2}}} + \frac{4\alpha_1\alpha_2}{(1+\alpha_2^2)} \frac{\cos(\frac{\theta_2}{2})}{r_2^{\frac{1}{2}}}\} + 0(1) \end{cases} \tag{38}$$

and

$$\begin{cases} \dot{u} = -\frac{3}{4} v(t).B(t)\{r_1^{-\frac{1}{2}} \cos\frac{\theta_1}{2} - \frac{2\alpha_1\alpha_2}{1+\alpha_2^2} r_2^{-\frac{1}{2}} \cos\frac{\theta_2}{2}\} + 0(1) \\ \dot{v} = -\frac{3}{4} v(t) B(t)\ \alpha_1\{r_1^{-\frac{1}{2}} \sin\frac{\theta_1}{2} - \frac{2}{1+\alpha_2^2} r_2^{-\frac{1}{2}} \sin\frac{\theta_2}{2}\} + 0(1) \end{cases} \tag{39}$$

An analog dynamic stress-intensity factor can be defined as

$$K_{ID} = \frac{3}{4}\mu B[\frac{4\alpha_1\alpha_2 - (1+\alpha_2^2)^2}{1+\alpha_2^2}] \tag{40}$$

Similarly for Mode II (B = 0)

$$\begin{cases} \sigma_{11} = \frac{3}{4}\mu A\{(1+\alpha_2^2)r_2^{-\frac{1}{2}} \sin\frac{\theta_2}{2} - (1+2\alpha_1^2-\alpha_2^2)r_1^{-\frac{1}{2}} \sin\frac{\theta_1}{2}\} + O(1) \\ \sigma_{12} = \frac{3}{4}\mu A.2\alpha_1\{r_1^{-\frac{1}{2}} \cos\frac{\theta_1}{2} - \frac{(1+\alpha_2^2)^2}{4\alpha_1\alpha_2} r_2^{-\frac{1}{2}} \cos\frac{\theta_2}{2}\} + O(1) \\ \sigma_{22} = \frac{3}{4}\mu A(1+\alpha_2^2)\{r_1^{-\frac{1}{2}} \sin\frac{\theta_1}{2} - r_2^{-\frac{1}{2}} \sin\frac{\theta_2}{2}\} + O(1) \end{cases} \tag{41}$$

with

$$K_{IID} = \frac{3}{4}\mu A\left[\frac{4\alpha_1\alpha_2-(1+\alpha_2^2)^2}{2\alpha_2}\right] \tag{42}$$

IV.2.2.2 Regularity of solution

In parallel to the regularity analysis of Chapter II for stationary crack problems we study smoothness of the functions Φ and Ψ. From the expansion (36) for j = 3 we have

$$\begin{cases} \Phi = r_1^{3/2}\{A \sin\frac{3}{2}\theta_1 + B \cos\frac{3}{2}\theta_1\} + W\phi_3 \\ \Psi = r_2^{3/2}\{-\frac{2\alpha_1}{1+\alpha_2^2} B \sin\frac{3}{2}\theta_2 + \frac{1+\alpha_2^2}{2\alpha_2} A \cos\frac{3}{2}\theta_2\} + W\psi_3 \end{cases} \tag{43}$$

In general $\Phi \in H^2(\Omega)$ and $\Psi \in H^2(\Omega)$ and also for the right hand sides in (16) we have $L_1 \in H^1(\Omega)$ and $L_2 \in H^1(\Omega)$. Since $-1 + 2 \leq \mathrm{Im}\lambda_j = \frac{3}{2} < -1 + k_1 + 2$ (i.e. $k_1 = 1$), from Theorem (1) Chapter II.6, we obtain

and

$$\begin{cases} W\phi_3 \in H^3(\Omega) \\ W\psi_3 \in H^3(\Omega) \end{cases}$$

i.e. the solutions Φ and Ψ can be asymptotically expanded as the sum of dominant singular terms and smoother functions $W\phi_3$ and $W\psi_3$. Similar expansions also hold for displacements u and v with the leading singularities given by (37). In this way the solution $u \in H^1(\Omega)$ and $v \in H^1(\Omega)$ (at any fixed time t) can be expanded containing smooth functions in $H^2(\Omega)$. Therefore, similarly to the analysis of stationary crack problems, we can incorporate the singular functions in any approximation scheme for solving moving crack problems and expect it to result in a convergent algorithm.

IV.3 FAILURE CRITERIA

The study of mechanisms of initial growth of a crack is important for both failure analysis of cracked structures and also determination of the initial conditions set for the propagation phase of the moving crack problem. We also notice that once a crack has started to move its subsequent motion should only depend on the local behaviour of the field variables. In general it would be reasonable to substitute the global energy balance equations with a local 'fracture criterion' as the whole energy dissipation takes place from the moving tip. In this section we review certain failure criteria that provide the required initial conditions for the moving crack problem.

IV.3.1 Griffith Criterion [74]

In a linearly elastic brittle material the Griffith energy criterion can be stated as follows: for a crack of length C to extend an amount δC, the change in the total energy released would be

$$\delta U = \delta W - \delta T; \begin{cases} T = \text{kinetic and strain energy} \\ W = \text{work of applied forces} \end{cases} \quad (1)$$

On the other hand, in order to create fresh surfaces in the material certain energy is required. This energy denoted by Γ is the "surface energy" of the crack. The extension of the crack would entirely depend on the availability of the minimum surface energy Γ, i.e.

$$\delta U \geq \Gamma \quad (2)$$

Griffith expresses Γ in terms of γ (surface tension) of solids by $\Gamma = 2C\gamma$. Equation (2) would then be written as

$$\delta U \geq 2C\gamma \quad (3)$$

Define the rate of energy release by

$$G = \frac{\delta U}{2\delta C} \quad (4)$$

The Griffith criterion can be written as:

$$G \geq \gamma \quad (5)$$

G can be regarded as the force tending to open the crack and its evaluation should only need a local knowledge of the field near the crack tip. This can be obtained for a semi-infinite crack in an infinite medium for, say, Mode I by calculating the work done at the crack as

$$G_1 = \frac{\pi(\kappa+1)}{8\mu} K_I^2, \quad \kappa = 3 - 4\nu \text{ for plane strain}$$

The Griffith criterion would then yield the following failure condition

$$K_I^2 \geq \frac{2\mu}{\pi(1-\nu)}\gamma$$

IV.3.2 Barenblatt's Criterion [75]

Barenblatt established the earlier conjecture that the position of the crack tip is determined by the condition of boundedness of stresses. This is to say that the stress intensity factors vanish there and the crack faces close smoothly (cusp shape) at the tip. Due to non-zero stress intensity factors calculated from the infinitesimal theory he postulated the existence of an 'end' region at the crack tip where the opposite faces of the crack are so close that the cohesive forces are operating on that area. This would resolve the discrepancy of the classical theory in giving unbounded stresses. Outside this region (the inner region) the continuum model holds and the effect of cohesive forces can be neglected. He assumes that the dimensions of the end region are very small in comparison with the largest dimension of the crack and that the distribution of the cohesive forces in the neighbourhood of points having its maximum intensity is independent of the loading condition. (The autonomy hypothesis.) Denoting by $K_{i\alpha}$ ($i = 1, 3$) the stress intensity factors due to cohesive forces acting on the end region and by K_{i0}, ($i = 1, 3$) the corresponding stress intensity factors for the forces acting on the inner region due to infinitesimal theory then the condition of finiteness of stresses is

$$K_{i0} + K_{i\alpha} = 0 \qquad (i = 1, 3) \tag{1}$$

For example, Barenblatt has shown that the stress intensity factor $K_{2\alpha}$ can be expressed in terms of the cohesion modulus K, regarded as a material constant, through

$$K_{2\alpha} = -\frac{K}{\pi} \tag{2}$$

so everywhere on the rim of the crack

$$K_{20} \leq \frac{K}{\pi} \tag{3}$$

with equality sign for a limiting case where any increase in the load would result in a movement of the tip.

The following hypothesis for crack initiation is given by Barenblatt: "for any brittle (or quasi-brittle) material there exists a universal function $\Phi(-K_{1\alpha}, -K_{2\alpha}, -K_{3\alpha})$ of the stress intensity factors of the cohesive force, such that:

$$\Phi(-K_{1\alpha}, -K_{2\alpha}, -K_{3\alpha}) \leq 0 \tag{4}$$

at all points on the rims of all cracks within the body. At points at which $\Phi = 0$ the state of stress is limiting in that the attainment of this state at some point on the rim makes the crack move at that point and any increase in the load which would have led to $\Phi < 0$ in fact leads to crack *propagation*." Because of (1) the initiation condition can be written in the form

$$\Phi(K_{10}, K_{20}, K_{30}) = 0 \tag{5}$$

If the limiting condition corresponds to the constant energy of rupture so that the density of energy Γ_0, expended in forming a new crack surface is constant, equation (5) is written as

$$\frac{\pi(1+\nu)}{E}\left[(1-\nu)(K_{20}^2+K_{30}^2)+K_{10}^2\right] = \Gamma_0 \tag{6}$$

Since Barenblatt has shown that

$$\Gamma_0 = \frac{(1-\nu^2)K^2}{\pi E} \tag{7}$$

(5) can be written as

$$\Phi(-K_{1\alpha},-K_{2\alpha},-K_{3\alpha}) = K_{2\alpha}^2 + K_{3\alpha}^2 + \frac{1}{1-\nu}K_{1\alpha}^2 - \frac{K^2}{\pi^2} \tag{8}$$

Willis [76] has proved the equivalence of these two fracture criteria and showed that the modulus of cohesion K is not a constant but depends on the speed of the crack and therefore is not so fundamental a quantity as the surface energy of Griffith.

IV.3.3 Sih's Mixed-Mode Criterion

When fracture occurs in a mixed mode, experimental evidence indicates that the crack does not extend in its plane (unlike Griffith's one) and hence the classical energy balance of Griffith is not directly applicable. In such a case there are two basic questions [77]:

1. critical loads for fracture to occur
2. initial direction of crack extension.

The strain energy density dU in an element dA = rdrdΘ is

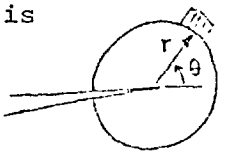

$$dU = \frac{1}{r}\left(a_{11}K_1^2+2a_{12}K_1K_2+a_{22}K_2^2\right)dA$$

K_1, K_2 are stress intensity factors for Mode I and II respectively and

$$a_{11} = \frac{1}{16\mu}(1+\cos\theta)(\kappa-\cos\theta)$$

$$a_{12} = \frac{1}{16\mu}\sin\theta\,[2\cos\theta - (\kappa-1)]$$

$$a_{22} = \frac{1}{16\mu}[(\kappa+1)(1-\cos\theta)+(1+\cos\theta)(3\cos\theta-1)]$$

$\kappa = 3-4\nu$ for plane strain, $\mu =$ shear modulus.

The strain energy density $\frac{dU}{dA}$ is singular of order $0(r^{-1})$ as $r \to 0$. Now define the strain energy density factor as

$$S = \lim_{r\to 0}\{r\frac{dU}{dA}\} = a_{11}K_1^2 + a_{12}K_1K_2 + a_{22}K_2^2$$

Sih states that:

(i) The initial crack growth takes place in the direction $\theta = \theta_0$ along which S possesses a minimum i.e.

$$\frac{\partial S}{\partial \theta} = 0 \to \theta = \theta_0; \quad -\pi < \theta_0 < \pi$$

(ii) Fracture is initiated when S reaches a critical value S_{cr}, i.e.

$$S = S_{cr} \text{ for } \theta = \theta_0$$

S_{cr} is assumed to be a material property.

Using this concept for a central crack of length 2a in an infinite medium under Mode I loading (σ) we find

$$S = \frac{\sigma^2 a}{16\mu}(1+\cos\theta)(\kappa-\cos\theta)$$

and

$$\frac{\partial S}{\partial \theta} = 0 \Rightarrow \theta_0 = 0$$

and

$$S_{cr} = \frac{(\kappa-1)\sigma^2 a}{8\mu}$$

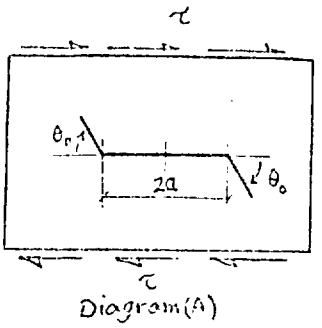

Diagram(A)

which can be related to the critical stress intensity factor $K_{1C} = \sigma\sqrt{a}$ as $S_{cr} = \frac{(\kappa-1)K_{1C}^2}{8\mu}$ and hence, for this problem, S_{cr} has similar implication as Irwin's idea of taking the critical stress intensity factor as a material constant.

The concept of critical strain energy is best demonstrated on a Mode II crack problem. For $K_1 = 0$, $K_2 = \tau\sqrt{a}$ (Diagram A)

$$S = \frac{\tau^2 a}{16\mu}[(\kappa+1)(1-\cos\theta) + (1+\cos\theta)(3\cos\theta-1)]$$

$$\frac{\partial S}{\partial \theta} = 0 \Rightarrow \cos\theta_0 = \frac{\kappa-1}{G}$$

and

$$S_{cr} = \frac{(-\kappa^2+18\kappa-1)}{192\mu}\tau^2 a$$

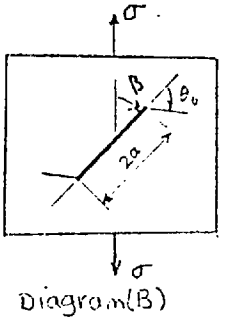

Diagram(B)

i.e. the crack does not initially extend at the crack plane. This has experimentally been verified on a number of materials and θ_0 measured. The agreement between the θ_0 from the S-criterion and reported experiments are good.

For an inclined crack in a plate in tension we have (Diagram B)

$$S = \sigma^2 a(a_{11}\sin^2\beta + 2a_{12}\sin\beta\cos\beta + a_{22}\cos^2\beta)\sin^2\beta$$

$$\frac{\partial S}{\partial \theta} = 0 \Rightarrow (\kappa-1) \sin(\theta_0-2\beta) - 2\sin 2(\theta_0-\beta) - \sin 2\theta = 0, \quad \beta \neq 0$$

It should be mentioned that the maximum stress criterion gives an angle which for an isotropic material is independent of the material properties and for large values of β is close to the S-criterion results. More details on this problem are given in [77].

IV.4 CRACK PROPAGATION AT THE LIMITING RAYLEIGH VELOCITY

In this section we discuss the possibility and implications of having a Rayleigh speed of crack propagation ($V = V_R$). From the earlier result in (32) (see IV.2.2.1) we know that the existence of a non-trivial solution to the problem is guaranteed if

$$(1+\alpha_2^2)^2 - 4\alpha_1\alpha_2 = 0$$

i.e.

$$V = 0 \quad \text{or} \quad V = V_R$$

Since we have analyzed the stationary case ($V = 0$) we exclude it here and only deal with $V = V_R$. In particular we want to see if this velocity can be regarded as an acceptable speed for propagating cracks and if so get numerical results for the problem.

Stroh [78] has apparently been the first stating that the velocity $V = V_R$ is the terminal velocity (i.e. the upper bound for all acceptable velocities). His heuristic proof is based on the assumption that the surface energy to be zero. He was then led to the conclusion that the local tensile stresses are zero and hence the crack can be thought of as a disturbance along a free surface which can only propagate at $V = V_R$.

By arguments based on the analysis of exact solutions of the dynamic equations of elasticity, several authors concluded that the terminal velocity is V_R. Craggs [72] considered steady propagation of a semi-infinite straight crack with symmetrically distributed normal and shear stresses applied on a part of the crack faces adjacent to the tip. Ang [79] dealing with an unsteady elastic field in an infinite body with a semi-infinite crack loaded normal to the crack surfaces suggests that when $V \to V_R$ a 'resonance' effect seems to be produced. Barenblatt [80] treats the wedging of brittle bodies. He assumes a zone of cohesive forces ahead of the crack to remove the stress singularities and as the conclusion states that as the crack velocity approaches the Rayleigh velocity, peculiar resonance phenomena arise.

In order to clarify the relation between 'resonance', say, in an electrical circuit and that in an elastic field when a free crack is running at $V = V_R$ we give the following explanation. In a circuit if the source supplies energy at a frequency ω which corresponds to the 'natural' frequency ω_n of the circuit (assuming that the energy could be supplied) then the oscillator would gain large amplitudes, in fact it tends to infinity for $\omega \to \omega_n$. If this provision of energy is continued one can theoretically reduce the amplitude of the alternating supply (but keeping the frequency locked at $\omega = \omega_n$) to almost zero at the input while still getting infinite amplitude of oscillations at the output. Now even if the source is removed the circuit would continue oscillating at its 'natural' frequency (assuming a conservative system).

In analogy with the circuit we have a free crack where the energy required to move it decreases with increasing velocity of the

crack tip and reaches zero at $V = V_R$ (if a constant velocity could be established at all). In fact the surface waves due to the dynamics of the problem (at V_R) would *interfere* with the tip motion. (This analogy should not be regarded as a perfect parallel, however.) So in a propagating crack problem once the constant velocity V_R is reached it will maintain this speed even if the external forces are removed. A crack in this state could be called a 'self-maintaining crack' and it could be arrested if any of the assumptions in the solution of the problem are violated (e.g. any change in the material property etc.).

Broberg [73] in treating the problem of a uniformly propagating crack assumes zero surface energy and for large values of time concludes that $V = V_R$ (Infinite body, finite length crack.) In fact by using (22) of IV.1 we can get the following expression (see also [81]) for the fracture power E in terms of stress-intensity factors K_I and K_{II}:

$$E = \frac{1+\nu}{E} V(t) \frac{1-\alpha_2^2}{-4\alpha_1\alpha_2+(1+\alpha_2^2)^2}[\alpha_1 K_I^2+\alpha_2 K_{II}^2]$$

From (40) and (42) we see that

(a) $K_I = K_{II} = 0$ if $V = V_R$

(b) $E = 0$ if $V = 0$ or $V = V_R$

i.e. fracture at the Rayleigh velocity proceeds without any loss of energy from the system.

It seems that the resonance phenomena at $V = V_R$ is not limited to the problem of moving cracks only. In the 'punch' problem the same pecularity arises as the punch velocity approaches V_R.

(It should also be mentioned that Eshelby [82] in studying the

velocity of motion of linear dislocations concludes that V_R is the upper limit for the velocity if the atomic nature of the material is taken into account.)

As to the experimental evidence, most of the experiments reported in the literature are based on Mode I fracture for specimen of finite dimensions. These dimensions are usually so small that the dynamic analysis of the problem can be valid only for very small intervals of time after fracture is initiated. Hence, in general, it is too much to expect that there would be enough time for the crack to settle down on a steady velocity as high as V_R before breaking the boundaries. However, in our particular application, i.e. extension of geological faults, the medium is large enough to allow for the crack to propagate at any physically possible velocity for any reasonable length of time. This provides a unique experiment that cannot be simulated in small-scale in laboratories.

Experimental results [78] for metals, glass, polymers etc. indicate velocities of propagation as high as $V = 0.78C_2 < V_R = 0.92C_2$. Regarding the nature of the measurements together with the material inhomogeneity and anisotropy (even for a perfectly brittle body) lower values for the upper limit of velocity is reasonable. It is also suggested that in real materials crack would run in a jerky manner, coming to rest and moving forward again. Such a process would give a mean crack velocity less than the limiting velocity (on seismograms, sometimes, there are indications of a stopping - and - starting phase (stick-slip mechanism) during the fault propagation).

Yoffe [71] showed that for a non-zero speed of crack propagation in Mode I the normal stress σ_{22} does not have its maximum on the crack line for velocities greater than a critical velocity V_{cr} ($V_{cr} < V_R$).

So if one uses a failure criterion such as the "maximum principal stress" then one can conclude that before the speed of the crack reaches V_R, due to symmetry, bifurcation takes place at the critical velocity V_{cr}.

By branching, the velocity is reduced and hence the upper limit for the velocity would, in this case, be $V_{cr} < V_R$.

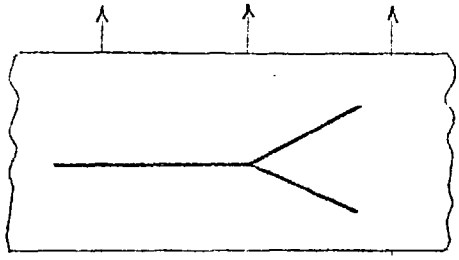

Bifurcated Crack (Mode I)

In conclusion for Mode I fracture : the upper limit is dictated by (known) failure criteria and is $V_{SS} \leq V_R$.

However for the general loading, due to lack of symmetry, bifurcation cannot happen and instead the crack would smoothly bend along a curved trajectroy in order to satisfy any failure criterion. This would possibly imply that under general loading conditions the crack starts to move from zero initial velocity to a critical velocity unsteadily along a straight line. For velocities of the accelerating crack greater than this critical velocity, the crack tends to curve, in a specific way, by changing its slope while increasing its velocity until the velocity approaches V_R where it is locked at this velocity with no further change in its speed or its trajectory.

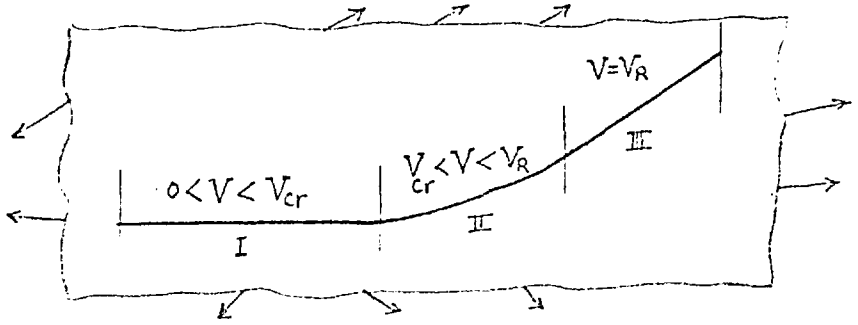

Trajectory of an Accelerating Crack

IV.5 NUMERICAL TREATMENT OF CRACK PROPAGATION PROBLEMS

IV.5.1 Current Techniques

Many authors have attempted to get solutions for moving crack problems. Using a finite difference technique (HEMP mode) Chen [83] presents plots of stress field for a number of time steps. With the inherent impossibility of simulating the propagating crack problem with the aid of any finite-difference scheme it is clear that this method cannot represent the true physical problem. However, his solution could be acceptable only as a limiting case ($V=V_R$) provided the tip of the crack is moved in a way consistent with this velocity.

Aboudi [84] has also used finite difference methods to solve the problem of an interface propagating crack. The use of finite differences for an interface problem introduces even more serious errors. This is due to the expected oscillatory behaviour (with the frequency of oscillations rapidly increasing as the crack tip is approached) of the stress field from the linear theory of elasticity for an interface crack [88]. Clearly, finite difference technique cannot take into account this feature and one expects more erroneous results as is reflected in the numerical values presented in the reference.

Employing a conventional finite element routine, Aberson et al [85] and Malluck [86] give numerical values for dynamic stress intensity factor (Mode I fracture). Their approach is to use the same finite element formulation as for standard dynamic problems (i.e. no term corresponding to fracture power). The moving crack is simulated by subsequent release of the nodes in front of the crack tip. The resulting displacements are then matched with the correct asymptotic solutions to extract the dynamic stress intensity factors. In the next section it becomes clear that the conventional finite elements correspond *only* to

$E \equiv 0$ (i.e. either for stationary cracks $V = 0$ or $V = V_R$ if the tip is moved exactly at this speed) and any attempt to extract *non-zero dynamic stress intensity factors* is bound to fail. In fact it is surprising that they get a non-zero value for K_I (for any crack velocity). However they state that their more accurate stress intensity factors correspond to higher crack velocities. Indeed as $V \to V_R$ then $K_I \to 0$ which represents the *only* consistent interpretation of the numerical values and hence the reason for getting more accurate results when $V \to V_R$.

Anderson [87(i-ii)] has also used finite element method for this problem. He does not take into account the dynamic effects while he considers the plastic deformation at the crack tip.

Nilsson [89] using the Wiener-Hopf technique has found dynamic stress intensity factor for a strip in mode I fracture. Other relevant references in this regard include [90]-[92].

IV.5.2 Approximation of the Variational Formulation for Unsteady Crack Propagation

IV.5.2.1 Finite elements in time and space

We have earlier seen that the moving crack problem can be represented by the solution u, to the following equation (see equation (25) Chapter IV.1)

$$(P): \quad \int_0^T \int_{D_\varepsilon} \ddot{u}\dot{v}\,dx\,dt + \int_0^T \int_{D_\varepsilon} \sigma_{ij}(u)\varepsilon_{ij}(\dot{v})\,dx\,dt - \int_0^T \oint_{C_\varepsilon} \sigma_{ij}(u)n_j\dot{v}\,ds\,dt =$$

$$\int_0^T \int_{D_\varepsilon} f\dot{v}\,dx\,dt + \int_0^T \int_C t\dot{v}\,ds\,dt, \quad \text{for all } V \in \bar{V}$$

$\varepsilon_x \to 0, \quad \varepsilon_y \to 0.$

With the asymptotic expressions (37)-(41) of (IV.1) for stresses and velocities near the tip it is obvious that we have to use an approximation

scheme capable of handling singularities in *both stresses and velocities*. Failure to do so will result in a *zero* fracture power which, in general, contradicts the physics of the problem.

Now we suggest that the only valid numerical scheme for an approximate solution of the problem is to use finite elements in *both time and space*.

The usual finite element technique as applied to hyperbolic systems is to reduce the time dependent problem to a sequence of elliptic systems at any instant of time by finite difference approximation of time derivatives involved. This is the technique that was applied to stationary dynamic crack problems. However, in the moving crack case since we have velocity singularity as well, any finite difference in time is bound to give *finite velocities* (velocities calculated from displacements are finite throughout the domain). As a consequence, the third term in the left hand side of (P) which involves a contour integration around a circuit would always be zero even though *stress* singularities are preserved.

The *approximating problem* (P_ℓ) is as follows:

(P_ℓ): Find $u_\ell \in \bar{V}_\ell$ such that $u_\ell - u_{0\ell} \in \bar{V}_\ell$ and

$$(\ddot{u}_\ell, \dot{v}_\ell)_{\bar{D}_\varepsilon} + a(u_\ell, \dot{v}_\ell)_{\bar{D}_\varepsilon} + b(u_\ell, \dot{v}_\ell)_{\bar{C}_\varepsilon} = (f, \dot{v}_\ell)_{\bar{D}_\varepsilon} + (t, \dot{v}_\ell)_{\bar{C}}, \quad \text{for all } v_\ell \in \bar{V}_\ell,$$

$\varepsilon_x \to 0$, $\varepsilon_y \to 0$ where $\bar{V}_\ell \subset \bar{V}$ is of finite dimensions.

Note: It is observed that (P_ℓ) is approximate in two ways, one approximation is due to discretization in time and space (represented by the symbol ℓ for discrete time interval (τ) and discrete space mesh of size (h)) and the other due to the size of the finite region C_ε as the formulation (P) is dependent on $\varepsilon_x \to 0$ and $\varepsilon_y \to 0$ in a particular way. We do not know the behaviour of the solution for different values of ε_x, ε_y, h and τ but

expect to get a convergent solution as $h \to 0$ and $\tau \to 0$ with small (compared to any characteristic length in the problem) ε_x and ε_y. These can be investigated by numerical experiments.

IV.5.2.2 Reduction to a set of simultaneous linear equations

We take the approximating space $\bar{V}_\ell$ to be spanned by the basis functions $f_i(x,y,t)$ i.e.

$$u = \sum_{i=1}^{m} f_i(x,y,t)\alpha_i \tag{1}$$

Then (P_ℓ) can be written as

$$(\sum_i \ddot{f}_i\alpha_i, \sum_j \dot{f}_j\beta_j)_{\bar{D}_\varepsilon} + a(\sum_i f_i\alpha_i, \sum_j \dot{f}_j\beta_j)_{\bar{D}_\varepsilon} + b(\sum_i f_i\alpha_i, \sum_j \dot{f}_j\beta_j)_{\bar{C}_\varepsilon} =$$

$$(f, \sum_j \dot{f}_j\beta_j)_{\bar{D}_\varepsilon} + (t, \sum_j \dot{f}_j\beta_j)_{\bar{C}}, \quad \text{for all } \beta_j,\ i,\ j = 1,\ldots,m$$

or alternatively

$$\sum_{i=1}^{m} \alpha_i \{(\ddot{f}_i, \dot{f}_j)_{\bar{D}_\varepsilon} + a(f_i, \dot{f}_j)_{\bar{D}_\varepsilon} + b(f_i, \dot{f}_j)_{\bar{C}_\varepsilon}\} = (f, \dot{f}_j)_{\bar{D}_\varepsilon} + (t, \dot{f}_j)_{\bar{C}}$$

$$\text{for all } j = 1, \ldots, m \tag{2}$$

This system can equivalently be written in the form:

$$K\alpha = F \tag{3}$$

where

$$K = \{k_{ij}\};\quad k_{ij} = (\ddot{f}_i, \dot{f}_j)_{\bar{D}_\varepsilon} + a(f_i, \dot{f}_j)_{\bar{D}_\varepsilon} + b(f_i, \dot{f}_j)_{\bar{C}_\varepsilon}$$

$$F = \{F_j\};\quad F_j = (f, \dot{f}_j)_{\bar{D}_\varepsilon} + (t, \dot{f}_j)_{\bar{C}}$$

and

$$\alpha = \{\alpha_i\},\quad i,\ j = 1,\ \ldots,\ m$$

Note: The space $\bar{V}_\ell$ incorporates the basis functions corresponding to displacements near the tip given by the asymptotic solution there (e.g. see equation (37) of IV.2 for near-tip displacements in Mode I).

While this scheme is conceptually easy, its computer implementation is difficult. The difficulty is due to two different reasons.

1. Choice of basis functions satisfying the conditions of interelement compatibility in time and space in the presence of singular functions.

2. The inherent large dimensions of the resulting system of equations.

With the present computer generations this poses serious storage problems (this is one reason for using finite difference in time in conjunction with finite elements in space for standard time-dependent problems).

The first difficulty could be alleviated if we are content with basis functions in our approximating space that are *not mathematically elegant* even though they preserve all the dominant features of the problem. Specifically we can extend the idea of quarter-point elements in 2-D space to 3 dimensions i.e. 2 space dimensions and time. For this we can use a three dimensional element having an *edge* along which stresses and velocities are unbounded. This element is computationally easy to implement.

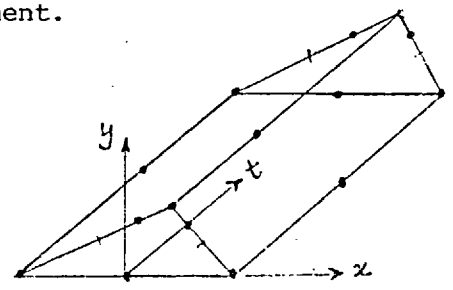

However, the second difficulty remains unresolved.

Note: The first difficulty could also be considered as the problem of

matching the global and local field variables. By deciding on a particular form for fracture power (in terms of the crack propagation speed V) we will be able to combine the global and local behaviour of the field to get both the unknown crack velocity V and field variables.

IV.5.2.3 Approximation of the Rayleigh problem

For the special case when the crack is propagating at the constant Rayleigh velocity V_R we know that the fracture power is zero and the singularities are absent. The only non-standard feature of the problem would then be that of a moving boundary into the medium. Moreover, we can use finite differences in time for this case (no velocity singularities). Therefore, we get round the difficulties for the general unsteady crack problem. In this case the problem is reduced to the following:

Find $u \in V$

$$(\ddot{u}\ ,v)_{D(t)} + a(u,v)_{D(t)} = (f,v)_{D(t)} + (t,v)_{C(t)} \quad \text{for all } v \in V$$

where

$$V = \{v \mid v \in (H^1(\Omega))^2,\ v=U \text{ on } \Gamma_U\}$$

This variational form is similar to the stationary crack problem analysed earlier in Chapter III with the only difference that the domain is now time-dependent. This is equivalent to saying that any finite-dimensional approximation of the problem results in a linear system of equations with a time-dependent dimension (i.e. as time goes on new surfaces are created in the material and hence the dimensions of the matrix K increase with time).

For Mode I fracture we can use symmetry and then the problem is

tractable as it would only require a change in the boundary conditions with time. It is clear, that in the presence of boundaries (i.e. reflected waves) for any finite domain $V = V_R$ remains as a consistent velocity for all time.

In the next chapter we will present numerical results for Mode I fracture at the Rayleigh velocity.

Chapter V

COMPUTATIONAL ASPECTS OF THE PROBLEM

V.1 INTRODUCTION

We have earlier seen that the standard approximate problem

$$(P_h) \qquad \begin{cases} \text{Find } u_h \in V_h \text{ such that} \\ a(u_h, v_h) = (f, v_h) \qquad \text{for all } v_h \in V_h \end{cases} \tag{1}$$

can be solved by Galerkin's method. In the method one looks for a solution to (P_h) in a finite-dimensional subspace $V_h \in V$ spanned by a linearly independent set of basis functions $w_1(x), \ldots, w_m(x)$. The solution u_h is then of the form:

$$u_h(x) = \sum_{i=1}^{m} \alpha_i w_i(x) \tag{2}$$

where the coefficients α_i, $i = 1, \ldots m$ are to be determined such that u_h satisfies (P_h) i.e.

$$\sum_{i=1}^{m} a(w_i, w_j)\alpha_i = (f, w_j), \qquad \text{for all } j = 1, \ldots, m \tag{3}$$

or

$$K\alpha = f \tag{4}$$

where $K_{ij} = a(w_i, w_j)$ is the stiffness matrix entry and $f_j = (f, w_j)$ is the load vector entry. Now we have to solve a linear system of simultaneous equations in terms of the unknown coefficients α_i, $i = 1, \ldots, m$.

We recall some of the basic properties of this solution as being the best L_2 approximation with the residual error orthogonal to the subspace V_h. (The admissible space is, obviously, $H^1(\Omega)$.)

For the standard dynamic problem we are concerned with

$$(P_h) \quad \begin{cases} \text{Find } u_h \in V_h \text{ such that} \\ (\ddot{u}_h, v_h) + a(u_h, v_h) = (f, v_h) \quad \text{for all } v_h \in V_h \end{cases} \tag{5}$$

then using Galerkin's solution in the form of (2) the problem is reduced to

$$\sum_{i=1}^{m} (w_i, w_j)\ddot{\alpha}_i + \sum_{i=1}^{m} a(w_i, w_j)\alpha_i = (f, w_j) \quad \text{for all } j = 1, \ldots, m \tag{6}$$

Thus the α_i's are the solution of system of ordinary differential equations:

$$M\ddot{\alpha} + K\alpha = f \tag{7}$$

where

$M_{ij} = (w_i, w_j)$ is the mass matrix entry

$K_{ij} = a(w_i, w_j)$ is the stiffness matrix entry

and

$f_j = (f, w_j)$ is the load vector entry

V.2 CHOICE OF BASIS FUNCTIONS

In earlier chapters we have seen that for any convergent finite element scheme we should incorporate the proper singularities of the solution in the approximating subspaces. For this reason we introduced the spaces V^k (see Chapter II.7) which can be interpreted

as the usual smooth spaces augmented by singular basis functions χ_i.

As to the practical implementation of this scheme, we will only be dealing with the space V^1 which includes the leading term singularity of the solution. With this we, theoretically, expect an order of convergence of two (see Chapter II) for displacements from any finite element method using polynomials of minimum degree one.

Before going into details of the basis functions we need to clarify two basic considerations: conformity and the patch test.

V.2.1 Conformity

For a differential equation of order 2m in the plane we want to know which piecewise polynomials lie in the admissible space $H^m(\Omega)$. The sufficient condition for conformity is then to have basis functions which together with their (m-1) derivatives are continuous across element boundaries. In case we choose our basis functions from polynomials (as we usually do) on each element, then they lie in H^m if and only if all derivatives of order less than m are continuous along interelement boundaries. Any violation of this rule would result in infinite strain energy and consequently a physically meaningless approximation. In the problems we are dealing with C^0 conformity is enough. However, in practice, some non-conforming elements have proved useful and reliable. The reason for their reliability is explained by the fact that the total strain energy is found by the sum of the contributions from each individual element and therefore the interelement discontinuities do not affect the finiteness of the strain energy. The reason for their popularity is in their simplicity for construction.

However, one should be very careful in using the non-conforming elements as in many cases they do not result in a convergent algorithm

and one has to have means to ensure the convergence before applying new elements to any particular problem. One such a tool has been devised by engineers and is called *the patch test*.

V.2.2 The Patch Test

This has a recent historical development since 1965 and we refer to the work of Irons [43] and references there.

The importance of the interelement continuity was earlier noticed for convergence. Irons, the originator of the empirical tool holds the idea that the patch test provides a necessary, and possibly sufficient, condition for convergence as $h \to 0$. Strang [42] proves that passing the patch test is, indeed, sufficient for convergence. However, by establishing upper bounds for the approximation error, Oliveira [93] proves that, in contradiction with the Irons' thinking, passing the patch test is *not a necessary condition* for convergence. He also demonstrates the *sufficiency* of the test for convergence. Moreover, he shows that contrary to Strang's argument [42] higher order patch tests are not necessary for higher order accuracy analysis and that, with the completeness condition satisfied, the order of the error involved is dependent on the order of the completeness condition.

Suppose that all polynomials P_ℓ of degree ℓ (with ℓ being the maximum order of derivatives appearing in the expression for the strain energy) are contained in the approximating space. Suppose also that around an arbitrary patch of elements, the boundary conditions are chosen such that the true solution within the patch is $u = P_\ell$. Then the patch test requires that the *approximation* u_h, computed by using non-conforming elements (i.e. ignoring δ-functions along the interelement boundaries) must also coincide with P_ℓ. When the test is passed, and

completeness conditions satisfied, then it is expected that the convergence would follow as in conforming models.

With this background on the conformity and patch test we are able to discuss the non-standard approximation we use for the crack problem.

V.2.3 Singular Basis Functions

There is a variety of ways to supplement a piecewise polynomial approximating space by proper singular functions to achieve the desired optimum rates of convergence. The efficiency of methods varies according to the degree to which the actual problem has been idealized.

a. The most straightforward method which thoroughly satisfies the theoretical requirements to improve rates of convergence of the technique is to augment the space of piecewise polynomials with the exact form of singular behaviour of the solution near the crack tip, i.e. the approximating space has the basis $\{w_i\}_{i=1}^{p}$ (usual piecewise polynomials) and $\{s_i\}_{i=1}^{q}$ (singular functions in the expansion of the exact solution). This idea has already been implemented for the problem of torsion of a cracked beam (i.e Laplace's equation) by Fix et al [94]. See also [95]. However, there are, even for this simplest problem, some computational difficulties associated with the evaluation of inner products involving singular functions and inversion of the resulting matrix. It is obvious that introduction of the functions destroys the band-structure of the matrix and in most cases the condition number of the matrix is much increased resulting in possible numerical instabilities. Eventhough there are ways out of these difficulties, the amount of effort involved might turn out to be too much, particularly, for equations of elasticity in plane domains. However, since in this method we have singular functions defined over a *fixed* domain (either on a part or on the whole of the domain), in practice, we have to be able to get the expected theoretical

rates of convergence. See [96] for application to a strip problem.

b. An alternative approach is the use of the so called 'singular elements'. In this approach one surrounds the crack tip with special elements over which the dominant singular behaviour is simulated. This method fits well into the standard finite element systems with the difference that one has to develop a new element type. In this category of elements fall the Wilson's elements [22] and Byskov's cracked elements [97] . For example, Wilson uses triangular elements with the following shape function at the crack tip

$$u = u_0 + \left[\frac{\theta_j-\theta}{\theta_j-\theta_i} u_i + \frac{\theta-\theta_i}{\theta_j-\theta_i} u_j\right] \left(\frac{r}{r_0}\right)^{\frac{1}{2}}$$

i.e. elements that preserve the exact $r^{\frac{1}{2}}$ behaviour but approximate in θ-direction.

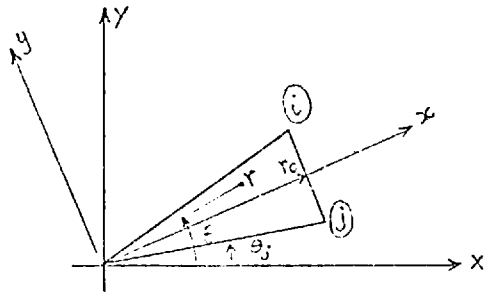

While numerical implementation of singular elements is relatively easy, there are two basic problems that make their convergence questionable. One is their strong non-conformity and the other is their support shrinking to zero as $h \to 0$. The non-conformity arises from the displacement discontinuity along the common boundary of the singular and the standard elements (they only match at the nodes). With this difficulty, good accuracy can only be obtained if the element sizes in the angular direction is significantly reduced. On the other hand, a basic assumption in convergence analysis of the standard finite element is that all elements have angles far from zero i.e. not too thin elements. It is not clear how

one can reconcile these two opposing conditions for convergence and whether there exists any critical element size for which reliable results could be obtained. We have implemented Wilson's crack (singular strain triangular -SST) element [22] and were not able to obtain the accuracy reported there. The explanation could be that either due to the preceding discussion we should not expect accurate enough solutions or he might have used (but not mentioned) a layer of auxiliary elements between singular and standard elements to reduce the degree of non-conformity present there. We also observed that these elements do not pass the patch test and hence their convergence is not guaranteed (in fact this element is *not* in static equilibrium).

The second difficulty of having singularities defined over a domain of *variable size* is practically less important. The reason for this is that singularities are limited to a very small neighbourhood of the crack tip and as long as they are present there, in principle, we have to get good accuracy. However, it is not known how small this region is and it seems the only way to get an estimate for the size of the region is by numerical evaluation. In this way one would expect to get convergent results as $h \to 0$ up to a critical element size h_c beyond which the behaviour would become erroneous. We will explain this further in the next approach.

c. A third approach, and by far the easiest of all, has been recently put forward, independently, in [98] and [99]. This method, referred to as the quarter-point approach is now widely used for static crack analysis.

In this approach by using standard quadratic isoparametric elements, and moving the mid-side nodes to quarter position one can produce square root singularities so desirable in linear fracture

mechanics.

The basic idea was initially demonstrated on a standard 8-node rectangular element and was shown that the square root singularities are present along the *element boundaries*.

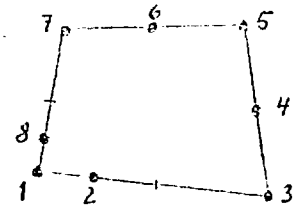

In a recent correct analysis, Barsoum [100] indicates that by moving the mid-side nodes, in an 8-node rectangular isoparametric element, to quarter position we get a stronger singularity 1/r within the element as well which is not appropriate for elastic crack analysis. However, the singular function $r^{\frac{1}{2}}$ could be produced if one side of the element is collapsed to zero length.

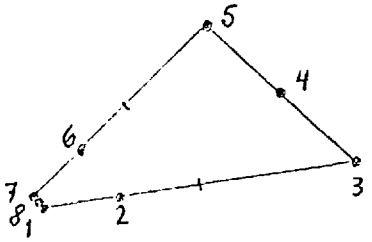

The collapsed rectangular elements are then the desired ones. (See also [101].)

d. Inspired by the above idea we use the standard 6-node isoparametric triangular element and move the mid-side nodes to quarter-position along the edges intersecting at the crack tip. Then following the above arguments one can show that these elements have the proper order of singularity ($r^{\frac{1}{2}}$). These imbedded singularity elements are easier than the collapsed 8-node elements to construct and implement.

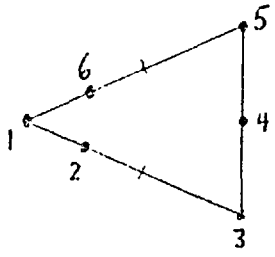

Take p(r,θ) an arbitrary point in the triangle 1-2-3 with the local coordinate system x-y.

For the isoparametric family of finite elements, the geometry within the element is approximated by the same interpolation functions that are used to specify the displacement field within the element, i.e.

$$u = \sum_{i=1}^{6} N_i u_i, \text{ etc.} \tag{1}$$

$$x = \sum_{i=1}^{6} N_i x_i, \text{ etc.} \tag{2}$$

where u_i and x_i are the nodal displacement and coordinate values respectively and N_i are the quadratic isoparametric functions over the triangle in terms of the well-known *area coordinates*, L_i, i = 1, ..., 3

$$N_1 = (2L_1-1)L_1$$

$$N_4 = 4L_1L_2 \tag{3}$$

etc.

Now we show that by proper positioning of the side nodes (4) and (6) along the edges of the triangle the shape function N_1 associated with the node (1) produces square root singularity $r^{\frac{1}{2}}$ when p moves along any arbitrary line θ = const. and hence the desired property for linear fracture application is derived.

We note that

$$x_1 = 0 \quad x_2 = h \quad x_3 = h \quad x_4 = h/4 \quad h_5 = h \quad x_6 = h/4$$

$$y_1 = 0 \quad y_2 = -\ell \quad y_3 = +\ell \quad y_4 = -\ell/4 \quad y_5 = 0 \quad y_6 = \ell/4 \tag{4}$$

substituting (3) and (4) into (2) we obtain:

$$x = (2L_1-1)L_1x0+(4L_1L_2+4L_1L_3)xh/4+[(2L_2-1)L_2+(2L_3-1)L_3]h+4L_2L_3.h$$

$$= h(1-L_1)^2 \qquad (5)$$

$$y = (2L_1-1)L_1x0+(-4L_1L_2+4L_1L_3)x\ell/4+[-(2L_2-1)L_2+(2L_3-1)L_3]\ell+4L_2L_3x0$$

$$= \ell(1-L_1-2L_2)(1-L_1)$$

where we have used $L_1 + L_2 + L_3 = 1$ to eliminate L_3 in x and y.

The radius r to point p is then given by:

$$r = \sqrt{x^2+y^2} = x\sqrt{1+(\frac{y}{x})^2} = h(1-L_1)^2\sqrt{1+\tan^2\theta} \qquad (6)$$

From (6) follows that

$$L_1 = 1 - \sqrt{\frac{r}{r_{m,\theta}}}\ ; \quad r_{m,\theta} = h\sqrt{1+\tan^2\theta} = \text{const for } \theta = \text{const} \qquad (7)$$

Substituting (7) into (3) we get:

$$N_1 = (1-2\sqrt{\frac{r}{r_{m,\theta}}})(1-\sqrt{\frac{r}{r_{m,\theta}}})$$

or

$$N_1 = 1 + 2(\frac{r}{r_{m,\theta}}) - 3\sqrt{\frac{r}{r_{m,\theta}}} \qquad (8)$$

i.e. the required $r^{\frac{1}{2}}$ singularity is available at the tip.

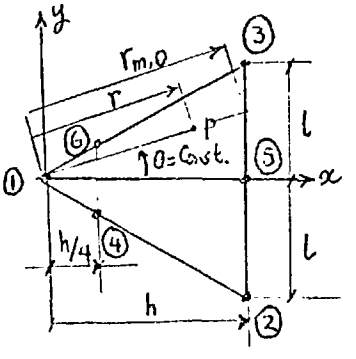

An important property of the elements in (c) and (d) category is that they are *conforming* elements and pass the *patch test*. Therefore the convergence of the algorithm using these elements is guaranteed. 6-node crack elements have been incorporated in the programme for both static and dynamic crack analysis.

V.3 TIME-DISCRETIZATION IN DYNAMIC PROBLEMS

The differential equation (7) can be reduced to a system of linear simultaneous equations by direct step-by-step integration in time. One method is the Newmark's scheme [102]. In this method we replace X_{n+1} and $\dot{X}_{n+1}$ by

$$X_{n+1} = X_n + \dot{X}_n.\tau + [(\tfrac{1}{2}-\beta)\ddot{X}_n+\beta\ddot{X}_{n+1}]\tau^2$$

$$\dot{X}_{n+1} = \dot{X}_n + [(1-\gamma)\ddot{X}_n+\gamma\ddot{X}_{n+1}]\tau \qquad (8)$$

where X_{n+1} and X_n denote the value of X(t) at times t_{n+1} and t_n respectively and $t_{n+1} - t_n = t_n - t_{n-1} = \tau$ is the time increment. Usually γ is taken to be $\frac{1}{2}$. With this value the equation (7) can be shown to reduce to

$$[M+\beta\tau^2K]X_{n+1} = [2M-\tau^2(1-2\beta)K]X_n - [M+\beta\tau^2K]X_{n-1} + \tau^2[\beta f_{n+1}+(1-2\beta)f_n +\beta f_{n-1}] \qquad (9)$$

$n = 1, \ldots, N$, where f_n is the value of f(t) at $t = t_n$.

Equation (9) presents a recursive formula for determination of X(t) at any given time step from previous information. It is clear that for dynamic problems the matrix to be inverted is the sum of contributions from both mass and stiffness matrices. The load vector also involves contributions from both the actual dynamic loading and past system response.

This scheme is known to be unconditionally stable for $\beta \geq \frac{1}{4}$ [103]. Also for the particular choice of $\beta = \frac{1}{4}$ it results in the minimum time-truncation error. It is for these reasons that we will exclusively be dealing with the Newmark's scheme with $\gamma = \frac{1}{2}$ and $\beta = \frac{1}{4}$. In fact, it is for these values of parameters that we have proved results on the rates of convergence for fully-discretized equations of elastodynamics (see Chapter III). For other methods of integration of equations of motion and on evaluation of their performance on a one-dimension problem we refer to [104] and [105].

The central difference method for numerical integration leads to equation (9) with $\beta = 0$. Therefore, the system is only conditionally stable and for large values of the time increment τ it becomes unstable.

Throughout our analysis we have used the *consistent mass matrix* i.e. the correct form for evaluation of the entries according to $M_{ij} = (w_i, w_j)$. On theoretical grounds, this seems to be the only option to calculate the mass matrix. However, many engineers have already idealized the mass distribution within each element by their equivalent lumped masses at the nodes. This results in a diagonal mass matrix. The great attraction in the lumping process, in conjunction with central difference schemes, comes from the fact that from equation (9), with $\beta = 0$ and M diagonal, *explicit* expressions for $X_1, \ldots, X_N$ are obtained. For large systems and when a large number of time steps are to be used, computational effort could greatly be reduced by having an explicit form [106]. While the lumping procedure for simple elements is rather easy there is a snag in finding a proper diagonal mass matrix for more sophisticated elements. For this reason some improved versions of diagonal mass matrices avoiding the inherent inaccuracies of lumping procedures have been developed [107].

One more point in connection with the starting procedure for the recursive relation (9) is in order. As the equation (9) only provides values for $x_2, \ldots, X_N$ we have to approximate X_1 from initial values X_0 and $\dot{X}_0$. Using the truncated Taylor series expansion for X_1 we have

$$X_1 = X_0 + \tau(\frac{\partial x}{\partial t})_0 + \frac{\tau^2}{4}[(\frac{\partial^2 x}{\partial t^2})_0 + (\frac{\partial^2 x}{\partial t^2})_1]$$

multiplying both sides by M and using (7) we obtain

$$[M+\frac{\tau^2}{4}K]X_1 = [M-\frac{\tau^2}{4}K]X_0 + \tau[M]\dot{X}_0 + (f_0+f_1)\frac{\tau^2}{4} \qquad (10)$$

so before using the recursive formula (9) we have to solve equation (10) to obtain X_1. It is to be noted that the matrices to be inverted in (9) and (10) are the same and hence we can invert $[M+\frac{\tau^2}{4}K]$ *once* and store it for further application of loads to get $X_1, \ldots X_N$.

V.4 NUMERICAL (SPATIAL) INTEGRATION OF THE APPROXIMATING PROBLEM

In error analysis of Chapter III we have assumed that [M] and [K] are evaluated exactly. Due to use of polynomials in finite elements these inner products and bilinear forms can easily be evaluated by *analytical* means over simple elements. However, these calculations are cumbersome for more complex elements and it is advantageous to use some standard quadrature rules for numerical evaluation of the matrices. In particular, for isoparametric elements it is essential to use numerical integration routines.

Numerical integration introduces some additional errors in the results. For the simple Sturm-Liouville equation in one-dimension

$$-(pu')' + qu = f$$

one can show [42] that the error in the strain using (k-1) Gauss points is of the order of h^k.

An interesting advantage of numerical integration is that it, generally, yields more accurate results. This is because we have an overstiff system in the Ritz method and by numerical integration we commit errors in the right direction (relaxation).

While we have not attempted to give estimates for the numerical quadrature-errors involved in our results, it seems that such estimates for equations of dynamic elasticity could be obtained by an approach similar to [108].

Throughout the analysis we have used Gaussian quadrature formulae. In each element there are a certain number of evaluation points $\xi_i = (x_i, y_i)$ - known as Gauss points - with weights w_i which depend on the geometry of the element and on the particular quadrature rule. A table of ξ_i and w_i values for quadrature rule over triangles has been provided by Cowper [109].

In particular, for the 6-node crack element we have implemented quadrature rules with varying numbers of Gauss points. The corresponding numerical values are presented in this chapter. A maximum of 12 Gauss points over triangles gives accurate enough results.

The convenience of numerical integration in handling singularities is also to be considered. It is known that the Jacobian matrix for crack elements become zero at the crack tip and therefore the transformation ceases to be valid. However, by using a finite number of Gauss points, and without having any such points at the tip, numerical integration presents a way out of the difficulty.

V.5 SOLUTION OF THE FINITE ELEMENT EQUATIONS

It was shown that any finite element approximation of both static and dynamic problems results in a set of linear equations of the following form (cf. equations (4) and (9)):

$$AX = b \tag{11}$$

where

$$A = \sum_k B^{(k)}, \quad b = \sum_k c^{(k)} \tag{12}$$

(A is an nxn symmetric, positive definite matrix). Each superscript represents an element so that the summation is over all the elements. The matrix $B^{(k)}$ has non-zeros only in position (i,j) which are such that variables x_i and x_j are associated with the k^{th} finite element so that it may be stored as a small full matrix of order the number of variables associated with the k^{th} element. Similarly the vector $c^{(k)}$ may be stored as a small full vector. With the condensed form of storage, small vectors of integers are needed to indicate which variables are associated with the columns of each small full matrix.

A finite element calculation usually involves three distinct phases:

1. calculation of the individual matrices $B^{(k)}$ and vectors $c^{(k)}$ (as small full matrices and vectors)

2. assembly of the overall problem (11)

and 3. solution of the overall problem (e.g. by the Gaussian elimination).

In phase (1) element matrices and load vectors are generated and stored. Usually phase (2) and phase (3) are combined. Considerable savings can be made if a backing store (e.g. disk) is used to store the overall matrix A.

For phase (3) analysis, considerable research has been devoted towards finding very efficient equation solvers. During recent years it has been recognised that in most cases direct solution of the equations is preferable to using an iterative technique [110]. Various direct solution procedures such as band-matrix techniques [111], frontal methods [112], nested dissections [113] etc. are available. Also see [114].

These equations can be solved using plane rotations or Householder transformation matrices. However, it is most efficient to use the basic Gauss elimination procedure described below.

V.5.1 Gaussian Elimination

We consider the sparse set of equations (11) without making any assumptions about the nature of the sparsity. We use variants of the method of Gaussian elimination, which may be summarized by the formulae

$$a_{ij}^{(k+1)} = a_{ij}^{(k)} - a_{ik}^{(k)}[a_{kk}^{(k)}]^{-1}a_{kj}^{(k)}, \quad (i, j > k) \tag{13}$$

and

$$b_{i}^{(k+1)} = b_{i}^{(k)} - a_{ik}^{(k)}[a_{kk}^{(k)}]^{-1}b_{k}^{(k)}, \quad (i > k) \tag{14}$$

which express the operations performed at the k^{th} step, $k = 1, \ldots, n$ beginning with $A^{(1)} = A$, $b^{(1)} = b$. This eventually leads to an upper triangular ssytem which can be solved by the back-substitution

$$x_k = [a_{kk}^{(k)}]^{-1}(b_k^{(k)} - \sum_{j=k+1}^{n} a_{kj}^{(k)} x_j), \quad k = n, n-1, \ldots 1 \tag{15}$$

Each $a_{ij}^{(k+1)}$ may overwrite $a_{ij}^{(k)}$ in storage and the "multipliers" $\ell_{ik} = a_{ik}^{(k)}[a_{kk}^{(k)}]^{-1}$ may overwrite $a_{ik}^{(k)}$. We will have obtained the desired triangular factorization

$$A = LU \tag{16}$$

where L is unit lower triangular with off-diagonal elements ℓ_{ik} and U is the upper triangular matrix $\{a_{ij}^{(i)},\ i \leq j\}$.

V.5.2 Numerical Stability

When large numbers are added to small ones in equation (14) numerical instability may occur as the information present in the small number is lost. In particular, a total loss of information results when a pivot $a_{kk}^{(k)}$ is zero and must seriously be avoided. It is also important to have some control over any partial loss of information. In fact the LU factorization obtained for A is the exact factorization of a perturbed matrix $A + \Delta$ where the perturbations Δ_{ij} are bounded.

In order to control the size of the largest matrix element at each stage we can introduce row and column interchanges if the matrix elements are of comparable size. This has the additional advantage of limiting the number of *fill-ins*, i.e. zero entries that become non-zero after elimination.

The algorithm we have used for solving the set of linear equations is known as the Irons' *frontal method* that is explained below.

V.5.3 Frontal Method

Irons [112] proposed a very useful technique for combining phases (2) and (3) of the process mentioned earlier. It depends on the fact that the elimination steps for a_{ij} involve subtracting the quantities

$$a_{i\ell}^{(\ell)} a_{\ell j}^{(\ell)} / a_{\ell\ell}^{(\ell)}, \quad \ell = 1, 2, \ldots, \min (i-1, j-1) \tag{17}$$

and the assembly operations involve adding the quantities $b_{ij}^{(k)}$ for all the finite elements k that involve variables i and j. These operations can be performed in any order. All that matters is that they must all be completed before row i or column j becomes pivotal. Irons therefore eliminates each variable as soon as its row and column is fully assembled. Variables not yet eliminated that are involved in elements that have been assembled constitute the "front", which separates the region of assembled elements from the rest. A full matrix can be used at each stage to hold rows and columns that correspond to the front. On assembly its order increases to accommodate any new variables. On an elimination, the pivotal row is written away to backing store and the size of the active matrix reduces by one. In this way variables frequently leave the front in a different order to that in which they entered it, so it may be necessary to perform a symmetric interchange on the full active matrix before an elimination. If the front never has more than m variables then we will need main storage for m(m+1)/2 variables to hold the active matrix at its largest.

The ordinary problem has now shifted from the variables to the elements. We want to order the elements for keeping a small front. This is likely to be somewhat easier manually since there are likely to be fewer elements than variables.

The storage demands of variable band methods and the front method are often similar. Each requires room for a symmetirc "active" matrix and a buffer for input-output operations. The orders of the largest active matrices will be actually identical (and equal to the maximal semi-band width) if the ordering makes the variables leave the front in the same order as they entered it (first in, first out). An example

where they differ, to the advantage of the frontal method, is where some variables are associated with just one element so that they can be eliminated immediately after the element is assembled. (This process is sometimes called "static condensation".) Similar, but less dramatic results may be obtained when some variables are associated with just two elements.

V.5.4 Operation Counts and Comparison

Some feeling for the relative merits of direct and iterative methods may be obtained by looking at the 5-point finite difference approximation to Laplace's equation in a square and a cube, in each case with s unknowns in each coordinate direction so that the number of unknowns are s^2 and s^3, respectively. Using direct methods the maximum semi-band width is s and s^2 and the number of multiplications is approximately $\frac{1}{4}s^4$ and $\frac{1}{7}s^7$. Using successive over-relaxation with parameter w (iterative method), the number of multiplications per iteration is about $2s^2$ and $2s^3$, the maximal eigenvalues are about $(1-4\pi^2/s^2)$ at w = 1 and $(1-2\pi/s)$ at the optimum w so that the number of iterations needed to gain a decimal is about $s^2/17$ at w = 1 and s/2.7 at w_{opt}. This corresponds to $s^3/1.3$ and $s^4/1.3$ multiplications per decimal in 2-D and 3-D, respectively, with the w_{opt}. It can be seen from these approximate figures that direct and iterative methods are likely to be fairly competitive in two dimensions while iterative methods are likely to be superior in three dimensions.

In a more general situation, much depends on the problem. Well conditioning and very large numbers of variables favour iterative methods, unless the structure results in little fill-ins for a direct method. The cost of direct method is dependent on the structure and not on conditioning.

For the dynamic problem where several sets of equations with the same matrix but different right hand sides are to be solved, the factorization may be retained so that the second and subsequent sets may be solved much more rapidly. For example, the operation counts of about $\frac{1}{4}s^4$ and $\frac{1}{7}s^7$ for Laplace's equation in a square and a cube, respectively, reduce to about $\frac{4}{3}s^3$ and $\frac{4}{5}s^5$, respectively. Iterative methods are able to use previously determined relaxation parameters and perhaps have a good first iterate, but this does not result in such a dramatic improvement. Direct methods are therefore superior to iterative methods more frequently for "many-off" cases than for "one-off" cases.

V.6 GENERAL PROGRAM ORGANIZATION

There are three distinct phases in any efficient computational implementation of solution technique discussed in earlier chapters. These are:

(i) data generation and processing phase

(ii) solution phase

(iii) post-solution processing phase.

As mentioned earlier an efficient development of a finite element system requires a good deal of experience and computer system engineering so that with the available central memory (25K-50K) a problem of medium size can be solved within reasonable time of the central processor. The program is employing the Iron's frontal processor (see [115] for details of implementation) and extends the range of applications to include singular elements and dynamic problems.

V.6.1 Data Generation and Processing Phase

In any idealisation of a structure we divide it into a finite number of elements of particular types. With each element is associated a number of nodes and each node has a finite degree of freedom. Within each element the distribution of loads and/or body forces can be specified.

Boundary conditions are accounted for by imposing relevant conditions on the nodes along the boundary. In this phase an automatic mesh generator is employed to provide the node coordinates, element connectivities, boundary conditions, element material properties, and loads on each element. The data input for each element is then stored in a long array of a variable length. The length of the array (dynamic array) is problem-dependent and after data processing, the program decides on the required maximum length of the dynamic array and proceeds to compute element stiffenss and/or mass matrices and retrieve them for the next sequence of computations. With detection of any error in data input the program terminates and returns to the next problem.

V.6.2 Solution Phase

With the element matrices already computed and stored in the dynamic vector array the frontal solution is employed to find the actual displacement solution. In order to reduce the amount of time required at the central processor for this phase, the very inner core of the frontal solution technique is written in basic language. Clearly, the maximum size of the problem is only decided by the amount of central memory available to the user. Another feature of the solution procedure is the use of random access disc transfers. This facility saves both peripheral and central processing time without any further use of central memory. It is recognised that the frontal solution

method employed in this work is one of the most efficient solution processors available for this purpose. The solution (i.e. displacement) obtained in this way is then stored in the dynamic vector for post-processing phase.

V.6.3 Post-Solution Phase

In this phase the element stresses and strains are computed from displacements and are stored on tape. The options in this phase are to output stresses/strains at either nodes or Gauss points. If necessary, reactions due to loading of the structure can also be output. From the stresses one can plot stress variations within each element. One point in order is that as the stresses at nodes are obtained by *extrapolation* of the stresses at Gauss points, there are some small errors involved in the process. Obviously, the most accurate result for any post-processing of solution is obtained by working directly with displacements. It is for this reason that we compute stress intensity factors from displacements and not stresses in the next section where computational results are presented.

V.7 COMPUTATIONAL RESULTS

While a full range of applications cannot be included in the thesis some results for certain problems are presented. These examples are chosen in a way to represent a wide range of applications of the system to problems for which comparison, even partially, can be made. These include problems in both dynamic and static analysis of fracture problems.

Note - throughout the analysis we use SI units.

V.7.1 Static Analysis

A central crack in a square sheet subject to pure tension is analysed as a model problem (Fig. 1).

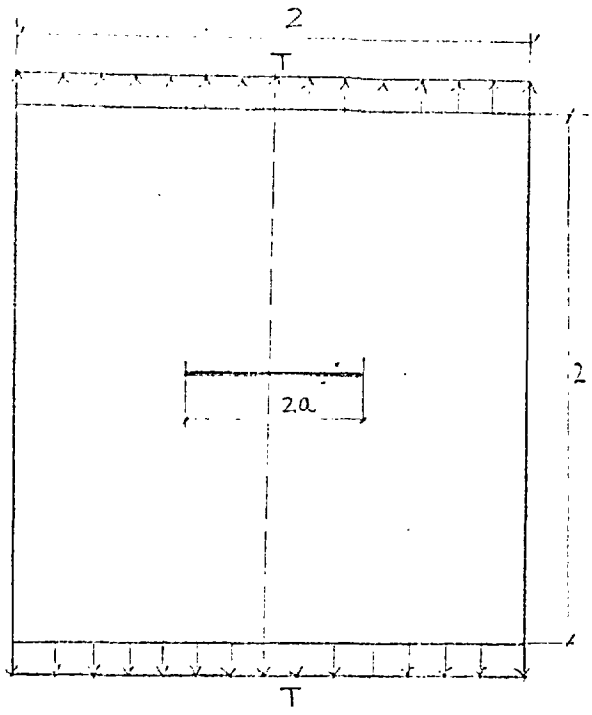

Fig. 1 - A Central Crack Problem

Using symmetry only one-quarter or one-half of the sheet is considered. The crack tip is surrounded by only four quarter-point triangular isoparametric elements and layers of ordinary 8-node quadrilateral isoparametric elements. The discrete structure is shown in Fig. 2.

Before proceeding any further we give a consistent procedure for derivation of stress intensity factors in a crack problem from displacements. This procedure is then used to extract the numerical values of stress intensity factors.

Consider an oblique crack at angle β (Fig. 3) at the tip B. Denoting by U and V the displacements in X-Y coordinates and by u and v the displacements in x-y coordinates we have

$$\begin{cases} U = u \cos \beta + v \sin \beta \\ \\ V = -u \sin \beta + v \cos \beta \end{cases} \tag{1}$$

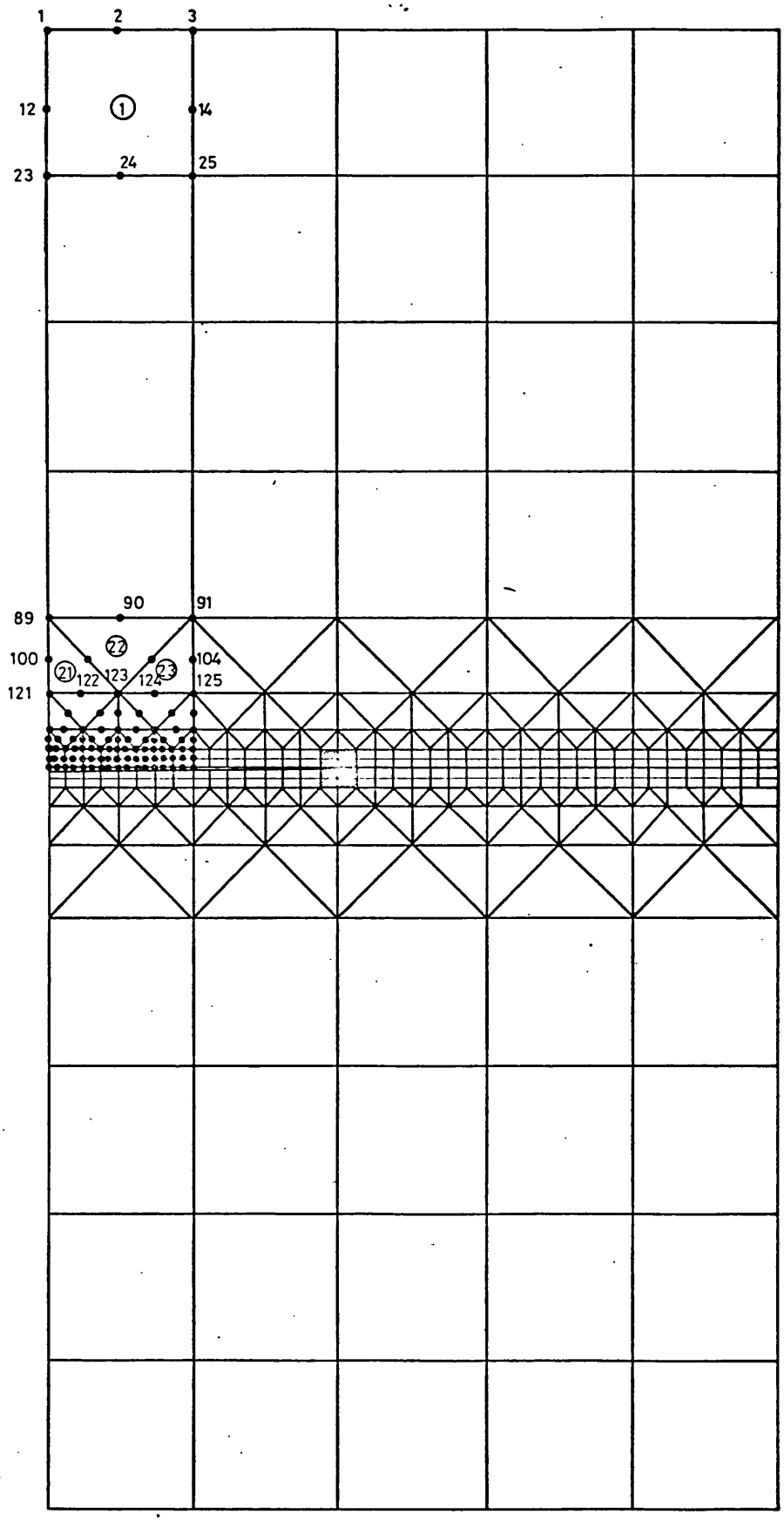

Fig 2a Fine - mesh. Finite element representation of a central crack

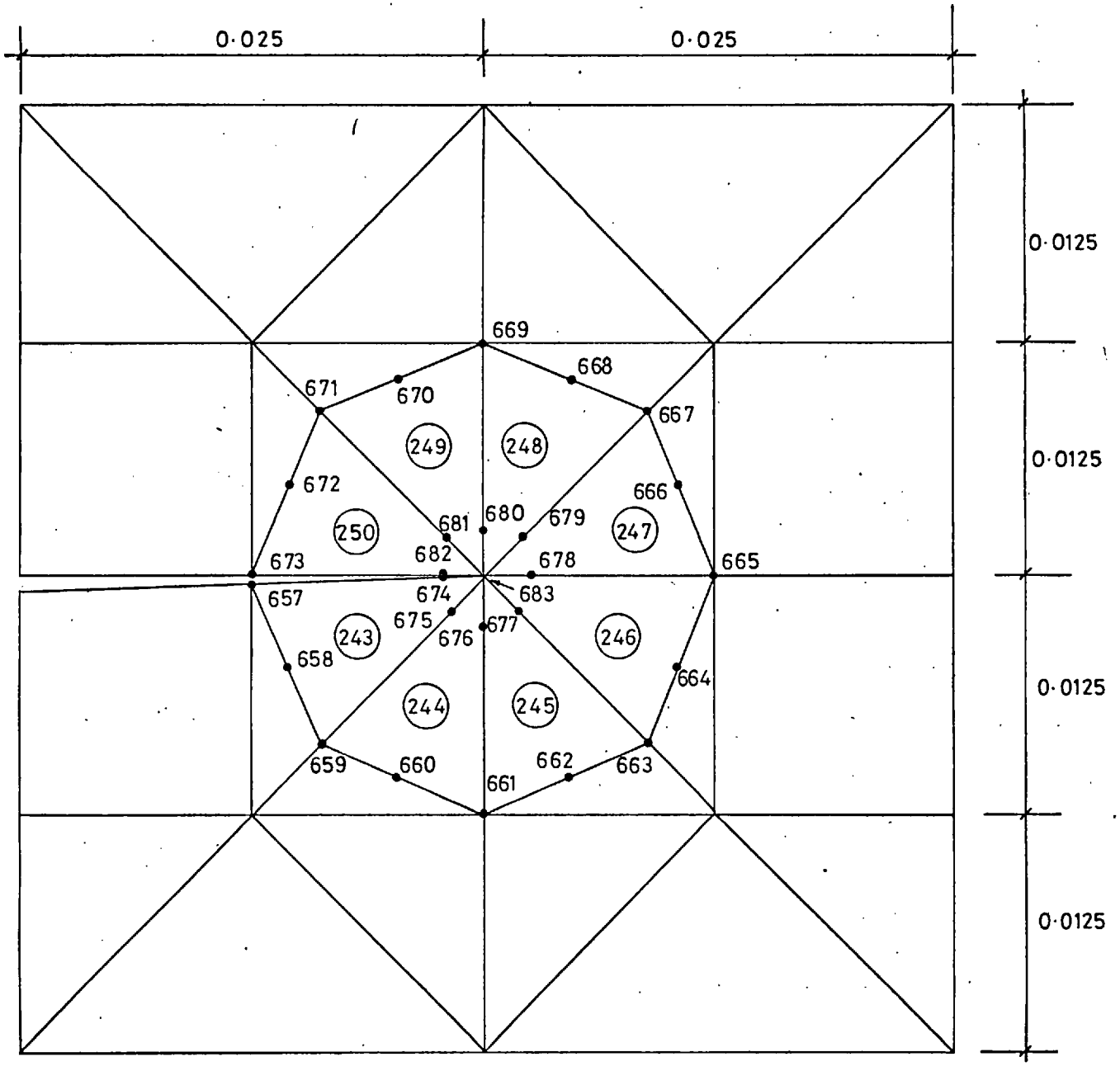

Fig 2 b Enlarged shaded arec in Fig. 2 a

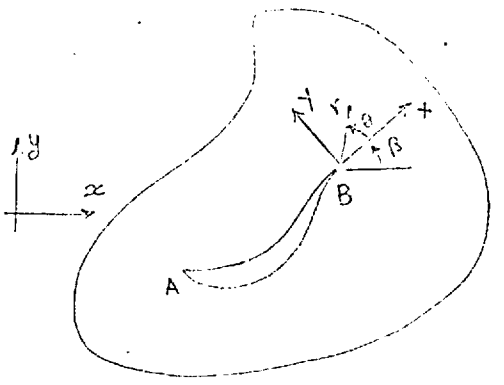

Fig(3)

Also with the known asymptotic expansion of the solution near the crack tip we have

$$\begin{pmatrix} U \\ V \end{pmatrix} = \begin{pmatrix} a_1 \\ a_2 \end{pmatrix} + \begin{pmatrix} b_1(\theta) \\ b_2(\theta) \end{pmatrix} \sqrt{r} + \begin{pmatrix} c_1 \\ c_2 \end{pmatrix} r + \ldots \qquad (2)$$

where r and θ are measured in the X-Y coordinate system and

$$\begin{pmatrix} b_1 \\ b_2 \end{pmatrix} = \frac{K_I}{G\sqrt{8\pi}} \begin{pmatrix} f_x \\ f_y \end{pmatrix} + \frac{K_{II}}{G\sqrt{8\pi}} \begin{pmatrix} g_x \\ g_y \end{pmatrix} \qquad (3)$$

where

$$\begin{pmatrix} f_x \\ f_y \end{pmatrix} = \begin{pmatrix} \cos \theta/2[\kappa-1+2 \sin^2\theta/2] \\ \sin \theta/2[\kappa+1-2 \cos^2\theta/2] \end{pmatrix}$$

and

$$\begin{pmatrix} g_x \\ g_y \end{pmatrix} = \begin{pmatrix} \sin \theta/2[\kappa+1+2 \cos^2\theta/2] \\ -\cos \theta/2[\kappa-1-2\sin^2\theta/2] \end{pmatrix}$$

$$\kappa = \frac{3-\nu}{1+\nu} \qquad \text{for plane stress}$$

(we can normalise K_I and K_{II} by dividing through $T\sqrt{\pi a}$ i.e. $H_I = \frac{K_I}{T\sqrt{\pi a}}$ and $H_{II} = \frac{K_{II}}{T\sqrt{\pi a}}$.)

By using quarter-point triangular elements of side length ℓ we can obtain parameters a_i, b_i and c_i in (2) from displacements at the crack tip (O),

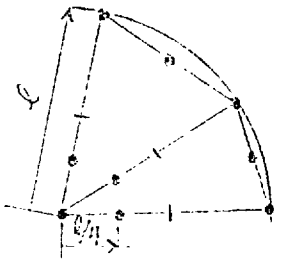

Fig(4)

quarter point ($\ell/4$) and nodes at $r = \ell$ at any angle θ. e.g. we have

$$\begin{pmatrix} b_1 \\ b_2 \end{pmatrix} = \begin{pmatrix} 4U(\ell/4)-U(\ell)-3U(O) \\ 4V(\ell/4)-V(\ell)-3V(O) \end{pmatrix} \frac{1}{\sqrt{\ell}} \quad . \tag{4}$$

As the oblique crack problem is normally solved in x-y system i.e. we usually have u and v, the stress intensity factors K_I and K_{II} are the solution to the following set of equations:

$$\begin{cases} K_I . f_x(\theta) + K_{II} f_y(\theta) = \dfrac{G\sqrt{8\pi}}{\sqrt{\ell}} \{[4u(\ell/4)-u(\ell)-3u(O)]\cos\beta + \\ \qquad\qquad [4v(\ell/4)-v(\ell)-3v(O)]\sin\beta\} \\ K_I g_x(\theta) + K_{II} . g_y(\theta) = \dfrac{G\sqrt{8\pi}}{\sqrt{\ell}} \{[4v(\ell/4)-v(\ell)-3v(O)]\cos\beta - \\ \qquad\qquad [4u(\ell/4)-u(\ell)-3u(O)]\sin\beta\} \end{cases} \tag{5}$$

It is noted that the new proposal for a correct interpretation of data for extraction of stress intensity factors requires the system (5) to be solved along each ray making an angle θ with the x-axis. This, in particular, implies that in any problem (either in pure shear or pure tension) we will determine K_I and K_{II} *simultaneously* but expect a comparatively small K_I (resp. K_{II}) for a crack in pure shear (resp. tension). In fact this also provides a good test for accuracy of the solution.

Table I - Central Crack Problem (fine mesh) Data and Displacements

D I S P L A C E M E N T S A T N O D E S

NODE NO.	DISPLACEMENT IN SYSTEM X-DIRECTION	DISPLACEMENT IN SYSTEM Y-DIRECTION
641	-.265757E+00	-.353033E+00
642	-.281744E+00	-.333300E+00
643	-.298091E+00	-.312400E+00
644	-.314591E+00	-.789300E+00
645	-.331619E+00	-.165420E+00
646	-.346766E+00	-.736900E+00
647	-.362827E+00	-.710240E+00
648	-.378802E+00	-.670033E+00
649	-.394701E+00	-.645100E+00
650	-.410569E+00	-.610115E+00
651	-.426359E+00	-.567033E+00
652	-.442063E+00	-.521137E+00
653	-.457628E+00	-.483350E+00
654	-.473202E+00	-.430240E+00
655	-.488196E+00	-.336435E+00
656	-.497289E+00	-.292531E+00
657	-.504647E+00	-.236541E+00
658	-.463053E+00	-.221530E+00
659	-.427084E+00	-.223420E+00
660	-.412844E+00	-.156810E+00
661	-.407123E+00	-.123930E+00
662	-.420400E+00	-.765230E-01
663	-.432621E+00	-.461130E-01
664	-.446502E+00	-.189410E-01
665	-.456910E+00	.365814E-09
666	-.446502E+00	.193111E-01
667	-.432621E+00	.461130E-01
668	-.420400E+00	.765230E-01
669	-.407123E+00	.120830E+00
670	-.412844E+00	.134120E+00
671	-.427084E+00	.203420E+00
672	-.463053E+00	.221530E+00
673	-.504647E+00	.239541E+00
674	-.514814E+00	-.119611E+00
675	-.474927E+00	-.100771E+00
676	-.462530E+00	-.589937E-01
677	-.473646E+00	-.212255E-01
678	-.482318E+00	.113416E-09
679	-.473646E+00	.212253E-01
680	-.462530E+00	.530337E-01
681	-.474927E+00	.100771E+00
682	-.514814E+00	.116611E+00
683	-.516662E+00	-.113661E-20
684	-.379764E+00	.297335E+00
685	-.378312E+00	.193135E+00
686	-.369354E+00	.115335E+00
687	-.400337E+00	.639943E-01
688	-.410782E+00	.294230E+00
689	-.404427E+00	.132031E+00
690	-.413429E+00	.777230E-01
691	-.418665E+00	.439333E-01
692	-.416734E+00	.223591E+00
693	-.425240E+00	.307715E-01
694	-.440790E+00	.233917E+00
695	-.441144E+00	.357115E-01
696	-.497269E+00	.292631E+00
697	-.439537E+00	.169337E-09
698	-.446750E+00	-.333317E+00
699	-.441144E+00	-.357115E-01
700	-.416734E+00	-.223531E+00
701	-.425240E+00	-.307715E-01
702	-.410782E+00	-.294230E+00
703	-.404427E+00	-.182031E+00
704	-.413429E+00	-.777230E-01
705	-.418665E+00	-.433333E-01
706	-.379764E+00	-.297353E+00
707	-.378312E+00	-.133133E+00
708	-.369354E+00	-.113533E+00
709	-.400337E+00	-.689343E-01
830	-.215050E-11	[illegible]

S U M M A R Y O F D A T A

TOTAL NUMBER OF ELEMENTS	=	434
TOTAL NUMBER OF NODES	=	1255
TOTAL NUMBER OF SUPPORT NODES	=	39
TOTAL NUMBER OF LOADING CASES	=	1

DYNAMIC VECTOR ARRAY REQUIREMENTS

DATA PROCESSING	=	7829
DATA STORAGE	=	7713
PRE-SOLUTION PROCESS	=	11939
SOLUTION PROCESS	=	17422
POST-SOLUTION PROCESS	=	4303
LOCATIONS AVAILABLE	=	25000

MAXIMUM FRONT WIDTH OF STIFFNESS MATRIX	=	180
MAXIMUM HALF BANDWIDTH OF STIFFNESS MATRIX	=	703
TOTAL NUMBER OF ACTIVE NODES	=	1145
TOTAL NUMBER OF EQUATIONS	=	2290

TIME FOR THIS PHASE = 37.721 SEC.

TIME USED TO PROCESS INPUT DATA = 88.472 SEC.

TIME AT CENTRAL PROCESSOR = 22 29.32. HRS/MINS/SECS

TIME USED IN PRE-SOLUTION PROCESS (ALL ELEMENT STIFFNESS MATRICES) = 54.423 SEC.

TIME AT CENTRAL PROCESSOR = 22.31.37. HRS/MINS/SECS

S O L U T I O N B Y F R O N T A L S P A R S E M A T R I X T E C H N I Q U E

MACHINE CODE INNER LOOPS AND DYNAMIC RANDOM ACCESS IN OPERATION

TIME USED FOR ASSEMBLY AND ELIMINATION WITH 1 RIGHT HAND SIDES = 236.990 SEC.

TIME USED IN BACK-SUBSTITUTION PROCESS WITH 1 RIGHT HAND SIDES = 6.779 SEC.

TIME AT CENTRAL PROCESSOR = 22.38.17. HRS/MINS/SECS

TOTAL AREA OF ELEMENTS = .200000E+01 SQ.

Now returning to the central crack problem we evaluate K_I and K_{II} along each ray $\theta = -180$ to $\theta = +180$ at intervals of 45°. In the fine meshes of figure 2 which represents only half of the strucutre, we have used a total of 434 isoparametric elements having 1255 nodes which results in a set of 2290 equations. The time for solving this problem is about 294 seconds on a CDC 6400. Summary of the data and the solution for displacement field near the crack tip is given in Table 1. From Table 1 and system (5) numerical values for H_I and H_{II} are obtained and presented in Table II(a). The variation of H_I and H_{II} with θ is plotted in Fig. 5.

θ	180°	135°	90°	45°	0°
H_I	1.1990	1.1930	1.1685	1.1407	1.1089
H_{II}	0.0069	0.0037	0.0077	0.0016	0.0000

Table II(a) - Variations of H_I and H_{II} with θ

Isida [18] has solved this problem using boundary collocation techniques and obtained $H_I = 1.216$ (assumes $H_{II} = 0.$). It is seen that the values of H_I and H_{II} in Fig. 5 have small variations with θ and the most accurate values (as compared with Isida's values of $K_I = 1.216$ and $K_{II} = 0$) are obtained by *averaging* the values obtained from $\theta = -180$ and $\theta = 180$ (i.e. along crack faces). The averaged values are $H_I = 1.199$ and $K_{II} = 0.000$ and hence we suggest that the most reliable results are obtained from crack opening displacements (COD).

The profile of the crack is sketched in Fig. 6 and as is expected, it has a local parabolic variation with distance from the crack tip.

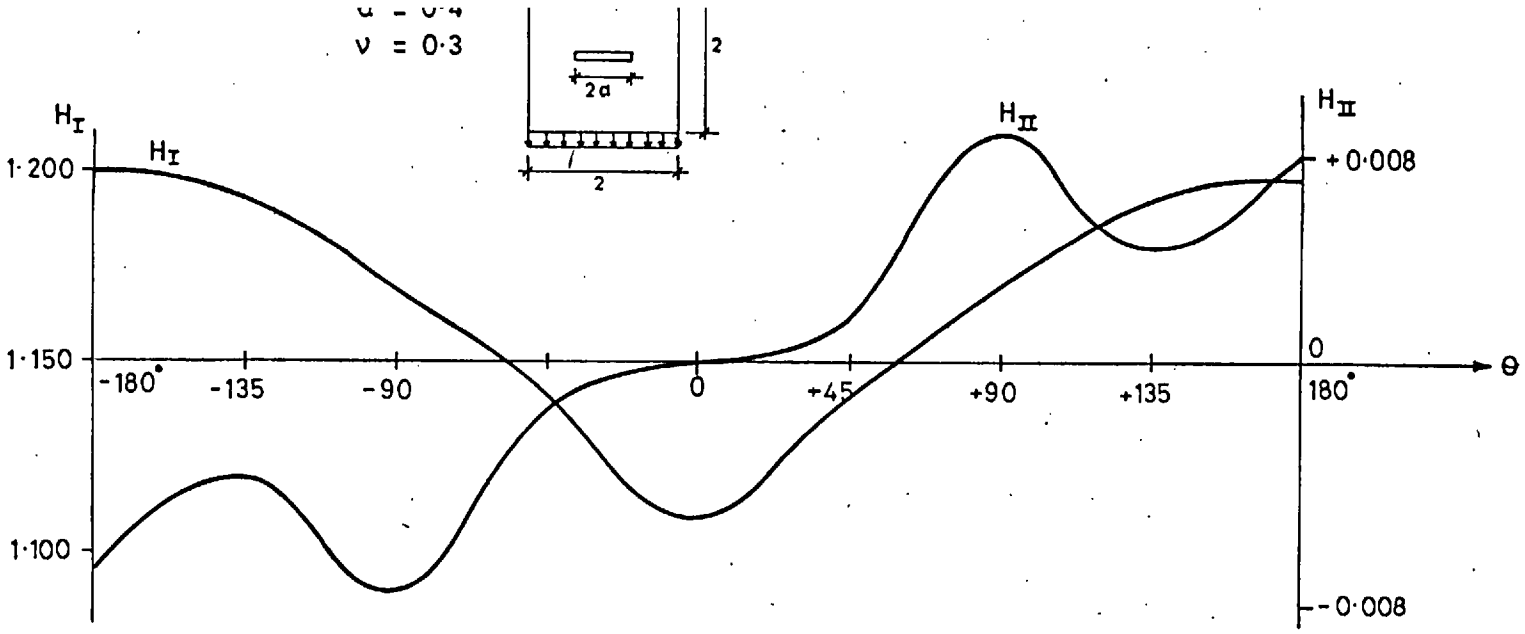

Fig. 5 Variations of H_I and H_{II} with θ for the central crack in tension

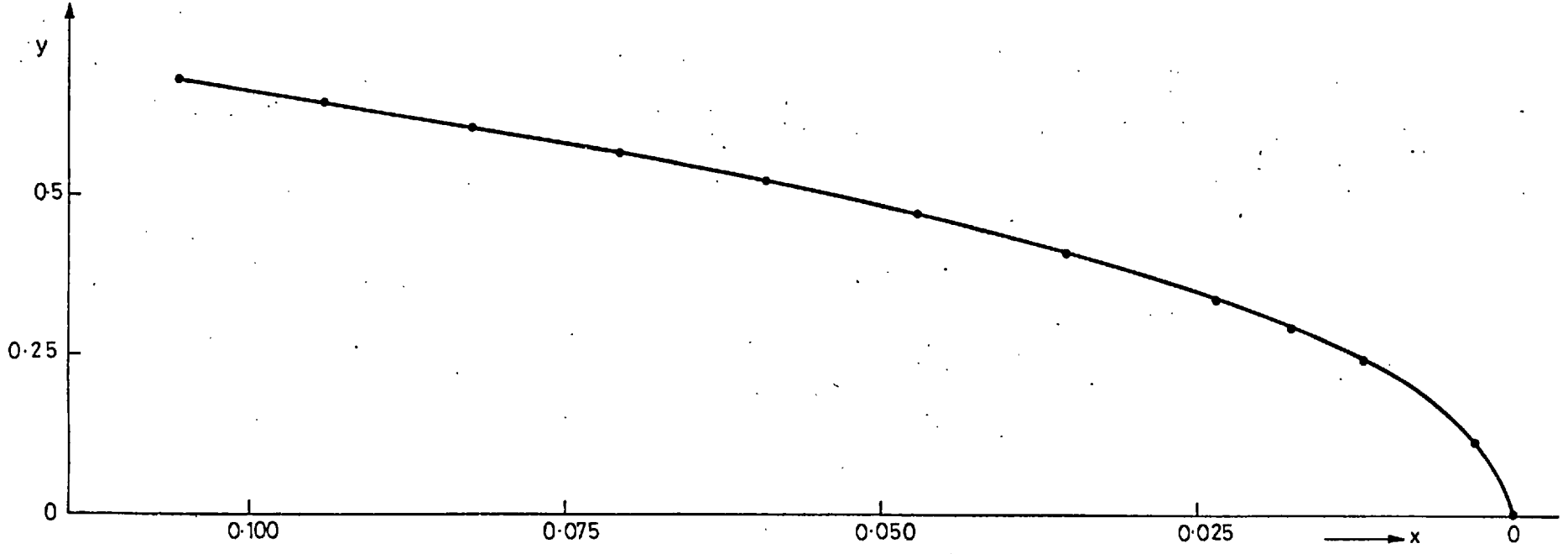

Fig 6. COD for central crack in tension

In this initial approximation we have used a rather fine discretization of the structure with 434 elements. To show the effectiveness of the techniques, using symmetry, the same structure is represented by only 34 isoparametric elements and 123 nodes. In this case a total of 246 equations has to be solved. (See fig. 7.) The solution time is only 2.4 seconds as compared with 294 seconds for the previous fine discretization of the problem (i.e. about 1 : 100).

The calculated stress intensity factors are given in Table II(b) below.

θ	180°	135°	90°	45°	0°
H_I	1.2043	1.1938	1.1642	1.1298	1.1130
H_{II}	0.0076	0.0079	0.0209	0.0159	0.0000

Table II(b) - Variations of H_I and H_{II} with θ

Table III summarizes data and gives displacements at the nodes for the coarse mesh. We obtain the following stress intensity factors from crack opening displacements (COD):

$$\begin{cases} H_I = 1.2043 \\ H_{II} = 0.0000 \end{cases}$$

which apparently, is even more accurate (as compared with Isida's values of $H_I^T = 1.216$ and $H_{II}^T = 0$ which are regarded as accurate up to four figures) than the corresponding results based on previous fine meshes.

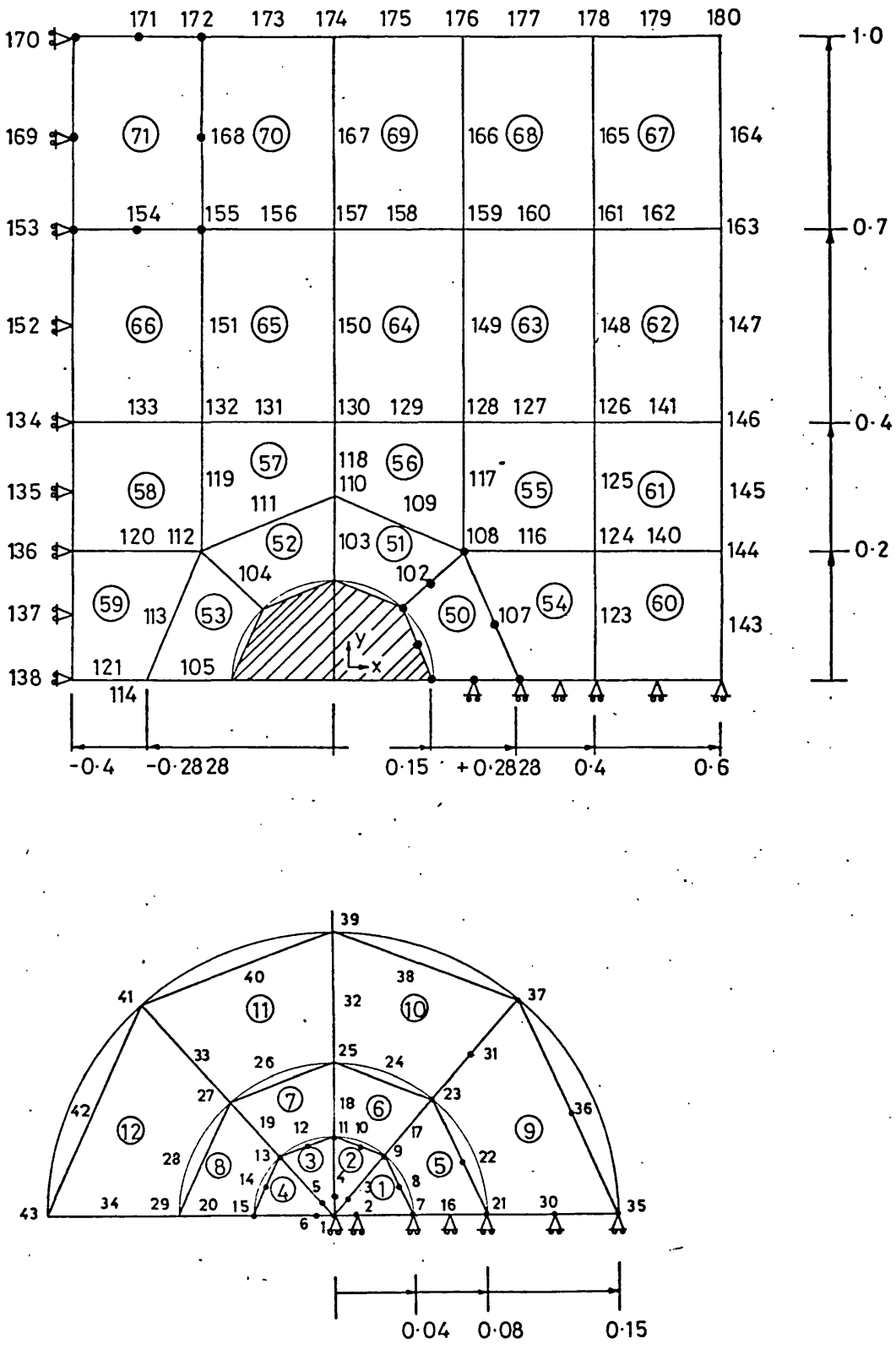

DETAIL OF SHADED AREA

Fig 7 Discrete structure of a central crack problem

D I S P L A C E M E N T S A T N O D E S

NODE NO.	DISPLACEMENT IN SYSTEM X-DIRECTION	DISPLACEMENT IN SYSTEM Y-DIRECTION
1	-.516475E-02	.754712E-13
2	-.457317E-02	[illegible]-12
3	-.447956E-02	.131273E-03
4	-.418693E-02	.10554[illegible]-02
5	-.43[illegible]7[illegible]4E-02	.131[illegible]E-02
6	-.505956E-02	[illegible]-02
7	-.41[illegible]E-02	[illegible]-02
8	-.469356E-02	.163[illegible]E-03
9	-.377464E-02	[illegible]-03
10	-.35[illegible]11E-02	.14[illegible]-02
11	-.322771E-02	[illegible]-02
12	-.325711E-02	[illegible]-02
13	-.3[illegible]17E-02	[illegible]-02
14	-.462271E-02	[illegible]-02
15	-.4711[illegible]1E-02	[illegible]-02
16	-.462517E-02	[illegible]-02
17	-.356671E-02	[illegible]-02
18	-.28[illegible]21E-02	.1765[illegible]-02
19	-.301144E-02	[illegible]-02
20	-.444795E-02	[illegible]-02
21	-.396316E-02	[illegible]-03
22	-.394[illegible]14E-02	.57561[illegible]-03
23	-.241796E-02	.1325[illegible]-02
24	-.29[illegible]69E-02	[illegible]-02
25	-.252967E-02	[illegible]-02
26	-.249653E-02	[illegible]-02
27	-.264[illegible]94E-02	[illegible]-02
28	-.336247E-02	.552575E-02
29	-.41[illegible]4E-02	[illegible]-02

R E A C T I O N S T O E A R T H

NODE NO.	FORCE IN SYSTEM X-DIRECTION	FORCE IN SYSTEM Y-DIRECTION
1	0	-.754732E+09
2	0	-.295579E+09
7	0	-.113567E+09
16	0	[illegible]
31	0	-.763975E+08
30	0	-.174[illegible]E+09
35	0	-.111[illegible]E+09
101	0	[illegible]
106	0	-.10[illegible]E+09
115	0	[illegible]E+09
122	0	-.12[illegible]E+09
134	-.145175E+09	0
135	.212115E+09	0
136	.345511E+09	0
137	.2[illegible]29E+09	0
138	.636557E+09	0
[illegible]	0	-.272379E+10
[illegible]	0	-.576841E+10
152	-.697762E+09	0
15[illegible]	-.429952E+09	0
159	-.141[illegible]40E+09	0
170	-.732192E+09	0

TOTAL FORCE -.584126E-03 -.200000E+10

S U M M A R Y O F D A T A

TOTAL NUMBER OF ELEMENTS = 34
TOTAL NUMBER OF NODES = 123
TOTAL NUMBER OF SUPPORT NODES = 22
TOTAL NUMBER OF LOADING CASES = 1

DYNAMIC VECTOR ARRAY REQUIREMENTS

DATA PROCESSING = 990
DATA STORAGE = 333
PRE-SOLUTION PROCESS = 1259
SOLUTION PROCESS = 1621
POST-SOLUTION PROCESS = 1195
LOCATIONS AVAILABLE = 5000

MAXIMUM FRONT WIDTH OF STIFFNESS MATRIX = 42
MAXIMUM HALF BANDWIDTH OF STIFFNESS MATRIX = 75
TOTAL NUMBER OF ACTIVE NODES = 123
TOTAL NUMBER OF EQUATIONS = 246

TIME FOR THIS PHASE = 1.075 SEC.

TIME USED TO PROCESS INPUT DATA = 4.543 SEC.
TIME AT CENTRAL PROCESSOR = 11.04.14. HRS/MINS/SECS

TIME USED IN PRE-SOLUTION PROCESS (ALL ELEMENT STIFFNESS MATRICES) = 5.088 SEC.
TIME AT CENTRAL PROCESSOR = 11.04.30. HRS/MINS/SECS

S O L U T I O N B Y F R O N T A L S P A R S E M A T R I X T E C H N I Q U E
MACHINE CODE INNER LOOPS AND DYNAMIC RANDOM ACCESS IN OPERATION

TIME USED FOR ASSEMBLY AND ELIMINATION WITH 1 RIGHT HAND SIDES = 2.988 SEC.
TIME USED IN BACK-SUBSTITUTION PROCESS WITH 1 RIGHT HAND SIDES = .374 SEC.
TIME AT CENTRAL PROCESSOR = 11.04.39. HRS/MINS/SECS

TOTAL AREA OF ELEMENTS = .100000E+01 SQ.

TOTAL TIME USED IN SOLVING PROBLEM = 13.998 SEC.

Table III - Central Crack Problem (coarse mesh) Data and Displacements

The percentage of the error involved can be calculated as

$$\% \text{ error} = \frac{\{(H_I^T - H_I)^2 - (H_{II}^T - H_{II})^2\}^{\frac{1}{2}}}{\{H_I^{T2} + H_{II}^{T2}\}^{\frac{1}{2}}}$$

$$= \frac{\{(1.2160-1.2043)^2+(0.0000-0.0000)^2\}^{\frac{1}{2}}}{\{(1.216)^2+(0.0000)^2\}^{\frac{1}{2}}} = 0.962$$

A possible explanation for this behaviour is that when using quarter-point singular elements we do not expect a uniform rate of convergence because with the mesh refinement we are necessarily reducing the size of the singular zone which violates the basic requirement for convergence. These relatively coarse and fine discretizations can be regarded as two extreme cases and for intermediate ones convergence has the following typical behaviour.

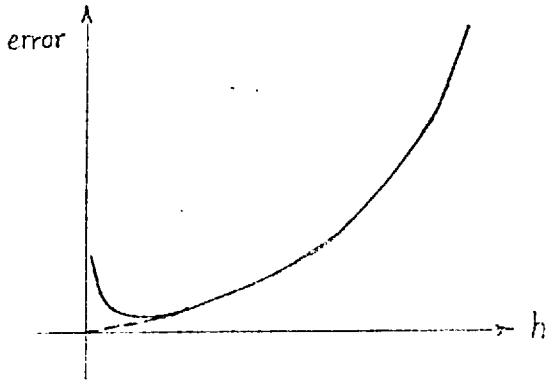

In other words we get reasonably accurate results if the discretization near the crack tip is not too coarse or too fine.

Since the stiffness matrix is numerically integrated we investigate the effects the total number of Gauss points (NGP) have on the numerical accuracy of the solution. We test the accuracy of the central crack problem with the relatively coarse mesh using different number of Gauss points. For the structure with 34 elements we use 3, 6 and 12 integration points in each quarter-point trianguler isoparametric elements while the number of integration points in other elements are kept constant at 3 (resp. 4) for ordinary triangular (resp. quadrilateral) isoparametric elements.

Table IV shows the corresponding numerical values obtained from COD.

NGP	3 (mid-side points)	3 (corner points)	6	12
H_I	1.119054	1.234625	1.211158	1.204302
H_{II}	0.000000	0.000000	0.000000	0.000000
% Error	-7.9772	+1.5317	-0.3982	-0.9621

Table IV - Effect of Number of Gauss Points (NGP) on H_I and H_{II}

As is noted from the table good accuracy is obtained using only 6 integration points inside each crack tip element.

Results for an edge crack (Fig. 8) and a double-edge crack (Fig. 9) using symmetry and the same discretization as in the central crack problem are as follows.

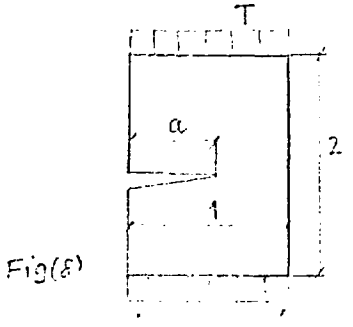

Fig(8)

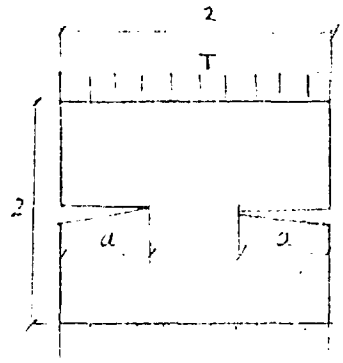

Fig(9)

For the edge crack problem using 12 Gauss points over singular elements and 4 Gauss points for quadrilateral isoparametric elements we obtain $H_I = 2.0620$ from the COD which is about 2.3% less than the approximate value $H_I = 2.11$ obtained by Tracey [116].

Similarly for the double-edge crack problem of Fig.(9) using 12 Gauss points and the same discretization as in the central crack problem we obtain $H_I = 1.2663$ from COD. This value can be compared with the interpolated (not accurate enough) value of $H_I = 1.227$ from [117].

As a further analysis of static crack problems we thoroughly analyse an oblique edge crack in a sheet subject to tensile forces (Fig. 10).

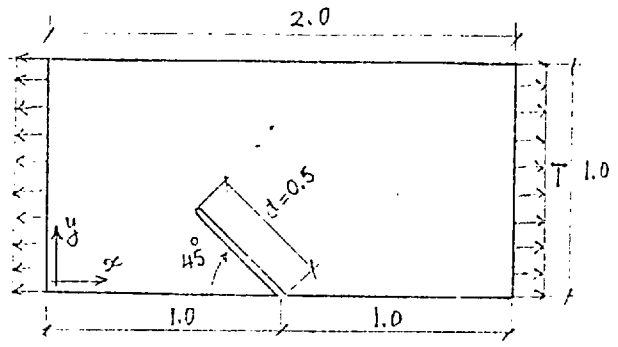

Fig(10)

The geometry and loading was specifically chosen from the Bowie's example [16, p. 51] so that the accuracy of the method can be tested on another model problem for which the stress intensity factors are known. For discretization mesh see Fig. 11. The data for this analysis and the corresponding solution near the tip of the crack are given in Table V. From system (5) and the displacement field we can simultaneously find $H_I = \frac{K_I}{T\sqrt{\pi a}}$ and $H_{II} = \frac{K_{II}}{T\sqrt{\pi a}}$. These values as obtained from displacements along each ray from the crack tip are shown in Table VI and are plotted in Fig. 12. In this problem in order to remove rigid body motion we have fixed the crack tip and restrained node at (x = 0, y = 0) in the vertical direction.

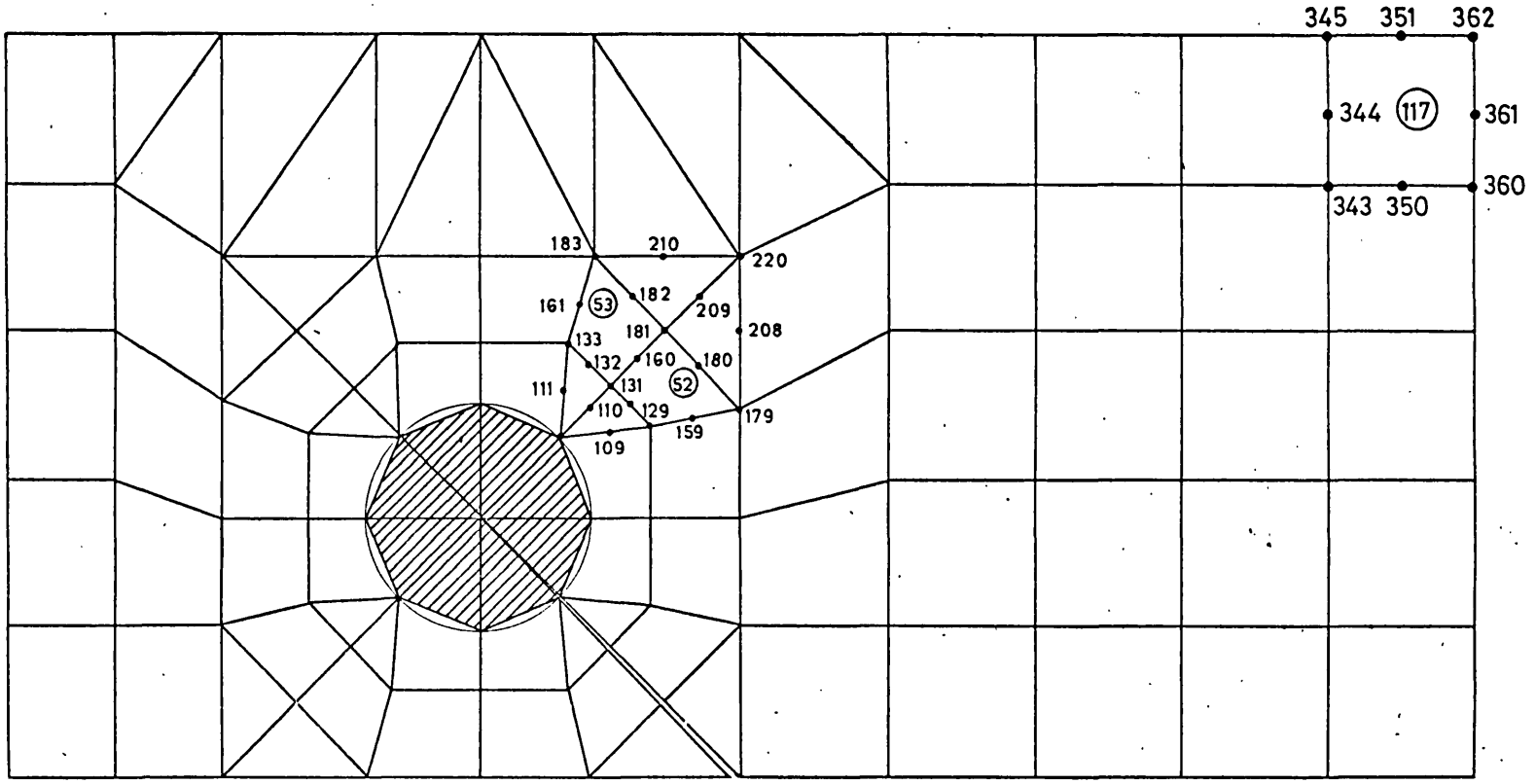

Fig 11a Finite element representation of an inclined edge crack problem

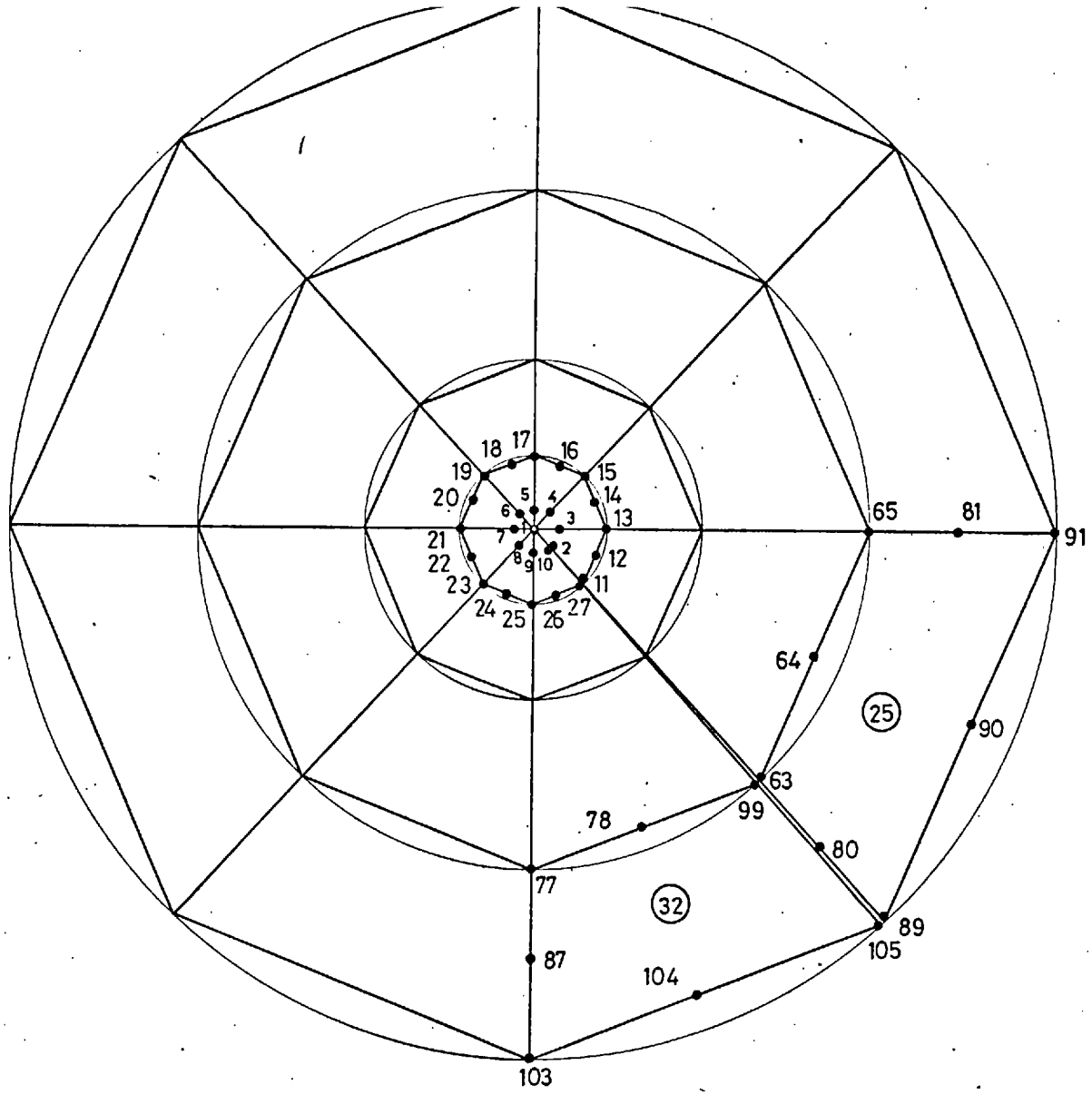

Fig 11 b. Enlarged shaded area in fig 11a.

D I S P L A C E M E N T S   A T   N O D E S

NODE NO.	DISPLACEMENT IN SYSTEM X-DIRECTION	DISPLACEMENT IN SYSTEM Y-DIRECTION
1	-.119779E-20	.232122E-21
2	.191635E-02	.748933E-03
3	.113060E-02	.963317E-03
4	.421523E-03	.737073E-03
5	.512303E-05	.499133E-03
6	-.355266E-03	.522521E-03
7	-.927418E-03	.625043E-03
8	-.159232E-02	.433503E-03
9	-.192073E-02	-.103475E-03
10	-.167883E-02	-.627351E-03
11	.416416E-02	.169731E-02
12	.314409E-02	.205375E-02
13	.233656E-02	.222273E-02
14	.133925E-02	.197240E-02
15	.656618E-03	.172303E-02
16	.957748E-04	.126441E-02
17	-.308436E-03	.105731E-02
18	-.571156E-03	.366215E-03
19	-.973964E-03	.925611E-03
20	-.131018E-02	.391701E-03
21	-.193170E-02	.105712E-02
22	-.239962E-02	.373317E-03
23	-.303802E-02	.723753E-03
24	-.331874E-02	.304637E-03
25	-.357189E-02	-.222673E-03
26	-.336066E-02	-.716347E-03
27	-.319312E-02	-.111913E-02
28	.573077E-02	.246513E-02
29	.350993E-02	.326551E-02
30	.667664E-03	.246533E-02
31	-.676278E-03	.135731E-02
32	-.147914E-02	.107425E-02
33	-.257165E-02	.123153E-02
34	-.387040E-02	.366530E-03
35	-.449136E-02	-.288037E-03
36	-.398966E-02	-.113613E-02
37	.706675E-02	.314337E-02
38	.524772E-02	.377213E-02
39	.370258E-02	.418317E-02
40	.194569E-02	.362714E-02
41	.613106E-03	.312221E-03
42	-.331230E-03	.220131E-02
43	-.106713E-02	.164533E-02
44	-.141272E-02	.121713E-02
45	-.195078E-02	.114331E-02
46	-.233254E-02	.121332E-02
47	-.318212E-02	.132335E-02
48	-.366755E-02	.125113E-02
49	-.455540E-02	.956537E-03
50	-.484091E-02	.381931E-03
51	-.510620E-02	-.333610E-03
52	-.498065E-02	-.102331E-02
53	-.457257E-02	-.159033E-02
54	.903926E-02	.420165E-02
55	.456092E-02	.362033E-02
56	.446795E-03	.412733E-02
57	-.173578E-02	.199733E-02
58	-.270365E-02	.116573E-02
59	-.386003E-02	.136914E-02
60	-.533161E-02	.103333E-02
61	-.601251E-02	-.403331E-03
62	-.531266E-02	-.183331E-02
63	.106239E-01	.322337E-02
64	.782466E-02	.627333E-02
65	.529636E-02	.593331E-02
66	.243519E-02	.537722E-02
67	.230146E-03	.503631E-02
68	-.125497E-02	.337631E-02
69	-.241656E-02	.223121E-02

S U M M A R Y   O F   D A T A

TOTAL NUMBER OF ELEMENTS = 117
TOTAL NUMBER OF NODES = 362
TOTAL NUMBER OF SUPPORT NODES = 2
TOTAL NUMBER OF LOADING CASES = 1

DYNAMIC VECTOR ARRAY REQUIREMENTS

DATA PROCESSING = 2249
DATA STORAGE = 2441
PRE-SOLUTION PROCESS = 4213
SOLUTION PROCESS = 3746
POST-SOLUTION PROCESS = 1343
LOCATIONS AVAILABLE = 25000

MAXIMUM FRONT WIDTH OF STIFFNESS MATRIX = 75
MAXIMUM HALF BANDWIDTH OF STIFFNESS MATRIX = 162
TOTAL NUMBER OF ACTIVE NODES = 362
TOTAL NUMBER OF EQUATIONS = 724

TIME FOR THIS PHASE = 3.649 SEC.

TIME USED TO PROCESS INPUT DATA = 14.177 SEC.
TIME AT CENTRAL PROCESSOR = 22.00.58. HRS/MINS/SECS

TIME USED IN PRE-SOLUTION PROCESS (ALL ELEMENT STIFFNESS MATRICES) = 14.830 SEC.
TIME AT CENTRAL PROCESSOR = 22.01.22. HRS/MINS/SECS

S O L U T I O N   B Y   F R O N T A L   S P A R S E   M A T R I X   T E C H N I Q U E
MACHINE CODE INNER LOOPS AND DYNAMIC RANDOM ACCESS IN OPERATION

TIME USED FOR ASSEMBLY AND ELIMINATION WITH 1 RIGHT HAND SIDES = 18.764 SEC.
TIME USED IN BACK-SUBSTITUTION PROCESS WITH 1 RIGHT HAND SIDES = 1.317 SEC.
TIME AT CENTRAL PROCESSOR = 22.01.57. HRS/MINS/SECS

Table V - Mixed-mode Crack Problem Data and Displacements

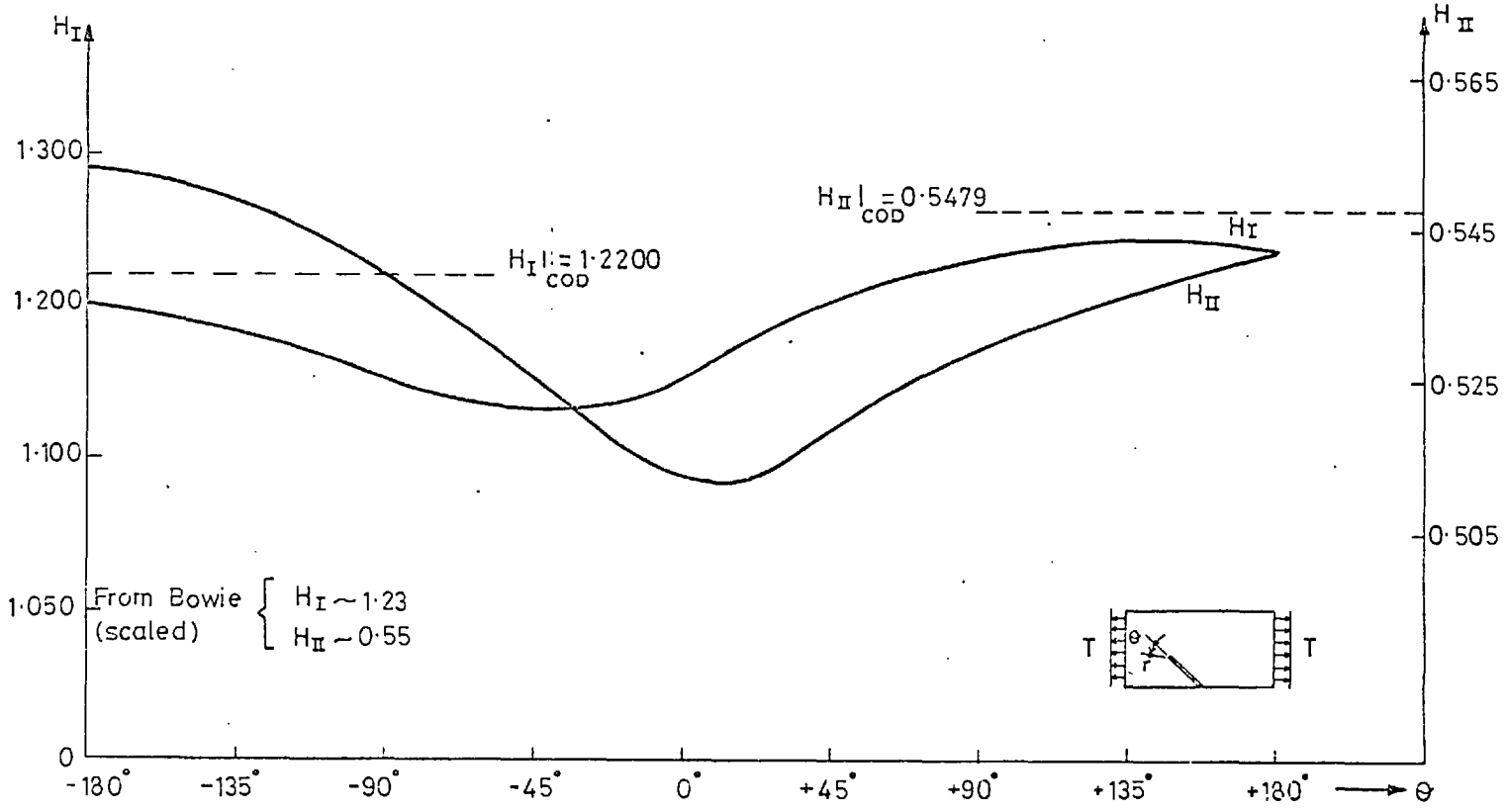

Fig.12 Variations of stress-intensity factors with θ

θ	-180°	-135^{0}	-90°	-45^{0}	0°
H_I	1.2017	1.1842	1.1569	1.1332	1.1512
H_{II}	0.5530	0.5496	0.5393	0.5268	0.5126

θ	45°	90°	135°	180°
H_I	1.2078	1.2350	1.2442	1.2384
H_{II}	0.5184	0.5293	0.5363	0.5425

Table VI - H_I and H_{II} for Mixed-Mode Crack

As is seen in Fig. 12 the most accurate values are again obtained from COD (i.e. averaging the values on $\theta = -180^{\circ}$ and $\theta = +180^{\circ}$). This in fact, is physically very appealing as in practice we can only measure the COD and then find the corresponding H_I and H_{II}. Also it is noted that the computed values compare well with those of Bowie's. The reason for these values being slightly less than Bowie's values might be due to the inherent underestimation of the displacement field in the approximation method. The COD for the mixed-mode crack problem is plotted in Fig. 13 for a small neighbourhood of the tip. The final distortion of the sheet if sketched in Fig. 14.

One can also find the state of stress in the sheet due to the tension T applied uniformly along the edges. While there is a number of ways to present the state of stresses we only plot the contours of maximum principal stress in Fig. 15 and Fig. 16. In the very inner core near the tip (Fig. 16) the state of stresses are very high and are given by the formulae (for $\frac{r}{a} < 0.02$)

$$
\begin{cases}
\dfrac{\sigma_{xx}}{T} = \dfrac{1}{\sqrt{2\left(\frac{r}{a}\right)}}\left\{1.2200\cos\dfrac{\theta}{2}\left(1-\sin\dfrac{\theta}{2}\sin\dfrac{3\theta}{2}\right) - 0.5479\sin\dfrac{\theta}{2}\left(2+\cos\dfrac{\theta}{2}\cos\dfrac{3\theta}{2}\right)\right\} \\[2ex]
\dfrac{\sigma_{xy}}{T} = \dfrac{1}{\sqrt{2\left(\frac{r}{a}\right)}}\left\{0.6100\sin\theta\cos\dfrac{3\theta}{2} + 0.5479\cos\dfrac{3\theta}{2}\left(1-\sin\dfrac{\theta}{2}\sin\dfrac{3\theta}{2}\right)\right\} \\[2ex]
\dfrac{\sigma_{yy}}{T} = \dfrac{1}{\sqrt{2\left(\frac{r}{a}\right)}}\left\{1.2200\cos\dfrac{\theta}{2}\left(1+\sin\dfrac{\theta}{2}\sin\dfrac{3\theta}{2}\right) + 0.27395\sin\theta\cos\dfrac{3\theta}{2}\right\}
\end{cases}
\tag{6}
$$

where $T = 0.2\times10^{10}$, $a = 0.5$ and r and θ are as shown in Fig. 12.

Now we can consider an edge-crack in a tensile sheet and assume that the crack has *branched off* at an angle of 135° from the crack line (Fig. 17). The COD for this problem is plotted in Fig. 17. The values of stress intensity factors obtained from the COD are

$$
\begin{cases}
H_I = 8.8220 \\[2ex]
H_{II} = -1.6286
\end{cases}
$$

See Table VII for computational data and results.

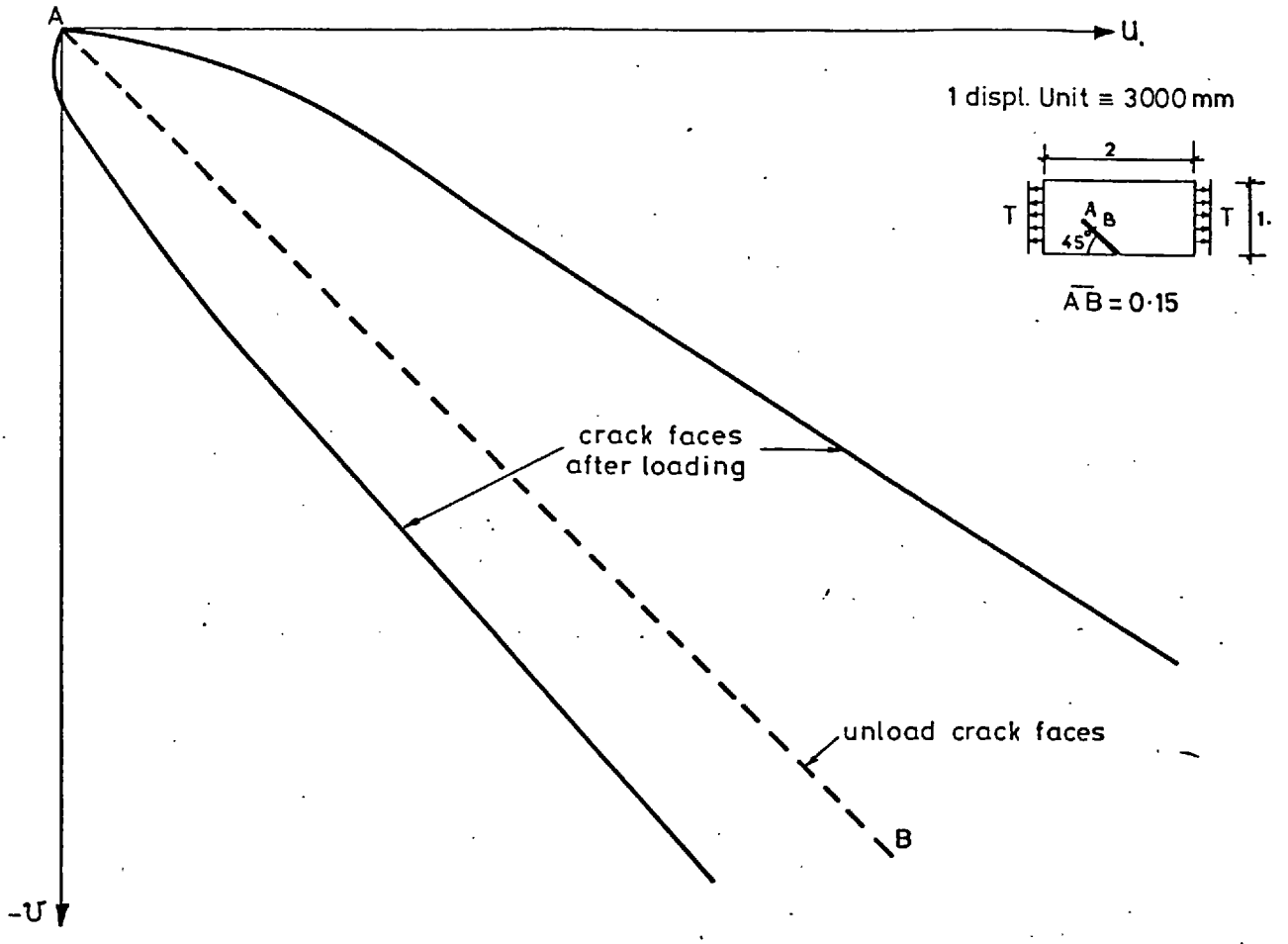

Fig. 13 Local (AB) mixed-mode crack opening displacement (COD)

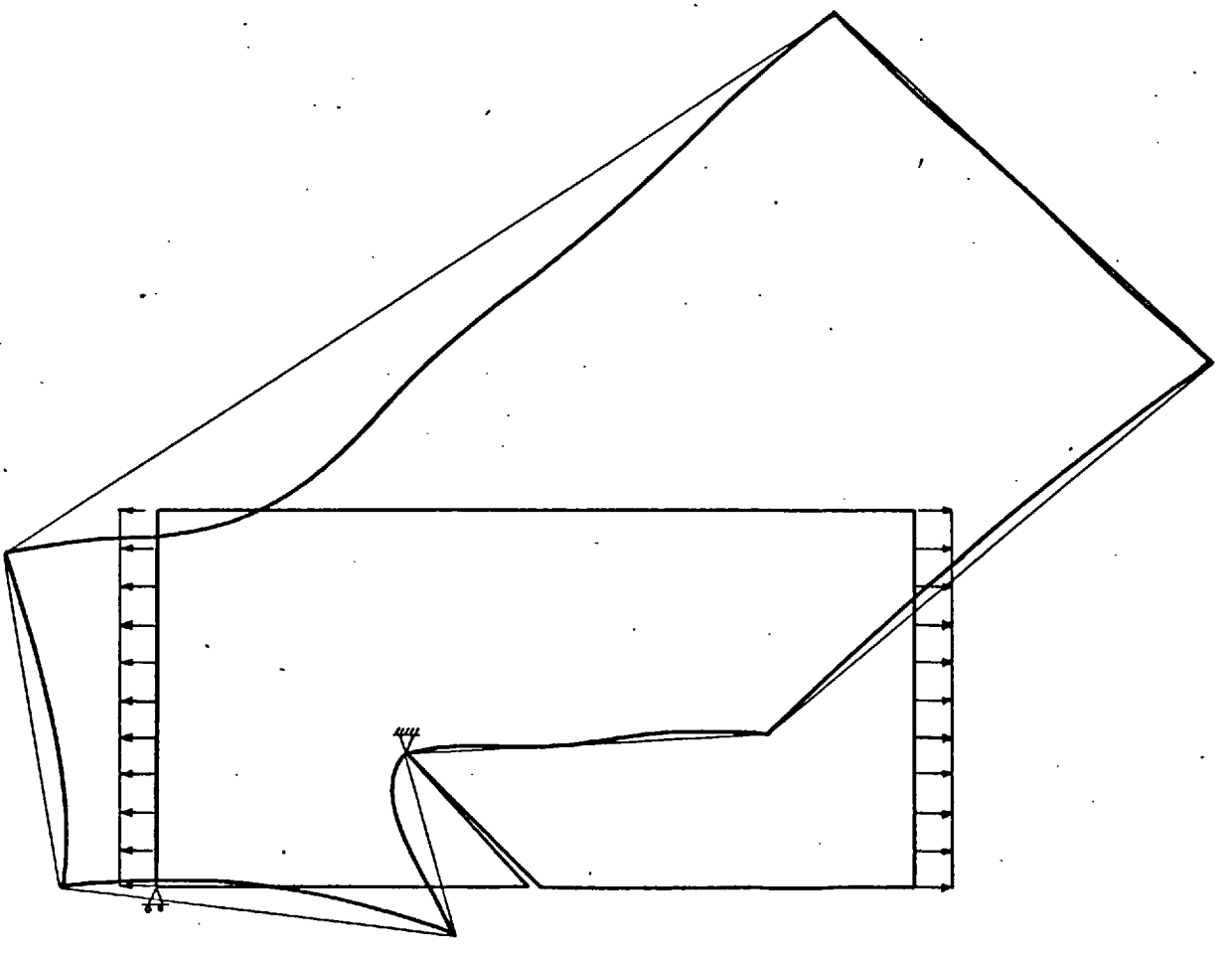

Fig. 14 Distortion of an edge-cracked sheet

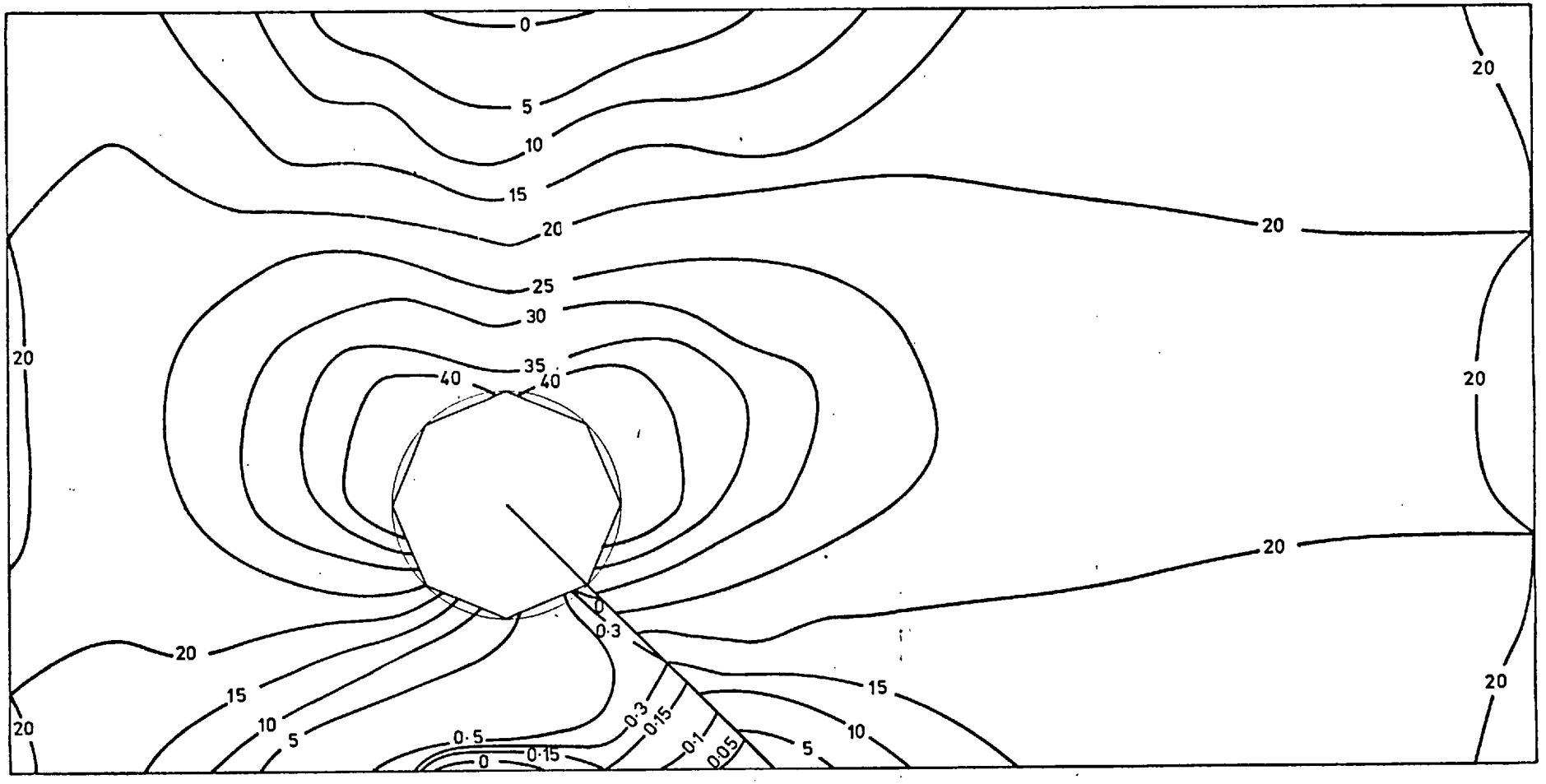

Fig 15 · Contours of maximum principal stress for the inclined crack problem

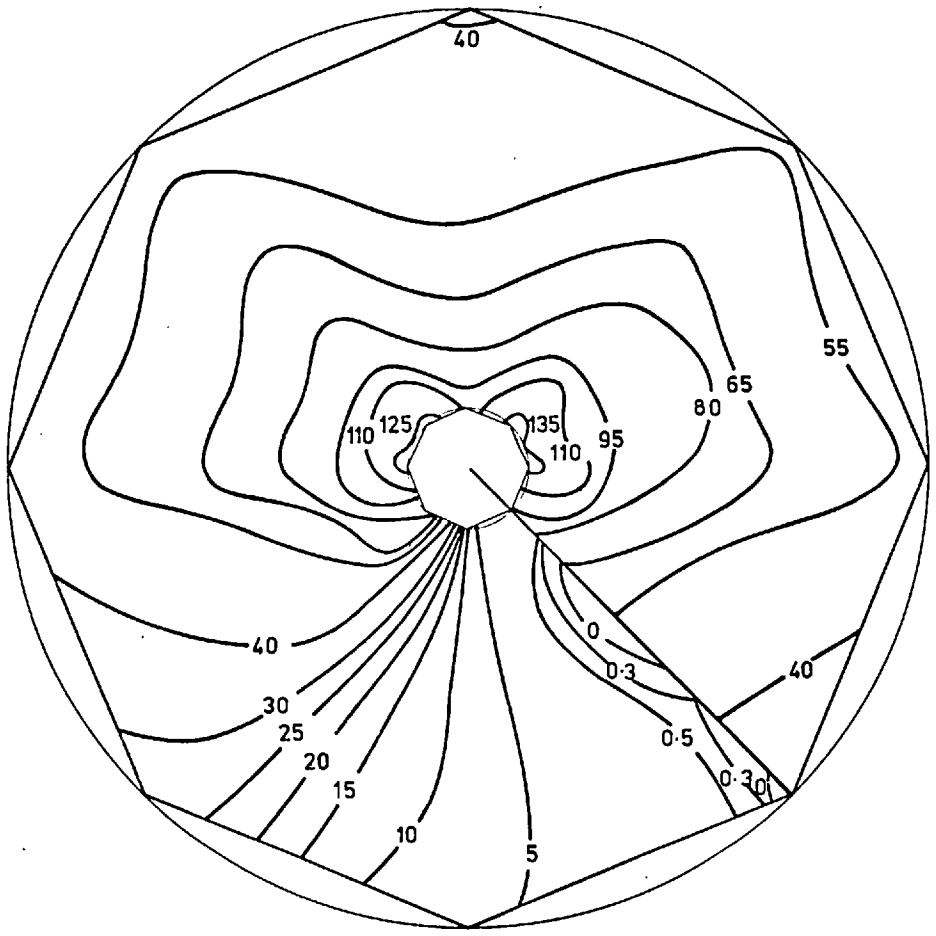

Fig 16 Contours of maximum principal stress near the crack tip for the inclined crack problem.

D I S P L A C E M E N T S   A T   N O D E S

NODE NO.	DISPLACEMENT IN SYSTEM X-DIRECTION	DISPLACEMENT IN SYSTEM Y-DIRECTION
1	.116777E+01	.562531E+01
2	.202235E+01	.676231E+01
3	.146734E+01	.693243E+01
4	.916053E+00	.871511E+01
5	.682559E+00	.620630E+01
6	.707358E+00	.533351E+01
7	.713564E+00	.559421E+01
8	.564346E+00	.539341E+01
9	.425031E+00	.512233E+01
10	.540548E+00	.461533E+01
11	.312216E+01	.303531E+01
12	.245293E+01	.136943E+01
13	.172250E+01	.363043E+01
14	.105845E+01	.333233E+01
15	.458057E+00	.312333E+01
16	.113735E+00	.735072E+01
17	-.116719E+00	.633335E+01
18	-.259324E-01	.624625E+01
19	.177496E-01	.595716E+01
20	.211760E+00	.557233E+01
21	.213009E+00	.536553E+01
22	.234478E+00	.523333E+01
23	.631661E-01	.499533E+01
24	-.794643E-02	.478135E+01
25	-.110656E+00	.431133E+01
26	-.629774E-01	.403333E+01
27	.723670E-01	.369413E+01
28	.396741E+01	.994153E+01
29	.197769E+01	.593543E+01
30	.213365E-01	.397543E+01
31	-.707861E+00	.723374E+01
32	-.510091E+00	.379712E+01
33	-.695423E-01	.511435E+01
34	-.136333E+00	.469133E+01
35	-.374666E+00	.399327E+01
36	-.170695E+00	.315671E+01
37	.473192E+01	.987677E+01
38	.343297E+01	.104143E+02
39	.213359E+01	.109133E+02
40	.776234E+00	.103541E+02
41	-.406072E+00	.343511E+01
42	-.596647E+00	.457235E+01
43	-.143015E+01	.754374E+01
44	-.110495E+01	.643311E+01
45	-.100439E+01	.571353E+01
46	-.526215E+00	.535547E+01
47	-.329779E+00	.485653E+01
48	-.176621E+00	.471517E+01
49	-.274626E+00	.441231E+01
50	-.392214E+00	.416333E+01
51	-.542033E+00	.365535E+01
52	-.492099E+00	.326433E+01
53	-.334559E+00	.274335E+01
54	.591626E+01	.111213E+02
55	.234976E+01	.125533E+02
56	-.110679E+01	.110551E+02
57	-.245990E+01	.793247E+01
58	-.176339E+01	.553312E+01
59	-.659190E+00	.443033E+01
60	-.411532E+00	.397737E+01
61	-.717248E+00	.323433E+01
62	-.516920E+00	.223333E+01
63	.710435E+01	.123333E+02
64	.477164E+01	.113333E+02
65	.253076E+01	.143333E+02
66	.220625E+00	.111333E+02
67	-.151224E+01	.122110E+02
68	-.276510E+01	.111111E+02
69	-.746559E+01	.116533E+01

S U M M A R Y   O F   D A T A

TOTAL NUMBER OF ELEMENTS = 117
TOTAL NUMBER OF NODES = 362
TOTAL NUMBER OF SUPPORT NODES = 13
TOTAL NUMBER OF LOADING CASES = 1

DYNAMIC VECTOR ARRAY REQUIREMENTS

DATA PROCESSING = 2249
DATA STORAGE = 2556
PRE-SOLUTION PROCESS = 4329
SOLUTION PROCESS = 3746
POST-SOLUTION PROCESS = 1376
LOCATIONS AVAILABLE = 25000

MAXIMUM FRONT WIDTH OF STIFFNESS MATRIX = 75
MAXIMUM HALF BANDWIDTH OF STIFFNESS MATRIX = 162
TOTAL NUMBER OF ACTIVE NODES = 362
TOTAL NUMBER OF EQUATIONS = 724

TIME FOR THIS PHASE = 3.874 SEC.

TIME USED TO PROCESS INPUT DATA = 15.355 SEC.
TIME AT CENTRAL PROCESSOR = 22.42.08. HRS/MINS/SECS

TIME USED IN PRE-SOLUTION PROCESS (ALL ELEMENT STIFFNESS MATRICES) = 15.418 SEC.
TIME AT CENTRAL PROCESSOR = 22.42.34. HRS/MINS/SECS

S O L U T I O N   B Y   F R O N T A L   S P A R S E   M A T R I X   T E C H N I Q U E

MACHINE CODE INNER LOOPS AND DYNAMIC RANDOM ACCESS IN OPERATION

TIME USED FOR ASSEMBLY AND ELIMINATION WITH 1 RIGHT HAND SIDES = 18.777 SEC.
TIME USED IN BACK-SUBSTITUTION PROCESS WITH 1 RIGHT HAND SIDES = 1.312 SEC.
TIME AT CENTRAL PROCESSOR = 22.43.13. HRS/MINS/SECS

Table VII - Branched Crack Problem Data and Displacements

$E = 0{\cdot}2 \times 10^{12}$
$T = E$
$\nu = 0{\cdot}3$
$H_I = 8{\cdot}8220$
$H_{II} = -1{\cdot}6286$

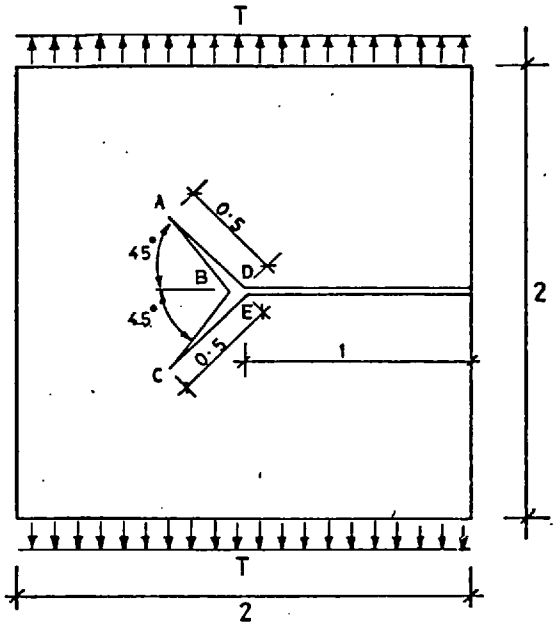

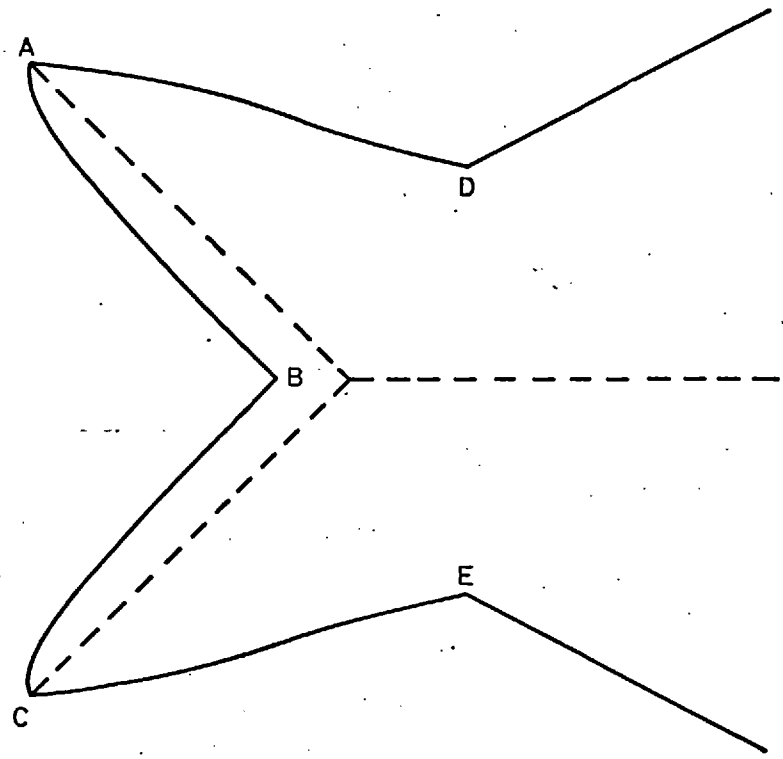

Fig. 17 The profile of a branched-crack after loading

Now we study the effects of anisotropy on the solution. Consider the previous central crack problem with only changes in the material properties as representing an orthotropic material with lines of material symmetry coinciding with the x- and y-axes of Fig. 18

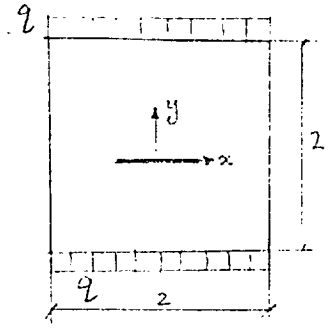

Fig(18)

and

$$\begin{cases} E_1 = 0.56\times10^{11} \\ \\ E_2 = 0.14\times10^{11} \end{cases} \qquad \text{elastic moduli}$$

$G_{12} = 0.1\times10^{11}$ shear modulus

$\nu_{12} = 0.3$ a poisson's ratio

$q = 0.2\times10^{10}$ load intensity

$a = 0.4$ half-crack length

The asymptotic displacement field is then given by [118, Ch. II]

$$u = K_I\sqrt{\frac{2r}{\pi}}\,\mathrm{Re}\left\{\frac{1}{s_1-s_2}\left[s_1p_2(\cos\theta+s_2\sin\theta)^{\frac{1}{2}} - s_2p_1(\cos\theta+s_1\sin\theta)^{\frac{1}{2}}\right]\right.$$

$$\left. + K_{II}\sqrt{\frac{2r}{\pi}}\,\mathrm{Re}\left\{\frac{1}{s_1-s_2}\left[p_2(\cos\theta+s_2\sin\theta)^{\frac{1}{2}} - p_1(\cos\theta+s_1\sin\theta)^{\frac{1}{2}}\right]\right\} + O(r)\right. \qquad (7)$$

$$v = K_I \sqrt{\frac{2r}{\pi}}\, \mathrm{Re}\left\{\frac{1}{s_1-s_2}\left[s_1 q_2 (\cos\theta + s_2 \sin\theta)^{\frac{1}{2}} - s_2 q_1 (\cos\theta + s_1 \sin\theta)^{\frac{1}{2}}\right]\right\}$$

$$+ K_{II} \sqrt{\frac{2r}{\pi}}\, \mathrm{Re}\left\{\frac{1}{s_1-s_2}\left[q_2 (\cos\theta + s_2 \sin\theta)^{\frac{1}{2}} - q_1 (\cos\theta + s_1 \sin\theta)^{\frac{1}{2}}\right]\right\} + O(r) \qquad (7)$$

where s_1 and s_2 are roots of the following equation:

$$a_{11}s^4 - 2a_{16}s^3 + (2a_{12}+a_{66})s^2 - 2a_{26}s + a_{22} = 0 \qquad (8)$$

the coefficients a_{ij} in the orthotropic case are given by:

$$a_{11} = \frac{1}{E_1}, \quad a_{16} = 0, \quad a_{12} = -\frac{\nu_{12}}{E_1} = -\frac{\nu_{21}}{E_2}, \quad a_{66} = \frac{1}{G_{12}}$$

$$a_{26} = 0 \quad \text{and} \quad a_{22} = \frac{1}{E_2}$$

From equation (8) we obtain

$$\begin{cases} s_1 s_2 = -\alpha_0 \\ s_1 + s_2 = i\sqrt{2(\alpha_0+\beta_0)} \end{cases}$$

where

$$\begin{cases} \alpha_0 = (E_1/E_2)^{\frac{1}{2}} \\ \beta_0 = \dfrac{E_1}{2G_{12}} - \nu_{12} \end{cases}$$

In (7) p_j and q_j are given by

$$\begin{cases} p_1 = a_{11}s_1^2 + a_{12} - a_{16}s_1 \\ p_2 = a_{11}s_2^2 + a_{12} - a_{16}s_2 \\ q_1 = \{a_{12}s_1^2 + a_{22} - a_{26}s_1\}/s_1 \\ q_2 = \{a_{12}s_2^2 + a_{22} - a_{26}s_2\}/s_2 \end{cases} \tag{9}$$

substituting for the elastic constants we obtain

$$\begin{cases} p_1 = -\left(\dfrac{1.3}{0.56\text{x}10^{11}}\right) & p_2 = -\left(\dfrac{4.3}{0.56\text{x}10^{11}}\right) \\ q_1 = \left(\dfrac{4.3}{0.56\text{x}10^{11}}\right)/i & q_2 = \left(\dfrac{2.6}{0.56\text{x}10^{11}}\right)/i \end{cases}$$

and

$$\begin{cases} s_1 = i \\ s_2 = 2i \end{cases}$$

From (7) along $\Theta = +180$ we obtain

$$\begin{cases} u = K_I\sqrt{\dfrac{2r}{\pi}}\,\text{Re}\left\{\dfrac{1.7i}{0.56\text{x}10^{11}}\right\} + K_{II}\sqrt{\dfrac{2r}{\pi}}\,\text{Re}\left\{\dfrac{3.0}{0.56\text{x}10^{11}}\right\} = \\ \qquad K_{II}\sqrt{\dfrac{2r}{\pi}}\,\dfrac{3.0}{0.56\text{x}10^{11}} \\ v = K_I\sqrt{\dfrac{2r}{\pi}}\,\text{Re}\left\{\dfrac{3.}{0.28\text{x}10^{11}}\right\} + K_{II}\sqrt{\dfrac{2r}{\pi}}\,\text{Re}\left\{-\dfrac{1.7i}{0.56\text{x}10^{11}}\right\} = \\ \qquad K_I\sqrt{\dfrac{2r}{\pi}}\,\dfrac{3.0}{0.28\text{x}10^{11}} \end{cases}$$

Similarly to the isotropic material treated before (equation (5)) we get

$$\begin{cases} K_I \sqrt{\frac{2}{\pi}} \frac{3.0}{0.28\times10^{11}} = \frac{4v(\ell/4)-v(\ell)-3v(0)}{\sqrt{\ell}} \\ K_{II} \sqrt{\frac{2}{\pi}} \frac{3.0}{0.56\times10^{11}} = \frac{4u(\ell/4)-u(\ell)-3u(0)}{\sqrt{\ell}} \end{cases} \qquad (\ell = 0.04)$$

in which along $\theta = 180^{\circ}$, K_I and K_{II} have decoupled.

Using Table VIII along $\theta = + 180^{\circ}$ we obtain

$$\begin{cases} H_I = \frac{K_I}{q\sqrt{\pi a}} = 1.1082 \\ H_{II} = \frac{K_{II}}{q\sqrt{\pi a}} = 0.0489 \end{cases}$$

and along $\theta = - 180^{\circ}$ we get

$$\begin{cases} H_I = 1.1082 \\ H_{II} = -0.0489 \end{cases}$$

The averaged values of H_I and H_{II} from $\theta = - 180^{\circ}$ and $\theta = + 180^{\circ}$ which correspond to H_I and H_{II} obtained from COD in the orthotropic case are given by

$$\begin{cases} H_I = 1.1082 \\ H_{II} = 0.000 \end{cases} \qquad (11)$$

The corresponding *interpolated* values from Bowie's work [119] are

Table VIII - Orthotropic Central Crack Problem Data and Displacements

SOLUTION BY FRONTAL SPARSE MATRIX TECHNIQUE

MACHINE CODE INNER LOOPS AND DYNAMIC RANDOM ACCESS IN OPERATION

TIME USED FOR ASSEMBLY AND ELIMINATION WITH 1 RIGHT HAND SIDES = 2.088 SEC.

TIME USED IN BACK-SUBSTITUTION PROCESS WITH 1 RIGHT HAND SIDES = .274 SEC.

TOTAL AREA OF ELEMENTS = .100000E+01 SQ.

MATERIAL PROPERTIES ORTHOTROPIC

FIRST ELEMENT IN SERIES	LAST ELEMENT IN SERIES	DIFFERENCE BETWEEN ELEMENTS	MODULUS OF ELASTICITY IN X-DIRECTION OF ORTHOTROPY	MODULUS OF ELASTICITY IN Y-DIRECTION OF ORTHOTROPY	SHEAR MODULUS OF ELASTICITY	POISSONS RATIO FOR INDUCED STRAIN IN X-DIRECTION OF ORTHOTROPY	ANGLE BETWEEN X-AXIS OF ORTHOTROPY AND REFERENCE X-AXIS
1	12	1	.5600E+11	.1400E+11	.1000E+11	.3000	0
50	71	1	.5600E+11	.1400E+11	.1000E+11	.3000	0

DISPLACEMENTS AT NODES

NODE NO.	DISPLACEMENT IN SYSTEM X-DIRECTION	DISPLACEMENT IN SYSTEM Y-DIRECTION
1	-.330524E-01	.727346E-13
2	-.273399E-01	.267355E-12
3	-.259860E-01	.575065E-02
4	-.245324E-01	.125510E-01
5	-.260550E-01	.183219E-01
6	-.321248E-01	.219413E-01
7	-.237619E-01	.175384E-12
8	-.239499E-01	.537335E-02
9	-.215175E-01	.125511E-01
10	-.134976E-01	.164035E-01
11	-.168361E-01	.251596E-01
12	-.174762E-01	.306412E-01
13	-.139443E-01	.370515E-01
14	-.233342E-01	.339555E-01
15	-.312336E-01	.416357E-01
16	-.225996E-01	.124819E-12
17	-.190503E-01	.157723E-01
18	-.133357E-01	.323351E-01
19	-.155891E-01	.451104E-01
20	-.284914E-01	.551930E-01
21	-.217492E-01	.727193E-13
22	-.202713E-01	.835599E-02
23	-.185513E-01	.126309E-01
24	-.133374E-01	.273309E-01
25	-.114362E-01	.377334E-01
26	-.113515E-01	.437333E-01
27	-.123403E-01	.519755E-01
28	-.135335E-01	.543125E-01
29	-.258342E-01	.576931E-01
30	-.210637E-01	.167176E-12
31	-.145554E-01	.234315E-01
32	-.863306E-02	.459416E-01
33	-.841398E-02	.616215E-01
34	-.243679E-01	.673357E-01
35	-.210917E-01	.115524E-12
36	-.179781E-01	.126737E-01
37	-.131469E-01	.279312E-01
38	-.967358E-02	.394710E-01
39	-.560281E-02	.532451E-01

SUMMARY OF DATA

STRUCTURE TYPE	=	PLANESTRESS
TOTAL NUMBER OF ELEMENTS	=	34
TOTAL NUMBER OF NODES	=	123
TOTAL NUMBER OF SUPPORT NODES	=	22
TOTAL NUMBER OF LOADING CASES	=	1

DYNAMIC VECTOR ARRAY REQUIREMENTS

DATA PROCESSING	=	980
DATA STORAGE	=	934
PRE-SOLUTION PROCESS	=	1763
SOLUTION PROCESS	=	1631
POST-SOLUTION PROCESS	=	1375
LOCATIONS AVAILABLE	=	5000

MAXIMUM FRONT WIDTH OF STIFFNESS MATRIX	=	42
MAXIMUM HALF BANDWIDTH OF STIFFNESS MATRIX	=	76
TOTAL NUMBER OF ACTIVE NODES	=	123
TOTAL NUMBER OF EQUATIONS	=	246

TIME FOR THIS PHASE = .795 SEC.

TIME USED TO PROCESS INPUT DATA = 3.494 SEC.

$$\begin{cases} H_I = 1.125 \\ \\ H_{II} = 0. \end{cases}$$

with an error of $\frac{1.1250-1.1082}{1.1250} = 1.49\%$ for the relatively coarse discretization of the sheet.

As the last example in static analysis we consider a central crack in a bi-material sheet (see figure).

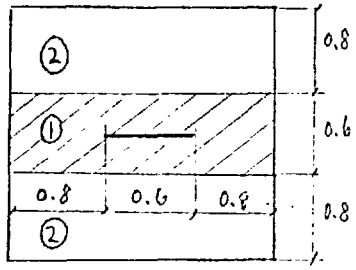

The physical data for the problem is as follows:

$$\begin{cases} E_1 = 0.2\text{x}10^{12} & E_2 = 0.5\text{x}10^{12} \\ & \text{and} \\ \nu_1 = 0.3 & \nu_2 = 0.25 \end{cases}$$

Using the same mesh as before we obtain the following values for the stress intensity factors:

$$\begin{cases} H_I = 1.0739 \\ \\ H_{II} = 0. \end{cases}$$

V.7.2 Dynamic Analysis

Consider the central crack problem of the previous section as a model for dynamic analysis. This time the uniform tension T is suddenly applied along the boundary (i.e. step load) and the time behaviour of the stress intensity factor $K_I(t)$ and other field variables are studied.

For this problem the same *spatial* finite element representation as in the previous section is used. Employing the Newmark's difference scheme (see Chapter II) and a consistent mass matrix we surround the crack tips by quarter-point singular elements. Eventhough the adopted difference scheme is unconditionally stable, in order to obtain an accurate result we have to use time-intervals (Δt) smaller than the time required for the longitudinal waves to travel across the smallest elements in the spatial discretization. With $E = 0.2\text{x}10^{12}$, $\nu = 0.3$ and $\rho = 5000$ (SI units) we have

$$c_1 = \sqrt{\frac{\lambda+2\mu}{\rho}} = \sqrt{\frac{E}{\rho}\frac{1-\nu}{(1+\nu)(1-2\nu)}} = 7338, \quad \text{longitudinal wave velocity}$$

$$c_2 = \sqrt{\frac{\mu}{\rho}} = \sqrt{\frac{E}{\rho}\frac{1}{2(1+\nu)}} = 3922, \quad \text{shear wave velocity}$$

$$V_R \simeq 0.9274 c_2 = 3638, \quad \text{Rayleigh wave velocity}$$

We choose $\Delta t = 4\mu s$ which is slightly less than the time required for waves to propagate across the singular (smallest) elements. Table IX presents the numerical displacement field after $t = 260\mu s$ from the application of the step load.

The profile of the crack tip at four different times is plotted in Fig. 19. From the COD variations with time we can extract the stress intensity factor $K_I(t)$ at any time using equations (5). For numerical values of the normalised stress intensity factor see Table X.

D I S P L A C E M E N T S   A T   N O D E S

NODE NO.	DISPLACEMENT IN X-DIRECTN	DISPLACEMENT IN Y-DIRECTN	NODE	DISPLACEMENT IN X-DIRECTN	DISPLACEMENT IN Y-DIRECTN	NODE	DISPLACEMENT IN X-DIRECTN	DISPLACEMENT IN Y-DIRECTN	NODE	DISPLACEMENT IN X-DIRECTN	DISPLACEMENT IN Y-DIRECTN
1	-.406813E-02	.364119E-12	2	-.319850E-02	.144426E-11	3	-.293663E-02	.476845E-03	4	-.274815E-02	.132664E-02
5	-.303484E-02	.273316E-12	6	-.391631E-02	.273297E-02	7	-.248761E-02	.565365E-12	8	-.246987E-02	.447095E-03
9	-.211333E-02	.107458E-02	10	-.187573E-02	.183313E-02	11	-.159226E-02	.272328E-02	12	-.171625E-02	.352780E-02
13	-.214758E-02	.452992E-02	14	-.276394E-02	.432541E-02	15	-.357689E-02	.526951E-02	16	-.230219E-02	.556205E-12
17	-.141761E-02	.175345E-02	18	-.112487E-02	.734614E-02	19	-.155791E-02	.541264E-02	20	-.348187E-02	.626752E-02
21	-.219241E-02	.396356E-12	22	-.204765E-02	.731323E-03	23	-.159255E-02	.161449E-02	24	-.121190E-02	.248107E-02
25	-.454633E-03	.386231E-02	26	-.791633E-03	.493372E-02	27	-.110503E-02	.618620E-02	28	-.217486E-02	.670242E-02
29	-.376519E-02	.721167E-02	30	-.209928E-02	.953737E-12	31	-.141592E-02	.209476E-02	32	-.227068E-03	.468360E-02
33	-.511166E-03	.735168E-02	34	-.304686E-02	.351021E-02	35	-.209434E-02	.683701E-12	36	-.138601E-02	.119184E-02
37	-.134972E-02	.261478E-02	38	-.659533E-03	.371197E-02	39	.123246E-03	.542320E-02	40	.251417E-03	.664273E-02
41	-.840664E-04	.827549E-12	42	-.116825E-02	.333501E-02	43	-.279652E-02	.935956E-02	101	-.225152E-02	.162103E-11
102	-.115795E-02	.357771E-02	103	.395513E-03	.554275E-02	104	.524295E-03	.973366E-02	105	-.211804E-02	.107927E-01
106	-.244305E-02	.667747E-12	107	-.133937E-02	.214545E-02	108	-.139758E-02	.437675E-02	109	-.265979E-03	.576645E-02
110	.518665E-03	.763150E-12	111	-.911741E-03	.917324E-02	112	.742684E-03	.108309E-01	113	-.193305E-03	.114255E-01
114	-.151251E-02	.119624E-01	115	-.365115E-03	.131121E-11	116	-.183088E-02	.414541E-02	117	-.101309E-02	.633232E-02
118	.378335E-03	.864313E-12	119	-.323739E-03	.103322E-01	120	.463210E-03	.121973E-01	121	-.619735E-03	.124192E-01
122	-.384712E-02	.941999E-12	123	-.289657E-02	.312255E-02	124	-.273046E-02	.408259E-02	125	-.258334E-02	.622215E-02
126	-.272866E-02	.842766E-12	127	-.312905E-02	.833332E-02	128	-.127235E-02	.826603E-02	129	-.525629E-03	.886401E-02
130	.593765E-04	.977115E-02	131	.533954E-03	.133147E-01	132	.664956E-03	.111275E-01	133	.391622E-03	.114098E-01
134	.133923E-12	.115937E-01	135	.468204E-12	.120792E-01	136	.328003E-12	.125375E-01	137	-.148175E-12	.128327E-01
138	-.257593E-12	.126145E-01	139	-.343173E-02	.245337E-11	140	-.351075E-02	.402019E-02	141	-.345550E-02	.612045E-02
142	-.417913E-02	.603932E-12	143	-.415503E-02	.231772E-12	144	-.416055E-02	.402121E-02	145	-.411064E-02	.614415E-02
146	-.416374E-02	.861164E-02	147	-.397654E-02	.111367E-11	148	-.293248E-02	.115938E-01	149	-.200133E-02	.108500E-01
150	-.380856E-03	.113666E-01	151	-.411335E-02	.117327E-01	152	-.136851E-12	.117654E-01	153	-.252419E-12	.129043E-01
154	-.553883E-02	.123742E-01	155	-.131173E-02	.133365E-01	156	-.150437E-02	.126375E-01	157	-.134732E-02	.126229E-01
158	-.277510E-02	.127739E-01	159	-.366306E-02	.127133E-11	160	-.285914E-02	.129074E-01	161	-.319929E-02	.131087E-01
162	-.315976E-02	.136347E-01	163	-.374175E-02	.135556E-01	164	-.384198E-02	.155362E-01	165	-.352326E-02	.150334E-01
166	-.278224E-02	.147121E-01	167	-.224836E-02	.142609E-01	168	-.195901E-02	.140657E-01	169	-.517098E-12	.129644E-01
170	-.855636E-13	.152584E-01	171	-.513985E-02	.151341E-01	172	-.101216E-02	.156074E-01	173	-.159686E-02	.154939E-01
174	-.202595E-02	.159541E-01	175	-.243074E-02	.153311E-01	176	-.361616E-02	.166898E-01	177	-.342740E-02	.165086E-01
178	-.361301E-02	.168773E-01	179	-.405955E-02	.167233E-01	180	-.463952E-02	.178319E-01			

R E A C T I O N S   T O   E A R T H

NODE NO.	FORCE IN SYSTEM X-DIRECTION	FORCE IN SYSTEM Y-DIRECTION
1	0	-.364119E+09
2	0	-.144426E+10
7	0	-.565365E+09
16	0	-.556205E+09
21	0	-.396356E+09
30	0	-.953737E+09
35	0	-.683701E+09
101	0	-.162103E+10
106	0	-.667747E+09
115	0	-.131121E+10
122	0	-.941999E+09
134	-.133923E+09	0
135	-.468204E+09	0
136	-.328003E+09	0
137	.148175E+09	0
138	.257593E+09	0
139	0	-.245337E+10
142	0	-.603932E+09
152	.136851E+09	0
153	.252419E+09	0
169	.517098E+09	0
170	.855636E+08	0
TOTAL FORCE	.467569E+09	-.126569E+11

S U M M A R Y   O F   D A T A

TOTAL NUMBER OF ELEMENTS = 34
TOTAL NUMBER OF NODES = 123
TOTAL NUMBER OF SUPPORT NODES = 22
TOTAL NUMBER OF LOADING CASES = 1

DYNAMIC VECTOR ARRAY REQUIREMENTS

DATA PROCESSING = 990
DATA STORAGE = 829
PRE-SOLUTION PROCESS = 1985
SOLUTION PROCESS = 1621
POST-SOLUTION PROCESS = 1419
LOCATIONS AVAILABLE = 25000

MAXIMUM FRONT WIDTH OF STIFFNESS MATRIX = 42
MAXIMUM HALF BANDWIDTH OF STIFFNESS MATRIX = 76
TOTAL NUMBER OF ACTIVE NODES = 123
TOTAL NUMBER OF EQUATIONS = 246

TIME FOR THIS PHASE = .793 SEC.

D Y N A M I C   C O N T R O L

VALUE OF TIME STEP = .400000E-05
ELAPSED NUMBER OF TIME STEPS FOR OUTPUT OF RESULTS = 1

TIME USED FOR ASSEMBLY AND ELIMINATION WITH 1 RIGHT HAND SIDES = 2.122 SEC.
TIME USED IN BACK-SUBSTITUTION PROCESS WITH 1 RIGHT HAND SIDES = .490 SEC.

Table IX - Dynamic Response of a Central Crack Problem at t = 260μs

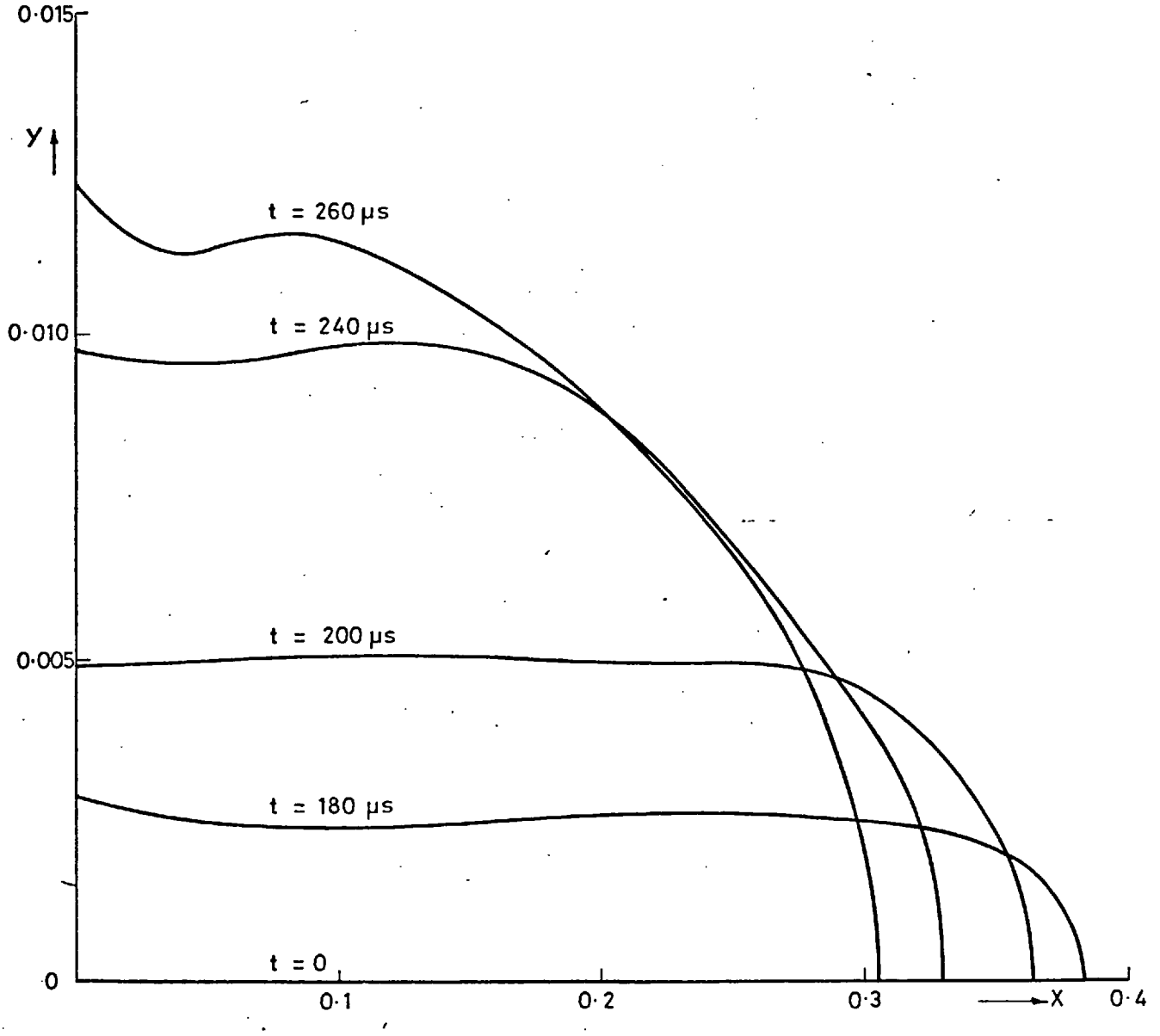

Fig.19 COD for the central crack problem due to step-load at four different times ($\Delta t = 4\,\mu s$)

TIME (μs)	H_I
0	0.000
12	-0.0002
24	0.0012
36	0.0007
48	-0.1026
60	0.1103
72	-0.1497
84	0.1025
96	0.0910
108	-0.0278
120	-0.1397
132	-0.0543
144	0.0881
156	0.3288
168	0.5871
180	0.7429
192	0.9152
204	1.0476
216	1.2196
228	1.2225
240	1.2707
252	1.2965
264	1.6408

TIME (μs)	H_I
276	1.5794
288	1.6839
300	1.8885
312	1.7167
324	1.9258
336	1.9477
348	2.0320
360	2.2899
372	2.3521
384	2.3827
396	2.3907
408	2.1046
420	2.4056
432	2.3370
444	2.3455
456	2.3518
468	2.3713
480	2.3221
492	2.5745
504	2.2336
516	2.3344
528	2.2401
540	2.3358

Table X - Stress-intensity-factor $H_I(t)$ at Different Times

$H_I(t)$ is also plotted in Fig. 20. As it is observed in this figure, before the first arrival of longitudinal waves there is some small-amplitude oscillations in $H_I(t)$ which is due to numerical cancellations and reinforcements of COD as calculated from (5). To see this more clearly we have plotted the time-variation of the displacement at the centre of the crack in Fig. 21. The same pattern for initial oscillations with small amplitudes is observed. As $H_I(t)$ is obtained from displacements at three nodes very close to the tip (i.e. equation (5)) the numerical inaccuracies involved could add or subtract, resulting in a slightly larger error for H_I. One way to reduce these oscillations is to choose a smaller time step (i.e. $\Delta t < 4\mu s$). However, we can hardly justify the use of a smaller time interval Δt without a simultaneous reduction in the size of the elements (h). Smaller time-increments (Δt) and mesh size (h) would then enable one to detect higher frequency components of displacements and stresses in the field.

The arrival time of different waves are marked in Figs. 20 and 21. In these figures p_1 (resp. s_1) represents the arrival time of the first longitudinal (resp. transverse) waves and prime on p_1 (e.g. p_1'', etc.) indicates later arrivals of the scattered longitudinal waves. Also R_{p_1} (resp. R_{s_1}) is the time required for the Rayleigh waves generated by the first incident longitudinal wave to travel from one crack tip to another and back to the point (0,0). Clearly, in the sheet of finite dimensions there are large number of different types of waves reflected from boundaries into the medium and as time rolls on the picture for H_I becomes more complex. However, the arrival times of some of the waves are shown on these figures to mark the more important features of the problem. As seen in Fig. 21 from about 480μs up to the time for which

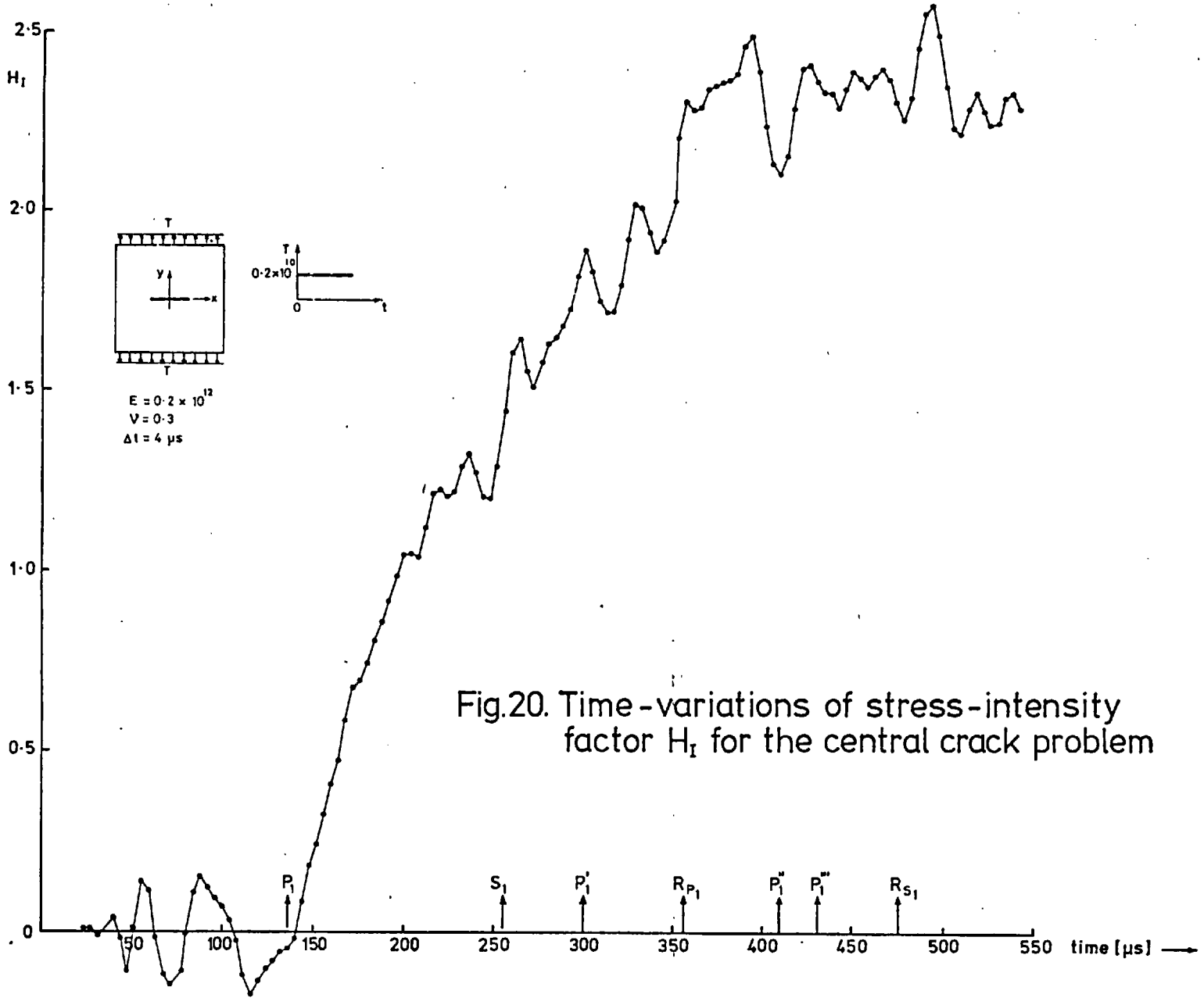

Fig.20. Time-variations of stress-intensity factor H_I for the central crack problem

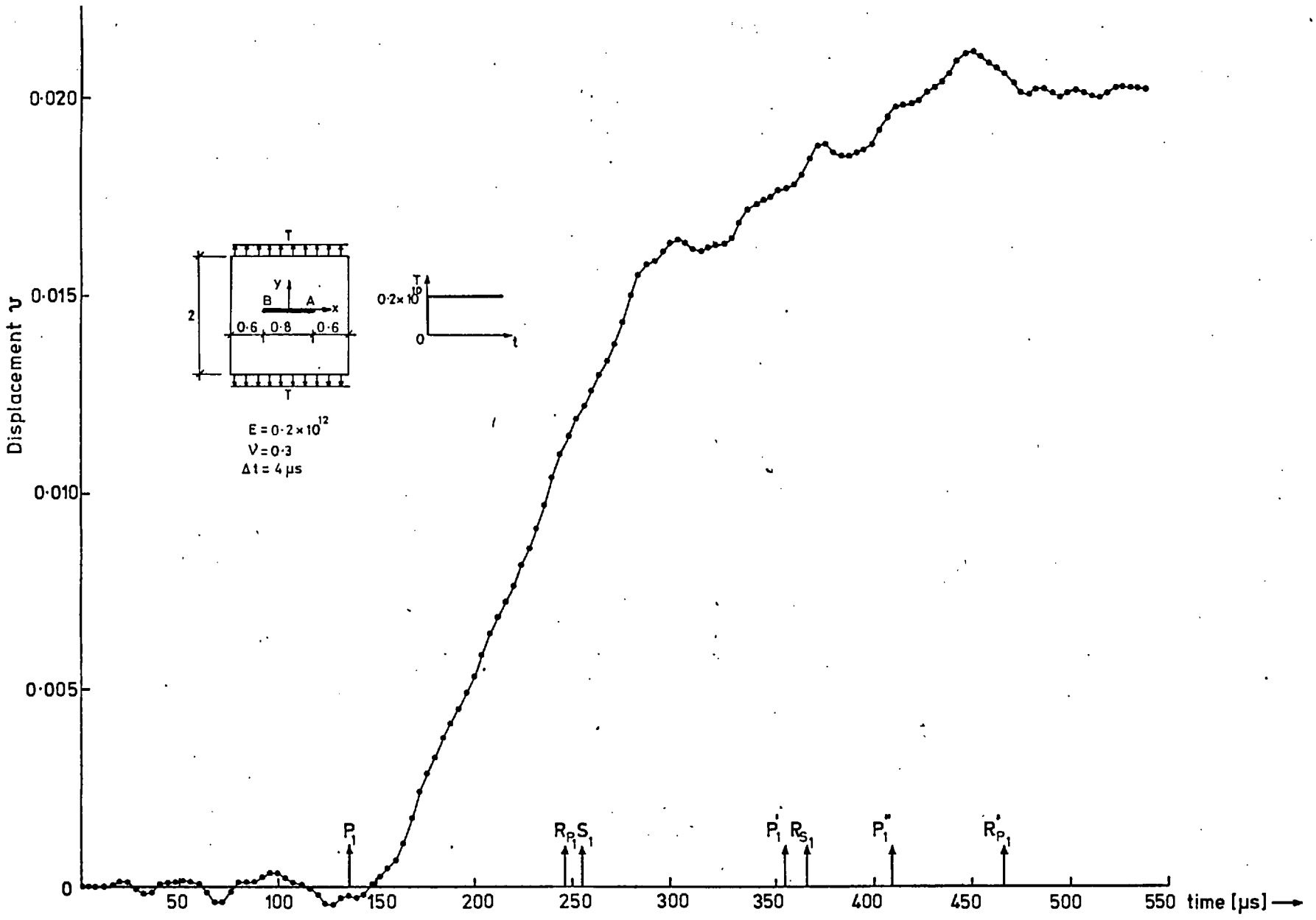

Fig.21 Time-variations of displacement υ at the centre (0,0) for the central crack problem

results are obtained the displacement shows an oscillatory behaviour around $v_s = 0.0201$ with very small amplitudes. The curve is plotted for 137 time steps of size $\Delta t = 4\mu s$. The time required for forward elimination of the resulting linear set of simultaneous equations is about 2.12 seconds while backward substitution for each time step takes about 0.49 seconds on a CDC 6400.

V.7.3 A Propagating Crack Problem

With the analysis in Chapter IV of a crack propagating at the Rayleigh velocity V_R we consider a crack developing from zero initial length at the centre of a tensile sheet and moving at a velocity V_R (Fig. 22). For this problem it is known that the stress intensity factors are zero. The data for this problem is as follows:

$$E = 200 \text{ Gpa}$$

$$\nu = 0.25$$

$$\rho = 5000 \text{ Kg/m}^3$$

which results in

$$c_1 = 6928 \text{ m/s}$$

$$c_2 = 4000 \text{ m/s}$$

$$V_R = 0.919 c_2 = 3676 \text{ m/s}$$

A finite element mesh for this problem is shown in Fig. 25. The problem is simulated by first applying static loads to a level that is assumed to initialize a crack at the centre of the sheet in the static field (i.e. field velocity is initially zero). The propagating crack is modelled by uniformly cutting through the material along the line immediatley ahead of the crack.

As we have discretized the structure in a finite number of elements we can simulate the crack propagation by the release of nodes in front of crack line at a rate

$$V_R = \dot{a}(t) = \lim_{\Delta t \to 0} \left[\frac{a(t+\Delta t) - a(t)}{\Delta t}\right]$$

where a(t) is the crack length at time t. In the time interval Δt we analyse a *stationary* crack of length $a(t+\Delta t)$ with a time increment $(\Delta t)' = \frac{\Delta t}{N}$ where N is an arbitrary integer (Fig. 16.).

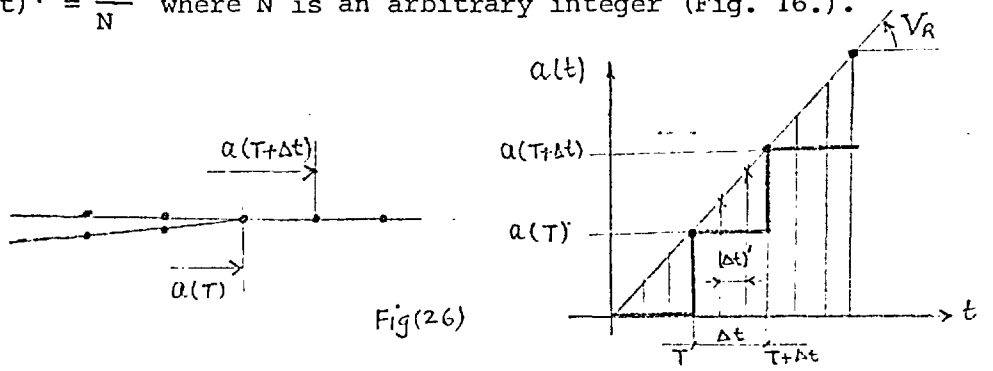

Fig(26)

As the smallest length in the elements is ½ we have taken $\Delta t = \frac{\frac{1}{2}}{3676} = 136.02 \times 10^{-6}$ s so that release of nodes results in almost uniform velocity V_R. Subsequent to the release of a node we analyse two stationary dynamic problems with $(\Delta t)' = \frac{\Delta t}{3}$ and crack length $a(T+\Delta t)$. This process is repeated for any desired period of time. The crack profile at two different times is shown in Fig. 23 and time variation of the displacement v due to propagation of the crack at an arbitrary point (x=1.0, y=1.0) is plotted in Fig. 24. There does not seem to be any values available in literature for comparison.

E = 200 GPa
ν = 0·25
ρ = 5000 Kg/m^3
Δt = 45·34 μs
$V = V_R$ = 3676 m/s

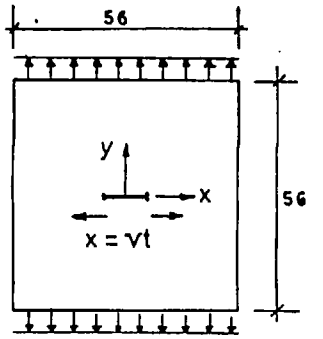

Fig. 22 The moving crack at Rayleigh velocity.

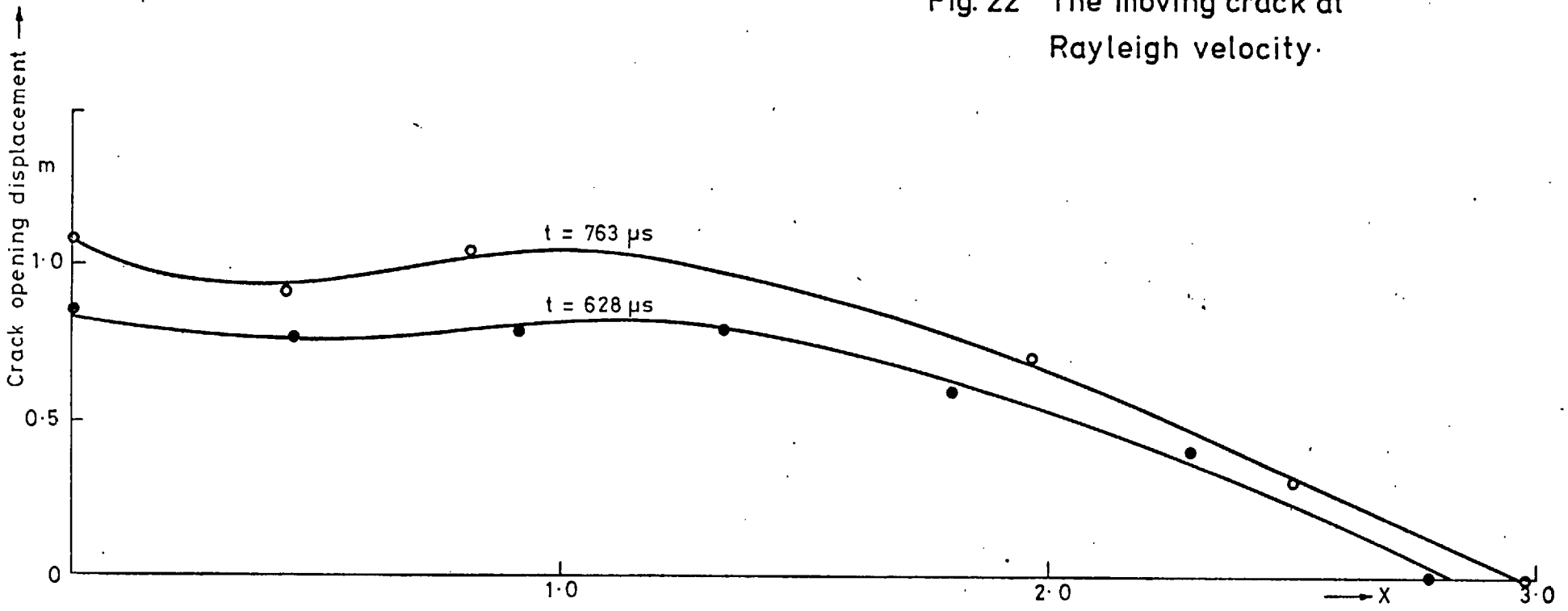

Fig 23 Crack profile of Rayleigh problem at different times

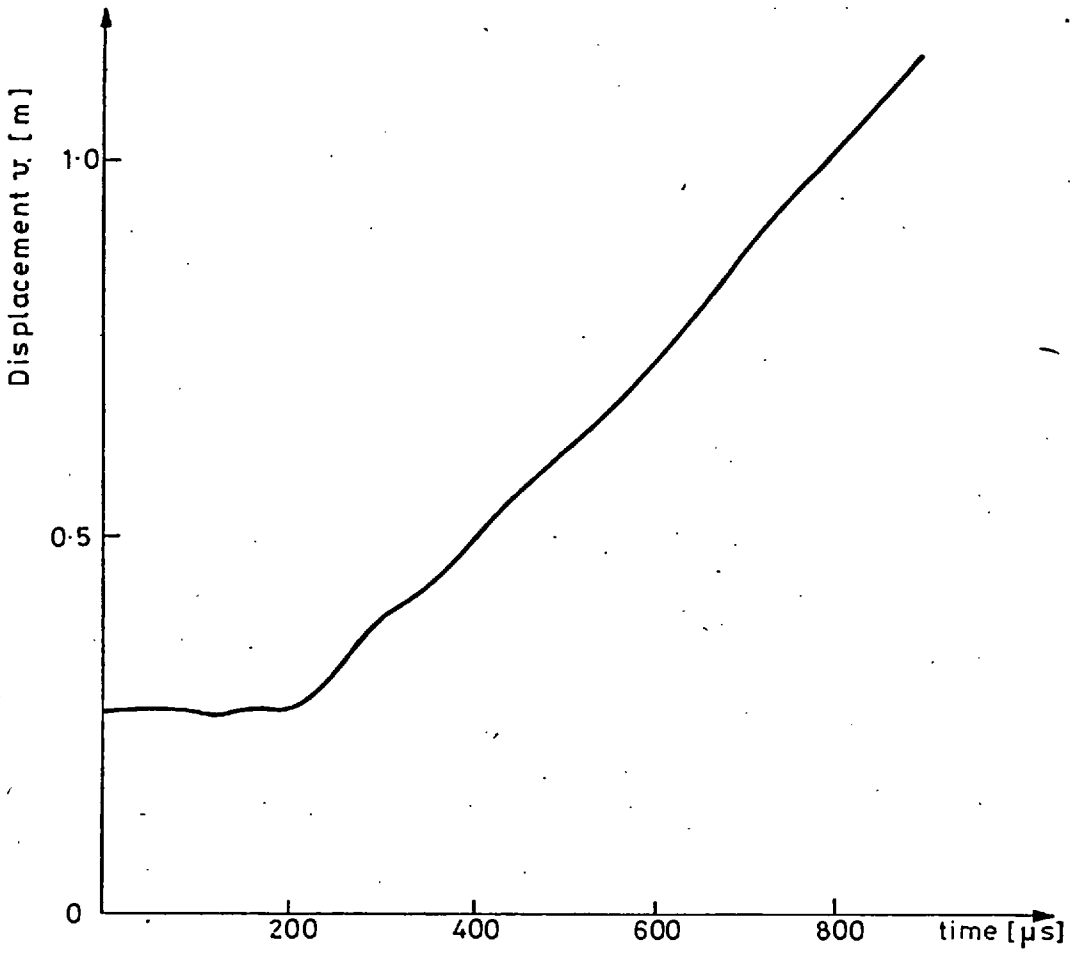

Fig. 24 Time-variation of displacement v at (x = 1·0, y = 1·0) in Rayleigh problem.

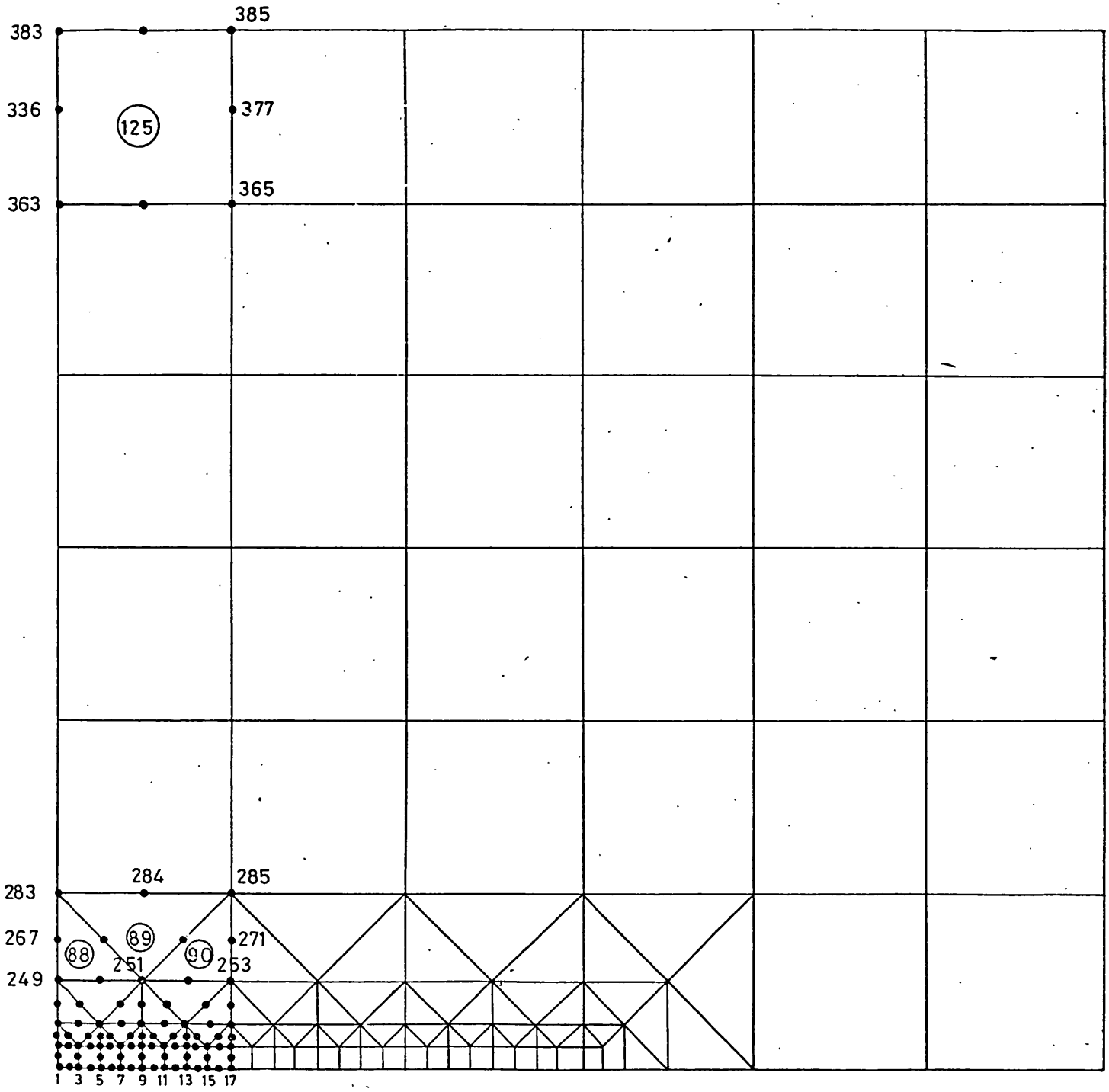

Fig 25 Finite element representation of Rayleigh Problem

REFERENCES

1. Muskhelishvili N.I., Some basic problems of mathematical theory of elasticity, P. Noordhoff, Groningen, 1963.

2. Sih G.C. et al, On the singular character of thermal stresses near a crack tip, J. Appl. Mech., 29, 1962, pp. 587-589.

3. Sih G.C., Fracture strength of a rectangular beam with surface cracks, SIAM, Vol. 12, No. 2, 1964, pp. 403-415.

4. Bowie O.L., Analysis of an infinite plate containing radial cracks originating at the boundary of an internal circular hole, J. Math. Phys., Vol. 35, 1956, pp. 60-71.

5. Bowie O.L., Rectangular tensile sheet with symmetric edge cracks, J. Appl. Mech., Vol. 31, 1964, pp. 208-212.

6. Neal D.M., Stress intensity factors for cracks emanating from rectangular cutouts, Int. J. Fracture Mech., Vol. 6, 1970, pp. 393-400.

7. Williams M.L., Stress singularities resulting from various boundary conditions in angular corners of plates in extension, J. Appl. Mech., 1952, pp. 526-528.

8. Williams M.L., On the stress distribution at the base of a stationary crack, J. Appl. Mech., 24, 1957, pp. 109-114.

9. Green A.E. and Zerna W., Theoretical elasticity, Oxford University Press, New York, 1954.

10. Sneddon I.N. and Srivastav R.P., The stress in the vicinity of an infinite row of collinear cracks in an elastic body, Proc. Royal Soc. Edin., A. 67, 1965.

11. Noble B., Methods based on the Wiener-Hopf technique for the solution of partial differential equations, Pergammon Press, New York, 1958.

12. Koiter W.T., Proc. Royal Neth. Acad. Sci., B59, 1956, pp. 354-365.

13. Knauss W.G., Stresses in an infinite strip containing a semi-infinite crack, J. Appl. Mech., Vol. 33, 1966, pp. 356-362.

14. Westmann R.A., Pressurized star crack, Jl. Math. Phys., Vol. 43, 1964, pp.191-198.

15. Baker B.R., Dynamic stresses created by a moving crack, J. Appl. Mech., 1962, pp. 449-458.

16. Sih G.C. (Ed.), Mechanics of fracture, methods of analysis and solution of crack problems, Vol. I, Noordhoff, 1973.

17. Bilby B.A. and Eshelby J.D., Fractur, Vol. I, Liebowitz (Ed.) Academic Press, New York, 1968.

18. Isida M., Methods of analysis and solutions of crack problems, G.C. Sih (Ed.), Noordhoff, Holland, 1973.

19. Chen Y.M. and Wilkins M.L., Elastodynamic crack problems in mechanics of fracture, Vol. IV, Chap. 6, Sih G.C. (Ed.), Noordhoff, 1977

20. Aberson J.A., Anderson J.M. and King W.W., ibid, Chap. 5.

21. Hilton P.D. and Sih G.C., Methods of analysis and solution of crack problems in mechanics of fracture, Sih G.C. (Ed.) Vol. 1, Chap. 8, 1973.

22. Wilson W.K., ibid, Chap. 9.

23. Tong P. and Pian T.H.H., On the convergence of the finite element method for problems with singularity, Int. J. Solids. Structures, Vol. 9, 1973, pp. 313-321.

24. Chan S.K., Tuba I.S. and Wilson W.K., On the finite element method in linear fracture mechanics, Eng. Fracture Mech., 2, 1970, pp. 1-17.

25. Nitche J. and Schatz A., On local approximation of L_2-projections on spline-subspaces, Applicable Analysis, 2, 1972, pp. 161-168.

26. Babuska I., Finite element method for domains with corners, Computing, Vol. 6, 1970, pp. 264-273.

27. Ben-Menaham, Radiation of seismic surface waves from finite moving sources, Bul. Seism. Soc. Am., Vol. 51, No. 3, 1961, pp. 401-435.

28. Haskell N.A., Elastic Displacements in the near field of a propagating fault, ibid, Vol. 59, No. 2, 1969, pp. 865-908.

29. Knopoff, Diffraction of elastic waves, J. of Accous. Soc. Am., Vol. 28, No. 2, 1956, pp. 217-229.

30. Ida Y., Stress concentration and unsteady propagation of longitudinal shear crack, J. Geophys. Res., Vol. 73, No. 16, 1968, pp. 5359-5376.

31. Ida Y. and Aki K., Seismic source time function of propagating longitudinal shear cracks, ibid, Vol. 77, No. 11, 1972, pp. 2034-2044.

32. Archambeau C.B., General theory of elastodynamic field sources, Review of Geophysics, Vol. 6, No. 3, 1968, pp. 241-288.

33. Eshelby J.D., The continuum theory of lattice defects, Solid State Physics, Vol. 3, Seitz F. and Turnball D. (Ed.) Academic Press, 1956.

34. Rice J.R., A path independent integral and the approximate analysis of strain concentration by notches and cracks, J. Appl Mech., Vol. 35, Trans. ASME, 1968, pp. 379-386.

35. Knowles J.K. and Sternberg E., On a class of conservation laws in linearized and finite elastostatics, Arch. Rat. Mech. Anal., Vol 44, No. 3, 1972, 00. 187-211.

36. Budiansky B. and Rice J.R., Conservation laws and energy-release rates, J. Appl. Mech., 1973, pp. 201-203.

37. Hellen T.K. and Blackburn W.S., The calculation of stress intensity factors for combined tensile and shear loading, Int. J. Fracture, Vol. 11, No. 4, 1975, pp. 605-617.

38. Nilsson F., A path-independent integral for transient crack problems, Int. J. Solids Structures, Vol. 9, 1973, pp. 1107-1115.

39. Gurtin E., On a path-independent integral for elastodynamics, Int. J. Fracture, Vol. 12, 1976, pp. 643-644.

40. Raviart P.A., The approximation of elliptic problems, Lecture Notes, Mathematics Department, Imperial College, 1975.

41. Zienkiewicz O.C., The finite element method in engineering science, 2nd. Ed., McGraw Hill, New York, 1972.

42. Strang G. and Fix G.J., An analysis of the finite element method, Prentice Hall Inc. Englewood Cliffs, N.J., 1973.

43. Aziz A.K. (Ed.) The Mathematical Foundation of the Finite Element Method with Applications to Partial Differential Equations, Symp. University of Maryland, Baltimore, June 1972, Academic Press, 1972.

44. Whiteman J.R. (Ed.), The Mathematics of Finite Elements and Applications, Conf. Brunel Univ., 1972, Academic Press, 1973.

45. Strang G., Approximation in the finite element method, Numer. Math., 19, 1972, pp. 81-98.

46. Strang G., Piecewise polynomials and the finite element method, Bul. Am. Math. Soc., Vol. 79, No. 6, 1973, pp. 1128-1137.

47. Bramble J.H. and Zlamal M., Triangular elements in the finite element method, Math. Comp., Vol. 24, No. 112, 1970, pp. 809-820.

48. Bramble J.H. and Hilbert S.R., Bounds for a class of linear functionals with applications to Hermite interpolation, Numer. Math., 16, 1971, pp. 362-369.

49. Bramble J.H. and Hilbert S.R., Estimation of linear functionals on Sobolev spaces with applications to Fourier transforms and spline interpolations, SIAM J. Num. Anal., Vol. 7, No. 1, 1970, pp. 112-124.

50. Zlamal M., On the finite element method, Numer. Math. 12, 1968, pp. 394-409.

51. Lions J.L. and Magenés E., Nonhomogeneous boundary value problems and applications, Vols. I and II, Springer Verlag, New York, 1972.

52. Ciarlet P.G. and Raviart P.A., General Lagrange and Hermite interpolation in R^n with applications to finite element methods, Arch. Rat. Mech. Anal., Vol. 46, 1972, pp. 177-199.

53. (i) Hlavaček I. and Nečas J., On inequalities of Korn's type, I - B.V.P. for elliptic systems of PDE, Arch. Rat. Mech. Anal., Vol. 36, 1970, pp. 305-311.

53. (ii) ibid, II - Applications to linear elasticity, pp. 312-334.

54. Gobert J. Une inegalité fundamentale de al théorie de l'elasticité, Bul Soc. Roy. Sci., Liège, No. 3-4, 1962, pp. 182-191.

55. Nečas J., Les méthodes directes en théorie des équations elliptiques, Masson, Paris, 1967.

56. Kadlec J., The regularity of the solution of the Poisson problem in a domain whose boundary is similar to that of a convex domain, Czechoslovak Math. J., Vol. 14, No. 89, 1964, pp. 386-393.

57. Agmon S., Douglis A. and Nirenberg L., Estimates near the boundary for solution of elliptic partial differential equations II, Comm. Pure Appl. Math., Vol. 17, pp. 35-92, 1964.

58. Agranovic M.S. and Visik M.I., Elliptic boundary value problems depending on a parameter, Soviet Math. Dokl., Vol. 4, 1963, pp. 325-329.

59. Kondratev V.A., Boundary problems for elliptic equations in domains with conical or angular points, Trans. Moscow Math. Soc. 16, 1968, pp. 227-313.

60. Bramble J.H. and Schatz A.H., Rayleigh-Ritz-Galerkin methods for Dirichlet's problem using subspaces without boundary conditions, Comm. Pure Appl. Math., Vol. 23, 1970, pp. 653-675.

61. Dupont T., L_2-estimates for Galerkin methods for second order hyperbolic equations, SIAM J. Num. Anal., Vol. 10, No. 5, 1973, pp. 880-889.

62. Baker G.A., Error estimates for finite element methods for second order hyperbolic equations, SIAM J. Num. Anal. Vol. 13, No. 4, 1976, pp. 564-576.

63. Wheeler M.F., A priori L_2-error estimates for Galerkin approximations to parabolic partial differential equations, SIAM J. Num. Math., Vol. 10, No. 4, 1973, pp. 723-759.

64. Duvaut G. and Lions J.L., Inequalities in mechanics and physics, (Trans. C.W. John), Springer Verlag, Berlin, 1976.

65. Craggs J.W., Fracture criteria for use in continuum mechanics, In Fracture of solids, Conf. Proc. Drucker D.C. and Gilamn J.J. (Ed.) 192, pp. 51-63, 1963.

66. Atkinson C. and Eshelby J.D., The flow of energy into the tip of a moving crack, Int. J. Fracture Mech., 4, 1968, pp. 3-8.

67. Freund L.B., Energy flux into the tip of an extending crack in an elastic field, J. of Elasticity, Vol. 2, No. 4, 1972, pp. 341-349.

68. Kostrov B.V. and Nikitin L.V., Some general problems of mechanics of brittle fracture, Archiwum Mechaniki Stosowanej, Vol. 6, No. 22, 1970, pp. 749-776.

69. Erdogan F., Crack propagation theories, In Fracture, Vol. II, Liebowitz (Ed.), Academic Press, 1968.

70. Sternberg E., On the integration of the equations of motion in the classical theory of elasticity, Arch. Rat. Mech. Anal., Vol. 6, 1960, pp. 34-50.

71. Yoffe E.H., The moving Griffith crack, Phil, Mag., Series 7, No. 42, 1951, pp. 739-750.

72. Craggs J.W., On the propagation of a crack in an elastic brittle material, J. Mech. Phys. Solids, Vol. 8, 1960, pp. 66-75.

73. Broberg K.B., The propagation of a brittle crack, Arkiv. für fysik, Band 18, nr. 10, 1960, pp. 159-192.

74. Griffith A.A., The phenomena of rupture and flow in solids, Phil. Trans. Series A, 221. 1921.

75. Barenblatt G.I., On the equilibrium due to brittle fracture, stability of isolated cracks, relation to energy theories, J. Appl. Math. and Mech., Vo. 23, 1959.

76. Willis J.R., A comparison of the fracture criteria of Griffith and Barenblatt, J. Mech. Phys. Solids, Vol. 15, 1967, pp. 151-162.

77. Sih G.C., Strain energy density factor applied to mixed mode crack problems, Int. J. Fracture, Vol. 10, No. 3, 1974, pp. 305-321.

78. Stroh A., A theory of the fracture of metals, Advances in Physics, Vol. 6, 1957, pp. 418-465.

79. Ang D.D., Elastic waves generated by a force moving along a crack, J. Math. and Physics, Vol. 38, 1959, pp. 246-256.

80. Barenblatt G.I. and Cherepanov G.P., On the wedging of brittle bodies, J. Appl. Math. Mech., Vol. 24, 1960, pp. 993-1014.

81. Freund L.B. and Clifton R.J., On the uniqueness of plane elastodynamic solutions for running cracks, J. of Elasticity, Vol. 4, No. 4, 1974, pp. 293-299.

82. Eshelby J.D., Uniformly moving dislocation, Proc. Phys. Soc., A62, Part V, No. 353A, 1949.

83. Chen Y.M. and Wilkins M.L., Numerical analysis of dynamic crack problems, chap. 6., in Mechancis of Fracture, Vol. 4, Sih G.C. (Ed.), Noordhoff, 1977.

84. Aboudi J., The dynamic stresses induced by moving interfacial cracks, Computer Methods in Appl. Mech. Eng., 10, 1977, pp. 303-323.

85. Anderson J.M., Aberson J.A. and King W.W., Finite element analysis of cracked structures subjected to shock loads, In Computational Fracture Mechanics, 2nd. Nat. Congress, Cal. (Rybicki E.F. et al. Ed.) 1975.

86. Malluck J.H., Crack propagation in finite bodies, PhD thesis, Georgia Institute of Technology, Atlanta, 1975.

87. Anderson H., (i) A finite element presentation of stable crack growth, J. Mech. Phys. Solids, Vol. 21, 1973, pp. 337-356.

(ii)Finite element treatment of a uniformly moving elastic-plastic crack tip, J. Mech. Phys. Solids, Vol. 22, 1974, pp. 285-308.

88. Atkinson C., On the stress intensity factors associated with cracks interacting with an interface between two elastic media, Int. J. Eng. Sci., Vol. 13, 1975, pp. 489-504.

89. Nilsson F., Dynamic stress intensity factors for finite strip problems, Int. J. Fracture Mech., Vol. 8, No. 4, 1972, pp. 403-411.

90. Bergkvist H., The motion of a brittle crack, J. Mech. Phys. Solids, Vol. 21, 1973, pp. 229-239.

91. Willis J.R., Crack propagation in viscoelastic media, J. Mech. Phys. Solids, Vol. 15, 1967, pp. 229-240.

92. Freund L.B. Crack propagation in an elastic solid subjected to general loading, Parts I and II, J. Mech. Phys. Solids, Vol. 20, 1972, pp. 129-140.

93. Arantes Oliveira E.R., The patch test and the general convergence criteria of the finite element method, Int. J. Solids Structures, Vol. 13, 1977, pp. 159-178.

94. Fix, G.J., Gulati S. and Wakoff G.I., On the use of singular functions with finite element approximation, J. of Computational Physics, Vol. 13, 1973, pp. 209-228.

95. Birkhoff G., Angular singularities of elliptic problems, J. Approximation Theory, Vol. 6, 1972, pp. 215-230.

96. Benzley S.E., Representation of singularities with isoparametric finite elements, Int. J. Num. Meth. Eng., Vol. 8, pp. 537-545, 1974.

97. Byskov E., The calculation of stress intensity factors using the finite element method with cracked elements, Int. J. Frac. Mech., Vol. 6, 1970, pp. 159-167.

98. Barsoum R.S., On the use of isoparametric finite element in linear fracture mechanics, Int. J. Num. Mech. Eng. Vol. 10, 1976, pp. 25-37.

99. Henshell R.D. and Shaw K.G., Crack tip finite elements are unnecessary, Int. J. Meth. Eng., Vol. 9, 1975, pp. 495-507.

100. Barsoum R.S., Triangular quarter-point elements as elastic and perfectly plastic crack tip elements, Int. J. Num. Meth. Eng., Vol. 11, 1977, pp. 85-98.

101. Levy N., et al, Small scale yielding near a crack in plane strain: a finite element analysis, Int. J. Fracture Mech., Vol. 7, No. 2, 1971, pp. 143-156.

102. Newmark N.M., A method of computation for structural dynamics, J. Eng. Mech. Div. Proc. ASCE, 85, EM3, 1959, pp. 67-94.

103. Fujii H., Finite element schemes: stability and convergence, in Advances in Computational Methods in Structural Mechanics and Design, Oden J.I. et al (Ed.) 1972, pp. 201-218.

104. Glowinski R., Lions J.L. and Trémolieres R., Analyse numérique des inéquations variationelles, Vol. II, Dunod, Paris, 1976.

105. Bathe K.J., Wilson E.L., Stability and accuracy analysis of direct integration methods, Earthquake Eng. Struct. Dynamics, Vol. 1, 1973, pp. 283-291.

106. Shantaram D., Owen D.R.J. and Zienkiewicz, Dynamic transient behaviour of two and three dimensional structures including plasticity, large deformation effects and fluid interaction, ibid, Vol. 4, 1976, pp. 561-578.

107. Hinton E., Rock T. and Zienkiewicz, A note on mass lumping and related processes, ibid, Vol. 4, No. 3, 1975, pp. 245.

108. Baker G. and Douglis V.A., The effect of quadrature errors on finite element approximation for second order hyperbolic equations, SIAM J. Num. Anal., Vol. 13, No. 4, pp. 577-598, 1976.

109. Cowper G.R., Gaussian quadrature formulae for triangles, Int. J. Num. Meth. Eng., Vol. 7, 1973, pp. 405-408.

110. Forsythe G. and Moler C.B., Computer solution of linear algebraic systems, Prentice Hall, New Jersey, 1967.

111. Jennings A., A compact storage scheme for the solution of symmetric linear simultaneous equations, Comp. J., Vol. 9, 1966, pp. 281-185.

112. Irons, B.U., A frontal solution program for finite element analysis, Int. J. Num. Meth. Eng., Vol. 2, 1970, pp. 5-32.

113. George J.A., Nested dissection of a regular finite element mesh, SIAM J. Num. Anal., Vol. 10. 1973, pp. 345-363.

114. Wilkinson J.H., The algebraic eigenvalue problem, Oxford University Press, Oxford, 1965.

115. Lyons L.P.R., A general finite element system with special reference to the analysis of cellular structures, PhD Thesis, University of London, 1977.

116. Freese C.E. and Tracey D.M., The natural isoparametric triangle versus collapsed quadrilateral for elastic crack analysis, Int. J. Fracture, Vol. 12, 1976, pp. 767-770.

117. Cartwright D.J. and Rooke D.P., Stress intensity factors, HMSO, 1976.

118. Liebowitz H. (Ed.) Fracture Vol. II, Mathematical Fundamentals, Academic Press, 1968.

119. Bowie O.I. and Freese C.E., Central crack in plane orthotropic rectangular sheet, Int. J. Frac. Mech., Vol. 8, No. 1, 1972.